ELUCIDATING THE ROLE OF BCL6 IN HELPER T CELL ACTIVATION, PROLIFERATION, AND DIFFERENTIATION

Kristin N. Hollister

Submitted to the faculty of the University Graduate School
in partial fulfillment of the requirements
for the degree
Doctor of Philosophy
in the Department of Microbiology and Immunology,
Indiana University

June 2014

Accepted by the Graduate Faculty of Indiana University, in partial fulfillment of the requirements for the degree of Doctor of Philosophy.

_____
Alexander L. Dent, Ph.D., Chairman

Doctoral Committee

_____
Randy R. Brutkiewicz, Ph.D.

March 7, 2014

_____
Maureen A. Harrington, Ph.D.

_____
Mark H. Kaplan, Ph.D.

ACKNOWLEDGEMENTS

I would like to thank my mentor, Dr. Alexander Dent. Without his guidance and support this work would not have been possible. He has been a phenomenal mentor, and any student would be lucky to have him as such. Also, I would like to thank my committee members, Dr. Randy Brutkiewicz, Dr. Mark Kaplan, and Dr. Maureen Harrington. I always looked forward to our meetings and the constructive criticism and helpful encouragement they provided. Several Dent lab members, past and present, contributed greatly to this work and enabled me to complete complex experiments resulting in excellent data. These people include Hao Wu, Arpita Mondal, and Ninah Clegg. Members of the Kaplan lab were also instrumental in assisting with the work presented here. In particular, I would like to acknowledge the contributions of Dr. Duy Pham, who provided excellent technical assistance with some of the assays presented in this thesis. Our collaborators at the University of Massachusetts Medical School played a pivotal role in ascertaining the data for our HIV-1 vaccine model. Dr. Shan Lu's group included Dr. Shixia Wang and Yuxin Chen.

I have been fortunate enough to be funded by multiple sources during my graduate studies, and I would like to thank Dr. Janice Blum, Dr. Hal Broxmeyer, and Dr. Stanley Spinola for providing me with financial support during my studies.

Finally, I would like to thank my family for providing me with the support and encouragement needed to make it through graduate school.

Kristin N. Hollister

ELUCIDATING THE ROLE OF BCL6 IN HELPER T CELL ACTIVATION, PROLIFERATION, AND DIFFERENTIATION

The transcriptional repressor BCL6 has been shown to be essential for the differentiation of germinal center (GC) B cells and follicular T helper (TFH) cells. The interaction of TFH and GC B cells is necessary for the development of high affinity antibodies specific for an invading pathogen. Germline BCL6-deficient mouse models limit our ability to study BCL6 function in T cells due to the strong inflammatory responses seen in these mice. To overcome this, our lab has developed a new BCL6 conditional knockout (cKO) mouse using the cre/lox system, wherein the zinc finger region of the BCL6 gene is flanked by loxP sites. Mating to a CD4-Cre mouse allowed us to study the effects of BCL6 loss specifically in T cells, without the confounding effects seen in germline knockout models. Using this cKO model, we have reaffirmed the necessity of BCL6 for TFH differentiation, including its role in sustained CXCR5 surface expression, a signature marker for TFH cells. This model also allowed us to recognize the role of BCL6 in promoting the expression of PD-1, another key surface marker for TFH cells. Without BCL6, $CD4^+$ T cells cannot express PD-1 at the high levels seen on TFH cells. Our discovery of DNMT3b as a target for BCL6 suggests BCL6-deficient T cells have increased DNA methyltransferase activity at the PD-1 promoter. This data establishes a novel pathway for explaining how BCL6, a transcriptional repressor, can activate genes. Experiments with the BCL6 cKO model have also established a role for BCL6 in naïve $CD4^+$ T cell activation. Furthermore, we did not observe increased differentiation of other helper T cell subsets, in contrast to what has been reported elsewhere with germline BCL6-deficient models. Unexpectedly, we found decreased T helper type 2 (Th2) cells, whereas mouse models with a germline mutation of BCL6 have increased Th2 cells. These results indicate that BCL6 activity in non-T cells is critical for controlling T cell differentiation. Finally, using an HIV-1 gp120 immunization model, we have, for the first time, shown BCL6-dependent GCs to be limiting for antibody development and affinity maturation in a prime-boost vaccine scheme.

Alexander L. Dent, Ph.D., Chairman

TABLE OF CONTENTS

List of Tables ix
List of Figures x
List of Abbreviations xiii
CHAPTER 1 – A GENERAL INTRODUCTION TO THE IMMUNE RESPONSE 1
Immune System Origins 1
The Innate Immune Response 1
Granulocytes 2
Monocytes, macrophages, dendritic cells 3
Major histocompatibility complex class II molecules 3
Natural killer cells 3
The Adaptive Immune Response 4
T helper type 1, type 2, type 17, and type 9 cells 4
Th-B cell interactions 6
Regulatory Th cells 8
Follicular T helper cells 8
Germinal Centers 9
Germinal center development 9
Somatic hypermutation and isotype class switching of B cells 11
Germinal center structure 12
Regulating the germinal center response 12
Goals of Research 14
CHAPTER 2 – DEVELOPMENT OF A NEW BCL6 CONDITIONAL KNOCKOUT MOUSE MODEL 15
Introduction 15
BCL6 structure and activity 15
BCL6 germline knockout mouse model 16
Materials and Methods 17
Results 20
Generation of $BCL6^{Neofl/Neofl}$ mice 20
Functional testing of $BCL6^{Neofl/Neofl}$ mice 21
Removal of the neomycin resistance gene 28
New germline knockout mice – $BCL6^{\Delta ZF/\Delta ZF}$ 29

BCL6$^{fl/fl}$ mice 33
Discussion 33
CHAPTER 3 – BCL6 IS NECESSARY FOR PROPER NAÏVE CD4^{+} T CELL ACTIVATION 37
Introduction 37
T cell development 37
Th cell activation signaling 37
Materials and Methods 40
Results 43
Efficient and complete deletion of BCL6 zinc finger exons in BCL6$^{+/fl}$ Cre^{CD4} mice 43
Skewed naïve and effector memory CD4^{+} T cell populations in BCL6$^{fl/fl}$ Cre^{CD4} mice 43
Skewed naive and effector CD4^{+} T cell populations confirmed in mixed bone marrow chimera model 44
Naïve/effector memory CD4^{+} T cell phenotype seen early after immunization and only exacerbates over time 48
Differences in T cell activation markers in BCL6$^{fl/fl}$ Cre^{CD4} mice 49
Levels of activation differ between *in vitro* and *in vivo* stimulation 49
Discussion 52
CHAPTER 4 – ROLE OF BCL6 IN Th CELL SUBSETS 56
Introduction 56
Th1 cells 56
Th2 cells 56
Th17 cells 57
BCL6 and Blimp-1 57
Treg cells 58
TFH cells 58
Materials and Methods 59
Results 62
Transcription levels of BCL6 vary with *in vitro* and *in vivo* stimulation 62
The role of BCL6 in Th1 cells 65
The role of BCL6 in Th2 cells 69

The role of BCL6 in Th17 cells 73
BCL6 influences Foxp3 expression in $CD4^+$ T cells 75
Blimp-1 is not increased in the absence of BCL6 78
IL-10 is suppressed by BCL6 81
BCL6 limits the proliferation of activated Th cells 84
Discussion 86
CHAPTER 5 – ROLE OF BCL6 IN TFH CELL SURFACE MARKER EXPRESSION 92
Introduction 92
CXCR5 expression by Th cells 92
ICOS expression by Th cells 92
PD-1 expression and signaling in Th cells 93
DNA methylation 93
Models for TFH differentiation 94
Methods and Materials 95
Results 98
Germinal center cells fail to develop at any time after immunization in $BCL6^{fl/fl}$ Cre^{CD4} mice 98
TFH surface marker expression in BCL6-deficient Th cells 101
PD-1 expression is altered in BCL6-deficient Th cells 105
BCL6 limits apoptosis in PD-1^{high} Th cells 107
Methylation and deacetylation machinery is increased in the absence of BCL6 107
The promoter region of PD-1 has increased binding of DNA-methyltransferases 109
Blocking methylation increases PD-1 expression, but not CXCR5 expression 111
Discussion 113
CHAPTER 6 – GERMINAL CENTER DYNAMICS IN AN HIV-1-gp120 DNA PRIME/PROTEIN BOOST VACCINE SCHEME 118
Introduction 118
Structure of HIV virion 118
Infection of $CD4^+$ T cells by HIV 118
Neutralizing antibodies 121

Methods and Materials 123
Results 125
Immunization with gp120-encoding DNA yields a stronger GC response than gp120 protein 125
Priming with gp120-encoding DNA enhances GCs and the proportion of TFH cells in spleen 126
Priming with gp120 DNA improves GC activity 129
Deletion of BCL6 results in a significant increase of gp120-specific IgG 131
Discussion 132
Future Directions 137
Appendix – Summary of mutant mice presented in this thesis 144
References 146
Curriculum Vitae

LIST OF TABLES

Table 1. Summary of microarray data with BCL6$^{fl/fl}$ Cre^{CD4} T cells 51
Table 2. Summary of mutant mice presented in this thesis 144

LIST OF FIGURES

Figure 1. Germinal center development 5
Figure 2. Different $CD4^+$ Th cell subsets 7
Figure 3. Antibody development 10
Figure 4. Germinal center cycling and regulation 13
Figure 5. BCL6 protein 16
Figure 6. Different versions of the BCL6 gene 21
Figure 7. Frequencies of $BCL6^{Neofl/Neofl}$ mice 22
Figure 8. Loss of GCs in $BCL6^{Neofl/Neofl}$ mice 23
Figure 9. Genotypic and phenotypic characterization of $BCL6^{Neofl/Neofl}$ mice 24
Figure 10. BCL6 expression $CD4^+$ T cells 25
Figure 11. Cytokine production of $CD4^+$ T cells from immunized mice 26
Figure 12. Cytokine production of cultured naïve $CD4^+$ T cells 27
Figure 13. Histology of lung and heart from $BCL6^{Neofl}$ and GL KO mice 27
Figure 14. Changes in *rorc* and *prdm1* expression under different cytokine environments 28
Figure 15. Alleles of new BCL6 mutant mice 29
Figure 16. Genotypic and phenotypic characterization of $BCL6^{\Delta ZF/\Delta ZF}$ mice 30
Figure 17. Cytokine skewing of $CD4^+$ T cells from $BCL6^{\Delta ZF/\Delta ZF}$ mice 31
Figure 18. Functional analysis of $BCL6^{fl/fl}$ mice 32
Figure 19. Proposed model for graded BCL6 expression in different Th subsets 36
Figure 20. Development of $CD4^+$ T cells 38
Figure 21. Early signaling events in TCR stimulation 39
Figure 22. Conditional deletion of BCL6 in T cells 44
Figure 23. $BCL6^{fl/fl}$ Cre^{CD4} mice have increased naïve and decreased memory $CD4^+$ T cell populations 45
Figure 24. Naïve and effector memory cell differences in $BCL6^{fl/fl}$ Cre^{CD4} mice remain in aged mice 46
Figure 25. $BCL6^{fl/fl}$ Cre^{CD4} have similar naïve/effector memory cell phenotype in competitive chimera model 47
Figure 26. Effector cell defect is consistent throughout immune response in $BCL6^{fl/fl}$ Cre^{CD4} mice 48
Figure 27. Decreased activation marker expression in $BCL6^{fl/fl}$ Cre^{CD4} mice 50

Figure 28. Differences in activation marker expression is dependent on type of naive CD4$^+$ T cell stimulation 52
Figure 29. Induction of BCL6 following immunization 63
Figure 30. Tbet transcript levels in the absence of BCL6 *in vivo* 64
Figure 31. IFNγ expression in the absence of BCL6 66
Figure 32. Tbet, but not IFNγ, is increased in the absence of BCL6 in *in vitro* cultures 68
Figure 33. GATA3 transcript levels are unchanged in the absence of BCL6 *in vivo* 69
Figure 34. IL-4 is decreased in BCL6-deficient CD4$^+$ T cells 70
Figure 35. GATA3 is marginally increased in BCL6-deficient CD4+ T cells in *in vitro* cultures 72
Figure 36. RORγt RNA levels are marginally increased in the absence of BCL6 *in vivo* 74
Figure 37. IL-17A secretion is not altered in the absence of BCL6 75
Figure 38. RORγt expression is reliant on BCL6 and exogenous cytokines for sustained expression 76
Figure 39. Foxp3 transcript levels are significantly reduced in BCL6-deficient CD4$^+$ T cells 77
Figure 40. Blimp-1 is decreased in CD4$^+$ T cells lacking BCL6 79
Figure 41. IL-10 is increased, in an intrinsic manner, in BCL6$^{fl/fl}$ Cre^{CD4} CD4$^+$ T cells 80
Figure 42. IL-10 is increased in different skewing culture conditions 83
Figure 43. BCL6 limits proliferation of activated CD4$^+$ T cells 85
Figure 44. Th17 differentiation and BCL6 91
Figure 45. BCL6$^{fl/fl}$ Cre^{CD4} mice fail to generate germinal centers 99
Figure 46. Antibody titers in BCL6$^{+/+}$ Cre^{CD4} and BCL6$^{fl/fl}$ Cre^{CD4} mice 100
Figure 47. CXCR5 expression in BCL6-deficient CD4$^+$ T cells 102
Figure 48. ICOS expression in BCL6-deficient CD4$^+$ T cells 103
Figure 49. PD-1 expression is altered in the absence of BCL6 104
Figure 50. BCL6 maintains the survival of PD-1^{high} TFH cells 106
Figure 51. Expression of methylation and deacetylation enzymes is increased in absence of BCL6 108
Figure 52. Dnmt3a and Dnmt3b bind to the *pdcd1* promoter region 110

Figure 53. The promoter region of *pdcd1* in BCL6$^{fl/fl}$ Cre^{CD4} mice is less acetylated than in BCL6$^{+/+}$ Cre^{CD4} mice 110
Figure 54. The promoter region of *cxcr5* in BCL6$^{fl/fl}$ Cre^{CD4} mice is less acetylated than in BCL6$^{+/+}$ Cre^{CD4} mice 111
Figure 55. Blocking methylation increases PD-1 expression, but not CXCR5 expression 112
Figure 56. Structure of HIV virion 119
Figure 57. Attachment and fusion of HIV to host cell 120
Figure 58. Binding sites of broadly neutralizing antibodies to HIV 121
Figure 59. Experimental design for testing DNA vs. protein priming 125
Figure 60. Germinal centers appear earlier with repeated immunizations 126
Figure 61. Increased germinal center activity after gp120 DNA priming 127
Figure 62. Enhanced GC B cells and TFH cell populations with gp120 DNA priming 128
Figure 63. Proportion of TFH cells increased with gp120 DNA priming 128
Figure 64. Priming with gp120-encoding DNA improves GC activity 130
Figure 65. Dynamics of transitional B cells during repeated immunizations 130
Figure 66. Experimental design for deletion of BCL6 131
Figure 67. Deletion of BCL6 in tamoxifen treated mice 132
Figure 68. Germinal centers are lost with deletion of BCL6 133
Figure 69. Tet1 and Tdg are up-regulated in the absence of BCL6 139
Figure 70. Cell cycle genes are up-regulated in the absence of BCL6 141

LIST OF ABBREVIATIONS

^{3}H	Tritiated thymidine
5caC	5-carboxylcytosine
5fC	5-formylcytosine
5hmC	5-hydroxymethylcytosine
5mC	5-methlycytosine
AID	Activation-induced deaminse
AIDS	Acquired immune deficiency syndrome
APC	Antigen presenting cell
AZA	5-Aza-2′-deoxycytidine
BCL6	B cell lymphoma 6
BCoR	BCL6 interacting corepressor
BCR	B cell receptor
BM	Bone marrow
CD40L	CD40 ligand
ChIP	Chromatin immunopreciptation
CHO	Chinease hamster ovary
cKO	Conditional knockout
CLP	Common lymphoid progenitor
CM	Central memory
CMP	Common myeloid progenitor
CTLA4	Cytotoxic T-lymphocyte antigen 4
CXCL13	C-X-C motif chemokine 13
CXCR5	C-X-C chemokine receptor type 5
DC	Dendritic cell
DN	Double negative
Dnmt	DNA methyltransferase
DP	Double positive
ELISA	Enzyme-linked immunsorbance assay
EM	Effector memory
ER	Endoplasmc reticulum
FACS	Fluorescence-activated cell sorting
FDC	Follicular dendritic cell

Foxp3	Forkhead box P3
FSC	Follicular stromal cell
GC	Germinal Center
GL	Germline
gp	Glycoprotein
H3ac	Acetylated histone 3
H4ac	Acetylated histone 4
HAART	Highly active anti-retroviral therapy
HDAC	Histone deacetylase
HIV-1	Human Immunodeficienty Virus-1
HSC	Hematopoeitic stem cell
i.m.	intra-muscular
i.p.	intra-peritoneal
i.v.	intra-venous
ICOS	Inducible T-cell costimulator
ICOSL	ICOS-ligand
ICS	Intracellular staining
Ig	Immunoglobulin
IL	Interleukin
IL-21R	IL-21 receptor
IL-2R	IL-2 receptor
IL-6R	IL-6 receptor
IP	Imunoprecipitation
iTreg	Induced Treg
KO	Knockout
Lck	Lymphocyte-specific protein tyrosine kinase
MB	Memory B cell
MeDIP	Methylated DNA immunoprecipitation
MFI	Mean fluorescense intensity
MHC	Major histocompatibility complex
MPP	Multipotent progenitors
МΦ	Macrophage
N-CoR	nuclear receptor corepressor
Neo	Neomycin resistance gene

NK	Natural killer cell
NKT	Natural killer T cell
nTreg	Natural Treg
NuRD	nucleosome remodeling and deacetylase
PCR	Polymerase chain reaction
PD-1	Programmed cell death protein 1
PNA	Peanut Agglutinin
Poz	Pox virus and zinc finger
qPCR	Quantative PCR
RAG	Recombination activating gene
RD 2	repression domain 2
RIP	RNA immunoprecipitation
RORγt	RAR-related orphan receptor gamma
RT	Reverse Transcriptase
SAP	SLAM-associated protein
SHP	Src homology region 2 domain-containing phosphatase-1
SLAM	Signaling lymphocytic activation molecule
SMRT	silencing mediator of retinoid and thyroid receptor
SP	Single positive
SRBC	Sheep red blood cells
STAT	Signal tansducer and activator of transcription
TB	Transitional B cell
TCR	T cell receptor
TDG	thymine DNA glycosylase
TET	Ten-Eleven-Translocation
TFH	Follicular T helper cell
TFR	Follicular regulatory T cell
TGF-β	Transforming growth factor beta
Th	T helper cell
Th1	T helper type 1 cell
Th17	T helper type 17 cell
Th2	T helper type 2 cell
Th9	T helper type 9 cell
ThN	Th neutral

Treg	Regulatory T cell
WT	Wild Type
Zap70	Zeta-chain-associated protein kinase 70
ZF	Zinc Finger
γδ	Gamma delta cell

CHAPTER 1 – A GENERAL INTRODUCTION TO THE IMMUNE RESPONSE

Immune System Origins

The immune response of mammals is a system which has been developed and fine-tuned by evolution over millions of years (1, 2). It enables higher order beings to survive in a world where bacteria and viruses cover nearly every surface. More than half a billion years ago, a genetic mutation took place which enabled jawed vertebrates, of which mammals are one type, to enhance their immune response by rearranging the genes of their immune cells (1). From that point forward, all descendants of this ancestral animal phylum were better suited to protect themselves from the dangers of infection, which is a main objective for any immune response (1). A second, and equally important attribute for immune cells, is to distinguish between self and non-self (2). Only by being able to recognize a foreign pathogen, while limiting damage to self-tissues, can an immune response be effective and lifesaving (2).

In humans, and mice (the animal used as a surrogate for humans in research studies), the immune response is broken down into two defined, but cooperative, parts: the innate and adaptive immune responses. Cells constituting both arms of the immune system develop through a process known as hematopoiesis, wherein self-renewing stem cells can give rise to progenitor cells, which, in turn, differentiate into mature immune cells (3-5). This process enables patients who must undergo radiation for cancer treatment, to have their entire immune system reconstituted from a stem cell transplant.

The Innate Immune Response

The first, and most important, layer of defense we have against pathogens is our outer anatomical barriers. Skin and mucosal surfaces are essential for protecting us from viruses, bacteria, and other pathogens in the outside world. In the event that this physical defense is compromised, such as from a cut in the skin, pathogens can gain entry into the body. When this occurs, innate immune cells detect the antigen and attempt to remove it. These cells all develop from a common myeloid progenitor cell (3-

5). Environmental cues will cause these progenitors to become either monocytes, neutrophils, basophils, eosinophils, or mast cells. Working together, these cells can help clear the majority of infections faced on a daily basis. By using their general defense mechanisms, these innate cells will eliminate pathogens before a person realizes he or she has been infected.

Granulocytes

Eosinophils, neutrophils, basophils, and mast cells are all considered granulocytes and differentiate from a precursor of the same name. These cells are so named because of the distinct granules visible when viewed under a microscope. Granules in eosinophils contain cytokines and enzymes, such as peroxidase and neurotoxin (6). Once they receive stimulating factors from the environment, in particular interleukin (IL)-5, these cells will release the contents of their granules, a process called degranulation (6). Those contents will then facilitate killing of infected cells and tissues or directly affect the pathogen. Dysregulation of these cells has been shown in a number of diseases, including asthma (6).

In the case of neutrophils, the cytokines contained within their granules can exacerbate the inflammatory response by recruiting additional immune cells to the point of infection (7). Also, release of reactive oxygen species facilitates killing of infected tissue. Unlike eosinophils, these cells also have the ability to phagocytose microorganisms or particles which have been marked for removal by other components of the immune response (7).

Mast cells and basophils share similar functions and, historically, basophils have been mistaken for a type of mast cell (8). However, more recent research has shown these two cells to be distinct linages of myeloid cells. While both cell types are rare, basophils are relatively short-lived, while mast cells can persist in tissues for weeks to months (8, 9). Both cell types play a role in allergy and inflammation. Among other things, the granules in these cells contain histamine, and, upon their release, can both mediate and exacerbate allergic responses. Furthermore, basophils help mediate the T helper type 2 (Th2) response (8, 9), which will be described further in a later section.

Monocytes, macrophages, dendritic cells

Monocytes are a unique type of innate cell in that they exit the bone marrow into circulation as a mature cell, but continue to differentiate into additional types of immune cells in the periphery. Once they leave the blood circulation and enter into tissues, such as spleen and lymph nodes, environmental cues will trigger these cells to differentiate into macrophages (MΦ) or dendritic cells (DC) (10, 11). These cells are phagocytes which present ingested antigen to T and B cells. The unique ability of these cells to present antigen to T helper (Th) cells classifies them as professional antigen presenting cells (APC) (12).

Major histocompatibility complex class II molecules

A requisite for professional APCs to present antigen to Th cells is their expression of major histocompatibility complex class II (MHC II) molecules on their cell surface. Unlike MHC class I (MHC I) molecules, which are expressed on every nucleated cell, MHC II expression is reserved to only professional APCs, of which MΦ and DCs are two types (13). Within the APC, the MHC II molecule is composed of an alpha and beta heavy chain and is assembled in the endoplasmic reticulum (ER). To stabilize the two subunits, a protein called invariant chain binds the groove where antigen will be loaded (13-15). This full-length protein is then cleaved, leaving only a small peptide, known as CLIP, within the antigen binding groove. After leaving the ER and trafficking through the Golgi apparatus, the MHC II molecule will migrate into the cytoplasm in an endosome. Meanwhile, pathogens are taken up from the outside, via phagocytosis, into phagosomes (13-15). Within phagosomes, pathogen is digested into peptide fragments. When an endosome containing an assembled MHC II molecule binds with a phagosome, another protein, called DM, will bind to MHC II, causing the release of CLIP. With the binding groove of the MHC II molecule available, peptide is loaded onto the complex and trafficked to the cell surface, where the antigen can then be presented to Th cells in the context of the MHC II molecule (13-15).

Natural killer cells

A final cell type imperative for the innate immune response is the natural killer (NK) cell.

Unlike APCs and granulocytes, NK cells are derived from a different progenitor cell in the bone marrow and, thus, are more closely related to cells of the adaptive response. NK cells survey the body, looking for cells which have decreased or no MHC I surface expression (16). This function evolved from the ability of pathogens, particularly viruses, to trigger down-regulation of MHC I on the surface of infected cells. Therefore, this is an efficient way for NK cells to detect infected cells, and when this occurs, NK cells release granules which contain enzymes that kill the infected cell (16).

The Adaptive Immune Response

Professional APCs are essential for the immune response because they serve as a link between the innate and the adaptive responses. Activation of this second layer of immunity is required if innate responses cannot clear an antigen. The acquired response is made up of two major cell types: B cells and T cells. They differentiate, as do NK cells, from a common lymphoid progenitor (4). While B cells develop in the bone marrow and further mature in the blood, T cells exit the bone marrow in their precursor form and traffic to the thymus, where they will undergo further maturation and selection processes. For a more detailed description of this process, please see the introduction of Chapter 3. T cells are activated by APCs, which acquire antigen from the periphery, typically from the site of infection, and travel to the nearest draining lymph node. Secondary lymphoid organs, such as the spleen and lymph nodes, are organized into different areas important for different aspects of the acquired immune response. Within a lymph node, professional APCs will interact with naïve Th cells, which are also referred to as $CD4^+$ T cells due to the expression of this particular co-receptor on their surface, in the T cell zone (Figure 1A). It is here where naïve Th cells are activated and, depending on the antigen presented and the cytokine environment, differentiate into one of several different Th subsets. Each Th subset, under the control of a unique master transcription factor, will secrete cytokines that facilitate removal of the specific pathogen present (Figure 2).

T helper type 1, type 2, type 17, and type 9 cells

During a viral infection, T helper type 1 (Th1) cells differentiate in the presence of IL-12

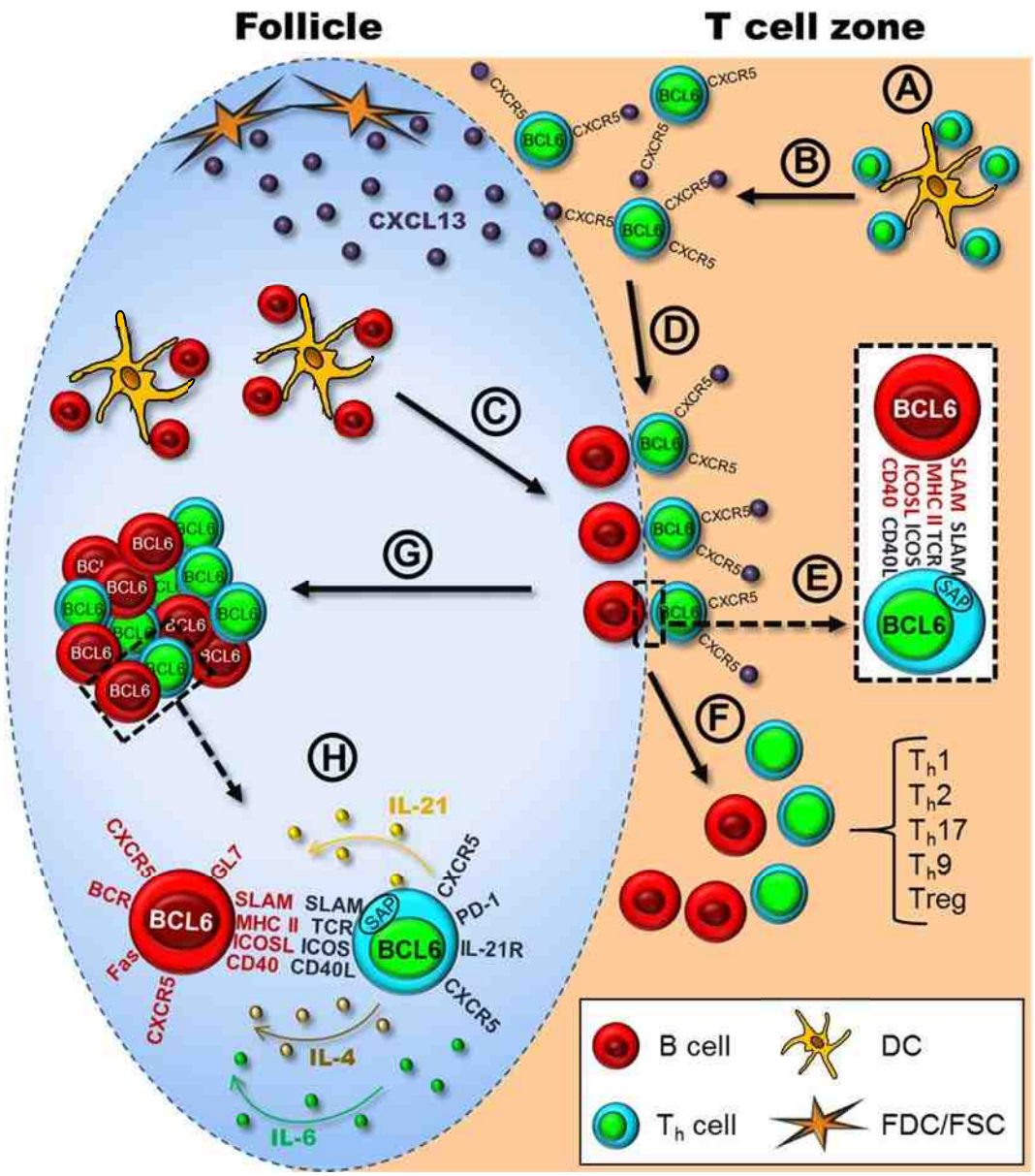

Figure 1. Germinal center development. A. Naïve CD4$^+$ Th cells are activated by professional APCs, such as DCs, within the T cell zone of secondary lymphoid organs. **B.** Once activated a subset of Th cells will up-regulate the transcriptional repressor BCL6 as well as the surface chemokine receptor, CXCR5. This allows them to follow the chemokine gradient of CXCL13, the ligand for CXCR5, toward the B cell follicle. Follicular dendritic cells (FDC) and stromal cells (FSC) secrete this chemokine to attract Th cells. **C.** While naïve Th cells are being activated and migrating toward the T-B cell border zone, B cells are also being activated by APCs within the B cell follicle. Once activated, these cells will also migrate to the border zone where they can interact with Th cells (**D**). **E.** The surface proteins necessary for these cognate interactions include MHC II/TCR, ICOSL/ICOS, CD40/CD40L, and SLAM/SLAM+SAP. SAP is an intracellular protein which signals downstream from the SLAM intracellular tail. SAP signaling is

crucial to maintain prolonged interactions between Th and B cells at this border zone. These interactions will license Th and B cells to take part in the germinal center (GC) reaction. **F.** If cells are not licensed to become part of the GC, the Th cells will down-regulate BCL6, migrate away from the B cell follicle, and differentiate into another Th subset. B cells not able to become GC B cells can also exit the follicle, where they will receive help from other Th cells and become extra-follicular plasma cells, which secrete lower affinity antibodies. **G.** Th and B cells which are properly licensed will up-regulate BCL6 and migrate back into the follicle to form transient structures known as GCs. **H.** B cells will up-regulate additional surface proteins, such as GL7, Fas, and different cytokine receptors. Th cells, now known as TFH cells, will up-regulate PD-1, IL-21R, as well as begin to secrete different cytokines, including their signature cytokine, IL-21, to influence changes in the GC B cells.

in response to viral peptides presented by MHC II molecules on APCs (17, 18). The master transcription factor of Th1 cells, Tbet, works with Signal Transducer and Activator of Transcription (STAT) 4 to clear the infection by secretion of Interferon gamma (IFNγ) (Figure 2). Th2 cells will differentiate in the presence of IL-4 during extracellular parasite infections (18, 19). Up-regulation of their master transcription factor, GATA3, in conjunction with STAT6 activity leads to secretion of signature cytokines, such as IL-4, IL-5, and IL-13 (Figure 2). Th2 cells have also been shown to play a substantial role in allergic responses. Antifungal and antimicrobial responses require T helper type 17 (Th17) differentiation, whose master transcription factor is RAR-related orphan receptor gamma (RORγt) (17, 18, 20) (Figure 2). Th17 cells have also been shown to trigger inflammation through the cytokines they secrete, including IL-17A and IL-22. T helper type 9 (Th9) cells are a relatively recently studied subset which have been shown to clear helminth infections. Th9 cells secrete their namesake cytokine, IL-9 (17, 20) (Figure 2). For a more detailed description of Th subsets and their functions, please see the introduction of Chapter 4.

Th-B cell interactions

Th cell subsets will interact with activated B cells to trigger isotype class switching, via cytokine signaling, and the differentiation of B cells into plasma cells. Plasma cells, whose sole job is to secrete antibodies to aid in clearing the infection, are a final differentiation state for B cells (21). The interactions of Th cells and B cells take place in the T cell zone and are referred to as extra-follicular antibody responses. The antibodies produced are not highly specific for the infecting antigen. However, these responses can arise quite quickly. In this way, extra-follicular antibodies can help to control the

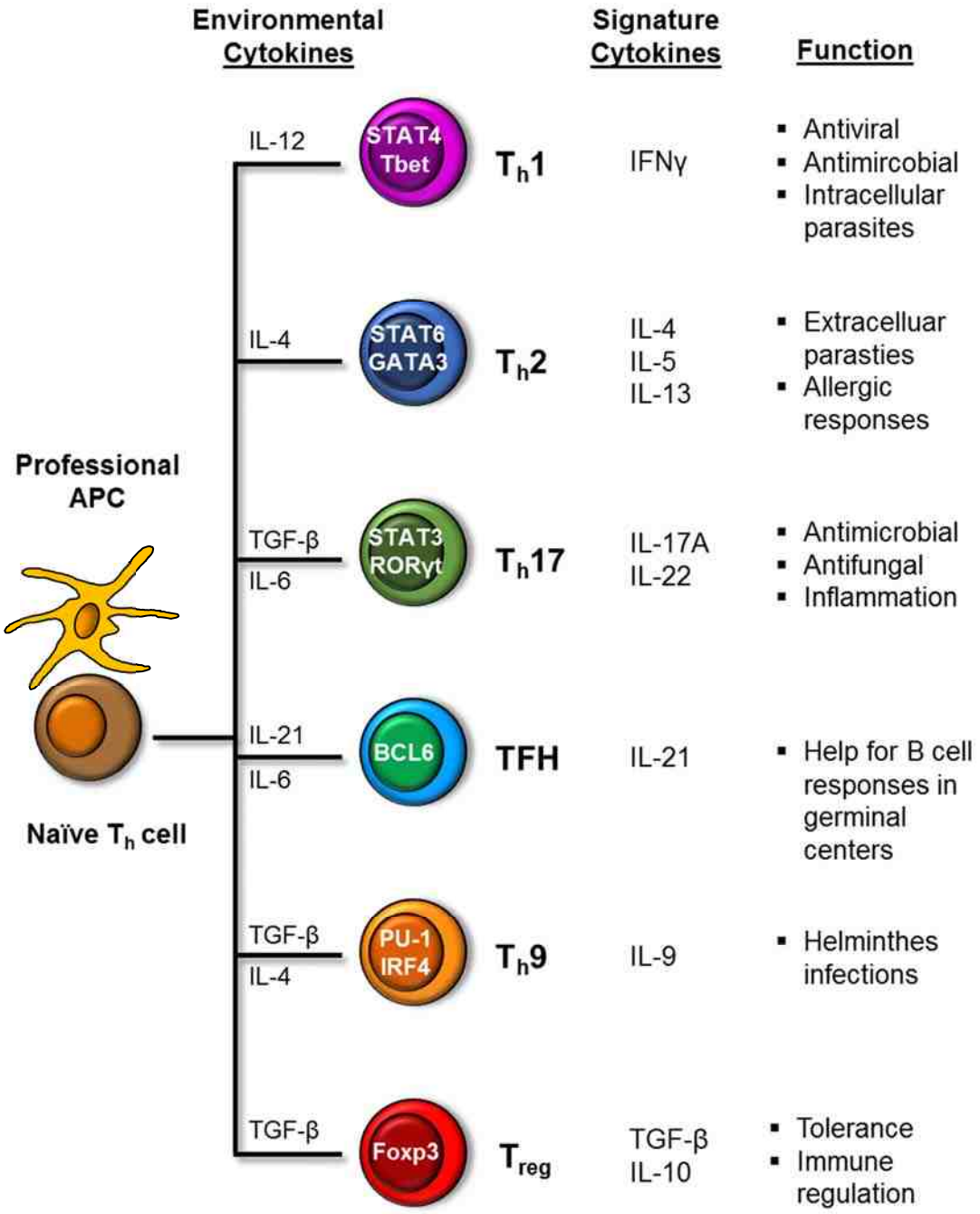

Figure 2. Different CD4⁺ Th cell subsets. Upon activation by a professional APC, naïve Th cells can differentiate into one of several subsets. The type of antigen being presented and cytokine environment will help direct these cells into a specific subset. Each subset is controlled by its own master transcription factor, and in some cases, specific STAT signaling. Additionally, each subset secretes its own signature cytokine. Only follicular Th cells (TFH) are defined by their location, rather than just their master transcription factor and cytokines. Regulatory T cells (Treg) are also unique in that they are responsible for repressing the activity of other Th subsets, rather than helping to activate the immune response.

infection, while more specific antibodies, which take longer to develop, are induced within the GC.

Regulatory Th cells

Regulatory T (Treg) cells play a slightly different role in the immune response. Natural Tregs, or nTreg cells, develop from the thymus and are responsible for maintaining the responses of other T cells via suppressive cytokines (17, 19). This ensures tolerance and limits auto-reactive T cell activity. A second set of Tregs, induced Tregs (iTreg), can differentiate from naïve Th cells in the periphery in the presence of polarizing cytokines. Induced Tregs cells have the same responsibilities as nTregs. Both types of Tregs are under the control of the same master transcription factor, forkhead box P3 (Foxp3) (Figure 2). Induced Treg cells have been shown to be differentiated *in vitro* in the presence of transforming growth factor beta (TGF-β) (17, 18).

Follicular T helper cells

The final subset of Th cells, follicular T helper (TFH) cells, is quite unique in that it performs its functions in a completely different area of the secondary lymphoid organ, compared to other Th subsets. Upon infection, TFH cells will differentiate regardless of what the antigen is or what the surrounding cytokine environment is *in vivo*. During initial activation, a subset of Th cells will up-regulate the transcription factor B cell lymphoma 6 (BCL6), as well as the chemokine receptor C-X-C chemokine receptor type 5 (CXCR5) (Figure 1B) (22, 23). This enables Th cells to follow the C-X-C motif chemokine 13 (CXCL13) chemokine gradient, which is secreted by follicular dendritic cells and stromal cells, toward the B cell follicle. Upon reaching the T/B cell border zone, these activated Th cells will have cognate interactions with activated B cells (Figure 1C-D) (24, 25). In addition to MHC II presentation of antigen to the T cell receptor (TCR), CD40/CD40Ligand (CD40L), ICOS/ICOSL, and SLAM/SLAM interactions are crucial to this process (Figure 1E). In particular the Slam Associated Protein (SAP) is a Th cell intracellular protein which has been shown to be necessary to prolong physical contact between the Th and B cells. These interactions are a licensing process in which some of the Th cells will become TFH cells and some B cells will travel back into the B cell area to have further interactions with TFH cells (23, 26). Without

SAP, this licensing event cannot take place, and TFH cells will not develop. Those Th cells which do not become TFH cells will down-regulate BCL6 and CXCR5, travel away from the border region, and differentiate into another type of Th subset (Figure 1F) (22, 25). Additionally, B cells not chosen to further interact with TFH cells can exit the B cell follicle and take part in extra-follicular interactions with other Th cells, as described above.

Germinal Centers

Germinal center development

The Th cells selected to become TFH cells at the border region will further up-regulate CXCR5 and the master transcription factor for TFH cells, BCL6. At this time, it is unclear what attributes a Th cell must have to be licensed to become a TFH cell, however one study has suggested the affinity of the TCR for the antigen being presented by the border region B cells is the deciding factor (27). TFH cells will then migrate into the B cell follicle and begin to form the structures known as germinal centers (GCs) (Figure 1G). GCs are transient structures which arise within the B cell area and are composed of TFH and B cells (28). It is here that GC B cells will undergo somatic hypermutation, making the antibodies they produce highly specific for the antigen present. Furthermore, isotype class switching takes place within GCs, which is a critical modification process to antibodies and is necessary to ensure efficient clearance of the pathogen.

After being licensed, TFH cells will be the first cell type to form the GC (22, 23). During their migration into the B cell follicle, these cells will up-regulate TFH signature surface markers, such as ICOS, programmed cell death protein 1 (PD-1), SLAM, CD40L, IL-21 receptor (IL-21R), and IL-6 receptor (IL-6R) (Figure 1H). The most commonly used markers to identify TFH cells are CXCR5 and PD-1. One day after TFH cells migrate into the B cell follicle, licensed B cells from the T/B border zone will likewise migrate back into the B cell area and join the TFH cells (22, 23). Like TFH cells, GC B cells highly express BCL6 (29). In addition to up-regulating IL-21R, ICOSL, and SLAM, the signature surface markers for GC B cells, Fas and GL7 become highly up-regulated once these cells have reached the GC (Figure 1H) (28).

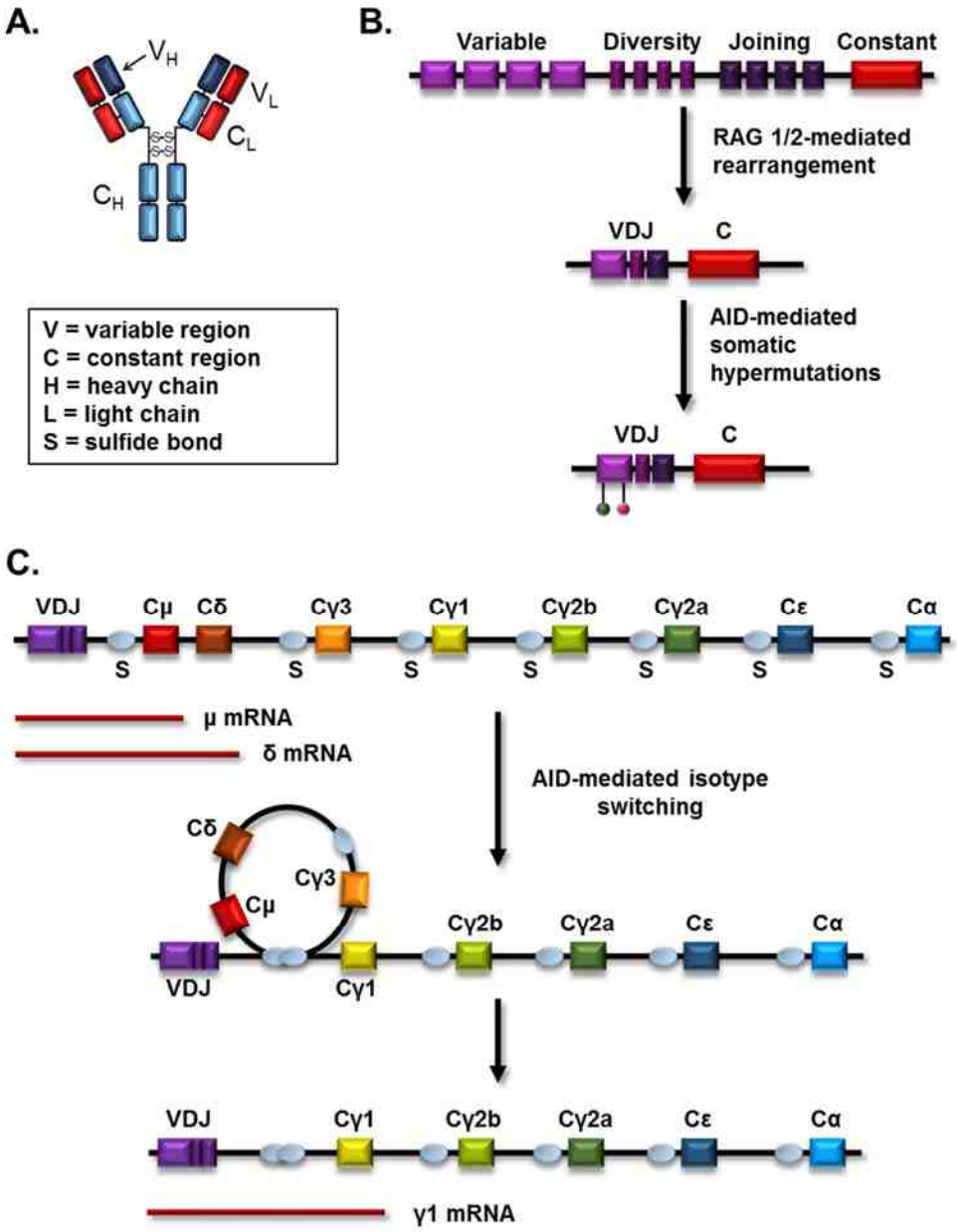

Figure 3. Antibody development. A. Antibodies are comprised of a heavy chain (H) and light chain (L), each with a variable region (V_H and V_L) and constant region (C_H and C_L). These components are all held together with disulfide bonds. The variable region will bind antigens, while the constant region is recognized by immune cells. **B.** The B cell receptor (BCR), which will become antibodies in plasma cells, is first formed by random gene rearrangement and selection of one variable region allele, one diversity allele, and one joining region allele. This is mediated by the recombination activating

gene, or RAG 1 and RAG 2 enzymes. In order to further diversity the BCR, and future antibodies, point mutations are introduced into the selected variable region. This is mediated by activation-induced deaminase, or AID, and is referred to as somatic hypermutation. **C.** The constant region of the BCR can be one of eight isotypes in mice. They are IgM (Cμ), IgD (Cδ), IgG3 (Cγ3), IgG1 (Cγ1), IgG2b (Cγ2b), IgG2a (Cγ2a), IgE (Cε), and IgA (Cα). The genes for the isotypes are arrayed along the Ig heavy chain locus, as shown in the diagram. Naïve B cells will express both IgM and IgD on their surface. Upon activation, cells will undergo isotype class switching, in which AID will recombine out intermediate constant genes, leaving the desired isotype gene directly following the VDJ segments. Once a particular constant gene is removed, the cell can no longer express that isotype.

Somatic hypermutation and isotype class switching of B cells

Within the GC, the antibody genes of B cells will undergo two very important maturation steps that lead to efficient clearance of a pathogen: somatic hypermutation and isotype class switching (28). Somatic hypermutation is the process by which small mutations are introduced into the variable region of the B cell receptor (BCR) (Figure 3 A-B). These genetic changes will alter the affinity the BCR has for a given epitope.

Isotype class switching refers to the process by which B cells, under the instruction of cytokine signals, change their BCR to the form which will best suit the antibody-mediated clearance of a pathogen. Naïve B cells will initially express two BCR immunoglobulin (Ig) isotypes: IgD and IgM (Figure 3C). Upon activation, naïve B cells will lose the ability to express IgD, thus making them only IgM positive (30). From there, B cells can undergo additional switching to other isotypes. These isotypes are IgM, IgG3, IgG1, IgG2b, IgG2a, IgE, and IgA (31). It is important to realize that, while a B cell can undergo additional isotype switching, it can never return to an earlier form, as that part of the gene has been permanently recombined out (30). For example, if an activated B cell mutates from IgM to IgG1, it can never again become IgM or IgG3 positive (Figure 3C). Additional changes will only lead to isotypes further down the Ig heavy chain locus, such as IgG2a or IgE. Cytokine signaling from the environment, and particularly from Th cells, can trigger further isotype class switching (31). Because certain antibodies are required for clearance of particular antigens, this is how Th cells are responsible for clearance of particular pathogens, albeit indirectly. For example, Th1 cells are cited as being responsible for clearance of certain bacteria. In the presence of IFNγ, which is secreted by Th1 cells, B cells will switch to an IgG2a isotype. However, in the presence

of Th2 cells, which secrete IL-4 in the presence of some parasites, B cells will adopt an IgG1 isotype. TFH cells have the unique ability to secrete the signature cytokines of all Th subsets, enabling them to direct GC B cell isotype switching, regardless of what antigen is being presented.

Germinal center structure

The GC itself is organized into two distinct areas: the dark zone and light zone (Figure 4). Within the dark zone, activated GC B cells will undergo clonal expansion and somatic hypermutation, which leads to increased numbers of B cells with enhanced affinity for the antigen (28, 32). TFH cells reside within the light zone where they interact with GC B cells, providing survival signals and secreting cytokines to direct isotype class switching of the BCR. GC B cells will continue to cycle back and forth between the light and dark zones, acquiring further affinity maturation and additional isotype switching, if necessary (28, 33). At some point, the GC B cells will cease cycling and exit the GC, as either memory B cells or plasma cells secreting the high affinity antibody that was developed during the GC process (28). The intracellular steps necessary to halt the cycling process and exit the GC are not well defined at this time. What is known is both memory B cells and plasma cells must down-regulate BCL6 in order to differentiate from a GC B cell state (33). This entire process, of GC formation, light/dark zone cycling, and development of memory B cells and plasma cells, takes several days to weeks. Typically, the peak of the GC response occurs between seven to ten days after infection or immunization. Once the antigen is cleared, the GC will dissipate, with its cells becoming either memory cells or dying by apoptosis (28). There is currently some evidence that TFH cells can become long-lived memory T cells in circulation (34).

Regulating the germinal center response

Regulation of the GC cycling process is crucial, as GC B cells which somatically mutate away from affinity for the presented antigen can be a hindrance to the immune response. If lower affinity B cells were allowed to survive and proliferate, they would take resources away from those cells progressing toward a more specific conformation. Furthermore, if a B cell were to somatically hypermutate and gain affinity for self-antigens, an autoimmune response would rapidly develop (28). For these reasons, the GC response

must be tightly controlled. To do so, the GC has at least two layers of mediation. First, if the somatic hypermutations of the GC B cells leads to lowered affinity for the antigen, these cells will not receive survival signals from TFH cells upon their return to the light zone, leading to apoptosis of the B cell (28). Secondly, a special subset of Th cells exists to control the TFH reaction. Follicular regulatory T (TFR) cells are a recently described subset which possess traits of both TFH and Treg cells (35, 36). These Th cells, like TFH cells, highly express BCL6 and CXCR5, and can migrate from the T cell zone into the GC. Their job is to regulate TFH responses, by suppressing auto-reactive T cells via the same methods as Treg cells. While TFR cells express BCL6, they also express the master transcription factor of Treg cells, Foxp3, at high levels. At this time,

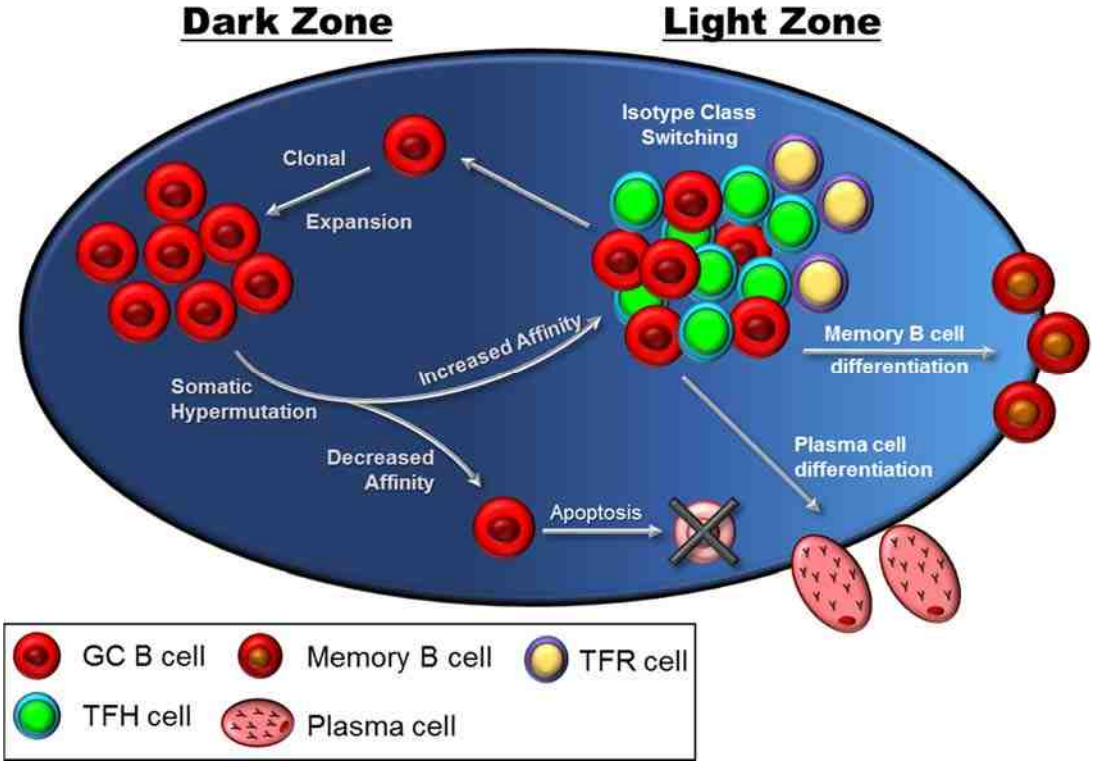

Figure 4. Germinal center cycling and regulation. The GC is comprised of a dark zone and a light zone. Within the dark zone, B cells will undergo clonal expansion as well as somatic hypermutation. Cells acquiring increased affinity via the somatic hypermutation will continue to receive help and survival signals from TFH cells. Further isotype class switching of the BCR is also done in the light zone, triggered by cytokines secreted from TFH cells. Those cells which decrease their affinity due to somatic hypermutation will not receive those signals, and thus are removed from the GC via apoptosis. This cycling from light to dark zone will continue until B cells down-regulate

BCL6 and exit the GC to become either memory B cells or plasma cells secreting high affinity antibodies. TFR are responsible for regulating TFH cells.
research into this subset suggests they are Treg cells which acquire the ability to express BCL6 and migrate into the GC (35, 36).

Goals of Research

While the role BCL6 plays in B cells, particularly GC B cells, has been extensively studied for approximately two decades, it is only in the last few years that researchers have begun to appreciate the role of BCL6 in Th cells. Since the first definitive papers describing TFH cells were published (37-40), many groups around the world have investigated these cells, what they do, where they migrate to, and how they are controlled. However, many questions remain unexplored. What are the kinetics of GC and TFH development over time? How do these cells develop? Does BCL6 play a role in other Th cells? What type of vaccine can enhance GC outcomes? This thesis seeks to address these questions and provide insights into how BCL6 controls gene expression, both in TFH and non-TFH Th cells.

CHAPTER 2 – DEVELOPMENT OF A NEW BCL6 CONDITIONAL KNOCKOUT MOUSE MODEL

INTRODUCTION

The transcriptional repressor BCL6 is made up of three major domains (Figure 5). First, the N-terminal Poz (Pox virus and zinc finger) domain binds specific corepressor proteins, including SMRT (silencing mediator of retinoid and thyroid receptor), N-CoR (nuclear receptor co-repressor), and BCoR (BCL-6 interacting corepressor) (41-44). These corepressors facilitate BCL6 repression, in part, by recruiting histone deacetylases (HDAC) to chromatin (45, 46). The BCL6 Poz domain can also directly bind HDAC1 (47). The central region of BCL6, known as repression domain 2 (RD 2), has been shown to directly bind MTA3, which is a subunit of the nucleosome remodeling and deacetylase (NuRD) complex (48, 49), as well as SIN3A, which, in combination with SMRT and HDACs, is part of a deacetylation complex (44, 47). Association with these corepressors and complexes allows BCL6 to effectively repress gene expression through chromatin remodeling. The RD 2 region also has sites for phosphorylation and acetylation, thus making this region responsible, in part, for turnover of BCL6 (44, 50). Finally, the C-terminal portion of BCL6 is composed of a zinc finger region, with six zinc fingers (51-53). Binding of the zinc fingers to DNA is sequence-specific and mediates transcriptional repression of BCL6 target genes (54-58).

Currently, there is no data demonstrating that BCL6 can activate genes directly. Therefore, the prevailing theory of how BCL6 can activate genes, particularly in the case of TFH and GC B cells, is by repressing other transcriptional repressors or by binding these suppressors and sequestering them away from their targets (46, 50). The exact mechanisms by which this is accomplished are not known, however this is one goal of my work. In order to better understand which genes BCL6 represses in a cell, germline knockout (GL KO) models have been employed to determine which genes were up-regulated in the absence of BCL6. Until now, these GL KO mice were the only models available to explore how BCL6 can up-regulate gene expression in primary T cells.

The problem with the BCL6 GL KO approach is the sickly nature of mice lacking both

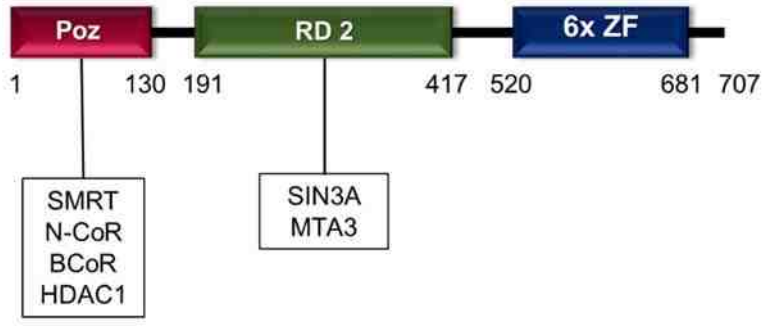

Figure 5. BCL6 protein. BCL6 contains a Poz domain which can bind protein, such as corepressors including SMRT, N-CoR, and BCoR, as well as directly bind HDAC1. The middle region is referred to as repression domain 2 (RD 2). It can also bind repression complexes via SIN3A and MTA3. The C-terminus contains six zinc fingers (ZF) and can bind DNA.

BCL6 alleles in all cell types (29, 59). To begin with, GL KO mice are too sick to breed (60), and, therefore, heterozygous mice must be used for mating purposes. Based on Mendelian probabilities, one quarter of the offspring of these mice should be homozygous for the deletion, however, in our hands, usually less than twenty five percent of mice born are KOs. Whether the mice homozygous for deletion die *in utero* or do not survive past birth remains unknown. In either case, mice lacking both alleles are difficult to acquire, and if they do survive, they are extremely sick, suffer from growth retardation, and rarely survive past eight weeks (29, 59). Additionally, they suffer from myocarditis and pulmonary vasculitis, which is characterized by an influx of eosinophils (29, 59). Furthermore, this type of inflammation has been described as Th2-mediated, as the Th cells from these mice have been shown to produce large amounts of Th2 cytokines (29, 59). Therefore, it is not practical to use these mice as *in vivo* models of BCL6 deletion.

To overcome these obstacles, most researchers have utilized different cell transfer models to investigate the role of BCL6 in Th cells. Transfer of mature, but naïve, Th cells into healthy recipient mice is a widely used and accepted method for studying loss of BCL6 in T cells, however, this strategy brings with it its own set of complications. For instance, it is highly likely the cytokine environment, resulting from Th2 inflammation, in GL KO mice has already conditioned the transferred cells to skew toward a Th2 phenotype (59, 61). Bone marrow transfers from GL KO mice to healthy irradiated recipients also run the risk of cells being preconditioned by the rampant inflammatory

disease seen in the GL KO mice and, furthermore, the bone marrow itself still contains the hyper-inflammatory myeloid cells which will produce the skewing cytokines in recipient mice. Additionally, these bone marrow chimera models are costly and time consuming, thus limiting their practicality. Therefore, it was necessary to develop a conditional KO (cKO) mouse model, in which BCL6 can be functionally deleted in specific subsets of cells, rather than globally, to investigate the role of BCL6 in different cell subsets.

MATERIALS AND METHODS

Mice and immunization

$BCL6^{Neofl/Neofl}$ mice on a mixed C57BL/6-129Sv background were generated at the Indiana University School of Medicine Transgenic and Knockout facility. LoxP sites were inserted into the BCL6 gene locus, flanking exons 7-9 encoding the zinc finger domain of BCL6, using standard molecular cloning and embryonic stem cell techniques. Cre^{Ella} mice, obtained from Jackson Labs, were used to remove the floxed Neomycin gene from the germline of knock-in mice. The following primer pairs were used to genotype different locations and versions of the mutant BCL6 allele as well as CD4 Cre-recombinase:

Neo-floxed:

5' loxP forward (5' –TGAAGACGTGAAATCTAGATAGGC– 3')
5' loxP reverse (5' –ACCCATAGAAACACACTATACATC– 3')
3' loxP + Neo gene forward (5' –GAGGCCACTTGTGTAGCGCCAAGT– 3')
3' loxP + Neo gene reverse (5' –CTACTCCTAAGCTTCCTTTAACAC– 3')

Floxed:

5' loxP forward (5' –TGAAGACGTGAAATCTAGATAGGC– 3')
5' loxP reverse (5' –ACCCATAGAAACACACTATACATC– 3')
3' loxP forward (5' –TCACCA ATCCCAGGTCTCAGTGTG– 3')
3' loxP reverse (5' –CTTTGTCATATTTCTCTGGTTGCT– 3')

ΔZF:

Deletion forward (5' –TGAAGACGTGAAATCTAGATAGGC– 3')

Deletion reverse (5' –CTACTCCTAAGCTTCCTTTAACAC– 3')

Also ensure mice are negative for "Floxed" genotyping bands

Cre-CD4

Forward (5' –ATCGCCATCTTCCAGCAGGCGCACT– 3')

Reverse (5' –ATTTCCGTCTCTGGTGTAGCTGAT– 3')

Mice were immunized i.p. with 1 x 10^9 sheep red blood cells (SRBC; Rockland Immunochemicals Inc., Gilbertsville, PA) in PBS.

Flow cytometry

Total spleen or thymus cells were incubated with anti-mouse CD16/CD32 (Fcγ receptor) for 20 minutes, followed by surface staining for the indicated markers. A fixable viability dye (eFluor 780, eBioscience) was used for all samples; manufacturer's directions were followed. The following antibodies were used for staining GC B cells: α-mCD19 Alexa Fluor 700, clone eBio1D3 (eBioscience); α-mB220 PE, clone RA3-682 (BD Bioscience); α-mFas Biotin, cat. # 554256 (BD Bioscience); Streptavidin-PECy7 (Biolegend); α-mGL7 APC, clone GL7 (BD Bioscience); PNA FITC (Vector Laboratories Inc.). The following antibodies were used to stain TFH cells: α-mCD3 Alexa Fluor 700, clone 500A2 (BD Bioscience); α-mCD4 PECy7, clone RM4-5 (BD Bioscience); α-mCXCR5 PerCP-efluor 710, clone SPRCL5 (eBioscience); α-mPD-1 APC, clone 29F.1A12 (Biolegend); α-mICOS FITC, clone C398.4A (eBioscience). Intracellular BCL6 was stained with α-h/mBCL6 V450, clone K112-9 (BD Horizon) or α-mBCL6 PE, clone mGI191E (eBioscience). Samples were run on a BD LSR II flow cytometer using FACSDiva software. Data was analyzed using FlowJo software.

***In vitro* stimulation**

Total $CD4^+$ T cells or naïve $CD4^+$ T cells were isolated via magnetic bead separation (Miltenyi Biotec). Effector memory cells were isolated via FACS. Cells were stimulated with plate-bound anti-CD3 (5 μg/ml) and anti-CD28 (10 μg/ml) antibodies (BD

Biosciences) at $1x10^6$ cells per mL. Th0 media conditions contain no cytokines or blocking antibodies, Th neutral (ThN) conditions contain anti-IFNγ and anti-IL-4 (10 μg/mL) (BD Biosciences) and TFH conditions contain IL-6 and IL-21 (10 ng/ml each (R&D Systems), plus anti-IFNγ, -IL-4 (10 μg/mL) and -TGF-β antibodies (20 μg/mL).

ELISA

Cytokines and antibody titers were measured via ELISA. Kits from BD Biosciences were used to measure cytokines, except IL-17, in which purified and biotin-labeled antibodies were used (BD Biosciences). Unless otherwise stated, both *in vitro* and *ex vivo* cells were isolated, as described above, and cultured for 5 days; IL-2 was used in all culture conditions when expanding cells. After 5 days, cells were restimulated with anti-CD3 antibody (5 μg/mL) for 18 – 24 hours, at which time supernatants were collected and analyzed.

Histology

Tissues were fixed in formalin and embedded in paraffin. Standard histological sections were cut and stained with hematoxylin and eosin. Samples were scored blindly on a 1-5 scale assessment of leukocytic infiltration, with 5 being the most inflamed. 0 = no sign of inflammation, 1 = hint of inflammatory cells, 2 = significant but small or rare patches of inflammatory cells, 3 = significant foci of inflammatory cells, 4= large foci of inflammatory cells taking up more than 50% of tissue, 5 = greater than 80% of tissue is filled with inflammatory cells.

Gene expression analysis

Total RNA was prepared using a kit (Qiagen) after lysis of the cells via Trizol (Life Technologies); cDNA was prepared with the Transcriptor First Strand cDNA synthesis kit (Roche). Quantitative PCR (qPCR) reactions were run by assaying each sample in triplicates using the Fast Start Universal SYBR Green Mix (Roche Applied Science) with custom primers or specific Taqman assays (ABI). Assays were run with a Stratagene Mx3000P Real-Time QPCR machine. Levels of mRNA expression were normalized to

beta-tubulin mRNA levels, and differences between samples analyzed using the ΔΔCT method. Primers for SYBR Green assays were previously described (14, 19).

Statistical Analysis

Statistical analysis was done using ANOVA with Tukey post hoc analysis on SPSS Statistics 20 software.

RESULTS

Generation of BCL6$^{Neofl/Neofl}$ mice

To generate a new cKO mouse model for BCL6, a targeting construct containing loxP sites and a neomycin (Neo) resistance gene within the zinc finger region was introduced into embryonic stem cells (Figure 6 A-B). Mice initially generated from these embryonic stem cells, henceforth referred to as BCL6-Neo-floxed (BCL6^{Neofl}), differ from GL KO mice in that they have the entire zinc finger region intact, but flanked by loxP sites ("floxed") with the addition of a Neo gene cassette 3' of exon 9, whereas the original GL KO mice have only exon 9 and part of exon 8 deleted, leading to only partial loss of the zinc finger domain (Figure 6 C). After mating heterozygous floxed mice (BCL6$^{+/Neofl}$), homozygous floxed mice were generated (BCL6$^{Neofl/Neofl}$).

When heterozygous parents were mated, BCL6$^{Neofl/Neofl}$ mice were born at equivalent rates to GL KO mice (−/−), and both mice were born at rates lower than the expected Mendelian frequency of twenty five percent (Figure 7 A). The percent of those homozygous mice that survived past weaning to at least eight weeks of age was higher for BCL6$^{Neofl/Neofl}$ mice than BCL6$^{-/-}$ mice, with approximately eighty six percent of Neofl/Neofl mice and sixty five percent of GL KO mice surviving (Figure 7 B). When the survival rates are taken into consideration along with birth rates, the probability of a GL KO mouse being born and surviving to eight weeks significantly drops below twenty five percent, while BCL6$^{Neofl/Neofl}$ mice are reduced to an eighteen percent chance (Figure 7 C). Phenotypically, BCL6$^{Neofl/Neofl}$ mice also appeared smaller and more hunched than littermates, similar to what is seen with GL KO mice.

A. Wild Type allele (+)

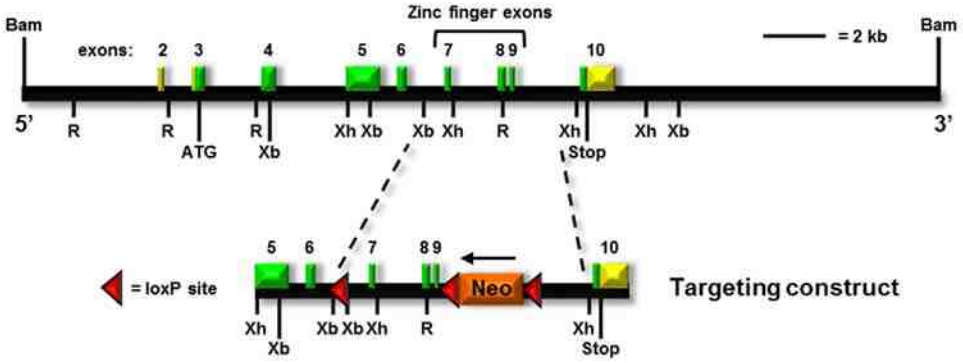

B. Floxed allele with Neo gene (Neofl)

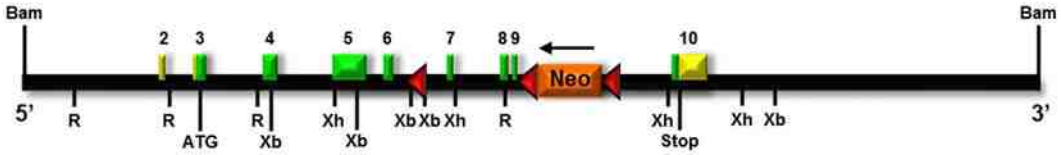

C. Germline Knockout (–)

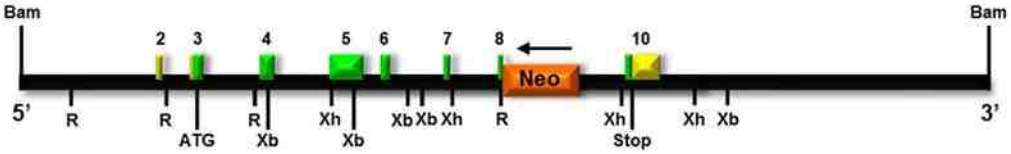

Figure 6. Germline and targeted BCL6. A. Schematic of the wild type BCL6 allele ($BCL6^{+}$) and a targeting construct containing BCL6 exons 7 through 9 and a Neomycin resistance gene (Neo) which was inserted into the wild type allele. **B.** The new BCL6-floxed allele containing a Neo gene ($BCL6^{Neofl}$). **C.** A schematic of BCL6 in the original GL KO mouse model ($BCL6^{-}$) in which part of exon 8 and all of exon 9 were deleted. The zinc finger region encoded by exon 7 is still fully intact.

Functional testing of $BCL6^{Neofl/Neofl}$ mice

To verify the functionality of the BCL6 gene before mating to a Cre recombinase mouse, $BCL6^{Neofl/Neofl}$ mice were immunized with sheep red blood cells (SRBC) and sacrificed ten days later. SRBC were used as an immunization because of their ability to induce

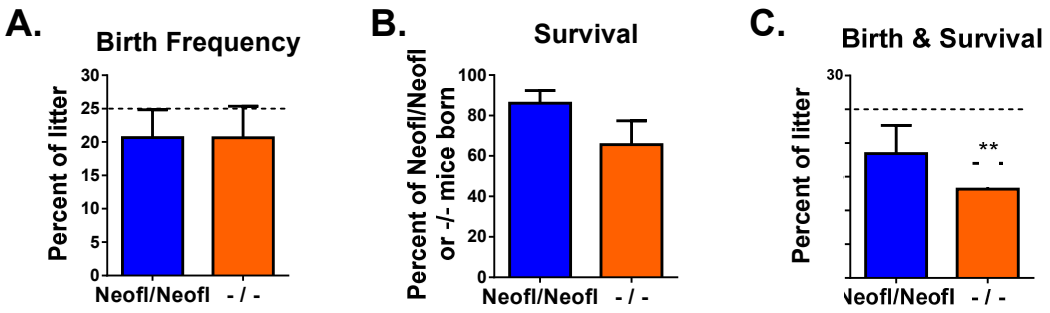

Figure 7. Frequencies of BCL6$^{Neofl/Neofl}$ mice compared to BCL6$^{-/-}$ mice. The frequencies of homozygous BCL6$^{Neofl/Neofl}$ and BCL6$^{-/-}$ mice born to heterozygous parents, and their deaths, were tracked over one year. **A.** The percent of BCL6$^{Neofl/Neofl}$ and BCL6$^{-/-}$ mice born in all litters which survived to weaning (3 weeks) when genotyping was done. **B.** Percentage of homozygous mice born that survived past 8 weeks. **C.** Percent of homozygous mice born and surviving past eight weeks in each litter. Mean ± SE; n = 15 (Neofl) and 30 (−/−) litters. **p < 0.01 by one sample *t* test (theoretical mean of 25%).

strong GC responses. Surprisingly, BCL6$^{Neofl/Neofl}$ mice had significantly reduced GC B cells and TFH cells as compared to wild type (WT) (BCL6$^{+/+}$) and heterozygous (BCL6$^{+/Neofl}$) mice (Figure 8 A-C). Furthermore, BCL6$^{Neofl/Neofl}$ mice had similar levels of GC cells to GL KO (BCL6$^{-/-}$) and unimmunized WT mice. Flow cytometry analysis of BCL6 in immunized mice showed a step-wise decrease in BCL6 protein expression as WT alleles were replaced with Neo-floxed alleles (Figure 9 A). These data would suggest that a functional transcript of BCL6 is not being produced with the presence of the neomycin resistance gene in the targeting construct. RNA analysis of *ex vivo* Th cells from immunized mice revealed a steep drop in full length transcript being produced in mice containing the targeting construct (Figure 9 B). In fact, RNA levels were comparable to that of cells from GL KO mice. This would suggest BCL6$^{Neofl/Neofl}$ mice may actually be more phenotypically similar to BCL6$^{-/-}$ mice than to WT mice. Since GL KO mice are much smaller than WT mice, the weights of BCL6$^{Neofl/Neofl}$ mice were analyzed and found to more be more similar to the sizes of BCL6$^{-/-}$ mice than BCL6$^{+/+}$ mice (Figure 9 C). However, the total CD4^{+} T cell and B cell populations in the spleen were found to be closer to the levels seen in WT mice (Figure 9 D).

To further investigate the defect in BCL6 transcription, naïve Th cells were isolated from unimmunized mice. When cells from the spleen and thymus were analyzed directly *ex vivo*, without *in vitro* stimulation, levels of BCL6 exon 8 transcript increased with the

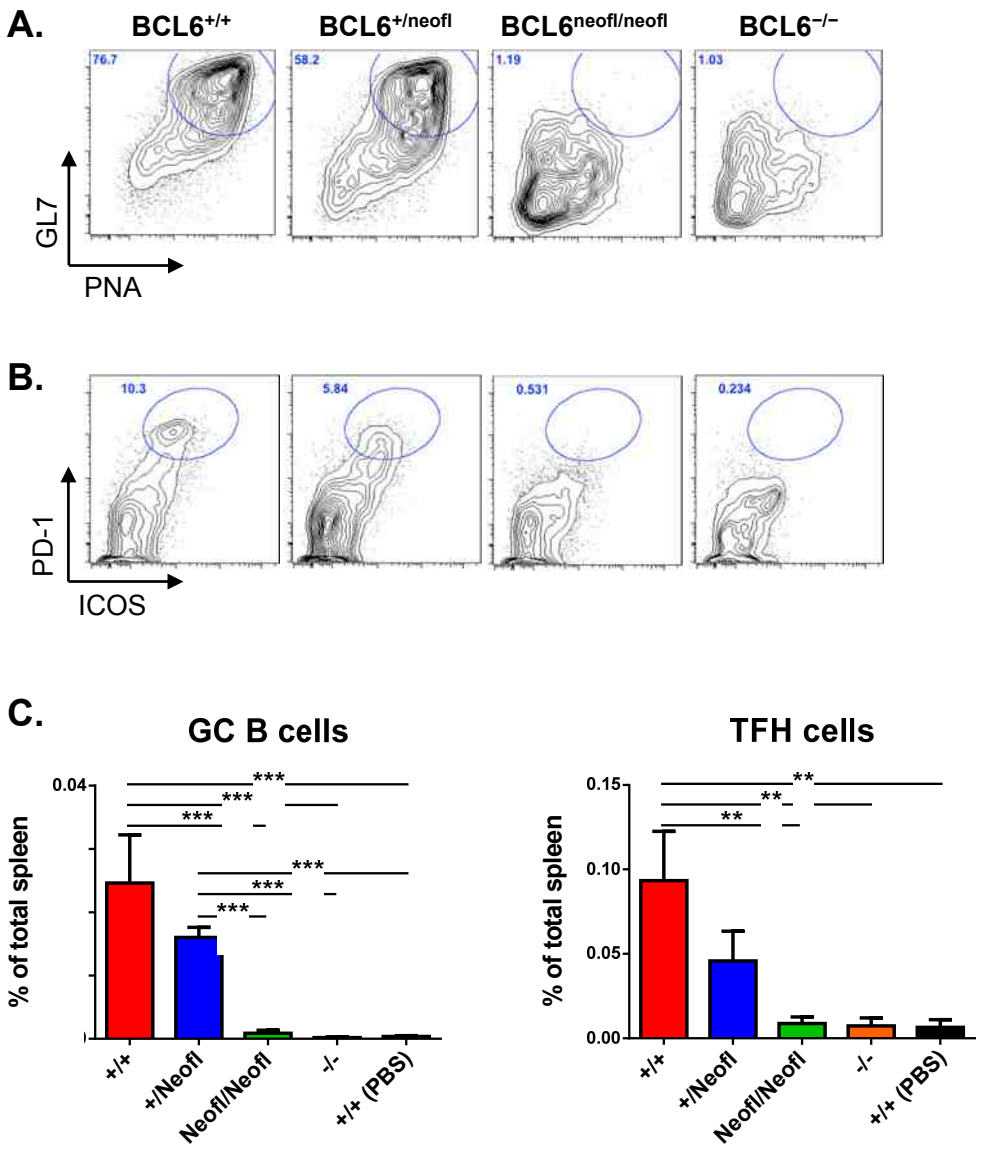

Figure 8. Loss of GCs in BCL6$^{Neofl/Neofl}$ mice. Wild type (BCL6$^{+/+}$), heterozygous (BCL6$^{+/Neofl}$), Neo-floxed (BCL6$^{Neofl/Neofl}$), and GL KO (BCL6$^{-/-}$) mice were immunized i.p. with SRBC and sacrificed on day 10. BCL6$^{+/+}$ mice injected with only PBS were used as negative controls. Spleen cells were analyzed via flow cytometry for GCs. **A.** Representative flow plots of GC B cell populations; gated on B220^{+} Fas^{+}. **B.** Representative flow plots of TFH cell populations; gated on CD4^{+} CXCR5^{+}. **C.** Graphs of GC B cells and TFH cells shown in **A-B**. Mean ± SE; n = 3 – 6. **p < 0.01, ***p < 0.001 by ANOVA; Tukey post hoc.

introduction of the floxed allele (Figure 10 A). Activation with anti-CD3 and anti-CD28 antibodies in Th0 culture conditions also revealed an increase in BCL6 transcript levels (Figure 10 B). Conversely, culturing cells in conditions which skew them toward a

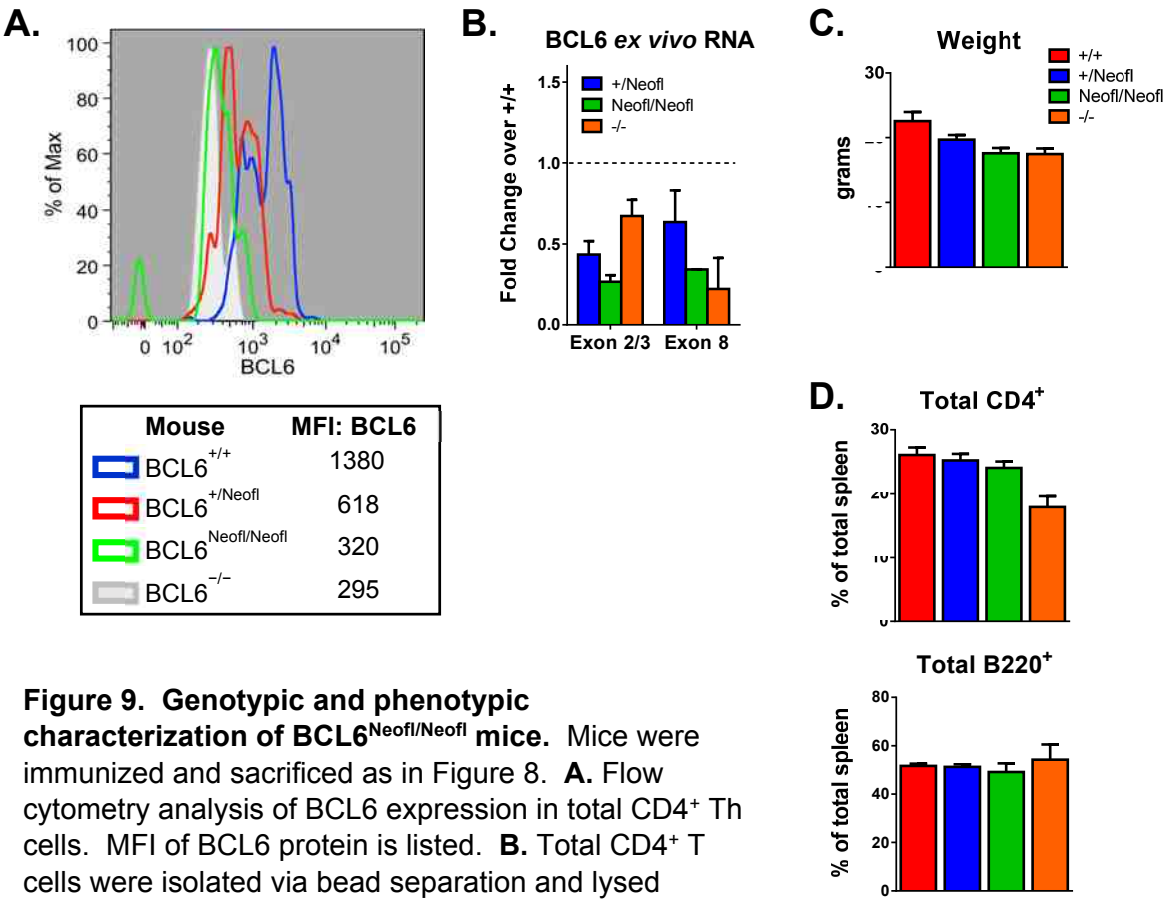

Figure 9. Genotypic and phenotypic characterization of BCL6$^{Neofl/Neofl}$ mice. Mice were immunized and sacrificed as in Figure 8. **A.** Flow cytometry analysis of BCL6 expression in total CD4$^+$ Th cells. MFI of BCL6 protein is listed. **B.** Total CD4$^+$ T cells were isolated via bead separation and lysed directly *ex vivo* for RNA analysis of BCL6 expression. Samples normalized to BCL6$^{+/+}$ levels (dotted line at 1.0). **C.** Weight of mice on day 10 after immunization. Mean ± SE. **D.** CD4$^+$ T cells and total B cells as percentage of total spleen. T cells gated on CD3$^+$ CD4$^+$; B cells gated on B220$^+$. Mean ± SE; n = 3 – 6.

TFH phenotype led to a drop in transcript levels compared to WT mice (Figure 10 C).

Any effects of decreased BCL6 transcription on cytokine secretion, after immunization, were abrogated in BCL6$^{Neofl/Neofl}$ mice. Only IL-17A and IFNγ appeared to be slightly increased in the BCL6$^{Neofl/Neofl}$ mice compared to BCL6$^{+/+}$ mice (Figure 11). Naïve Th cells isolated from uninfected mice and activated for five days in Th0 conditions showed a similar result with IL-17A being increased over BCL6$^{+/+}$ mice (Figure 12). After five days, only BCL6$^{-/-}$ mice showed a substantially different cytokine profile from other mice (Figure 12). This lack of inflammatory cytokines in BCL6$^{Neofl/Neofl}$ mice likely contributed to the absence of disease, as these mice had reduced lung vasculitis compared to GL KO mice and only a few BCL6$^{Neofl/Neofl}$ mice had marginally increased myocarditis

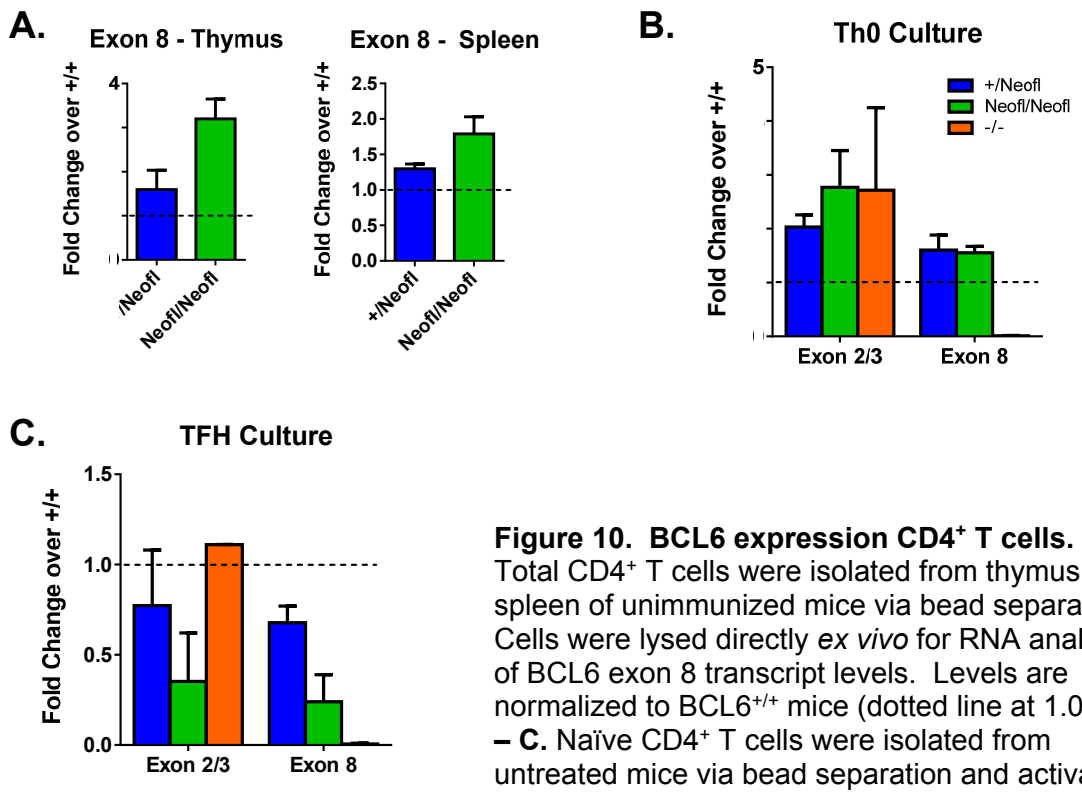

Figure 10. BCL6 expression CD4⁺ T cells. A. Total CD4⁺ T cells were isolated from thymus and spleen of unimmunized mice via bead separation. Cells were lysed directly *ex vivo* for RNA analysis of BCL6 exon 8 transcript levels. Levels are normalized to $BCL6^{+/+}$ mice (dotted line at 1.0). **B – C.** Naïve CD4⁺ T cells were isolated from untreated mice via bead separation and activated with anti-CD3 and anti-CD28 antibodies for 4 days in (**B**) Th0 or (**C**) TFH culture conditions. On day 4, cells were harvested and restimulated with anti-CD3 and anti-CD28 for 5 hours in Th0 media, after which they were lysed for RNA analysis. Transcript levels of different BCL6 exons were measured via qPCR. Levels are normalized to $BCL6^{+/+}$ levels (dotted line at 1.0). Mean ± SE.

compared to $BCL6^{+/Neofl}$ mice (Figure 13).

Because the transcriptional and functional changes seen in $BCL6^{Neofl/Neofl}$ mice appeared to be more of a knock-down rather than full knockout phenotype, we decided to further investigate the effects of having decreased levels of BCL6 expression, compared to WT and GL KO mice. Total Th cells were isolated from mice immunized with SRBC and sacrificed ten days later. After culturing for five days *in vitro* under Th0 conditions, cells were briefly restimulated with antibodies before being lysed for RNA analysis. Because cytokine data suggested these *ex vivo* cells could be skewing toward a Th17 phenotype (Figure 11-12), cells were analyzed for transcript levels of *rorc*, the gene which encodes the master transcription factor for Th17 cells. Interestingly, $BCL6^{Neofl/Neofl}$ Th cells showed a large increase in *rorc* expression over WT mice (Figure 14 A). Furthermore, *prdm1*, the gene coding for Blimp1, was found to only be marginally increased with loss of functional BCL6 transcript (Figure 14 A). This is particularly interesting because

previous work by others has demonstrated the reciprocal expression of Blimp1 and BCL6 (62). To further investigate the effects of graded BCL6 expression on Th17 cell differentiation, naïve $CD4^+$ T cells were isolated, activated with antibodies, and cultured for five days in either Th0 or TFH-skewing culture conditions. After a brief restimulation, cells were lysed and RNA expression measured. Under the non-skewing conditions of Th0 culture, *rorc* levels were substantially increased over WT in all mouse types, whereas under TFH conditions, levels remained comparable to $BCL6^{+/+}$ mice (Figure 14 B). Once again, under both culture conditions, *prdm1* did not increase with loss of BCL6 (Figure 14 B). This lack of increased *prdm1* expression, particularly in GL KO mice, is again interesting, considering the established dogma.

Analysis of $BCL6^{Neofl/Neofl}$ mice has thus demonstrated a functional defect in full length BCL6 expression. Not only have we found decreased full transcript of BCL6 being generated in $BCL6^{Neofl/Neofl}$ mice (Figure 9B), but the ability for GC B cells and TFH cells to develop in these mice is severely and significantly reduced as well (Figure 8).

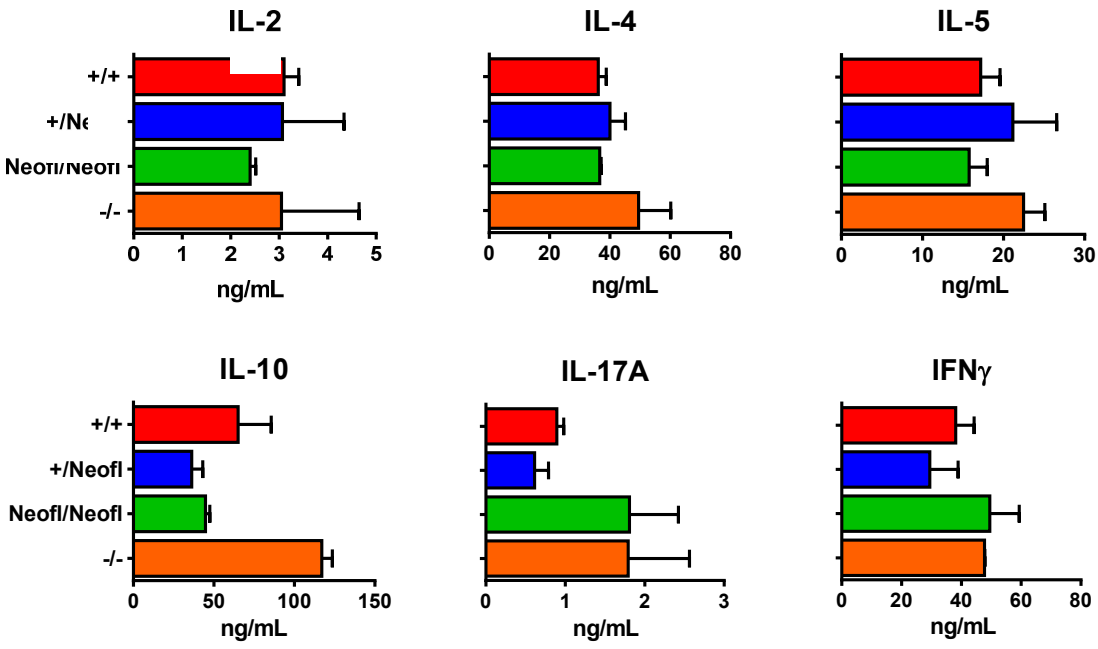

Figure 11. Cytokine production of $CD4^+$ T cells from immunized mice. Mice were immunized as in Figure 8. Total $CD4^+$ T cells were isolated via bead separation and stimulated for 5 days with anti-CD3 and anti-CD28 antibodies in Th0 media. On day 5, cells were harvested and restimulated overnight with anti-CD3 antibody. Supernatants were analyzed for cytokines via ELISA. Mean ± SE; n = 2 – 3.

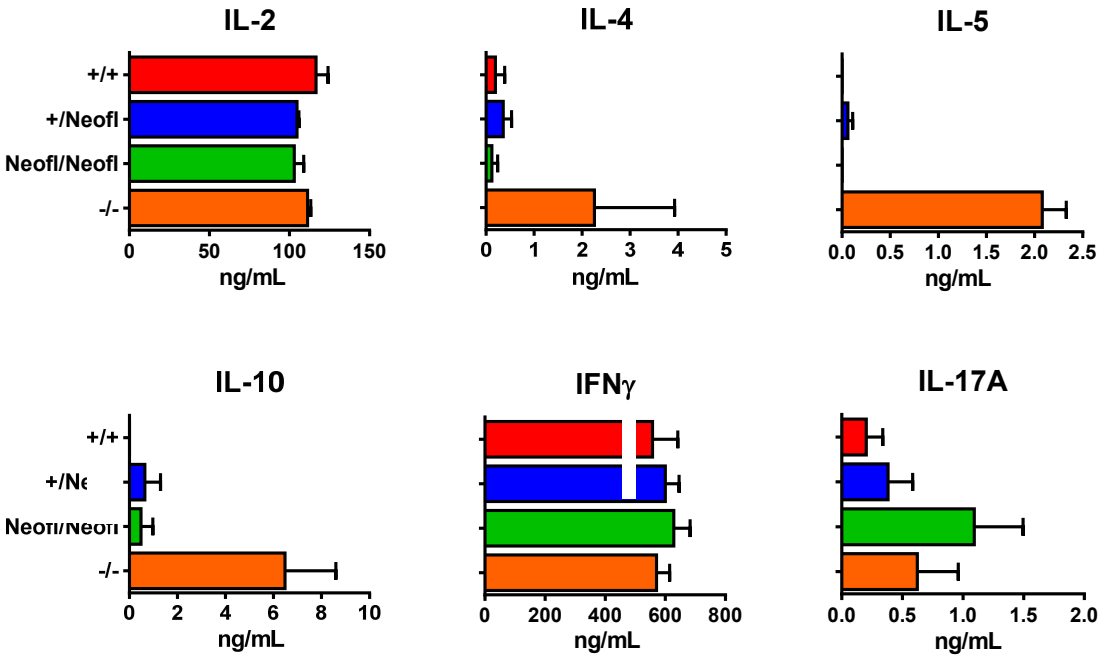

Figure 12. Cytokine production of cultured naïve CD4$^+$ T cells. Naïve CD4$^+$ T cells were isolated via bead separation from unimmunized mice. Cells were activated with anti-CD3 and anti-CD28 antibodies in Th0 culture conditions for 5 days. Cells were then restimulated overnight with anti-CD3 antibody. Supernatants were analyzed for cytokines via ELISA. Mean ± SE; n = 2 – 3.

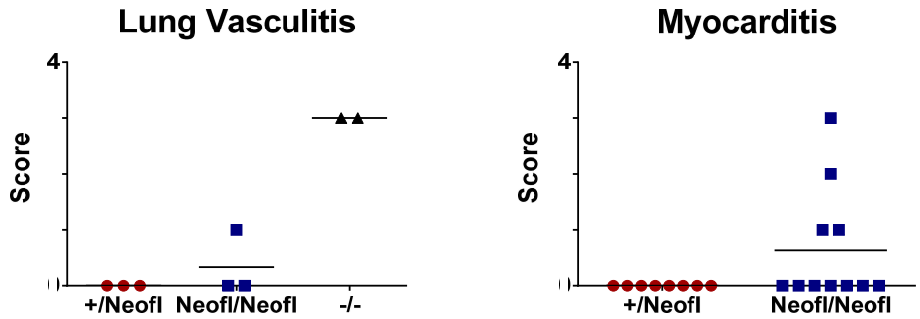

Figure 13. Histology of lung and heart from BCL6^{Neofl} and GL KO mice. Mice were immunized as in Figure 8, and heart and lungs were taken for histological analysis. Samples were scored blindly. Individual scores are shown with the mean.

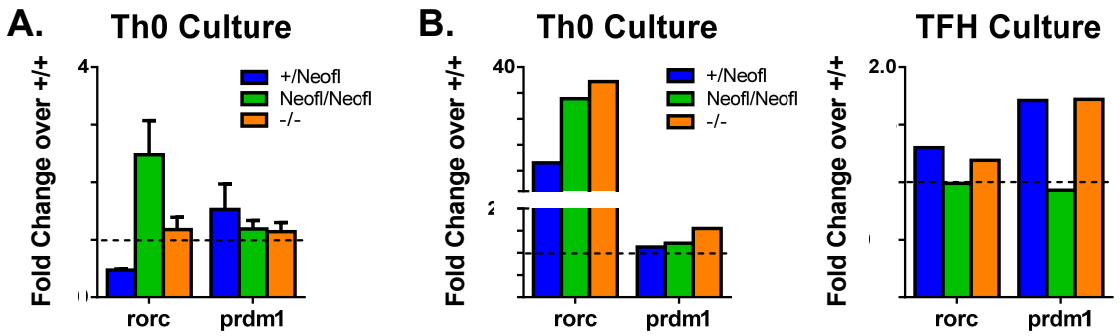

Figure 14. Changes in *rorc* and *prdm1* expression under different cytokine environments. A. Mice were immunized as in Figure 8. Total $CD4^+$ T cells were isolated via bead separation, activated with anti-CD3 and anti-CD28 antibodies, and cultured for 5 days in Th0 culture conditions. On day 5, cells were restimulated with anti-CD3 antibody for 5 hours, then lysed for RNA analysis. Transcript levels of *rorc* and *prdm1* are normalized to $BCL6^{+/+}$ levels (dotted line at 1). Mean ± SE. **B.** Naïve $CD4^+$ T cells were isolated and cultured as in Figure 10 **B-C**. Transcript levels are normalized to $BCL6^{+/+}$ levels (dotted line at 1.0).

Therefore, without modifications to the inserted targeting construct, these mice could not be used for further development as a cKO model.

Removal of the neomycin resistance gene

To rectify the defective BCL6 transcription in $BCL6^{Neofl/Neofl}$ mice, it was determined the neomycin resistance gene needed to be removed. To do so, Cre^{EIIa} mice were obtained from the Jackson Laboratory and mated to $BCL6^{Neofl/Neofl}$ mice. Cre^{EIIa} mice express a Cre recombinase under the control of the adenovirus EIIa promoter, which is active early in mouse development. Therefore, the EIIa-Cre recombinase will target and delete genomic DNA between two loxP sites in GL lineage cells. Since our BCL6 Neo-floxed construct contains three loxP sites, a total of three different deletions could result. Either the zinc fingers (exons 7 – 9), the Neo gene, or both could be removed (Figure 6 B). Two new mouse alleles resulted from this deletion process. First, a new GL KO mouse was generated by deleting the entire zinc finger region and neomycin resistance gene, henceforth referred to as $BCL6^{\Delta ZF/\Delta ZF}$ mice (Figure 15 A). Secondly, and more importantly, the neomycin resistance gene was successfully deleted, leaving the zinc finger region intact, flanked by two loxP sites, creating a floxed-BCL6 ($BCL6^{fl/fl}$) mouse (Figure 15 B).

A. New GL KO allele ($BCL6^{\Delta ZF}$)

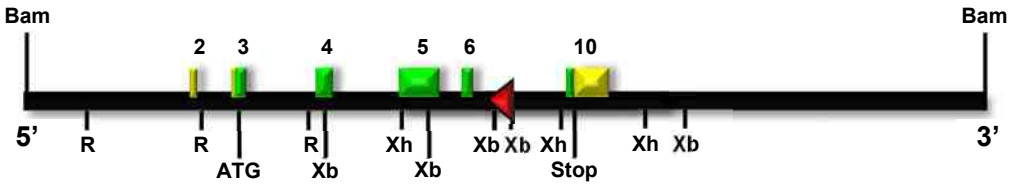

B. Floxed allele (fl)

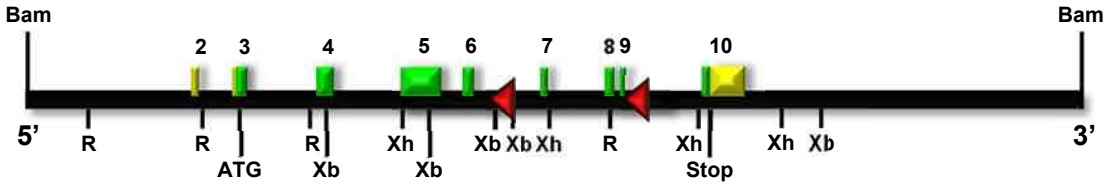

Figure 15. Alleles of new BCL6 mutant mice. A. Schematic of new GL KO mouse ($BCL6^{\Delta ZF}$) developed by mating to a Cre^{EIIa} mouse, which resulted in deletion of the entire zinc finger region and neomycin resistance gene. **B.** Schematic of BCL6 allele in new BCL6-floxed mouse ($BCL6^{fl}$). The neomycin resistance gene was removed by mating to a Cre^{EIIa} mouse, which constitutively expresses Cre recombines and will remove any segment flanked by two loxP sites.

New germline knockout mice – $BCL6^{\Delta ZF/\Delta ZF}$

The novelty of this new GL KO mouse ($BCL6^{\Delta ZF/\Delta ZF}$) is that rather than only having a partial deletion of the zinc finger region, as the original GL KO mouse ($BCL6^{-/-}$) has (Figure 6 C), the entire region is now deleted, as well as the neomycin resistance gene (Figure 15 A). To verify this deletion, naïve Th cells were isolated from untreated $BCL6^{\Delta ZF/\Delta ZF}$ and littermate controls. Cells were stimulated for two days with anti-CD3 and anti-CD28 antibodies in Th0 culture conditions, then lysed for RNA analysis. As shown in Figure 16 A, transcript levels of BCL6 exons 2/3 were reduced in $BCL6^{\Delta ZF/\Delta ZF}$ mice compared to the levels seen in littermate controls; as expected, exon 8 transcripts were nonexistent.

Work by several groups, including our own, has consistently shown the original BCL6 GL KO mouse ($BCL6^{-/-}$) to skew toward a Th2-like phenotype and to develop systemic

inflammation. To assess the phenotype of our new GL KO mice, naïve BCL6$^{\Delta ZF/\Delta ZF}$ and littermate control mice were sacrificed and analyzed. Like the original GL KOs, BCL6$^{\Delta ZF/\Delta ZF}$ mice were smaller than littermate controls (Figure 16 B). Spleen cells were then isolated and analyzed. No differences in T or B cell populations were observed in BCL6$^{\Delta ZF/\Delta ZF}$ mice compared to controls (Figure 16 C). When naive Th cells were isolated and activated with anti-CD3 and anti-CD28 antibodies for four days in Th0 culture conditions, the cytokines produced after an overnight restimulation showed a slightly different pattern than expected. Like traditional GL KO mice, Th cells fromBCL6$^{\Delta ZF/\Delta ZF}$ mice produced increased levels of IL-17A and IL-10 (Figure 17 A). Unlike BCL6$^{-/-}$ mice, activated naïve Th cells from BCL6$^{\Delta ZF/\Delta ZF}$ mice showed a reduction in IFNγ secretion, as the GL KO typically has similar levels of this cytokine to WT mice. Most interestingly, however, was the lack of increased IL-4 production; amounts produced by BCL6$^{\Delta ZF/\Delta ZF}$ mice were equivalent to control mice.

In a separate experiment, effector memory (EM) cells (CD44^{hi} CD62L^{-}) from BCL6$^{+/+}$, BCL6$^{Neofl/Neofl}$, and BCL6$^{\Delta ZF/\Delta ZF}$ mice were isolated via FACS and stimulated for 24 hours with anti-CD3 and anti-CD28 antibodies in Th0 culture conditions. Like the four day culture with naïve Th cells, EM cells failed to show increased IL-4 secretion in

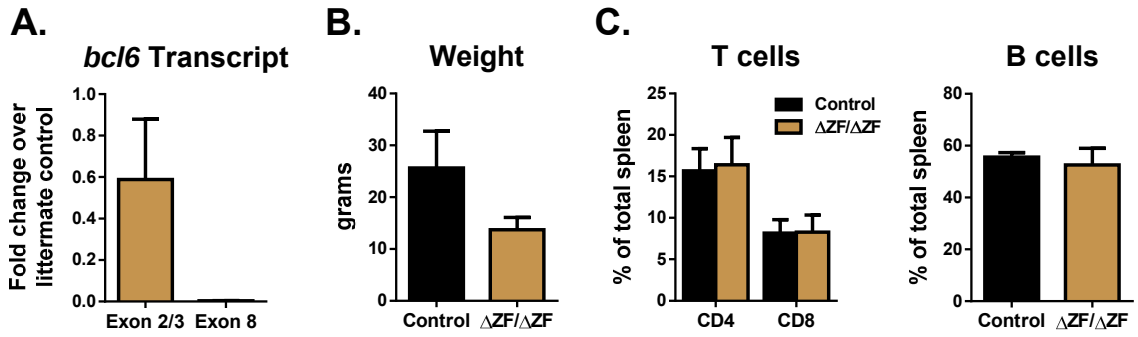

Figure 16. Genotypic and phenotypic characterization of BCL6$^{\Delta ZF/\Delta ZF}$ mice. A. Naïve CD4^{+} T cells were isolated from unimmunized BCL6$^{\Delta ZF/\Delta ZF}$ mice and littermate controls. Control mice were a mixture of BLC6$^{+/+}$ and BCL6$^{+/\Delta ZF}$ mice. Cells were activated with anti-CD3 and anti-CD28 antibodies in Th0 media for 48 hours, then lysed for RNA analysis. Transcript levels are normalized to littermate control levels (dotted line at 1.0). Mean ± SE. **B.** Weights of unimmunized BCL6$^{\Delta ZF/\Delta ZF}$ mice and littermate controls. Mean ± SE. **C – D.** CD4^{+} T, CD8^{+} T, and B cell populations were analyzed via flow cytometry from the spleen of unimmunized mice. T cells gated on CD3^{+} and CD4^{+} or CD3^{+} CD8^{+}; B cells gated on B220^{+} CD19^{+}. Mean ± SE.

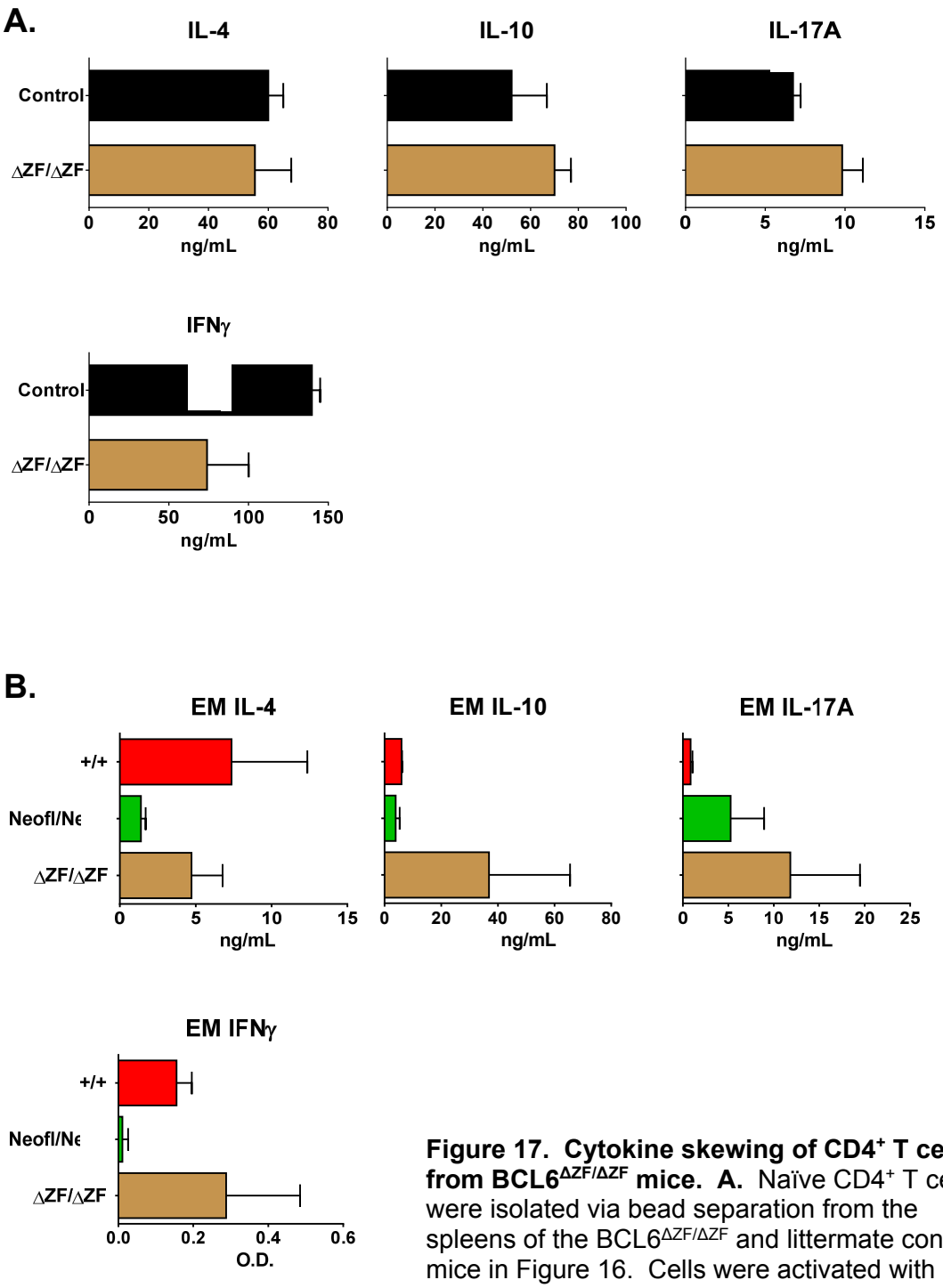

Figure 17. Cytokine skewing of CD4⁺ T cells from BCL6$^{\Delta ZF/\Delta ZF}$ mice. A. Naïve CD4⁺ T cells were isolated via bead separation from the spleens of the BCL6$^{\Delta ZF/\Delta ZF}$ and littermate control mice in Figure 16. Cells were activated with anti-CD3 and anti-CD28 antibodies in Th0 culture conditions for 4 days, after which they were restimulated overnight with anti-CD3 and anti-CD28 antibodies. Supernatants were collected and cytokine levels measured via ELISA. Mean ± SE. **B.** Effector memory (EM) CD4⁺ T cells (CD44⁺ CD62L⁻) were isolated via FACS from the spleens of unimmunized BCL6$^{+/+}$, BCL6$^{Neofl/Neofl}$, and BCL6$^{\Delta ZF/\Delta ZF}$ mice. EM cells were stimulated for 24 hours via anti-CD3 and anti-CD28 antibodies in Th0 media. Supernatant cytokine levels were measured via ELISA. Mean ± SE.

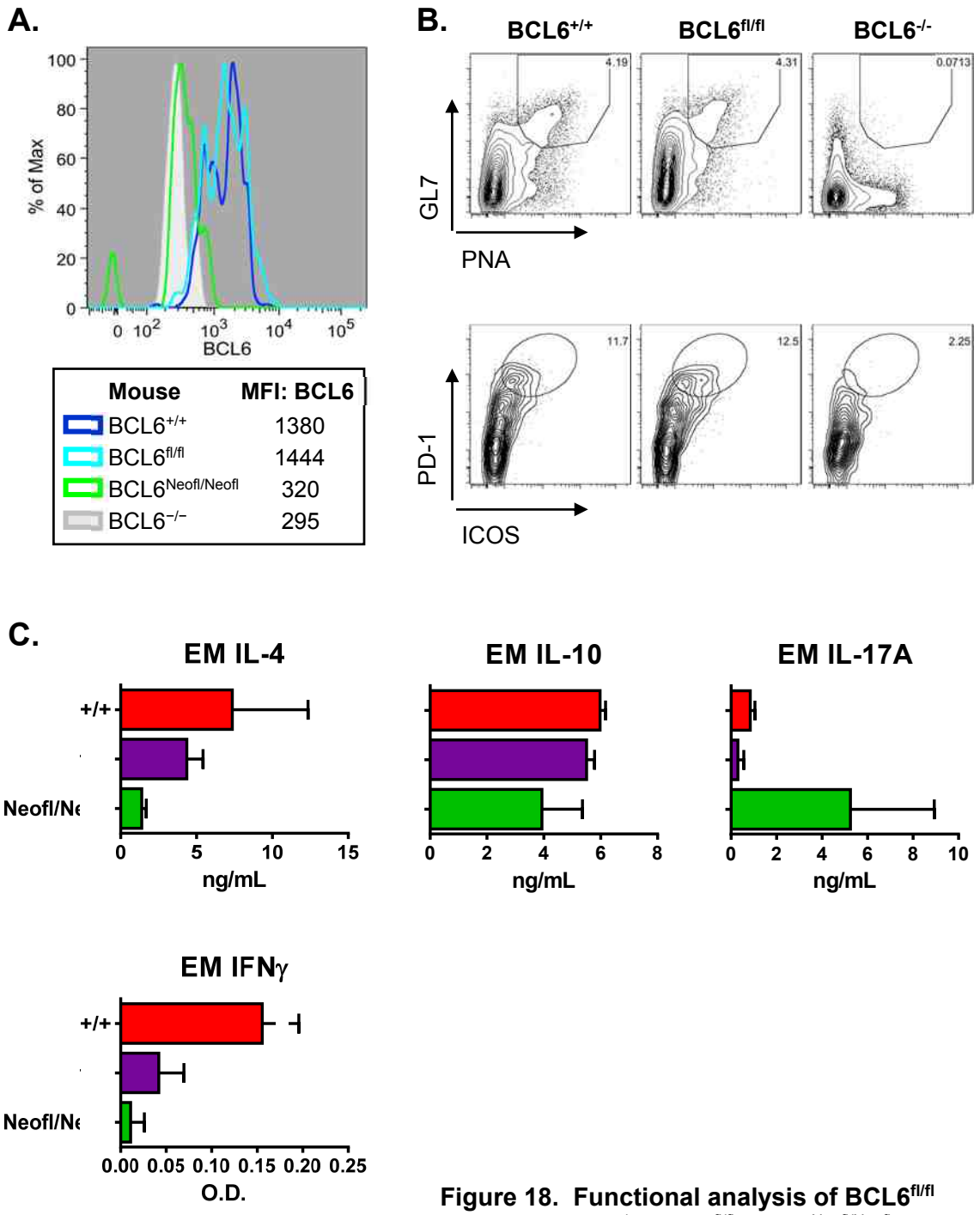

Figure 18. Functional analysis of BCL6$^{fl/fl}$ mice. A. BCL6$^{+/+}$, BCL6$^{fl/fl}$, BCL6$^{Neofl/Neofl}$, and BCL6$^{-/-}$ mice were immunized i.p. with SRBC and sacrificed on day 9. Spleen CD4^{+} T cells were analyzed for BCL6 protein expression via flow cytometry MFI of BCL6 protein is shown. **B.** Representative flow plots of mice immunized in (**A**). GC B cells (top) were gated on B220^{+} CD19^{+} Fas^{+}. TFH cells (bottom) were gated on CD3^{+} CD4^{+} CXCR5^{+}. **C.** EM CD4^{+} T cells (CD44^{+} CD62L^{-}) were isolated via FACS from the spleens of unimmunized BCL6$^{+/+}$, BCL6$^{fl/fl}$, and BCL6$^{Neofl/Neofl}$ mice. EM cells were stimulated for 24 hours via anti-CD3 and anti-CD28 antibodies in Th0 media. Supernatant cytokine levels were measured via ELISA. Mean ± SE.

$BCL6^{\Delta ZF/\Delta ZF}$ mice, while IL-10 levels remained increased (Figure 16 B). IFNγ in EM cells was equivalent to $BCL6^{+/+}$ mice. Of interest was the seemingly step-wise increase in IL-17A levels with the disruption of the zinc finger region (Figure 17 B). This cytokine data would suggest that our new GL KO mouse, with the entire zinc finger removed, does not skew toward a Th2 phenotype.

$BCL6^{fl/fl}$ mice

After $BCL6^{Neofl/Neofl}$ mice were mated to Cre^{EIIa} mice, some offspring were found to have only the neomycin resistance gene deleted, leaving the zinc fingers, flanked by two loxP sites, intact (Figure 15 B). These mice, termed $BCL6^{fl/fl}$, needed to be tested in order to assess whether the lack of GCs seen in $BCL6^{Neofl/Neofl}$ was indeed due to the presence of the neomycin resistance gene or because of some other factor. To test the functionality of the BCL6 allele in homozygous $BCL6^{fl/fl}$ mice, SRBC were again injected i.p. and mice were sacrificed on day nine. Removal of the neomycin resistance gene successfully restored BCL6 protein, as measured by flow cytometry (Figure 18 A). Functionality of the gene was also reestablished, as GC B cell and TFH populations were present at WT levels in $BCL6^{fl/fl}$ mice (Figure 18 B). When EM Th cells were isolated from naïve mice and activated for 24 hours with antibodies in Th0 culture conditions, the cytokine profile of $BCL6^{fl/fl}$ mice more closely resembled that of WT mice, rather than $BCL6^{Neofl/Neofl}$ mice (Figure 18 C). The increased IL-17A secretion from $BCL6^{Neofl/Neofl}$ effector memory Th cells seen here supports the earlier findings which suggest $BCL6^{Neofl/Neofl}$ mice may be skewing toward a Th17 phenotype. With the restoration of BCL6 protein and function, these $BCL6^{fl/fl}$ mice are a functional floxed mouse which can be used for conditional deletion.

DISCUSSION

Due to the complexities associated with using the original BCL6 GL KO mouse ($BCL6^{-/-}$) a cKO mouse model needed to be developed to better understand the role of BCL6 in different cell subsets. Here, using a targeting construct containing loxP sites flanking the zinc finger region of the gene, we have created a new mouse model which can do just

that. The first version of these mice, BCL6-Neo-floxed ($BCL6^{Neofl/Neofl}$) mice proved to be unusable for our purposes of cKO. However, they, in themselves, seem to be a novel BCL6 knock-down model. These mice are perplexing in that they lack BCL6 function *in vivo*, but show increases in transcript expression in *ex vivo* uncultured cells and in Th0 cultured cells. One reason for the increase in exon 8 expression could be due to transcription of the neomycin resistance gene. As shown in Figure 6, the Neo gene actually runs in an antisense direction to the rest of the BCL6 gene. Therefore, transcription of this gene could result in exons 8 and 9 being transcribed as well. Also, BCL6 self-represses its own transcription, and if functional protein is not being produced, this self-repression cannot take place. Therefore $BCL6^{Neofl/Neofl}$ T cells may have increased BCL6 RNA levels due to lack of self-repression, even at basal levels. However, in *ex vivo* cells from immunized mice and in Th cells cultured in TFH-skewing conditions, we show a decrease in BCL6 transcript compared to $BCL6^{+/+}$ mice. This may have more to do with the ability of WT cells to increase BCL6, rather than a decrease in BCL6 transcription in $BCL6^{Neofl/Neofl}$ mice. In TFH-skewing cultures and in immunized mice, Th cells will be pushed to up-regulate BCL6. Therefore, cells which are impeded from doing so, i.e. T cells from $BCL6^{+/Neofl}$, $BCL6^{Neofl/Neofl}$, and $BCL6^{-/-}$ mice, will not be able to achieve the normal increase seen in $BCL6^{+/+}$ T cells. Therefore, the decrease in transcript expression in $BCL6^{Neofl/Neofl}$ mice likely has more to do with WT cells raising the threshold.

The lack of functional BCL6 expression in $BCL6^{Neofl/Neofl}$ mice, while having a devastating effect on GCs, had few effects on Th cell cytokine secretion. IL-4 was not substantially increased, as is typically seen with GL KO mice. The one cytokine that stood out, though, was IL-17A. It was increased in *ex vivo* cultured Th cells (Figure 11), in naïve Th cells, *in vitro* cultured cells (Figure 12) and in *in vitro* stimulated effector memory cells (Figure 18 C). *Ex vivo* Th cells showed a more than two-fold increase in *rorc* expression, the master transcription factor for Th17 cells. This increase was also seen in Th0 cultured naïve Th cells. When comparing $BCL6^{-/-}$, $BCL6^{Neofl/Neofl}$ mice, and $BCL6^{+/+}$ mice, it appeared $BCL6^{Neofl/Neofl}$ mice have an intermediate phenotype, as they have reduced body weight, lack of GCs, and reduced BCL6 protein, similar to GL KO mice. However, their Th cell cytokine profile matched more closely to WT mice, and their inflammation, as determined by histology, was more of an intermediate level (Figure 13). Based on this, I would propose a model wherein graded BCL6 expression

results in the differentiation of different Th subsets. High BCL6 leads to TFH cells, while complete loss of BCL6 protein leads to Th2 cell development, as has been previously published (59, 61). Finally, an intermediate level of BCL6 transcript leads to TH17 differentiation (Figure 19). Because TFH cells and Th17 cells have been shown to share some characteristics, such as reliance on IL-6 and STAT3 for differentiation, utilization of c-maf, and secretion of IL-21(17, 19, 24, 63), this model seems plausible.

One caveat to the graded expression model, though, is the development and analysis of a new GL KO mouse ($BCL6^{\Delta ZF/\Delta ZF}$). These mice failed to show the Th2-type skewing seen in the original KO mice ($BCL6^{-/-}$). The observations made with $BCL6^{\Delta ZF/\Delta ZF}$ mice suggests multiple explanations for the phenotype seen in $BCL6^{-/-}$ mice. First of all, having only partial zinc finger deletion, as is the case with $BCL6^{-/-}$ mice, could result in a BCL6 protein with partial nucleic acid binding capabilities. What the binding capabilities of this truncated protein are has not been investigated, and thus cannot be ruled out as a possible explanation for the Th2 phenotype in these mice. Secondly, the background of the mice may play a larger role in the skewing of Th cells than previously appreciated, as the original GL KO mice, while on a mixed background, are slightly different than our new mice, which are mixed C57BL/6-129Sv. Therefore, having 129Sv genes may somehow be affecting Th cell cytokine production. Furthermore, the endogenous microbiota/microflora found in these mice likely plays a role in augmenting the immune response, and since our new GL KO mice are housed in a somewhat different environment (subtle changes in mouse housing and feeding) than the original KO mice, this difference may be a contributing factor to the differences seen. In any case, the conclusions about BCL6 function using $BCL6^{-/-}$ mice must be revaluated using the new GL KO and, more importantly, with our new cKO mouse, as these cKO mice will be able to control for extrinsic effects from other cells on the cells of interest, which is not possible in a GL KO of any kind. This is the major reason we developed these new $BCL6^{fl/fl}$ mice. Now researchers can tightly control which cells have BCL6 deleted and know any effects they see are due solely to loss of the gene in those cells.

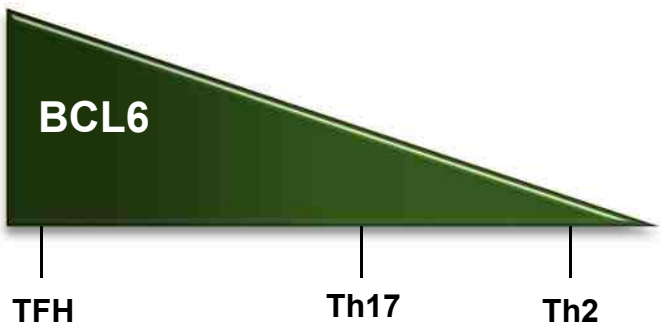

Figure 19. Proposed model for graded BCL6 expression in different Th subsets. Published data has established BCL6 as the master transcription factor for TFH cells. These cells also express BCL6 at the highest levels of all the Th subsets. Conversely, reports have shown BCL6 to repress GATA3, the master transcription factor for Th2 cells. Thus, little-to-no BCL6 is expressed in these cells. Data presented here has demonstrated $BCL6^{Neofl/Neofl}$ mice to be a BCL6 knock-down model, rather than knockout. Based on RNA and cytokine analysis of these mice, showing increased *rorc* expression and IL-17A secretion, both signature markers for TH17 cells, it seems plausible that an intermediate level of BCL6 could lead a cell to skew toward a Th17 phenotype.

CHAPTER 3 – BCL6 IS NECESSARY FOR EFFICIENT NAÏVE CD4$^+$ T CELL ACTIVATION

INTRODUCTION

Like all immune cells, CD4$^+$ T cells originate from a process known as hematopoiesis, wherein hematopoietic stem cells, which have the ability to self-renew, differentiate into multipotent progenitors (MMP) (Figure 20) (64-66). These cells can then give rise to myeloid cells via a common myeloid progenitor (CMP), or to lymphocytes, including B cells, by differentiating into a common lymphoid progenitor (CLP) (66-68). The CLP can exit the bone marrow and migrate to the thymus, where terminal T cell development commences (64, 66, 67, 69). First, cells referred to as double negative (DN), because they express neither CD4 nor CD8, differentiate from the CLP (69-72). From there, cells are selected for and become double positive (DP), as they begin to express both CD4 and CD8 on the cell surface (69-72). Further environmental signals will enable these cells to become single positive (SP) for either CD4 or CD8 (69, 70, 72, 73). At this point, T cells are considered mature and can exit the thymus into circulation (69, 70, 72). These mature, but naïve, T cells can enter secondary lymphoid organs, such as the spleen and lymph nodes, where they sample antigens being presented by APCs (74). If the TCR of a T cell, in this case that of a CD4$^+$ T cell, is specific for the presented antigen, it will be activated, begin to proliferate, and carry out effector functions to aid in pathogen clearance.

For a CD4$^+$ T cell to be properly activated, a complicated signal cascade must take place. First, the TCR binds the MHC II/antigen complex on an APC (Figure 21) (74-76). At the same time, CD4, functioning as a coreceptor, must bind to the MHC II molecule presenting the antigen (77, 78). TCR engagement triggers the mobilization and recruitment of the lymphocyte-specific protein tyrosine kinase (Lck) to the CD4 intracellular tail (71, 75-78). Lck will then become phosphorylated, converting it to an active state (77). Activated Lck will phosphorylate the zeta chain of the CD3 complex, thus recruiting another protein kinase, Zap70 (71, 75-78). Once relocated to the CD3 zeta chain, Zap70 becomes phosphorylated, either by Lck or via auto-phosphorylation (71, 78). Now in an active state, Zap70 will trigger a cascade of

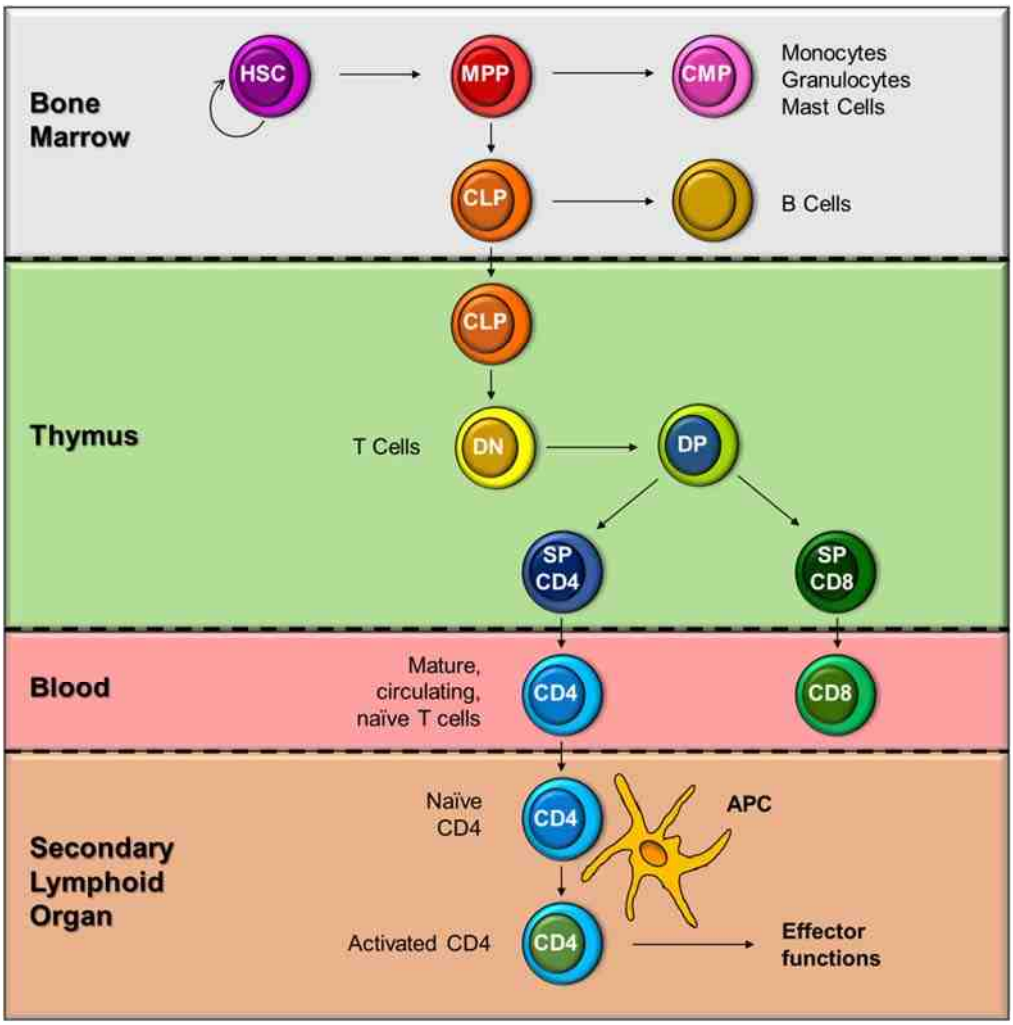

Figure 20. Development of CD4$^+$ T cells. All immune cells originate from hematopoietic stem cells (HSC) in the bone marrow (BM). These self-renewing cells can differentiate into mulitpotent progenitors (MPP), which will, in turn, differentiate into common myeloid progenitors (CMP). These cells give rise to monocytes, granulocytes, and mast cells. Alternately, MMPs can differentiate into common lymphoid progenitors (CLP), which will become immune cells of the acquired response. If the CLP does not differentiate into the B cell linage within the BM, a CLP can exit the marrow and migrate to the thymus, where it will give rise to T cells. First, a CLP will differentiate into what is known as a double negative (DN) T cell, as these cells do not express either of the coreceptors, CD4 or CD8. However, expression of the TCR β chain, along with other surface markers, denotes them as T cells. Environmental signals will next trigger surface expression of both CD4 and CD8 on these cells, leading them to become double positive (DP) cells. Finally, further environmental signals and selection events in the thymus will cause these cells to cease expressing one of the coreceptors and become single positive (SP) for either CD4 or CD8. These cells are now considered mature naïve T cells, and will exit the thymus into the circulation. Frequent encounters with APCs allow T cells the chance to become activated and take part in pathogen clearance. For CD4$^+$ T cells, this typically occurs in secondary lymphoid organs, such as the spleen or lymph nodes. These activated T cells can then acquire effector functions to aid in the clearance of the pathogen.

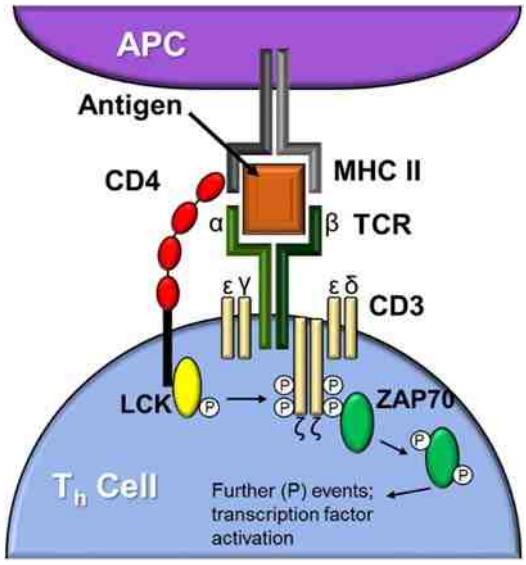

Figure 21. Early signaling events in TCR stimulation. When an APC presents antigen to a CD4$^+$ Th cell in the context of the MHC class II molecule, several cascade events must take place for proper signaling and activation of the T cell. First, the TCR, made up of an α and β chain, will bind the antigen and make contact with the MHC class II molecule. Additionally, the CD4 coreceptor must bind the MHC class II molecule on the APC for proper signaling. This leads to recruitment of the intracellular protein kinase called lymphocyte-specific protein tyrosine kinase, or Lck. The intracellular tail of CD4 will phosphorylate (P) Lck, thus transforming it into its active state. This kinase can then phosphorylate the tail of the CD3 zeta (ζ) chain. CD3 is a signature surface marker for T cells. It is composed of several different chains and clusters around the TCR. In the context of CD4$^+$ T cells, these chains are typically the epsilon (ε), delta (δ) and zeta (ζ) chains. Phosphorylation of the zeta chain leads to recruitment of the zeta-chain-associated protein kinase 70 (Zap70). Once localized to CD3, Zap70 is phosphorylated by Lck, thus activating it. From here, Zap70 will trigger a cascade of downstream phosphorylation events, eventually leading to the activation of transcription factors which will trigger T cell proliferation and differentiation.

sequential phosphorylation events (76-78). Downstream factors, such as MAP kinases, are essential parts of this signal cascade (76, 77), which culminates in the activation of critical gene expression pathways, such as NFAT, fos, and jun transcription factors. These, in turn, trigger up-regulation of activation markers, such as IL-2, IL-2 receptor alpha (IL-2Rα), cytotoxic T-lymphocyte antigen 4 (CTLA4), CXCR5, and CD69 (74, 76, 77, 79, 80). These activated CD4$^+$ T cells will then differentiate into one of several subsets, depending on the antigen and cytokine environment, to carry out effector functions (Figure 2).

At this time, a role for BCL6 in naïve Th cell activation has not been established.

Although CXCR5 has been shown to be up-regulated early after activation, research has demonstrated this to be independent of BCL6 expression (81). Recently, two publications have shown BCL6 to become up-regulated very early after activation, but do not show data that BCL6 is essential for activation (22, 23). Using our new cKO mouse model, we investigated the activation status of $CD4^+$ T cells in multiple *in vivo* and *in vitro* models.

MATERIALS AND METHODS

Mice and immunizations

$Bcl6^{fl/fl}$ mice were mated to CD4-cre mice (82) to generate $Bcl6^{fl/fl}$ Cre^{CD4} mice. Mice with the wild type BCL6 allele were bred to CD4-Cre mice for use as controls ($BCL6^{+/+}$ Cre^{CD4}). The floxed allele was genotyped by PCR using the following primers:

5' loxP forward (5' – TGAAGACGTGAAATCTAGATAGGC – 3')
5' loxP reverse (5' – ACCCATAGAAACACACTATACATC – 3')
3' loxP forward (5' –TCACCA ATCCCAGGTCTCAGTGTG–3')
3' loxP reverse (5' – CTTTGTCATATTTCTCTGGTTGCT–3')

Cre-CD4 transgene was genotyped using the following primers:

Forward (5' –ATCGCCATCTTCCAGCAGGCGCACT– 3')
Reverse (5' –ATTTCCGTCTCTGGTGTAGCTGAT– 3')

Mice were immunized i.p. with 1 x 10^9 sheep red blood cells (SRBC; Rockland Immunochemicals Inc., Gilbertsville, PA) in PBS.

Chimera mice

For mixed bone marrow chimera experiments, RAG-1-deficient mice (83) were sub-lethally irradiated with 350 rads. The following day, bone marrow from $Bcl6^{fl/fl}$ Cre^{CD4} ($CD45.2^+$) and BoyJ ($CD45.2^-$) mice was harvested and cells mixed in equal amounts. Irradiated RAG mice received tail vein injections of 5x10^6 cells. Mice were rested for approximately three months before immunization. Mice were bred under specific

pathogen-free conditions at the laboratory animal facility at IUSM and were handled according to protocols approved by the IUSM Animal Use and Care Committee.

Flow cytometry

Total spleen or thymus cells were incubated with anti-mouse CD16/CD32 (Fcγ receptor) for 20 minutes, followed by surface staining for the indicated markers. A fixable viability dye (eFluor 780, eBioscience) was used for all samples. The following antibodies were used to stain naïve and memory T cells: α-mCD3 Alexa Fluor 700, clone 500A2 (BD Bioscience); α-mCD4 PECy7, clone RM4-5 (BD Bioscience); α-mCD8a APC, clone 53-6.7 (BD Bioscience); α-mCD44 PE, clone IM7 (eBioscience); α-mCD62L FITC, clone MEL-14 (BD Bioscience). $CD25^+$ cells were stained using α-mCD25 PE CF594, clone PC61 (BD Horizon). $CD69^+$ cells were stained with α-mCD25 PerCPCy 5.5, clone H1.2F3 (Biolegend). The GL3 Ab (Biolegend) was used to detect γδ T cells and NKT cells were identified with α-galactosylceramide-loaded CD1d tetramers obtained from the NIH tetramer core facility.

For chimera experiments, the following antibodies were used: Bone marrow – α-mCD3 Alexa Fluor 700, clone 500A2 (BD Bioscience); α-mB220 PE, clone RA3-6B2 (BD Bioscience); α-mCD11b Biotin, clone M1/70 (eBioscience) with Streptavidin-PECy7 (Biolegend); α-mCD45.2 PerCPCy 5.5, clone 104 (BD Bioscience); Thymus – α-mCD3 Alexa Fluor 700, clone 500A2 (BD Bioscience); α-mCD4 FITC, clone H129.19 (BD Bioscience); α-mCD8a APC, clone 53-6.7 (BD Bioscience), α-mCD45.2 PerCPCy 5.5, clone 104 (BD Bioscience); Spleen – α-mCD3 Alexa Fluor 700, clone 500A2 (BD Bioscience); α-mCD4 PerCPCy 5.5, cloneRM4-5 (eBioscience); α-mCD8a APC, clone 53-6.7 (BD Bioscience); α-mCD44 PE, clone IM7 (eBioscience); α-mCD62L FITC, clone MEL-14 (BD Bioscience); α-mCD45.2 PECy7, clone 104 (Biolegend). Samples were run on a BD LSR II flow cytometer using FACSDiva software. Data was analyzed using FlowJo software.

***In vitro* stimulation**

Total $CD4^+$ T cells were isolated via magnetic bead separation (Miltenyi Biotec); Cells

were stimulated with plate-bound anti-CD3 (5 μg/mL) and anti-CD28 (10 μg/mL) antibodies (BD Biosciences) for 24 hours at $1x10^6$ cells/mL in Th0 media conditions, which contain no cytokines or blocking antibodies.

Gene expression analysis

Total RNA was prepared using a kit (Qiagen) after lysis of the cells via Trizol (Life Technologies); cDNA was prepared with the Transcriptor First Strand cDNA synthesis kit (Roche). Quantitative PCR (qPCR) reactions were run by assaying each sample in triplicates using the Fast Start Universal SYBR Green Mix (Roche Applied Science) with custom primers or specific Taqman assays (ABI). Assays were run with a Stratagene Mx3000P Real-Time QPCR machine. Levels of mRNA expression were normalized to beta-tubulin mRNA levels, and differences between samples analyzed using the ΔΔCT method. Primers for SYBR Green assays were previously described (14, 19).

Microarrays

Naïve $CD4^+$ T cells were isolated via FACS using the following surface markers: $CD3^+$ $CD4^+$ $CD62L^+$ $CD44^-$. A cell viability gate was also used. Cells were activated *in vitro* with anti-CD3 and anti-CD28 antibodies, as described above, in Th0 or TFH media conditions. TFH conditions contain IL-6 and IL-21 [10 ng/ml each (R&D Systems)], plus anti-IFNγ (10 μg/mL), anti-IL-4 (10 μg/mL), and anti–TGF-β (20 μg/mL) antibodies. Cells were cultured for 20 hours. Cells were lysed, RNA prepared using an RNeasy kit (Qiagen), and cDNA prepared with the Transcriptor First Strand cDNA synthesis kit (Roche). Affymetrix gene expression microarrays were carried out by Center for Medical Genomics at the Indiana University School of Medicine.

Statistical analysis

Statistical analysis was done using IBM SPSS Statistics 21 software. Statistics for microarray data was done using GraphPad Prism software. In all figures, $*p < 0.05$, $**p < 0.01$, $***p < 0.001$.

RESULTS

Efficient and complete deletion of BCL6 zinc finger exons in BCL6$^{+/fl}$ Cre^{CD4} mice

After BCL6$^{fl/fl}$ mice were generated and found to be able to form normal GC responses, these mice were mated to CD4-Cre mice. CD4-Cre mice express a Cre recombinase enzyme under the control of the CD4 promoter. This means that the floxed zinc fingers of BCL6 (Figure 22 A) will be deleted in all T cells, since CD4 expression is turned on during early T cell development in the thymus. After the first mating, heterozygous BCL6$^{+/fl}$ Cre^{CD4} mice were generated. Spleen cells from these mice were FACS sorted for B cells and CD4$^+$ T cells. PCR analysis revealed efficient deletion of the zinc fingers in CD4$^+$ T cells, but not in B cells, of Cre-expressing mice (Figure 22 B). Heterozygous mice were then mated to produce BCL6$^{fl/fl}$ Cre^{CD4} offspring.

Skewed naïve and effector memory CD4$^+$ T cell populations in BCL6$^{fl/fl}$ Cre^{CD4} mice

Eight week old, untreated BCL6$^{+/+}$ Cre^{CD4} and BCL6$^{fl/fl}$ Cre^{CD4} mice were first analyzed for T cell development. Thymic cells were analyzed for proportions of double positive CD4 CD8 cells (Figure 23 A), single positive CD4 and CD8 cells (Figure 23 B), natural killer T cells, and gamma delta T cells (Figure 23 C). The spleens of eight to twelve week old untreated mice were also analyzed for T_{reg} populations (Figure 23 D). In all cases, no differences in T cell populations were found between BCL6$^{+/+}$ Cre^{CD4} and BCL6$^{fl/fl}$ Cre^{CD4} mice. Unimmunized mice were also assessed for naïve and effector memory T cell populations in the spleen. In the case of CD8$^+$ T cells, no differences were found between the two mouse strains (Figure 23 E). However, naïve CD4$^+$ T cells were significantly increased in the spleen of BCL6$^{fl/fl}$ Cre^{CD4} mice as compared to BCL6$^{+/+}$ Cre^{CD4} mice. After immunizing mice i.p. with SRBC and sacrificing nine days later, the naïve CD4$^+$ T cell population in BCL6$^{fl/fl}$ Cre^{CD4} mice remained significantly increased (Figure 23 G – H), while no differences in total CD4$^+$ or CD8$^+$ T cells were found (Figure 23 F). Furthermore, while CD8$^+$ T cells showed no differences in naïve or effector memory cells in either mouse type, the BCL6$^{fl/fl}$ Cre^{CD4} mice now showed a significant loss in the CD4$^+$ effector memory cell population (Figure 23 G – H). These data suggest that BCL6, specifically in CD4$^+$ T cells, plays a role in naïve Th cell activation.

As mice age, they are exposed to more environmental antigens, and thus, trend toward having more activated T cells. To see if the skewing of naïve and effector memory cell populations seen in BCL6$^{fl/fl}$ Cre^{CD4} mice decreased with age, BCL6$^{+/+}$ Cre^{CD4} and BCL6$^{fl/fl}$ Cre^{CD4} mice were aged to thirteen months and sacrificed without immunizing. Still, at this advanced age, BCL6$^{fl/fl}$ Cre^{CD4} mice continued the trend of having increased naïve and decreased effector memory CD4^{+} T cells (Figure 24).

Skewed naive and effector CD4^{+} T cell populations confirmed in mixed bone marrow chimera model

The finding that naïve and effector memory Th cell populations were skewed in the absence of BCL6 was further verified in a mixed bone marrow chimera model. Bone

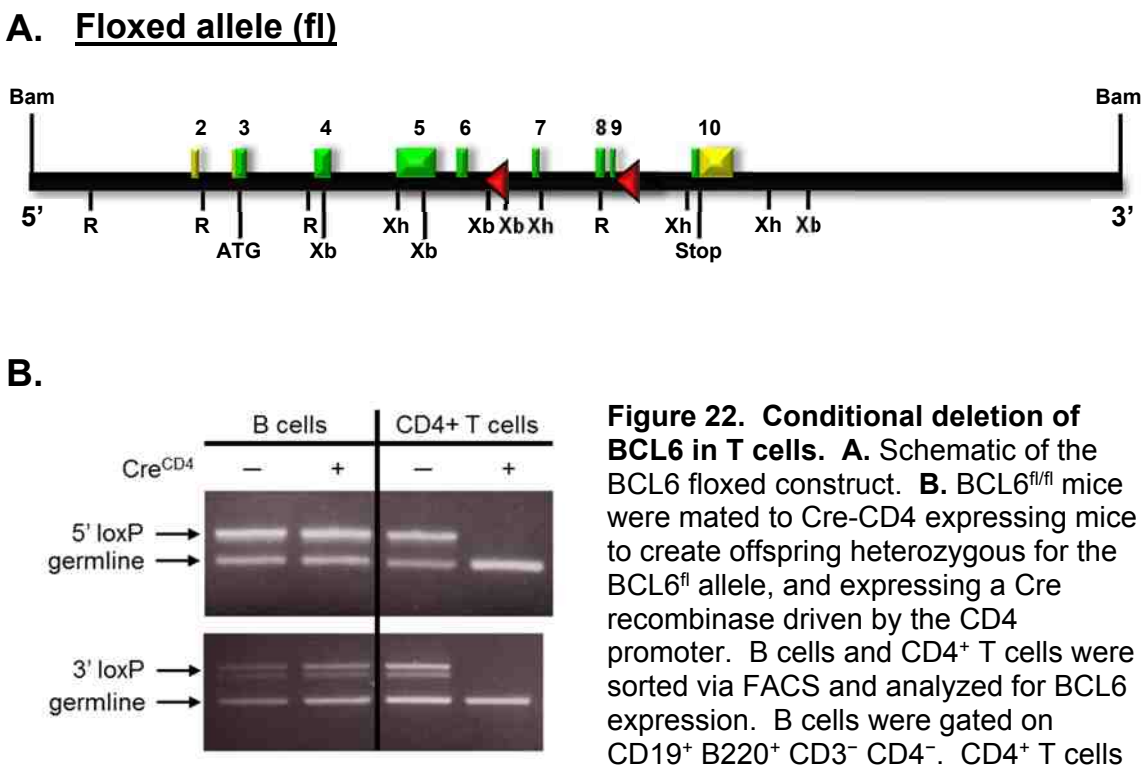

Figure 22. Conditional deletion of BCL6 in T cells. A. Schematic of the BCL6 floxed construct. **B.** BCL6$^{fl/fl}$ mice were mated to Cre-CD4 expressing mice to create offspring heterozygous for the BCL6^{fl} allele, and expressing a Cre recombinase driven by the CD4 promoter. B cells and CD4^{+} T cells were sorted via FACS and analyzed for BCL6 expression. B cells were gated on CD19^{+} B220^{+} CD3^{-} CD4^{-}. CD4^{+} T cells were gated on CD19^{-} B220^{-} CD3^{+} CD4^{+}. B cells expressed both a wild type allele (germline) and floxed allele (5' loxP and 3' loxP), regardless of Cre expression. CD4^{+} T cells not expressing a Cre-CD4 recombinase also expressed both versions of the BCL6 allele. However, cells from those mice mated to Cre^{CD4} mice expressed a wild type allele but not a floxed allele, as evidenced by the lack of a band in both the 5' loxP and 3' loxP regions. This demonstrates successful conditional knockout of the BCL6 zinc finger region in T cells.

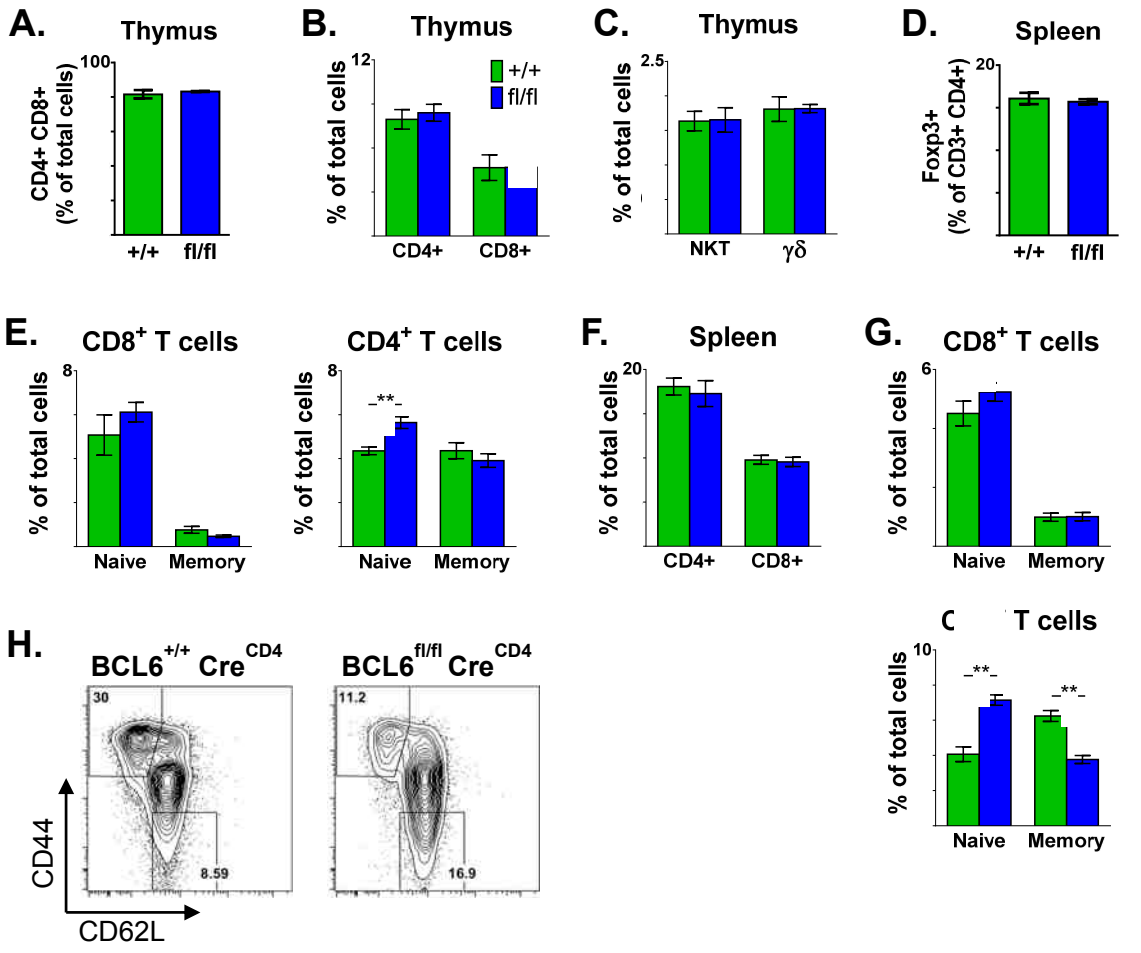

Figure 23. BCL6$^{fl/fl}$ Cre^{CD4} mice have increased naïve and decreased effector memory CD4^{+} T cell populations. Untreated 8 week old BCL6$^{+/+}$ Cre^{CD4} and BCL6$^{fl/fl}$ Cre^{CD4} mice were sacrificed and analyzed for T cell populations. **A.** Double positive T cells in thymus. **B.** Single positive CD4 and CD8 T cells in thymus. **C.** Natural killer T cells (NKT) and gamma delta T cells (γδ) in thymus. **D.** Treg cells in spleen of unimmunized mice. Shown as percent of total CD3^{+} CD4^{+} T cells. **E.** Naïve and effector memory cell populations in the spleen of unimmunized mice. CD4^{+} and CD8^{+} cells gated on CD3^{+}. Naïve cells gated on CD62L^{+} CD44^{-}. Effector memory cells gated on CD62L^{-} CD44^{hi}. N = 3 – 4; mean ± SE. **F – H.** Mice were immunized i.p. with SRBC and sacrificed on day 9. **F.** T cell populations in spleen. Cells gated on CD3^{+}. **G.** Naïve and effector memory cells in spleen. Cells gated as in (**E**). N = 4; mean ± SE. **H.** Representative flow plots of CD4^{+} cells in (**G**). Cells gated on CD3^{+} CD4^{+}. **p < 0.01 by *t* test.

marrow from BCL6$^{fl/fl}$ Cre^{CD4} and BoyJ mice was harvested, mixed equally, and transferred via tail vein injections into irradiated RAG-deficient mice. After resting the mice for approximately three months, mice were immunized i.p. with SRBC and sacrificed nine days later. Both the bone marrow and spleen reconstituted equally with

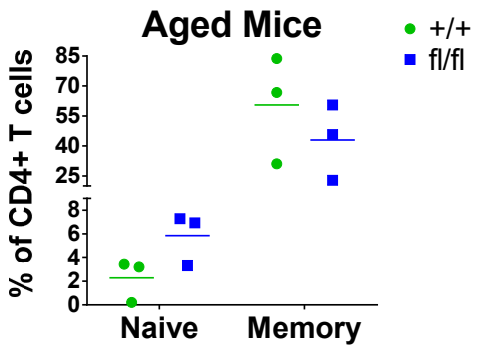

Figure 24. Naïve and effector memory cell differences in aged BCL6$^{fl/fl}$ Cre^{CD4} mice remain in aged mice. BCL6$^{+/+}$ Cre^{CD4} and BCL6$^{fl/fl}$ Cre^{CD4} mice were left untreated and aged to 13 months. Mice were sacrificed and spleen cells analyzed for naïve and effector memory CD4^{+} T cells. Cells gated as in Figure B. N = 3; bar = mean.

BCL6$^{fl/fl}$ Cre^{CD4} (CD45.2^{+}) and BoyJ (CD45.2^{-}) cells (Figure 25 A). Only the thymus showed slightly, but significantly, more cells coming from the BoyJ donor cells (CD45.2^{-}). Within the bone marrow, the B cells repopulated evenly from both donor marrows, however, macrophage and T cell populations were found to be disproportionally of CD45.2^{+} and CD45.2^{-} origins, respectively (Figure 25 B). Most thymus T cells were of equal CD45.2^{+} and CD45.2^{-} proportions (Figure 25 C). Only the CD4^{+} T cells in the thymus were shown to be proportionally more of CD45.2^{-} origin. However, when the cell populations were calculated as a percent of the total thymus cells, any differences were equalized (Figure 25 D), suggesting these differences were negligible. Within the spleen, T cells from BoyJ donor marrow (CD45.2^{-}) made up a significantly larger proportion of CD8^{+} and CD4^{+} T cells, as well as a significantly higher percentage of T cells in the total spleen (Figure 25 E – F). These data, combined with the increase in CD45.2^{-} T cells in the bone marrow (Figure 25 B), suggest BCL6 plays a role in the survival of T cells exiting the thymus into circulation.

When CD4^{+} naïve and effector memory cell populations were analyzed in the spleen, the phenotype of the earlier experiment repeated. Even though the BoyJ cells (CD45.2^{-}) made up a significantly larger proportion and percent of the total CD4^{+} T cells in the spleen, BCL6$^{fl/fl}$ Cre^{CD4} (CD45.2^{+}) T cells constituted a significantly larger proportion of the naïve cell population, while still lacking the ability to make effector memory cells (Figure 25 G). Because BoyJ cells disproportionally constituted a larger percentage of T cells in the spleen, we employed a different gating strategy to eliminate this bias and

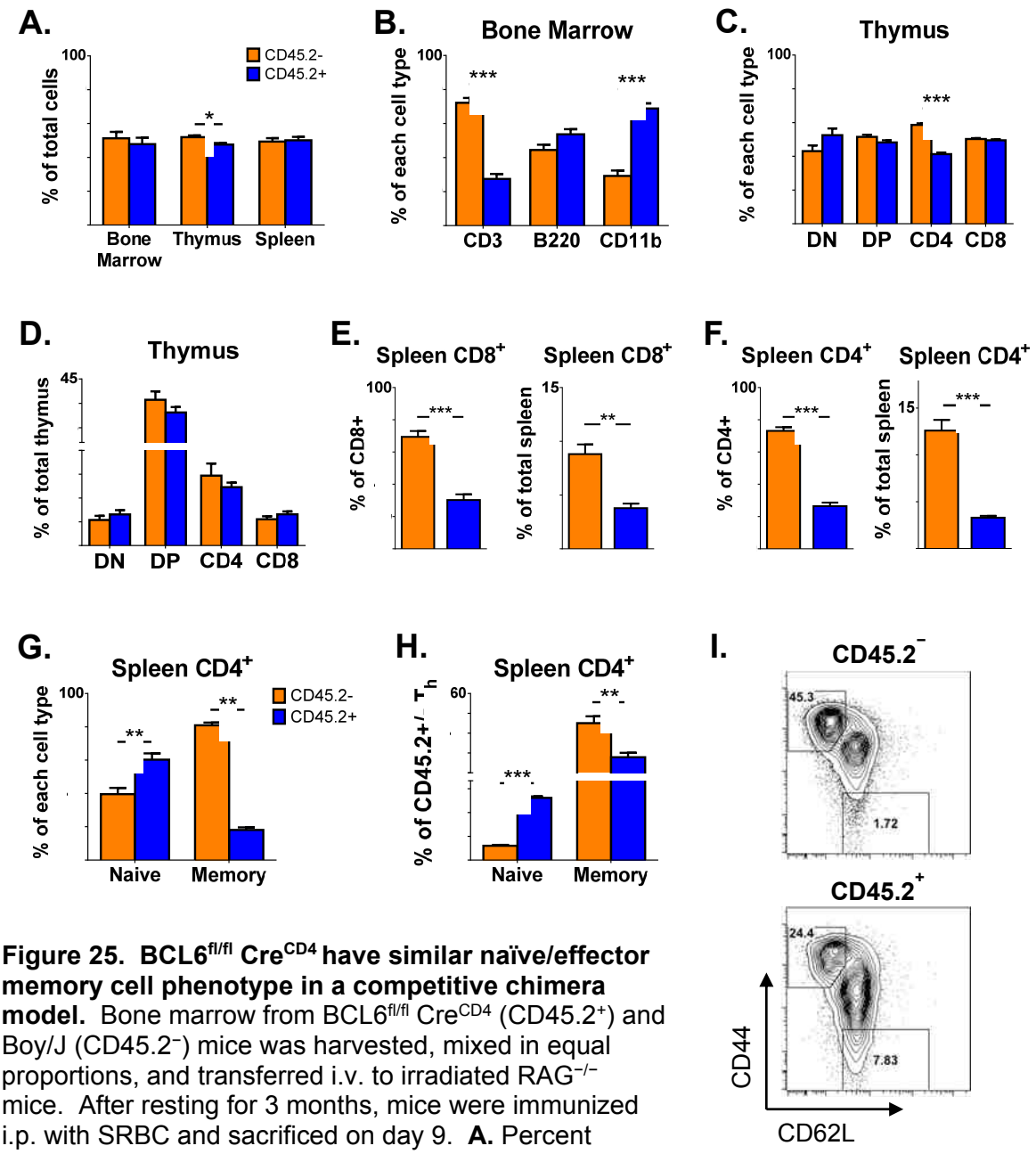

Figure 25. BCL6$^{fl/fl}$ Cre^{CD4} have similar naïve/effector memory cell phenotype in a competitive chimera model. Bone marrow from BCL6$^{fl/fl}$ Cre^{CD4} (CD45.2$^+$) and Boy/J (CD45.2$^-$) mice was harvested, mixed in equal proportions, and transferred i.v. to irradiated RAG$^{-/-}$ mice. After resting for 3 months, mice were immunized i.p. with SRBC and sacrificed on day 9. **A.** Percent reconstitution of bone marrow, thymus, and spleen. **B.** Proportion of each donor cell type found in CD3, B220, and CD11b cell subsets in bone marrow. **C.** Proportion of each donor cell type constituting double negative (DN) cells, double positive (DP), CD4$^+$, and CD8$^+$ cell populations in the thymus. Cells gated on live cells (DN), live cells, CD4$^+$, and CD8$^+$ (DP), live cells and CD4$^+$, or live cells and CD8$^+$, respectively. **D.** Percent of each cell type of total thymus cells. Cells gated as in (**C**). **E.** Proportion of each donor cell type constituting the spleen CD8$^+$ T cell population (left) and percent of each donor CD8$^+$ T cell population in the total spleen (right). Cells gated on CD3$^+$ CD8$^+$. **F.** Same populations as (**E**), except for CD4$^+$ T cells. Cells gated on CD3$^+$ CD4$^+$. **G.** Proportion of each donor cell type constituting splenic naïve and effector memory CD4$^+$ T cells. Cells gated for naïve and memory populations as in Figure B. **H.** Percent of each donor CD4$^+$ T cell population which were naïve or effector memory

cells. Cells gated, in order, on $CD3^+$ $CD4^+$ $CD45.2^{+/-}$, followed by naïve and memory gates used in Figure B. Shown as percent of $CD3^+$ $CD4^+$ $CD45.2^-$ or $CD3^+$ $CD4^+$ $CD45.2^+$ cells. N = 5; mean ± SE. **p< 0.01, ***p < 0.001 by *t* test. **I**. Representative flow plots of naïve and effector memory cells in (**H**).

investigate the ability of each donor cell type to remain naïve or become activated effector memory cells. To do this, spleen cells were first gated on total $CD3^+$ $CD4^+$ cells, then on CD45.2 expression. Next, each CD45.2 population was gated on naïve and effector memory cells, thus allowing us assess the percentage of these cell types within the context of each donor. When this was done, cells from $BCL6^{fl/fl}$ Cre^{CD4} ($CD45.2^+$) mice were still shown to have significantly more naïve cells and fewer effector memory cells compared to the proportions found in the BoyJ cell population (Figure 25 H – I). This data demonstrates an intrinsic role for BCL6 in the activation of naïve $CD4^+$ T cells.

Naïve/effector memory $CD4^+$ T cell phenotype seen early after immunization and only exacerbates over time

Next, we wanted to test the differences in these cell populations early after immunization to see if at any time the two cell populations are equivalent in +/+ and fl/fl mice. $BCL6^{+/+}$ Cre^{CD4} and $BCL6^{fl/fl}$ Cre^{CD4} mice were immunized i.p. with SRBC and sacrificed one, three, and five days after. On all days, the total $CD4^+$ T cell population was the same in

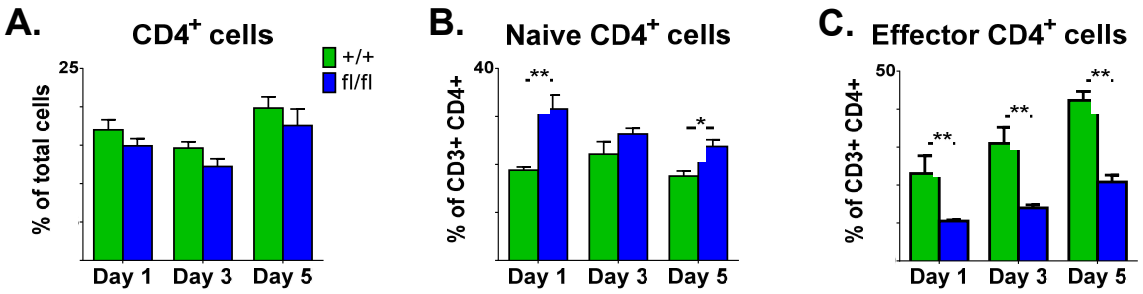

Figure 26. Effector cell defect is consistent throughout immune response in $BCL6^{fl/fl}$ Cre^{CD4} mice. $BCL6^{+/+}$ Cre^{CD4} and $BCL6^{fl/fl}$ Cre^{CD4} mice were immunized i.p. with SRBC and sacrificed 1, 3 and 5 days after immunization. Spleen cells were analyzed. **A.** $CD4^+$ T cells in spleen at each time point. Percent of total spleen. Cells gated on $CD3^+$. **B.** Naïve cells at each time point. Cells gated on $CD3^+$ $CD4^+$ $CD62L^+$ $CD44^-$. Shown as percent of Th cells. **C.** Effector memory cells at each time point. Cells gated on $CD3^+$ $CD4^+$ $CD62L^-$ $CD44^{hi}$. Shown as percent of Th cells. Mean ± SE; n = 3 – 4 per group, per time point. *p < 0.05, **p < 0.01 by *t* test.

both mice (Figure 26 A). However, like day nine, the naïve Th cells in BCL6$^{fl/fl}$ Cre^{CD4} were increased at all time points, while the effector memory population was significantly decreased on all days tested (Figure 26 B – C). This data shows that the differences in naïve and effector memory cell populations between BCL6$^{+/+}$ Cre^{CD4} and BCL6$^{fl/fl}$ Cre^{CD4} mice are seen before immunization and only increase over time after immunization.

Differences in T cell activation markers in BCL6$^{fl/fl}$ Cre^{CD4} mice

To further investigate the activation defect in T cells lacking functional BCL6, unimmunized BCL6$^{+/+}$ Cre^{CD4} mice and BCL6$^{fl/fl}$ Cre^{CD4} mice were analyzed for surface markers of activation on CD4^{+} T cells (Day 0). While the percentage of total CD4^{+} and CD4^{+} naïve T cells expressing CD25, also known as IL-2Rα, was not different between +/+ and fl/fl mice (Figure 27 A), another activation marker, CD69, decreased among total and naïve CD4^{+} T cells in BCL6$^{fl/fl}$ Cre^{CD4} mice (Figure 27 B). Therefore, while naïve BCL6$^{fl/fl}$ Cre^{CD4} mice do not have decreases in CD25^{+} Th cells, they do have fewer naïve and total CD4^{+} cells expressing the activation marker CD69.

After immunizing with SRBC, mice were again assessed for activation markers. On day nine after immunization, naïve CD4^{+} T cells from BCL6$^{fl/fl}$ Cre^{CD4} mice had significantly less CD25 expression, as well as significantly fewer Th cells expressing CD69, both total CD4^{+} and naïve CD4^{+} T cells (Figure 27 A – B). Therefore, after immunization, BCL6$^{fl/fl}$ Cre^{CD4} mice had fewer T cells expressing surface activation markers compared to BCL6$^{+/+}$ Cre^{CD4} mice. To assess activation markers at the RNA level early after immunization, mice were immunized and sacrificed as in Figure 26. Analysis of total CD4^{+} T cells revealed significant decreases at the RNA level of *il2rα* (Figure 27 C) and *ctla4* across several early time points. Transcripts of *il2*, however, were not decreased until day five (Figure 27 C). Taken together, this data strengthens the earlier findings that BCL6 plays a role in naïve CD4^{+} T cell activation.

Levels of activation differ between *in vitro* and *in vivo* stimulation

In order to better understand the global gene changes in CD4^{+} T cells in our cKO mice, two microarray analyses were done. Naïve BCL6$^{+/+}$ Cre^{CD4} mice and BCL6$^{fl/fl}$ Cre^{CD4} mice were sacrificed and naïve CD4^{+} T cells isolated from spleen via FACS. T cells

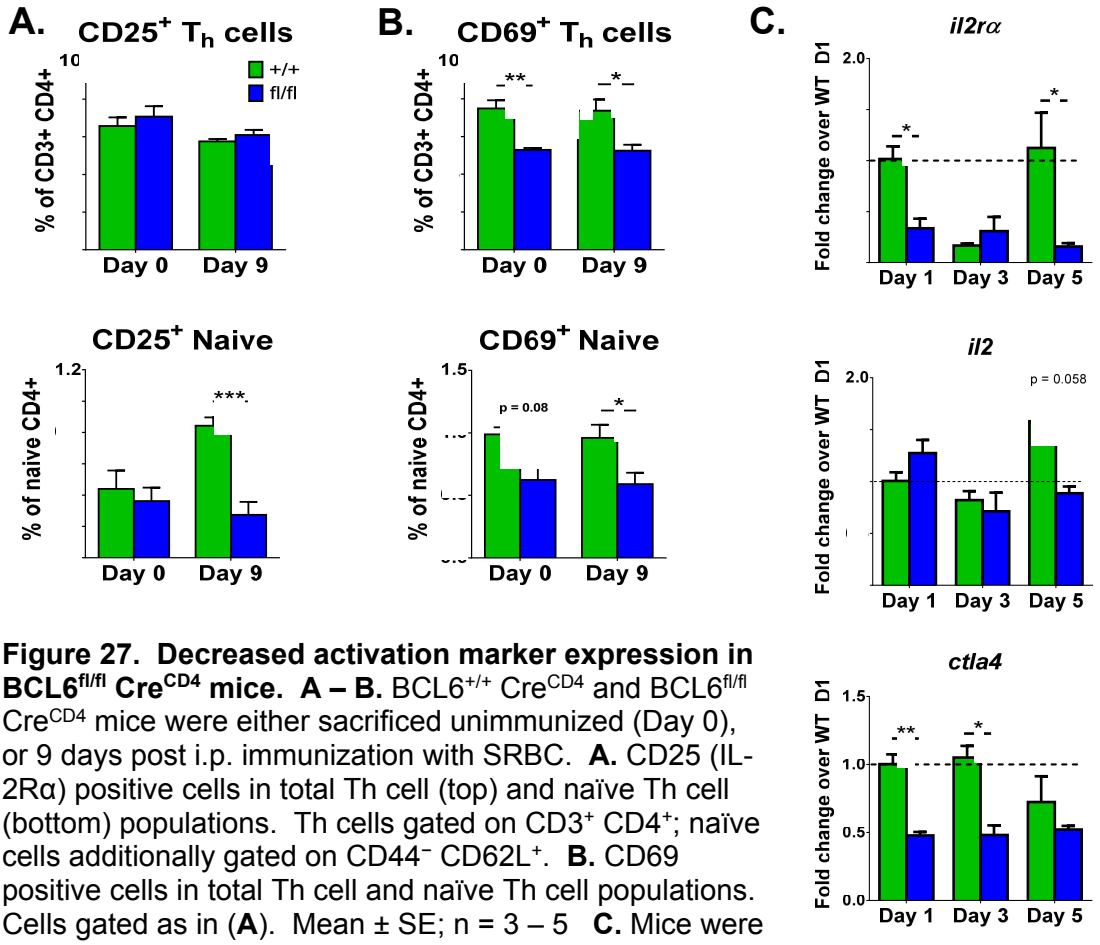

Figure 27. Decreased activation marker expression in BCL6$^{fl/fl}$ Cre^{CD4} mice. A – B. BCL6$^{+/+}$ Cre^{CD4} and BCL6$^{fl/fl}$ Cre^{CD4} mice were either sacrificed unimmunized (Day 0), or 9 days post i.p. immunization with SRBC. **A.** CD25 (IL-2Rα) positive cells in total Th cell (top) and naïve Th cell (bottom) populations. Th cells gated on CD3$^+$ CD4$^+$; naïve cells additionally gated on CD44$^-$ CD62L$^+$. **B.** CD69 positive cells in total Th cell and naïve Th cell populations. Cells gated as in (**A**). Mean ± SE; n = 3 – 5 **C.** Mice were immunized i.p. with SRBC and sacrificed 1, 3, and 5 days after. Total CD4$^+$ T cells were isolated via bead separation and lysed for RNA directly *ex vivo*. All samples normalized to +/+ Day 1 (dotted line at 1.0). Mean ± SE; n = 3 – 4 per group, per time point. *p < 0.05, **p < 0.01, ***p < 0.001 by *t* test.

were then activated *in vitro* with anti-CD3 and anti-CD28 antibodies in either Th0 or TFH culture conditions. After an overnight stimulation, cells were lysed for RNA analysis. As shown in Table 1, both culture conditions yielded similar numbers of genes significantly changed ($p < 0.05$) in fl/fl mice, compared to +/+ controls. Furthermore, the majority of those genes were down-regulated in fl/fl mice (< -1.1 fold), with only one quarter to one third being increased (> 1.1 fold). With fewer up-regulated genes in activated naïve CD4$^+$ T cells from BCL6-deficient mice, the case for BCL6 having a role in naive cell activation is strengthened.

Specific activation markers were analyzed in the microarrays (Figure 28 A). While *il2* and *il2rα* were shown to be significantly reduced in BCL6$^{fl/fl}$ Cre^{CD4} mice over time

Table 1. Summary of microarray data with BCL6$^{fl/fl}$ Cre^{CD4} T cells

	Th0 conditions	TFH conditions
# genes changed ($p < 0.05$)	3255	3502
# genes increased > 1.1 fold	824 (25%)	1102 (34%)
# genes decreased < -1.1 fold	1495 (46%)	1476 (42%)

Using Affymetrix gene expression arrays for total mouse genome, analyzing ~ 35,000 genes, naïve CD4 T cells were activated for 20 hours with anti-CD3 and anti-CD28 antibodies under either Th0 culture conditions (no cytokines or blocking antibodies), or TFH culture conditions (+IL-6 +IL-21, blocking antibodies to IFNγ, IL-4 and TGFβ). Fold increase/decrease in BCL6$^{fl/fl}$ Cre^{CD4} cells relative to BCL6$^{+/+}$ Cre^{CD4} cells.

(Figure 27 C), the microarray gave mixed results, with *il2* being significantly reduced in TFH conditions, while *il2rα* was either unchanged or slightly increased under TFH polarizing conditions (Figure 28 A). CXCR5, a surface marker up-regulated on many Th cells after initial activation, was shown to be decreased, specifically under Th0 conditions. The transcription factors *fos* and *jun* were also shown to be significantly reduced under TFH culture conditions. Lck, the protein kinase responsible for downstream signaling of TCR stimulation, was significantly reduced in both culture conditions, suggesting efficient TCR signaling is not being achieved. The gene encoding Zap70 kinase, a direct downstream target phosphorylation target of Lck kinase and critical for TCR signaling, was also significantly reduced in TFH conditions. One gene, however, *atf3*, was significantly increased in both *in vitro* conditions. Because ATF3 has been shown to limit cell proliferation, this further adds credence to the limited activation potential of naïve Th cells in BCL6$^{fl/fl}$ Cre^{CD4} mice. Interestingly, the changes seen overnight with antibody stimulation of naïve Th cells was not necessarily replicated *in vivo* in total Th cells. As already shown, *il2rα* was significantly decreased 24 hours after immunization in total CD4$^+$ T cells (Figure 27 C), but the microarray shows it unchanged or slightly increased in certain culture conditions. Likewise, while *atf3* and *fos* were shown to be significantly up and down-regulated, respectively, during the *in vitro* stimulation, total CD4$^+$ T cells analyzed *ex vivo* 24 hours after mouse immunization show this trend not to hold true for T cells of mixed activation states (Figure 28 B). In fact, *atf3* is shown to be decreased in BCL6$^{fl/fl}$ Cre^{CD4} mice over time, while *fos* never reaches significant differences at any time point after immunization. Only *cxcr5*, whose initial expression has been shown to be BCL6-independent, but prolonged expression reliant on BCL6, is consistent with the microarray data. Total Th cells had lowered *cxcr5*

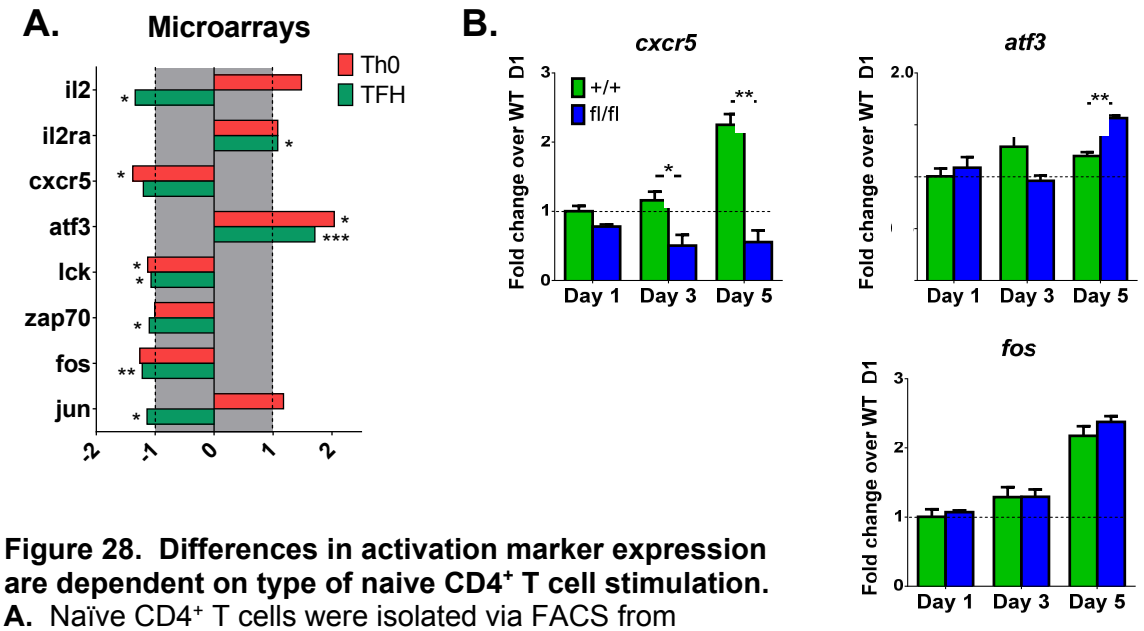

Figure 28. Differences in activation marker expression are dependent on type of naive CD4⁺ T cell stimulation. **A.** Naïve CD4⁺ T cells were isolated via FACS from unimmunized BCL6$^{+/+}$ Cre^{CD4} and BCL6$^{fl/fl}$ Cre^{CD4} mice. Cells were activated *in vitro* under Th0 or TFH culture conditions. After 20 hours, cells were lysed for RNA analysis via microarray. Bars represent gene expression in BCL6$^{fl/fl}$ Cre^{CD4} cells in the different culture conditions compared to BCL6$^{+/+}$ Cre^{CD4} mice. Differences are either greater than 1.0 or less than –1.0. *p < 0.05, **p < 0.01, ***p < 0.001. **B.** Mice were immunized i.p. with SRBC and sacrificed 1, 3, and 5 days after. Total CD4⁺ T cells were isolated via bead separation and lysed for RNA directly *ex vivo*. All samples normalized to +/+ Day 1 (dotted line at 1). Mean ± SE; n = 3 – 4 per group, per time point. *p < 0.05, **p < 0.01, by *t* test.

mRNA expression twenty four hours after immunization as well as three days after. As these are both early time points, it is likely CXCR5 gene expression is not reliant on BCL6. While overall, *in vitro* CD4⁺ T cells from BCL6$^{fl/fl}$ Cre^{CD4} mice had fewer genes activated than BCL6$^{+/+}$ Cre^{CD4} mice, the status of different activation marker genes seems to be dependent on the type and duration of stimulation.

DISCUSSION

While BCL6 has been shown to be essential for the differentiation of TFH and GC B cells, a role for BCL6 in naïve Th cell activation has not yet been established. Experiments using GL BCL6-deficient mice have not shown a lack of naïve cell activation. However, this is most likely because of the ongoing inflammatory responses in these mice. Due to this environment, T cells would be poised for activation, and

published reports have shown an increase in the effector memory populations in these mice, even when unimmunized. Here, we demonstrate, for the first time, an intrinsic role for BCL6 in naïve $CD4^+$ T cell activation.

Even when mice are not immunized and housed in a pathogen-free environment, environmental factors still exist which can trigger an immune response. Therefore, unimmunized mice have a measurable effector T cell population. In this environment, $BCL6^{fl/fl}$ Cre^{CD4} mice have a comparable effector memory cell population to $BCL6^{+/+}$ Cre^{CD4} mice, but have significantly more naïve $CD4^+$ T cells (Figure 23 E). Even over an extended period of time, untreated $BCL6^{fl/fl}$ Cre^{CD4} mice trend toward having more naïve cells and fewer activated ones (Figure 24). This would suggest that at basal levels, these mice are able to activate cells to environmental factors to the same degree as $BCL6^{+/+}$ Cre^{CD4} mice, while having an increased pool of naïve cells. Whether this naïve population has more cells of greater TCR diversity or just increased cell numbers of similar diversity cannot be determined from these studies, however, it is likely the latter.

Soon after immunization, $BCL6^{fl/fl}$ Cre^{CD4} mice fail to enhance their effector population, while retaining their naïve Th cell percentages (Figure 26 C). This would suggest the differences seen in naïve and effector memory populations in these mice is in fact due to an activation defect, and not because of loss of activated cells. If naïve cells were in fact being activated, but lost soon after to cell death, the effector cell percentages would be comparable between fl/fl and +/+ mice at earlier time points, which they are not (Figure 26 C).

A mixed bone marrow chimera was done to verify the intrinsic nature of the activation defect in $CD4^+$ T cells from $BCL6^{fl/fl}$ Cre^{CD4} mice. In this experiment, the wild type cells (BoyJ; $CD45.2^-$) were able to activate a substantial percentage of their $CD4^+$ T cells into an effector state, while cells from $BCL6^{fl/fl}$ Cre^{CD4} mice ($CD45.2^+$) retained a much higher percentage of naïve cells (Figure 25 H). These data, which verify the findings of the earlier *in vivo* experiments, demonstrate an intrinsic role for BCL6 in naïve Th cell activation. Furthermore, while the bone marrow of these mice was reconstituted with equivalent percentages of each donor cell type and the donor populations were mostly similar in the thymus, CD4 T cells in the periphery (spleen and bone marrow) were derived significantly more from BoyJ ($CD45.2^-$) donor cells. While further analysis must

be done to confirm, these data would suggest a role for BCL6 in T cell survival after exiting the thymus.

To further verify an activation defect in BCL6$^{fl/fl}$ Cre^{CD4} mice, we assessed activation marker expression in a variety of *in vivo* and *in vitro* models. CD25, also known as IL-2Rα, is an early indicator of CD4^{+} T cell activation. Th cells from unimmunized mice showed no differences in surface expression. However, after injection with SRBC, CD4^{+} T cells that were very recently presented with antigen, which is to say they are CD25^{+} but also retain naïve surface markers, had significantly fewer cells expressing CD25 when they were from BCL6$^{fl/fl}$ Cre^{CD4} mice (Figure 27 A). This would suggest that Th cells from the naïve pool in BCL6$^{fl/fl}$ Cre^{CD4} mice are not able to up-regulate this activation marker as well as BCL6$^{+/+}$ Cre^{CD4} Th cells. Furthermore, another surface marker for activation, CD69, was significantly decreased on all CD4^{+} T cells from BCL6$^{fl/fl}$ Cre^{CD4} mice, both before and after immunization, again supporting the finding of an activation defect in these mice (Figure 27 B).

At the RNA level, *il2rα* and *il2*, a cytokine up-regulated after activation, were down-regulated over time in BCL6$^{fl/fl}$ Cre^{CD4} Th cells, although not consistently. In an *in vitro* activation model assessed by microarray, only *il2* expression was found to be decreased, while *il2rα* transcripts were up-regulated (Figure 27 C, G A). These markers, however, are not the only marks of activation. Others, such as CTLA4, CXCR5, Lck, Zap70, Fos, and Jun, were all shown to be significantly down-regulated in the Th cells of BCL6$^{fl/fl}$ Cre^{CD4} mice, both in *in vivo* and *in vitro* models (Figure 27 C, G). Further indication of an activation defect in BCL6$^{fl/fl}$ Cre^{CD4} mice was exhibited by the overall results of the microarray, which showed nearly half of all genes were down-regulated in BCL6$^{fl/fl}$ Cre^{CD4} Th cells, as compared to BCL6$^{+/+}$ Cre^{CD4} cells (Table 1). Together, this surface expression data and RNA analysis demonstrates a reduced activation potential of CD4^{+} T cells in BCL6$^{fl/fl}$ Cre^{CD4} mice.

These data are not without limitations. The Th cells assessed *ex vivo* are a mixture of activated and unactivated cells. Therefore, RNA data from the time course experiment is not useful for demonstrating small nuances in gene expression changes. Instead, this data represents the overriding gene differences seen in cells, regardless of their activation status. Later time points, such as day five, have more activated cells at this

time due to clonal expansion. During *in vitro* activation, all cells have equal opportunity to achieve an active state, regardless of their TCR affinity. Therefore, data presented in the microarray is more representative of the gene changes seen soon after activation, as these cells were assessed less than 24 hours after plating. Microarray analysis is often criticized for not being as sensitive to changes as qPCR analysis is, however, many of the genes with significant changes in the microarray were confirmed with qPCR, and in most cases the differences were exacerbated with this analysis (data not shown). Taken together, the flow analysis of *in vivo* immunization models and RNA analysis of *in vitro* activated cells demonstrate an inherent activation defect in the naïve Th cells of $BCL6^{fl/fl}$ Cre^{CD4} mice.

CHAPTER 4 – ROLE OF BCL6 IN Th CELL SUBSETS

INTRODUCTION

Nearly thirty years ago researchers recognized that $CD4^+$ Th cells differentiated into distinct subsets which secrete specific cytokine profiles and are dependent on the antigen and cytokine environment present (84, 85). The original paradigm of Th1 and Th2 cells, secreting IFNγ and IL-4, respectively, has since been expanded to include many Th cell subsets, including Th17 (86, 87), Treg (88, 89), TFH (37, 38), Th9 (90, 91), and, in humans, Th22 (92, 93). Each subset has been classified based on their cytokine profile, master transcription factors, and, in the case of Treg and TFH cells, their specific activity and location (Figure 2). Because Th9 and Th22 cells are not yet as well defined as the other subsets, my work here will focus primarily on Th1, Th2, Th17, Treg, and TFH subsets.

As mentioned previously, Th1 cells are controlled by the master transcription factor Tbet, whose gene name is *tbx21* (17-19, 26). These cells will mainly respond to intracellular pathogens, such as virus and bacteria, and secrete IFNγ in response. Recent literature has shown a role for BCL6 in Th1 cells. While one group demonstrated repression of BCL6 by Tbet (94), another group demonstrated that the interaction of the two transcription factors is necessary for proper regulation of IFNγ secretion, whereby BCL6 represses Tbet-mediated IFNγ transcription in cells already producing IFNγ (95). Using a mixed bone marrow chimera, another group demonstrated an increase in IFNγ production by BCL6 KO Th cells, further supporting the findings that BCL6 is crucial for proper regulation of IFNγ secretion (39). However, these studies evaluated the role of BCL6 in Th1 cells from the stand point of Tbet KO mice and by using BCL6 GL KO mice. Therefore, as yet, no one has characterized the expression of Tbet and IFNγ in a BCL6-deficient mouse that lacks the pro-inflammatory environment of mice with a GL mutation. Our new cKO mouse model will enable us to address this issue.

Th2 cells were originally thought to be the main B cell helpers, however that role has since been attributed to TFH cells (26). Th2 cells will differentiate under the control of the master transcription factor, GATA3, and secrete the signature cytokine, IL-4 (17-20, 26).

Research by us and others has shown a role for BCL6 in Th2 cells, wherein the transcriptional repressor will limit GATA3 expression at the post-transcriptional level (61). Furthermore, in the absence of BCL6, Th2 cytokines are substantially increased, while over-expression of BCL6 leads to sharp decreases in IL-4 production (59, 61). Research using the original GL KO mice has shown a dramatic skewing of Th cells toward a Th2 phenotype. Secretion of inflammatory Th2 cytokines in these mice leads to myocarditis and pulmonary vasculitis, which is largely due to an influx of eosinophils (29, 59). However, again, these studies were done using BCL6 GL KO mice and thus carry with them the confounding effects of BCL6-deficiency in other cells. Therefore, our new mouse model will allow us to truly recognize the role of BCL6 in this Th cell subset.

The most recent Th cell subset to be fully described is Th17 cells. $CD4^+$ T cells will differentiate into Th17 cells in the presence of IL-6, IL-23 and TGFβ, and, under the control of RORγt (*rorc*), secrete its namesake cytokine, IL-17 (17, 20, 26, 63, 96). Existing literature on the role of BCL6 in Th17 cells is somewhat inconclusive. In our work, BCL6 appears to inhibit Th17 differentiation to some degree, but the gene itself is up-regulated in a Th17-inducing cytokine environment *in vitro* (97). Others have found IL-17 secretion to be enhanced in the absence of BCL6 (39). Finally, using a retroviral over-expression model, researchers have shown BCL6 to repress IL-17A and IL-17F production in an *in vitro* setting, while not affecting RORγt transcription (98). The relationship between BCL6, the master transcription factor for TFH cells, and Th17 cells is especially interesting when you consider the similarities between TFH and Th17 cells. Both cell types require IL-6 for their differentiation, both have been shown to secrete IL-21, both necessitate the phosphorylation of STAT3 for their differentiation, and both rely on c-maf, IRF4, and BATF for down-stream signaling (17, 24, 63, 96, 99, 100). We hope to better understand the relationship between BCL6 and Th17 differentiation with our new model.

An interesting dichotomy between the Th1, Th2, and Th17 subsets versus TFH cells is the reciprocal expression of BCL6 and Blimp-1. While BCL6 is highly up-regulated in TFH cells, Blimp-1 is repressed. Furthermore, while in Th1, Th2, and Th17 cells BCL6 is only present at low levels, if at all, Blimp-1 is more highly expressed (62, 99). Extensive studies have been done to investigate the role of Blimp-1, encoded by the gene *prdm1*, in Th cell subsets. For instance, researchers have found Blimp-1 to play a crucial role,

in conjunction with BCL6, in regulating the balance between Th1 and Th2 differentiation. While BCL6 has been shown to be important in Th1 cells, as mentioned above, Blimp-1 is not expressed in this subset (101). Conversely, BCL6 is repressed in Th2 cells by Blimp-1, thus allowing GATA3 expression and Th2 differentiation (101). Using Blimp-1 KO and cKO models, researchers have found that BCL6 expression is markedly enhanced in the absence of Blimp-1, also a transcriptional repressor (101-103). Furthermore, using a retroviral vector for over-expressing Blimp-1 *in vitro*, researchers have shown it can severely reduce BCL6 protein levels (62). Interestingly, most of the work regarding BCL6-Blimp-1 interactions has focused around the latter, using Blimp-1 KO mice and over-expression of Blimp-1. Once again, our mouse model, wherein BCL6 is specifically deleted in T cells, enables us to revisit the question of the relationship of these two transcriptional repressors and assess how much control BCL6 has over Blimp-1.

The final non-TFH cell subset to be discussed in this section is Treg cells. These cells, whether they be iTreg or nTreg cells, are dependent on the expression of Foxp3 (19, 104). As their name suggests, regulatory Th cells work to limit the immune response by eliminating self-reactive T cells in the periphery. While the processes by which they achieve that objective are still not fully understood, one way in which they repress such T cells is by secretion of IL-10 (105, 106). Although not exclusively produced by Treg cells, this anti-inflammatory cytokine limits Th cell activity through paracrine or autocrine signaling (107). With regards to BCL6 expression, recently, two groups have published evidence of Treg cells up-regulating the transcription factor, which triggered increased surface expression of CXCR5, facilitating the migration of these cells into the GC (35, 36). Once there, these follicular regulatory Th (TFR) cells added an additional level of regulation to the immune response. Furthermore, BCL6 has been shown to repress GATA3 in Treg cells (108). Therefore, while studies have demonstrated the dual expression of both BCL6 and Foxp3, at this time no one has yet to determine whether Foxp3 expression is reliant on BCL6, or vice versa.

With the determination that TFH cells are in fact a unique Th cell subset (37, 38, 109), and BCL6 their master transcription factor (39, 98), researchers have since worked to determine how Th cells differentiate into this subset and what effects BCL6 has in other Th subsets. The relationship between TFH cells and the other subsets is complicated.

The ability of TFH cells to produce the signature cytokines of other Th cells, as well as the ability for some subsets to express BCL6, particularly Treg cells, has only added to the controversy in the field as to whether TFH cells are a distinct subset or if they are merely a Th cell which has adopted an altered genotypic and phenotypic profile to migrate into the GC (19, 20, 26). Further complicating things is the plasticity of Th cells and their ability to change into, or adopt, partial characteristics of a different subset (17, 19). Therefore, fully understanding the role BCL6 plays in the differentiation and proliferation of non-TFH subsets may help to settle some of these disagreements concerning the plasticity of TFH cells. Here, we present data which shows little role for BCL6 in suppressing the differentiation of Th1, Th2, and Th17 subsets, while its expression seems to be essential for IL-4 secretion and expression of Foxp3 by Th cells.

MATERIALS AND METHODS

Mice and immunizations

$BCL6^{+/+}$ Cre^{CD4} and $BCL6^{fl/fl}$ Cre^{CD4} mice were generated and genotyped as described in Chapter 3. $BCL6^{\Delta ZF/\Delta ZF}$ mice were generated and genotyped as described in Chapter 2. $BCL6^{fl/fl}$ Cre^{LysM} mice were generated by mating $BCL6^{fl/fl}$ mice to B6.129P2-$Lyz2^{tm1(cre)Ifo}$/J mice (LysM-Cre), which were obtained from The Jackson Laboratory (cat. # 004781). These mice have a knock-in cre recombinase in the lysosome 2 allele, thus placing cre under the control of the Lyz2 promoter. In this model, BCL6 will be deleted in all myeloid cells. Because the LysM-Cre recombinase is a knock-in allele, only mice heterozygous for cre will be functional conditional knockout mice. Therefore, two different genotypings must be done for cre recombinase: one for the wild type allele, and one for the knock-in.

The following primer sets were used for LysM cre typing:

WT forward (5’ –TTACAGTCGGCCAGGCTGAC– 3’)
WT reverse (5’ –CTTGGGCTGCCAGAATTTCTC– 3’)
Knock-in forward (5’ –ATCGCCATCTTCCAGCAGGCGCAC– 3’)
Knock-in reverse (5’ –ATTTCCGTCTCTGGTGTAGCTGAT– 3’)

The following primer sets were used to detect the BCL6 floxed allele:

5’ loxP forward (5’ –TGAAGACGTGAAATCTAGATAGGC– 3’)
5’ loxP reverse (5’ –ACCCATAGAAACACACTATACATC– 3’)
3’ loxP forward (5’ –TCACCA ATCCCAGGTCTCAGTGTG– 3’)
3’ loxP reverse (5’ –CTTTGTCATATTTCTCTGGTTGCT– 3’)

Mice were immunized i.p. with 1 x 10^9 sheep red blood cells (SRBC; Rockland Immunochemicals Inc., Gilbertsville, PA) in PBS.

Flow cytometry

Total spleen or thymus cells were incubated with anti-mouse CD16/CD32 (Fcγ receptor) for 20 minutes, followed by surface staining for the indicated markers. A fixable viability dye (eFluor 780, eBioscience) was used for all samples. The following antibodies were used to stain naïve and memory T cells: α-mCD3 Alexa Fluor 700, clone 500A2 (BD Bioscience); α-mCD4 PECy7, clone RM4-5 (BD Bioscience); α-mCD8a APC, clone 53-6.7 (BD Bioscience); α-mCD44 PE, clone IM7 (eBioscience); α-mCD62L FITC, clone MEL-14 (BD Bioscience). For Tbet staining, cells were fixed and permeabilized using the Foxp3 / Transcription Factor Staining Buffer Set (eBioscience) according to manufacturer guidelines. Intracellular cytokine staining (ICS) was done as follows: cells were stained for surface markers, followed by a fixable viability dye (eBioscience). Cells were fixed for 10 minutes in the dark at room temperature in 2% formaldehyde. Cells were washed 1x with PBS, then 2x in permeabilization buffer (0.1% saponin + 2% BSA in PBS). Cells were then stained for α-mIL-4 APC, clone 11B11 (eBioscience), α-mIL-17A PE, clone eBio17B7 (eBioscience), α-mIFNγ Alexa Fluor 488 , clone XMG1.2 (Biolegend), and α-mIL-10 PECy7, clone JES5-16E3 (Biolegend) for 30 minutes at 4 °C in permeabilization buffer, washed, and analyzed via flow cytometry. Samples were run on a BD LSR II flow cytometer using FACSDiva software. Data was analyzed using FlowJo software.

Cell isolation and *in vitro* stimulation

Total $CD4^+$ T cells were isolated via magnetic bead separation (Miltenyi Biotec); effector memory cells (EM), central memory cells (CM), and naïve $CD4^+$ T cells were isolated via FACS. EM cells were gated on $CD3^+$ $CD4^+$ $CD44^{hi}$ $CD62L^-$, CM cells gated on $CD3^+$

$CD4^+$ $CD44^{hi}$ $CD62L^+$, and naïve cells gated on $CD3^+$ $CD4^+$ $CD44^-$ $CD62L^+$. Propidium iodide was used as a viability gate.

Naïve, EM, and CM cells were stimulated with plate-bound anti-CD3 (5 μg/ml) and anti-CD28 (10 μg/ml) antibodies (BD Biosciences) for varying times at $1x10^6$ cells/mL. Total spleen cells were stimulated with LPS for 24 hours at $1x10^7$ cells/mL. Th0 media contains no cytokines or blocking antibodies; ThN media contains anti-IFNγ and anti-IL-4 blocking antibodies (10 μg/mL) (R&D Systems); TFH media contains anti-IFNγ (10 μg/mL), anti-IL-4 (10 μg/mL) and anti-TGFβ (20 μg/mL) (R&D Systems) blocking antibodies, as well as IL-6 and IL-21 cytokines (50 ng/mL each) (PeproTech). Th1 media contains anti-IL-4 (10 μg/mL) blocking antibody plus IL-12 (10 ng/mL) (PeproTech); Th2 media contains anti-IFNγ (10 ug/mL) blocking antibody plus IL-4 (10 ng/mL) (PeproTech); Th17 media contains anti-IL-4 and anti-IFNγ (10 ug/mL each) blocking antibodies plus IL-6 (10 ng/mL) and TGFβ (1 ng/mL) (PeproTech).

Gene expression analysis

Total RNA was prepared using a kit (Qiagen) after lysis of the cells via Trizol (Life Technologies); cDNA was prepared with the Transcriptor First Strand cDNA synthesis kit (Roche). Quantitative PCR (qPCR) reactions were run by assaying each sample in triplicates using the Fast Start Universal SYBR Green Mix (Roche Applied Science) with custom primers or specific Taqman assays (ABI). Assays were run with a Stratagene Mx3000P Real-Time QPCR machine. Levels of mRNA expression were normalized to beta-tubulin mRNA levels, and differences between samples analyzed using the ΔΔCT method. Total cellular RNA was prepared and analyzed for gene expression as described in Chapter 2. Custom primers used with SYBR Green analysis were *prdm1, il4, ifnγ, il17a,* and *il10*; primers used with Taqman assays were *tbx21, rorc, foxp3,* and *gata3*.

Microarrays

Naïve $CD4^+$ T cells were isolated via FACS using the following surface markers: $CD3^+$ $CD4^+$ $CD62L^+$ $CD44^-$. A cell viability gate was also used. Cells were activated *in vitro* with anti-CD3 and anti-CD28 antibodies, as described above, in Th0 or TFH media

conditions. TFH conditions contain IL-6 and IL-21 [10 ng/ml each (R&D Systems)], plus anti-IFNγ (10 μg/mL), anti-IL-4 (10 μg/mL), and anti–TGF-β (20 μg/mL) antibodies. Cells were cultured for 20 hours. Cells were lysed, RNA prepared using an RNeasy kit (Qiagen), and cDNA prepared with the Transcriptor First Strand cDNA synthesis kit (Roche). Affymetrix gene expression microarrays were carried out by Center for Medical Genomics at the Indiana University School of Medicine.

Thymidine incorporation assay

Naïve $CD4^+$ T cells were isolated via FACS; cells were gated on $CD3^+$ $CD4^+$ $CD62L^+$ $CD44^-$. Cells were then activated in Th0 media with different concentrations of anti-CD3 and anti-CD28 antibodies (BD Bioscience) in round bottom, 96-well plates; 20,000 cells/well in 100 uL media. Some cells were e plated without antibodies to measure baseline proliferations (0x0). Other concentration combinations include 1 ug/mL anti-CD3 + 2 ug/mL anti-CD28, 5 ug/mL anti-CD3 + 2 ug/mL anti-CD28, and 10 ug/mL anti-CD3 + 10 ug/mL anti-CD28. After 48 hours, tritiated thymidine was added at 1 uCi per well. Eighteen hours later, plates were frozen and later thawed and assessed for thymidine incorporation via a scintillation counter. Incorporation presented as corrected counts per minute (CCPM). Data points for cells activated with antibodies have respective baseline counts (0x0) subtracted.

Statistical analysis

Statistical analysis was done using IBM SPSS Statistics 21 software. Statistics for microarray data was done using GraphPad Prism software. In all figures, $*p < 0.05$, $**p < 0.01$, $***p < 0.001$.

RESULTS

Transcription levels of BCL6 vary with *in vitro* and *in vivo* stimulation

During *in vivo* immunization, BCL6 is up-regulated in Th cells, particularly in those which will become TFH cells. In $BCL6^{+/+}$ Cre^{CD4} mice, without immunization (i.e. PBS given as

a control injection) we see BCL6 expressed at basal levels in total CD4$^+$ T cells (Figure 29 A). Nine days after immunization with SRBC, these T cells, without *ex vivo* stimulation, have a significant increase in BCL6 transcript levels (Figure 29 A). Therefore, *in vivo* immunization with SRBC is a reliable method for inducing BCL6 in CD4$^+$ T cells.

In order to assess the effects of stimulating T cells *ex vivo* after immunization, a time course experiment was done to study increases in BCL6 expression over the duration of the immune response. BCL6$^{+/+}$ Cre^{CD4} mice were immunized with SRBC and sacrificed one, three, and five days after the injections. Total CD4$^+$ T cells were isolated from spleen and either lysed directly *ex vivo* or stimulated *in vitro* with antibodies for 24 hours before being lysed for RNA analysis. RNA from cells lysed directly *ex vivo* show levels of BCL6 significantly increasing by day five after immunization (Figure 29 B). However, when the same T cells were stimulated overnight, the amount of BCL6 RNA was significantly decreased at all time points (Figure 29 B). This demonstrates the detrimental effect *in vitro* stimulation has on already high levels of BCL6 transcript. In

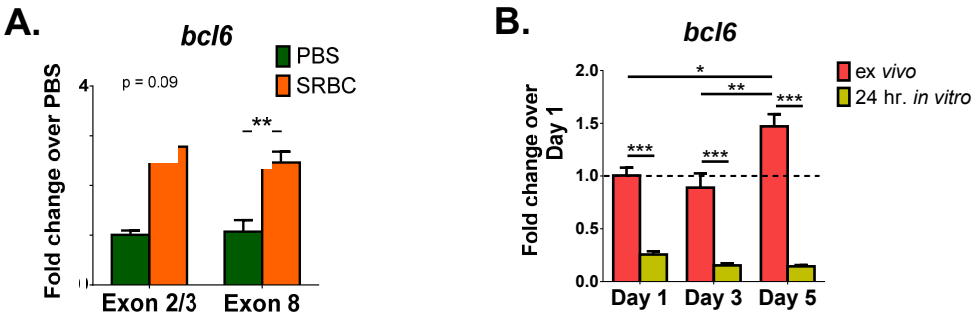

Figure 29. Induction of BCL6 following immunization. A. BCL6$^{+/+}$ Cre^{CD4} mice were immunized i.p. with SRBC or PBS as a control. Mice were sacrificed 9 days after and total CD4$^+$ T cells were isolated from spleen via bead separation. Cells were lysed directly *ex vivo* for RNA analysis. Samples were analyzed for BCL6 exon 2/3 and exon 8 expression via qPCR. Samples normalized to PBS samples for each exon. Mean ± SE; **p < 0.01 by *t* test. **B.** BCL6$^{+/+}$ Cre^{CD4} mice were immunized i.p. with SRBC and sacrificed 1, 3, and 5 days after. Total CD4$^+$ T cells were isolated from spleen via bead separation. Half the isolated cells were lysed directly *ex vivo* for RNA analysis and half were stimulated for 24 hours with anti-CD3 and anti-CD28 antibodies in Th0 media before being lysed for RNA analysis. Samples were analyzed via qPCR for BCL6 exon 8 expression. All samples are normalized to Day 1 *ex vivo* lysed cells (dotted line at 1.0). Mean ± SE; *p < 0.05, **p < 0.01, ***p < 0.001 by 2-way ANOVA; Tukey post hoc.

fact, the higher the transcript levels were in the *ex vivo* samples, the lower the levels seem to be in the stimulated samples. Therefore, this data serves as a caution for the interpretation of *in vitro* stimulated results. While we expect BCL6 levels to be notably high in the Th cells of immunized mice, as is shown in Figure 29 A, *in vitro* stimulation significantly abrogates these levels, and thus could be changing any downstream effects of high BCL6 expression. Therefore, whenever possible, we present data from cells harvested directly *ex vivo* without *in vitro* stimulation, as this is shown to alter BCL6 expression in WT Th cells.

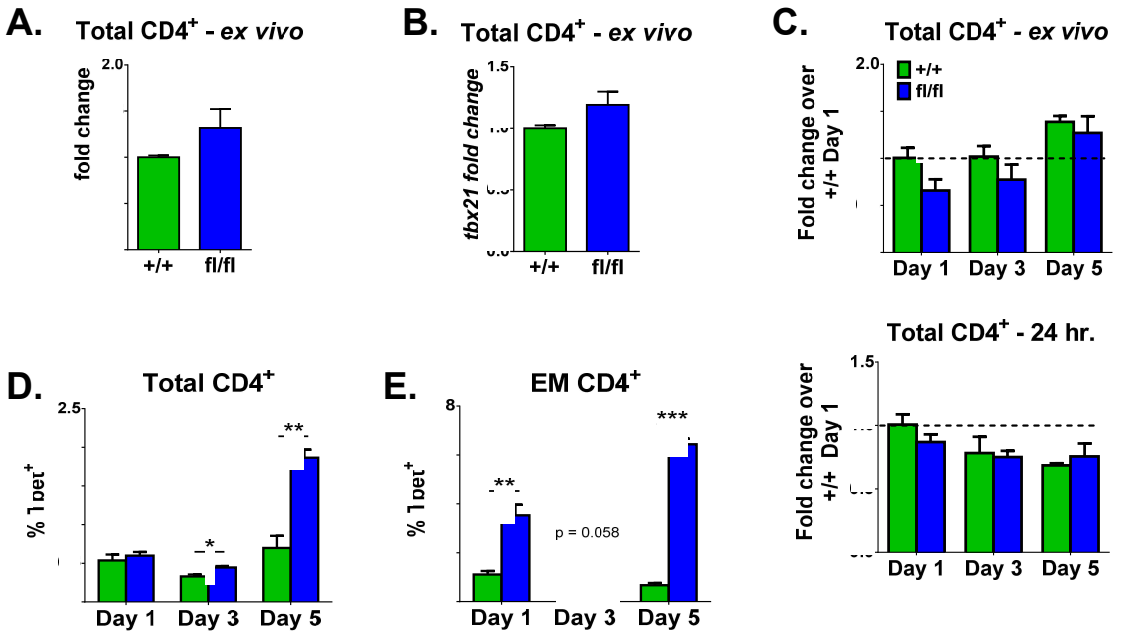

Figure 30. Tbet transcript levels in the absence of BCL6 *in vivo*. A. RNA expression of *tbx21* in total CD4$^+$ T cells from unimmunized BCL6$^{+/+}$ Cre^{CD4} and BCL6$^{fl/fl}$ Cre^{CD4} mice. Total CD4$^+$ T cells isolated via bead separation and lysed for RNA analysis directly *ex vivo*. **B.** RNA expression of *tbx21* in mice immunized i.p. with SRBC and sacrificed on day 9. Total CD4$^+$ T cells isolated via bead separation and lysed for RNA analysis directly *ex vivo*. **C.** BCL6$^{+/+}$ Cre^{CD4} and BCL6$^{fl/fl}$ Cre^{CD4} mice were immunized i.p. with SRBC and sacrificed 1, 3, and 5 days after. Total CD4$^+$ T cells were isolated via bead separation. RNA expression of *tbx21* in cells directly *ex vivo* (top) or after 24 stimulation with anti-CD3 and anti-CD28 antibodies in Th0 media (bottom). Samples normalized to Day 1 +/+ (dotted line at 1.0). **D.** Mice were immunized and sacrificed as in (**C**). CD4$^+$ T cells were stained for expression of Tbet. Cells gated on CD3$^+$ CD4$^+$. **E.** Percent of effector memory (EM) cells expressing Tbet in mice from (**D**). Mean ± SE; *p < 0.05, **p < 0.01, ***p < 0.001 by *t* test.

The role of BCL6 in Th1 cells

BCL6 has been shown to interact with Tbet in multiple models. Here, using our new cKO mouse model, we show minimal effects of BCL6 loss on Th1 differentiation. When total $CD4^+$ T cells were isolated from unimmunized $BCL6^{+/+}$ Cre^{CD4} and $BCL6^{fl/fl}$ Cre^{CD4} mice and analyzed for Tbet transcript directly *ex vivo*, $BCL6^{fl/fl}$ Cre^{CD4} mice showed only marginally increases in *tbx21* levels (Figure 30 A). The same was seen in Th cells from mice immunized with SRBC and sacrificed on day nine (Figure 30 B).

To investigate whether *tbx21* transcript levels were significantly increased earlier in the immune response, a time course experiment was done in which mice were immunized with SRBC and sacrificed one, three, and five days after immunization. In cells lysed directly *ex vivo* for RNA, *tbx21* levels were similar, with cells from $BCL6^{fl/fl}$ Cre^{CD4} mice showing slightly decreased levels at earlier time points (Figure 30 C). When cells were stimulated *ex vivo* for 24 hours, still no differences were seen over five days. Interestingly, while cells analyzed *ex vivo* show a slight increase in *tbx21* levels over time, those stimulated overnight seemed to have decreased *tbx21* transcript over time. However, the levels of *tbx21* transcript seen in total $CD4^+$ T cells did not replicate at the protein level. When total Th cells were analyzed for Tbet via flow cytometry, $BCL6^{fl/fl}$ Cre^{CD4} mice significantly increased protein levels over $BCL6^{+/+}$ Cre^{CD4} cells beginning on day three (Figure 30 D). When the effector memory (EM) population, which are highly activated Th cells, was specifically analyzed, we saw increases in Tbet at all time points (Figure 30 E). Therefore, while *tbx21* transcript levels were minimally affected by loss of BCL6 in $BCL6^{fl/fl}$ Cre^{CD4} mice, Tbet protein levels were significantly elevated in the absence of BCL6.

To fully understand if there is skewing of Th cells toward a Th1 type in $BCL6^{fl/fl}$ Cre^{CD4} mice, $CD4^+$ T cells were analyzed for IFNγ expression and secretion. After immunization with SRBC, $BCL6^{+/+}$ Cre^{CD4} and $BCL6^{fl/fl}$ Cre^{CD4} mice were sacrificed on day nine. Total $CD4^+$ T cells were isolated and stimulated with antibodies overnight or with PMA and ionomycin for five hours and cytokines analyzed via flow cytometry. Analysis of overnight supernatants from +/+ and fl/fl Th cells showed no difference in IFNγ concentrations, as was also the case for $CD4^+$ T cells analyzed via flow cytometry for intracellular cytokine staining (ICS) (Figure 31 A-C). When transcript levels of *ifnγ*

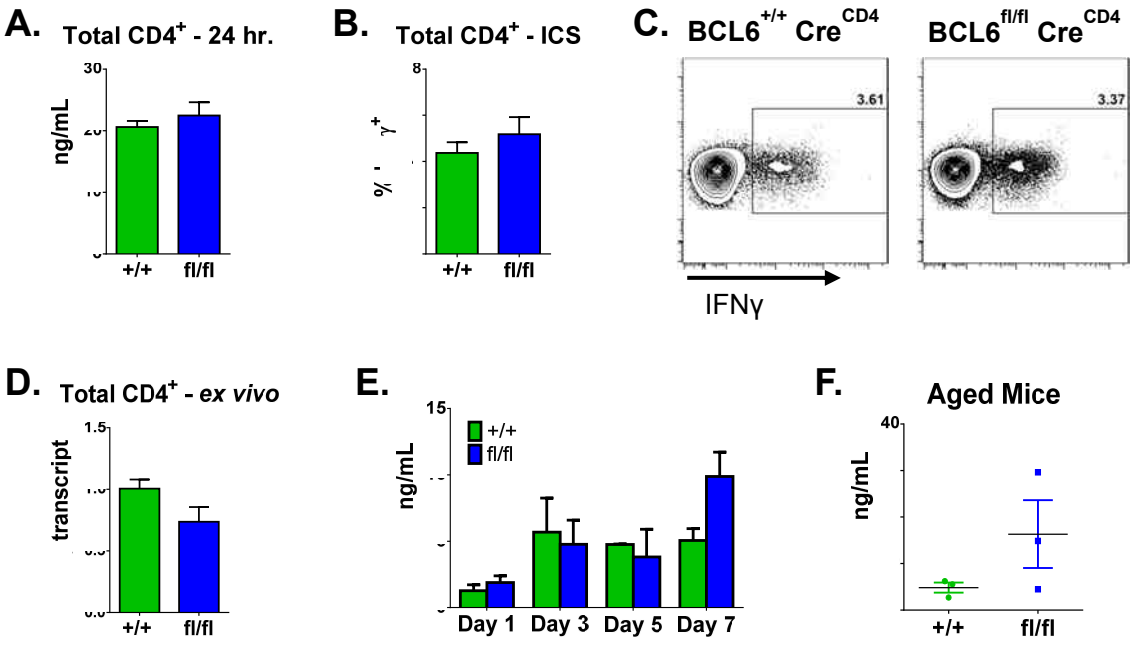

Figure 31. IFNγ expression in the absence of BCL6. A. BCL6$^{+/+}$ Cre^{CD4} and BCL6$^{fl/fl}$ Cre^{CD4} mice were immunized i.p. with SRBC and sacrificed on day 9. Total CD4$^+$ T cells were isolated from spleen via bead separation and stimulated *in vitro* with anti-CD3 and anti-CD28 antibodies in Th0 media for 24 hours. Supernatants were analyzed for IFNγ via ELISA. **B.** Mice were immunized and sacrificed as in (**A**). Total CD4$^+$ T cells were isolated from spleen via bead separation and stimulated for 5 hours *in vitro* with PMA and ionomycin. IFNγ levels were assessed via ICS. Cells gated on CD3$^+$ CD4$^+$. **C.** Representative flow plots of ICS in (**B**). **D.** Mice were immunized, sacrificed, and CD4$^+$ T cells isolated as in (**A**). T cells were lysed directly *ex vivo* for RNA analysis. IFNγ transcript levels assessed via qPCR; normalized to +/+. **E.** BCL6$^{+/+}$ Cre^{CD4} and BCL6$^{fl/fl}$ Cre^{CD4} mice were immunized i.p. with SRBC and sacrificed 1, 3, 5, and 7 days afterward. Total CD4$^+$ T cells were isolated via bead separation and stimulated for 24 hours with anti-CD3 and anti-CD28 antibodies in Th0 media. Supernatants were assessed for IFNγ via ELISA. **F.** BCL6$^{+/+}$ Cre^{CD4} and BCL6$^{fl/fl}$ Cre^{CD4} mice were aged to 13 months and sacrificed without immunization. Total CD4$^+$ T cells were isolated via bead separation and stimulated for 24 hours with anti-CD3 and anti-CD28 antibodies in Th0 media. IFNγ levels in supernatants were measured via ELISA. Mean ± SE.

were assessed in total CD4$^+$ cells taken directly *ex vivo* from the spleen, BCL6$^{fl/fl}$ Cre^{CD4} T cells showed only a marginal decrease in RNA levels (Figure 31 D). Therefore, there is little difference in IFNγ expression and secretion in the Th cells of BCL6$^{fl/fl}$ Cre^{CD4} mice nine days after immunization, as compared to BCL6$^{+/+}$ Cre^{CD4} mice.

Conversely, to assess changes in IFNγ at earlier time points after immunization, mice were injected with SRBC and sacrificed one, three, five, and seven days afterward.

While BCL6$^{fl/fl}$ Cre^{CD4} mice did not have significantly higher levels of IFNγ at any time point, the CD4^{+} T cells did trend toward more IFNγ on day seven (Figure 31 E).

To investigate whether Th1 skewing occurs later in the life of BCL6$^{fl/fl}$ Cre^{CD4} mice, both cKO and control mice were aged for thirteen months. Without immunization, total CD4^{+} T cells were isolated from spleen and stimulated overnight with antibodies. While IFNγ levels in the supernatant of BCL6$^{fl/fl}$ Cre^{CD4} mice was slightly increased compared to control mice, the difference was not significant (Figure 31 F).

While *in vivo* modeling is important to understand changes of physiological relevance, we also wanted to investigate whether Th1 skewing of BCL6$^{fl/fl}$ Cre^{CD4} naïve Th cells occurs *in vitro* under a variety of culture conditions. When naïve CD4^{+} T cells were isolated from cKO and control mice, then activated under Th0, ThN, or TFH culture conditions overnight, *tbx21* transcript levels were found to be significantly increased in BCL6$^{fl/fl}$ Cre^{CD4} cells in non-skewing Th0 conditions, while these mice had significantly less *tbx21* expression under TFH culture conditions (Figure 32 A). To examine whether the increase in *tbx21* levels in Th0 culture conditions was due to increased IFNγ secretion working in an autocrine fashion, naïve CD4^{+} T cells were activated with antibodies for 24 hours in Th0 media. No differences in IFNγ secretion from +/+ and fl/fl Th cells were found (Figure 32 B). Therefore, the increase in *tbx21* transcript in naïve Th cells under non-skewing culture conditions is likely due to intrinsic factors. When naïve Th cells were activated *in vitro* for five days, a significant decrease in IFNγ production was found in the absence of BCL6 (Figure 32 C). Therefore, while the cytokine levels of total CD4^{+} T cells from *in vivo* immunized mice were unchanged over several time points, it appears IFNγ secretion in *in vitro* activated cells requires expression of BCL6 to sustain its levels over time. Interestingly, EM cells, which are Th cells that have been activated *in vivo*, from unimmunized mice showed no difference in IFNγ levels after overnight *in vitro* stimulation (Figure 32 B). Therefore, differences in IFNγ secretion by activated Th cells may be altered by the *in vitro* stimulation itself.

Under neutral culture conditions, i.e. blocking IFNγ and IL-4, Tbet transcript levels increased significantly over time in BCL6$^{fl/fl}$ Cre^{CD4} cells compared to BCL6$^{+/+}$ Cre^{CD4} cells (Figure 32 D). Therefore, in the absence of IFNγ signaling, BCL6 may be working to limit *tbx21* expression over time. Finally, when naïve CD4^{+} T cells were isolated from

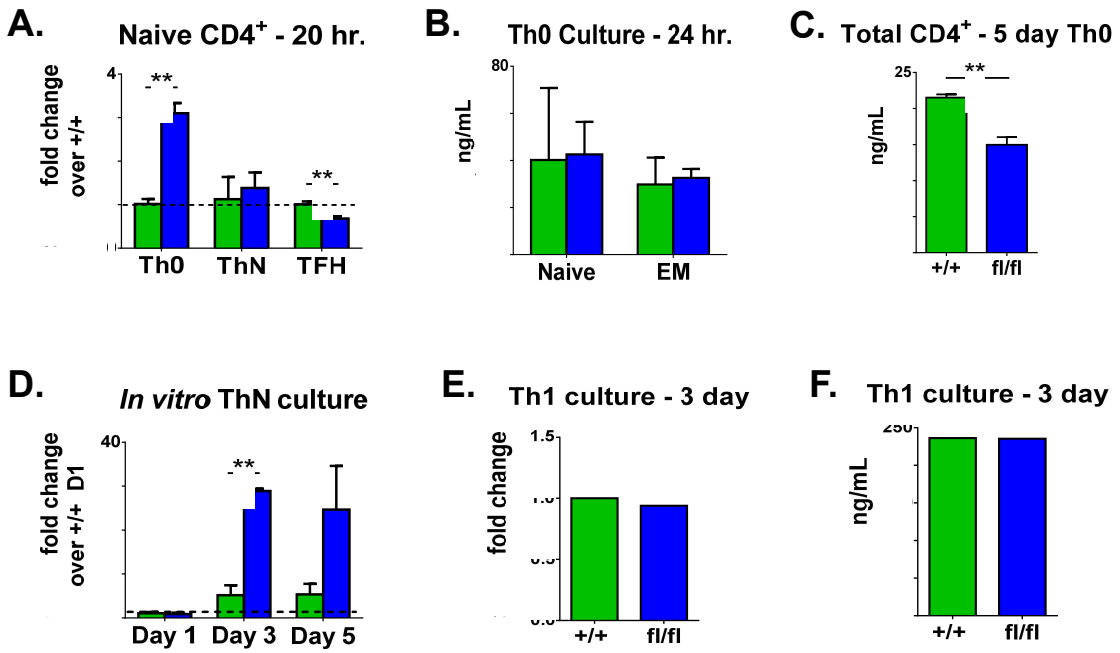

Figure 32. Tbet, but not IFNγ, is increased in the absence of BCL6 in *in vitro* cultures. A. Naïve CD4^{+} T cells were isolated from BCL6$^{+/+}$ Cre^{CD4} or BCL6$^{fl/fl}$ Cre^{CD4} mice via FACS and stimulated with anti-CD3 and anti-CD28 antibodies in Th0, ThN, or TFH culture conditions for approximately 20 hours. RNA expression of *tbx21* was assessed by microarray (Th0) or qPCR (ThN and TFH) analysis. **B.** Naïve and effector memory (EM) cells were isolated from unimmunized mice via FACS. Cells were stimulated with anti-CD3 and anti-CD28 antibodies in Th0 culture conditions for 24 hours. IFNγ concentrations in supernatants measured via ELSA. **C.** Total CD4^{+} T cells were isolated from unimmunized mice via bead separation and activated as in (**B**) in Th0 media for 5 days. After a 6 hour restimulation with anti-CD3 and anti-CD28, supernatants were collected and tested for IFNγ secretion via ELISA. **D.** Naïve CD4^{+} T cells were isolated via FACS and stimulated with anti-CD3 and anti-CD28 antibodies in ThN culture conditions. Cells were harvested and analyzed 1, 3, and 5 days after stimulation for *tbx21* RNA expression via qPCR. **E.** Naïve CD4^{+} T cells were isolated via FACS and activated with anti-CD3 and anti-CD28 antibodies under Th1 polarizing culture conditions for 3 days, then restimulated in Th0 conditions for 6 hours. RNA levels of *tbx21* were assessed via qPCR. **F.** Cells from (**E**) were also restimulated in Th0 conditions for 18 hours and supernatant collected for analysis via ELISA. Mean ± SE; **p < 0.01 via *t* test.

BCL6$^{+/+}$ Cre^{CD4} and BCL6$^{fl/fl}$ Cre^{CD4} mice and activated under Th1 skewing conditions for three days, no differences in *tbx21* transcript levels or IFNγ secretion was seen (Figure 32 E – F).

The role of BCL6 in Th2 cells

Published literature has shown that BCL6 can limit Th2 differentiation. However those studies were done using GL KO mice. Here, we are able to assess BCL6's role in these Th cells without the confounding effects of the inflammatory environment seen in the original GL KO mice.

When total $CD4^+$ T cells were tested for GATA3 transcript in $BCL6^{+/+}$ Cre^{CD4} and $BCL6^{fl/fl}$ Cre^{CD4} mice both before and after immunization, no differences in RNA levels were seen. Naïve mice had no significant differences in *gata3* expression; however fl/fl mice trended toward slightly higher levels (Figure 33 A). After immunization, on day nine (Figure 33 B), as well as earlier in the immune response (Figure 33 C-top), no significant differences were seen in *gata3* transcript levels. Stimulating cells overnight with antibodies only further equalized the levels between +/+ and fl/fl Th cells (Figure 33 C-bottom).

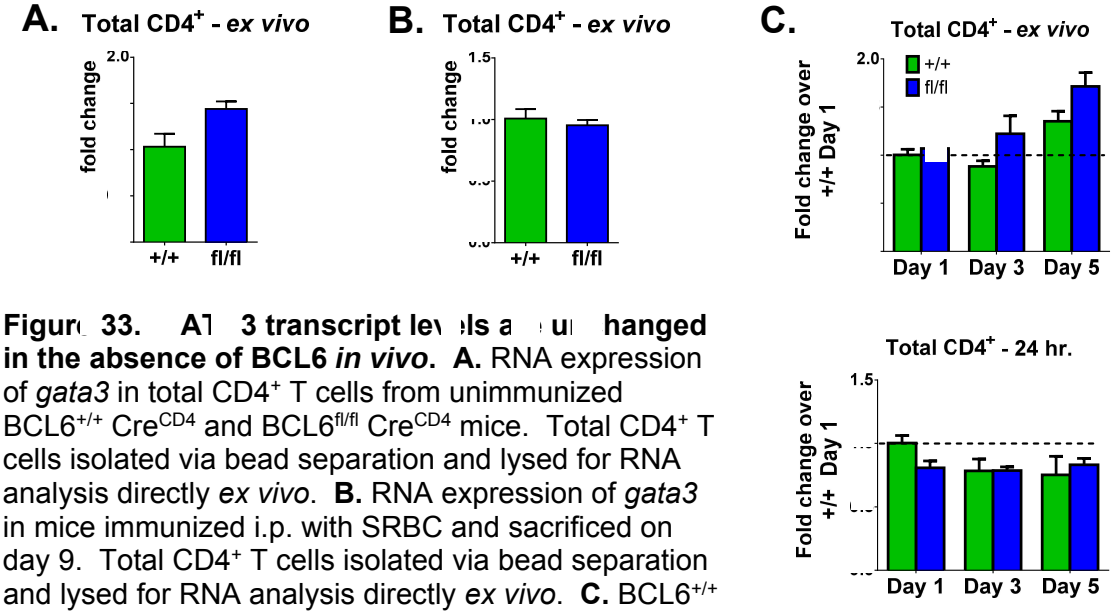

Figur 33. A 3 transcript le ls a u hanged in the absence of BCL6 *in vivo*. A. RNA expression of *gata3* in total $CD4^+$ T cells from unimmunized $BCL6^{+/+}$ Cre^{CD4} and $BCL6^{fl/fl}$ Cre^{CD4} mice. Total $CD4^+$ T cells isolated via bead separation and lysed for RNA analysis directly *ex vivo*. **B.** RNA expression of *gata3* in mice immunized i.p. with SRBC and sacrificed on day 9. Total $CD4^+$ T cells isolated via bead separation and lysed for RNA analysis directly *ex vivo*. **C.** $BCL6^{+/+}$ Cre^{CD4} and $BCL6^{fl/fl}$ Cre^{CD4} mice were immunized i.p. with SRBC and sacrificed 1, 3, and 5 days after. Total $CD4^+$ T cells were isolated via bead separation. RNA expression of *gata3* in cells lysed directly *ex vivo* (top) or after 24 stimulation with anti-CD3 and anti-CD28 antibodies (bottom) in Th0 media. Samples normalized to Day 1 +/+ (dotted line at 1.0). Mean ± SE.

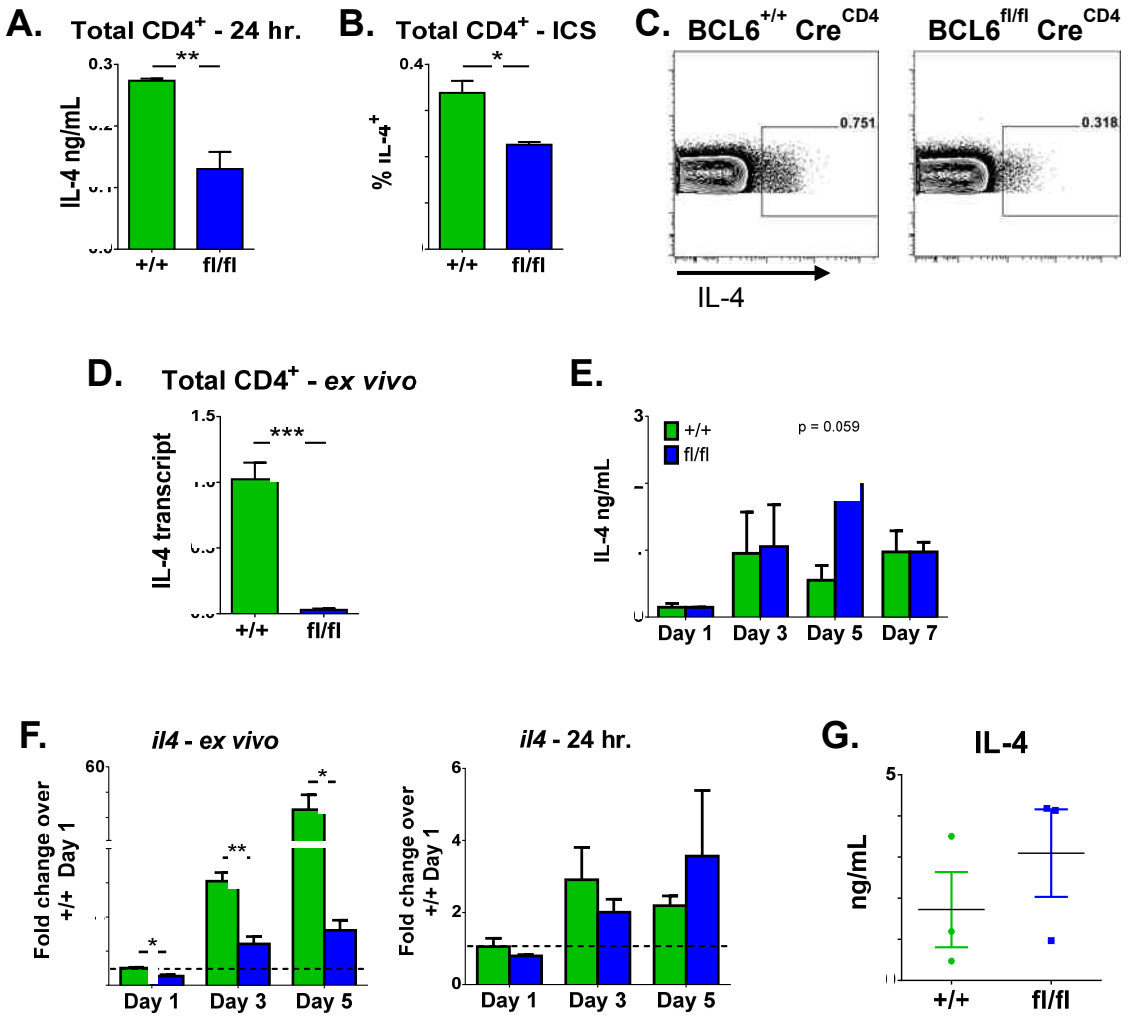

Figure 34. IL-4 is decreased in BCL6-deficient CD4⁺ T cells. A. BCL6$^{+/+}$ Cre^{CD4} and BCL6$^{fl/fl}$ Cre^{CD4} mice were immunized i.p. with SRBC and sacrificed on day 9. Total CD4⁺ T cells were isolated from spleen via bead separation and stimulated *in vitro* with anti-CD3 and anti-CD28 antibodies in Th0 media for 24 hours. Supernatants were analyzed for IL-4 via ELISA. **B.** Mice were immunized and sacrificed as in (**A**). Total CD4⁺ T cells were isolated from spleen via bead separation and stimulated for 5 hours *in vitro* with PMA and ionomycin. IL-4 levels were assessed via ICS. Cells gated on CD3⁺ CD4⁺. **C.** Representative flow plots of ICS in (**B**). **D.** Mice were immunized, sacrificed, and CD4⁺ T cells isolated as in (**A**). T cells were lysed directly *ex vivo* for RNA analysis. IL-4 transcript levels assessed via qPCR; normalized to +/+. **E.** BCL6$^{+/+}$ Cre^{CD4} and BCL6$^{fl/fl}$ Cre^{CD4} mice were immunized i.p. with SRBC and sacrificed 1, 3, 5, and 7 days afterward. Total CD4⁺ T cells were isolated via bead separation and stimulated for 24 hours with anti-CD3 and anti-CD28 antibodies in Th0 media. Supernatants were assessed for IL-4 via ELISA. **F.** Mice were immunized and sacrificed as in (**E**). Total CD4⁺ T cells were isolated via bead separation. RNA expression of *il4* in cells lysed directly *ex vivo* (left) or after 24 stimulation with anti-CD3 and anti-CD28 antibodies in Th0 media (right). Samples normalized to Day 1 +/+ (dotted line at 1.0). **G.** BCL6$^{+/+}$

Cre^{CD4} and $BCL6^{fl/fl}$ Cre^{CD4} mice were aged to 13 months and sacrificed without immunization. Total $CD4^+$ T cells were isolated via bead separation and stimulated for 24 hours with anti-CD3 and anti-CD28 antibodies in Th0 media. IL-4 levels in supernatants were measured via ELISA. Mean ± SE. *$p < 0.05$, **$p < 0.01$, ***$p < 0.001$ by *t* test.

Immunized mice were also analyzed for IL-4 secretion, as this is the signature cytokine for Th2 cells. Interestingly, total $CD4^+$ T cells from immunized mice showed significant decreases in IL-4 production when stimulated either overnight with antibodies (Figure 34 A) or for several hours with PMA and ionomycin and assessed via ICS (Figure 34 B-C). When Th cells from these mice were tested for *il4* transcript *ex vivo*, without stimulation, *il4* RNA was significantly reduced in the absence of BCL6 (Figure 34 D). To see if this defect in IL-4 production occurs early after immune activation, mice were immunized with SRBC and sacrificed one, three, five, and seven days later. Total $CD4^+$ T cells were stimulated overnight with antibodies and supernatants analyzed. Five days after immunization, $BCL6^{fl/fl}$ Cre^{CD4} cells showed increased IL-4, but IL-4 concentrations decreased by day seven (Figure 34 E). Therefore, the decrease on day nine is likely due to a continued decrease in production by fl/fl Th cells. Transcript levels of *il4*, however, did not match the trend seen in protein levels. While cells from both types of mice consistently increased *il4* transcript over time, BCL6-deficient Th cells had significantly less transcript compared to WT cells (Figure 34 F-left) when assessed directly *ex vivo*. When cells were stimulated overnight with antibodies, *il4* RNA was not different between the two groups (Figure 34 F-right), and seemed to match the trends seen in IL-4 secretion (Figure 34 E). Therefore, determining the effects of BCL6 on IL-4 expression and secretion can be complicated by the type of stimulation used.

Older mice are more prone to disease and have increased numbers of activated T cells. Therefore, we wished to assess IL-4 levels in these mice to see if their $CD4^+$ T cells would skew toward a Th2 type later in life. At thirteen months, unimmunized mice were sacrificed and total $CD4^+$ T cells isolated. After an overnight stimulation with antibodies, supernatants were tested for IL-4. While no significant difference was found, $BCL6^{fl/fl}$ Cre^{CD4} cells trended toward higher IL-4 secretion (Figure 34 G).

Because we observed altered *il4* and *gata3* transcript levels with *in vitro* stimulation, we wanted to assess the ability of $CD4^+$ T cells to adopt a Th2-like phenotype in different *in*

vitro culture conditions. When naïve Th cells were isolated from mice and activated with antibodies in Th0, ThN, and TFH culture conditions overnight, *gata3* expression was increased in fl/fl cells under all conditions, and significantly so in Th0 and ThN media (Figure 35 A). When cells were cultured for up to five days in ThN media, however, fl/fl cells had only marginally increased *gata3* expression on days one and three after activation, and approached a statistical increase by day five (Figure 35 B). Under non-skewing, Th0 conditions, naïve fl/fl cells secreted only slightly increased levels of IL-4

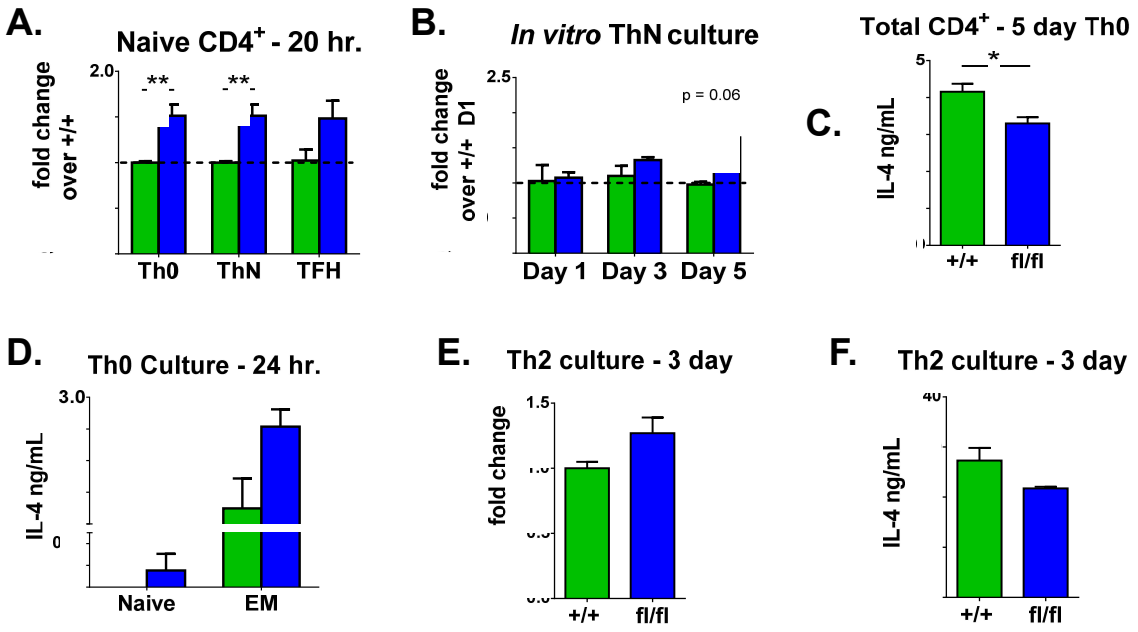

Figure 35. GATA3 is marginally increased in BCL6-deficient CD4⁺ T cells in *in vitro* cultures. A. Naïve CD4⁺ T cells were isolated from BCL6$^{+/+}$ Cre^{CD4} or BCL6$^{fl/fl}$ Cre^{CD4} mice via FACS and stimulated with anti-CD3 and anti-CD28 antibodies in Th0, ThN, or TFH culture conditions for approximately 20 hours. RNA expression of *gata3* was assessed by microarray (Th0 and TFH) or qPCR (ThN) analysis. **B.** Naïve and effector memory (EM) cells were isolated from unimmunized mice via FACS. Cells were stimulated with anti-CD3 and anti-CD28 antibodies in Th0 culture conditions for 24 hours. IL-4 concentrations in supernatants measured via ELISA. **C.** Total CD4⁺ T cells were isolated from unimmunized mice via bead separation and activated as in (**B**) in Th0 media for 5 days. After a 6 hour restimulation with anti-CD3 and anti-CD28, supernatants were collected and tested for IL-4 secretion via ELISA. **D.** Naïve CD4⁺ T cells were isolated via FACS and stimulated with anti-CD3 and anti-CD28 antibodies in ThN culture conditions. Cells were harvested and analyzed 1, 3, and 5 days after stimulation for *gata3* RNA expression via qPCR. **E.** Naïve CD4⁺ T cells were isolated via FACS and activated with anti-CD3 and anti-CD28 antibodies under Th2 polarizing culture conditions for 3 days, then restimulated in Th0 conditions for 6 hours. RNA levels of *gata3* were assessed via qPCR. **F.** Cells from (**E**) were also restimulated in Th0 conditions for 18 hours and supernatant collected for analysis via ELISA. Mean ±

SE; **p < 0.01 via *t* test.

compared to +/+ after twenty four hours, however EM cells from the same mice, stimulated for the same amount of time, in the same manner, showed a further increase in IL-4 production (Figure 35 D). However, when naïve cells were activated in Th0 media for five days, followed by an overnight restimulation, IL-4 secretion from fl/fl cells was shown to be significantly reduced (Figure 35 C). In the presence of Th2-skewing cytokines, neither GATA3 transcript, nor IL-4 production, was significantly changed. Therefore, while GL KO mice have typically shown an overwhelming skewing of Th cells toward a Th2 phenotype, here we do not see evidence of that skewing. GATA3 transcript levels are only marginally increased overall, depending on the stimulation method, and IL-4 is actually reduced, both *in vivo* and *in vitro* during longer-term cultures.

The role of BCL6 in Th17 cells

Previous work by our lab has shown BCL6 to have a role in promoting Th17 differentiation through suppression of Th2 differentiation (97). However, that work was done using a BCL6 GL KO model. Here we are able to better understand the role of BCL6 in Th17 cells in the absence of inflammatory cytokines *in vivo*. In our new model, BCL6-deficient $CD4^+$ T cells show only marginal increases in *rorc* expression, the gene that encodes RORγt, both before and nine days after immunization (Figure 36 A-B). At earlier time points in the immune response, $CD4^+$ T cells from fl/fl mice show an increase in *rorc* transcription, and significantly so on day five after injection (Figure 36 C-top). However, when these T cells are stimulated *ex vivo* with antibodies for 24 hours, fl/fl Th cells drastically reduce their *rorc* expression compared to +/+ cells (Figure 36 C-bottom).

Next, we evaluated the expression and secretion of IL-17A, the signature cytokine of Th17 cells. Nine days after immunizing mice with SRBC, no differences were seen in IL-17A secretion, either by ELISA (Figure 37 A) or by ICS (Figure 37 B-C). Transcript levels of *il17a* assessed in total $CD4^+$ T cells lysed directly *ex vivo* showed no difference in RNA levels either (Figure 37 D). In a time course experiment, where mice were sacrificed one, three, five, and seven days after immunization, total $CD4^+$ T cells stimulated with antibodies overnight showed significantly more IL-17A secretion by

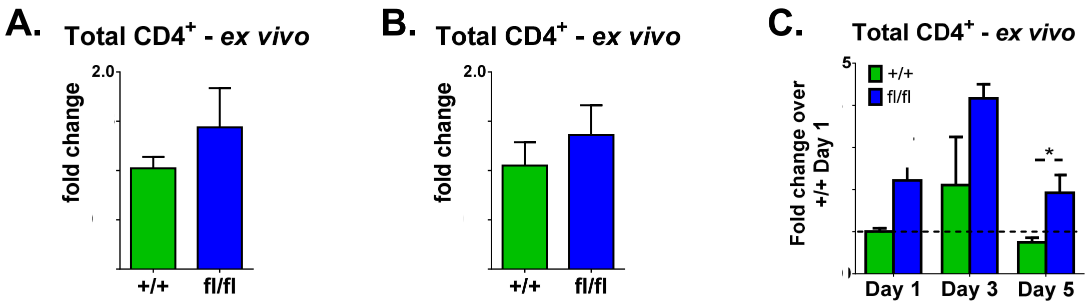

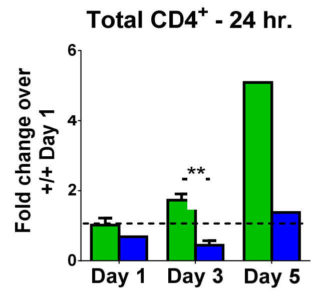

Figure 36. RORγt RNA levels are marginally increased in the absence of BCL6 *in vivo*. A. RNA expression of *rorc* (RORγt) in total CD4+ T cells from unimmunized BCL6$^{+/+}$ Cre^{CD4} and BCL6$^{fl/fl}$ Cre^{CD4} mice. Total CD4+ T cells isolated via bead separation and lysed for RNA analysis directly *ex vivo*. **B.** RNA expression of *rorc* in mice immunized i.p. with SRBC and sacrificed on day 9. Total CD4+ T cells isolated via bead separation and lysed for RNA analysis directly *ex vivo*. **C.** BCL6$^{+/+}$ Cre^{CD4} and BCL6$^{fl/fl}$ Cre^{CD4} mice were immunized i.p. with SRBC and sacrificed 1, 3, and 5 days after. Total CD4+ T cells were isolated via bead separation. RNA expression of *rorc* in cells lysed directly *ex vivo* (top) or after 24 stimulation with anti-CD3 and anti-CD28 antibodies (bottom) in Th0 media. Samples normalized to Day 1 +/+ (dotted line at 1.0). Mean ± SE; $^{*}p < 0.05$, $^{**}p < 0.01$ by *t* test.

BCL6-deficient T cells only on day five; all other time points showed no difference in cytokine production (Figure 37 E). Finally, aged mice were assessed for any T cell skewing associated with aging, and no difference was seen between +/+ and fl/fl Th cells, although BCL6$^{fl/fl}$ Cre^{CD4} mice trended toward more IL-17A production (Figure 37 F). In *in vitro* cultures of naïve Th cells, levels of *rorc* and IL-17A depended on the media environment. Naïve CD4+ T cells isolated from BCL6$^{+/+}$ Cre^{CD4} and BCL6$^{fl/fl}$ Cre^{CD4} mice activated with antibodies in Th0, ThN, or TFH media showed increases in *rorc* transcription only with the presence of TFH-skewing cytokines (Figure 38 A). Furthermore, naïve Th cells from fl/fl mice in Th0 media did not secrete more IL-17A; neither did EM cells, which have been previously activated *in vivo*, after 24 hours in Th0 media (Figure 38 B). When naïve cells were cultured *in vitro* in Th0 media for five days, IL-17A production was significantly reduced in BCL6-deficient mice (Figure 38 C). In the limiting environment of ThN media, fl/fl naïve CD4+ T cells showed significantly reduced levels of *rorc* three days after activation (Figure 38). By day five, however, no difference was seen between the two cell types, as +/+ Th cells had reduced their *rorc* levels to that of the fl/fl cells. Conversely, in the presence of Th17-skewing cytokines, after three days

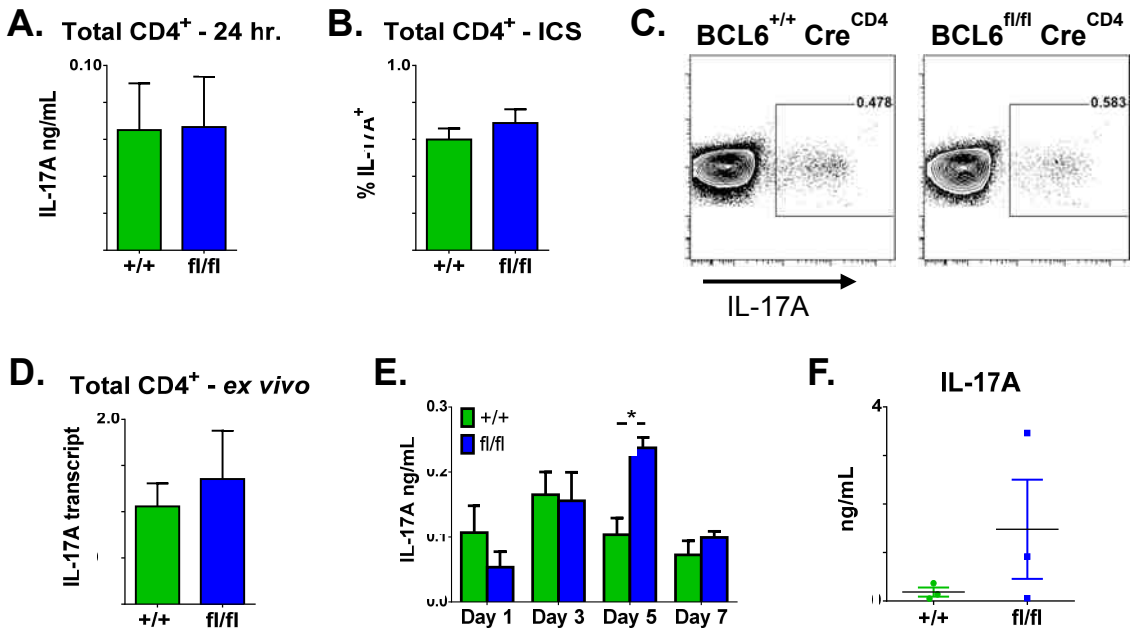

Figure 37. IL-17A secretion is not altered in the absence of BCL6. A. BCL6$^{+/+}$ Cre^{CD4} and BCL6$^{fl/fl}$ Cre^{CD4} mice were immunized i.p. with SRBC and sacrificed on day 9. Total CD4$^+$ T cells were isolated from spleen via bead separation and stimulated *in vitro* with anti-CD3 and anti-CD28 antibodies in Th0 media for 24 hours. Supernatants were analyzed for IL-17A via ELISA. **B.** Mice were immunized and sacrificed as in (**A**). Total CD4$^+$ T cells were isolated from spleen via bead separation and stimulated for 5 hours *in vitro* with PMA and ionomycin. IL-17A levels were assessed via ICS. Cells gated on CD3$^+$ CD4$^+$. **C.** Representative flow plots of ICS in (**B**). **D.** Mice were immunized, sacrificed, and CD4$^+$ T cells isolated as in (**A**). T cells were lysed directly *ex vivo* for RNA analysis. IL-17A transcript levels assessed via qPCR; normalized to +/+. **E.** BCL6$^{+/+}$ Cre^{CD4} and BCL6$^{fl/fl}$ Cre^{CD4} mice were immunized i.p. with SRBC and sacrificed 1, 3, 5, and 7 days afterward. Total CD4$^+$ T cells were isolated via bead separation and stimulated for 24 hours with anti-CD3 and anti-CD28 antibodies in Th0 media. Supernatants were assessed for IL-17A via ELISA. **F.** BCL6$^{+/+}$ Cre^{CD4} and BCL6$^{fl/fl}$ Cre^{CD4} mice were aged to 13 months and sacrificed without immunization. Total CD4$^+$ T cells were isolated via bead separation and stimulated for 24 hours with anti-CD3 and anti-CD28 antibodies in Th0 media. IL-17A levels in supernatants were measured via ELISA. Mean ± SE; *$p < 0.05$ by *t* test.

rorc was increased in BCL6-deficient T cells (Figure 38 E), while IL-17A production was only marginally increased (Figure 38 F).

BCL6 influences Foxp3 expression in CD4$^+$ T cells

Work by our lab has shown BCL6 to play a role in Treg cells, wherein BCL6 suppresses GATA3 and Th2 cytokine secretion by the regulatory cells, thus facilitating their

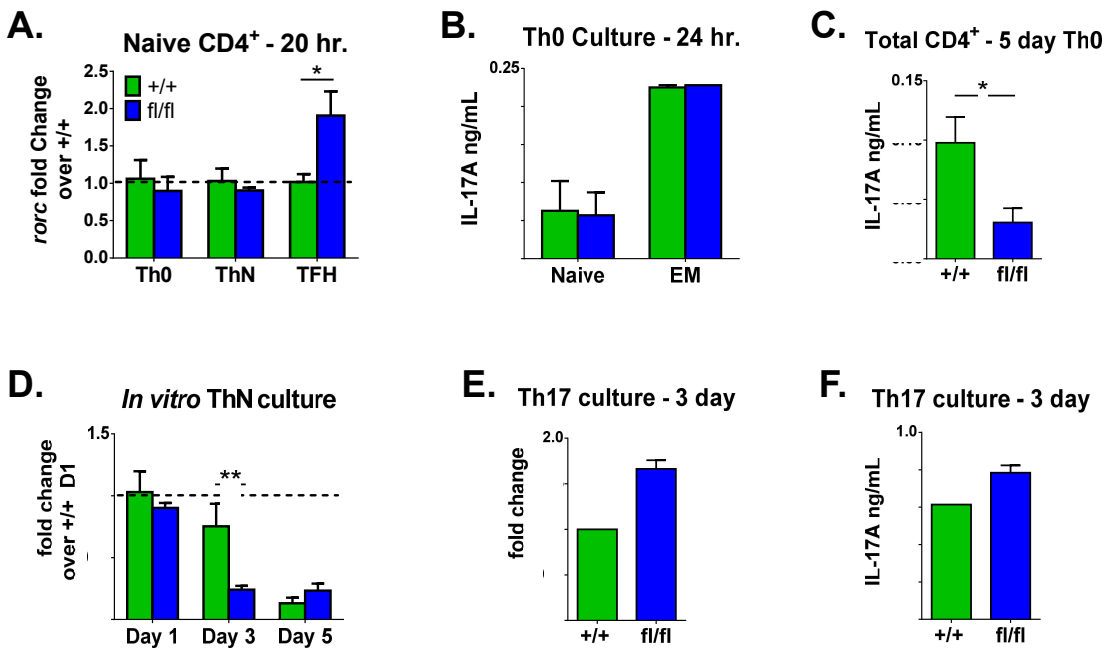

Figure 38. RORγt expression is reliant on BCL6 and exogenous cytokines for sustained expression. A. Naïve $CD4^+$ T cells were isolated from $BCL6^{+/+}$ Cre^{CD4} or $BCL6^{fl/fl}$ Cre^{CD4} mice via FACS and stimulated with anti-CD3 and anti-CD28 antibodies in Th0, ThN, or TFH culture conditions for approximately 20 hours. RNA expression of *rorc* was assessed by microarray (Th0 and TFH) or qPCR (ThN) analysis. **B.** Naïve and effector memory (EM) cells were isolated from unimmunized mice via FACS. Cells were stimulated with anti-CD3 and anti-CD28 antibodies in Th0 culture conditions for 24 hours. IL-17A concentrations in supernatants measured via ELSA. **C.** Total $CD4^+$ T cells were isolated from unimmunized mice via bead separation and activated as in (**B**) in Th0 media for 5 days. After a 6 hour restimulation with anti-CD3 and anti-CD28, supernatants were collected and tested for IL-17A secretion via ELISA. **D.** Naïve $CD4^+$ T cells were isolated via FACS and stimulated with anti-CD3 and anti-CD28 antibodies in ThN culture conditions. Cells were harvested and analyzed 1, 3, and 5 days after stimulation for *rorc* RNA expression via qPCR. **E.** Naïve $CD4^+$ T cells were isolated via FACS and activated with anti-CD3 and anti-CD28 antibodies under Th17 polarizing culture conditions for 3 days, then restimulated in Th0 conditions for 6 hours. RNA levels of *rorc* were assessed via qPCR. **F.** Cells from (**E**) were also restimulated in Th0 conditions for 18 hours and supernatant collected for analysis via ELISA. Mean ± SE; *$p < 0.05$, **$p < 0.01$ via *t* test.

suppressive nature and not promoting further inflammation (108). However, once again, these experiments were done using GL KO mice. Also, recent work by others has identified a specific subset of Treg cells which can traffic into the GC and contribute an additional layer of regulation to the cell activity there (35, 36). These studies show BCL6 and Foxp3 being co-expressed in these cells, with BCL6 facilitating the migration of the Treg cells into the GC. Therefore, it has been established that these two master

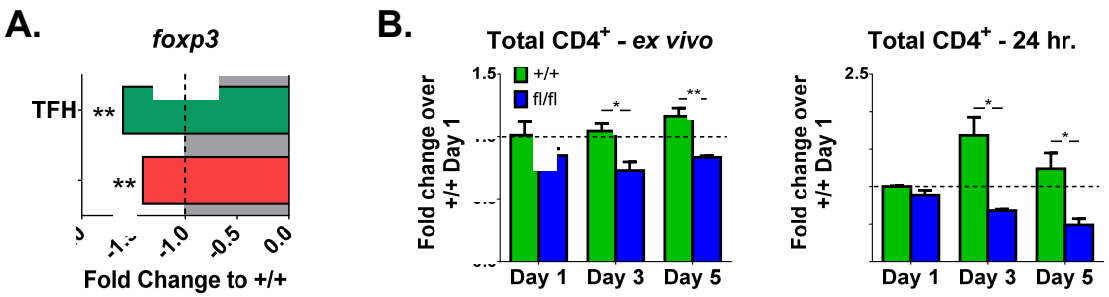

Figure 39. Foxp3 t nscript levels are significantly reduced in BCL6-deficient CD4⁺ T cells. A. Naïve CD4⁺ T cells were isolated from BCL6$^{+/+}$ Cre^{CD4} and BCL6$^{fl/fl}$ Cre^{CD4} mice via FACS. Cells were activated with anti-CD3 and anti-CD28 antibodies in Th0 or TFH media for 20 hours before lysing for RNA. Transcript levels of Foxp3 were assessed via microarray. BCL6$^{fl/fl}$ Cre^{CD4} transcript levels are shown relative to +/+ (dotted line at -1.0) in each culture condition. Mean shown; **p < 0.01. B. Mice were immunized i.p. with SRBC and sacrificed 1, 3, and 5 days after. Total CD4⁺ T cells were isolated via bead separation. RNA expression of *foxp3* in cells lysed directly *ex vivo* (left) or after 24 stimulation with anti-CD3 and anti-CD28 antibodies (right) in Th0 media. Samples normalized to Day 1 +/+ (dotted line at 1.0). Mean ± SE; *p < 0.05, **p < 0.01 by *t* test.

transcription factors can be co-expressed, but what effects BCL6 has specifically on Foxp3 expression has not been explored in a non-GL KO mouse model.

As shown in Figure 23 D in Chapter 3 of this thesis, no differences in Foxp3⁺ CD4⁺ T cells in the spleen of unimmunized mice were found between BCL6$^{+/+}$ Cre^{CD4} and BCL6$^{fl/fl}$ Cre^{CD4} mice. To investigate what role BCL6 may have on Foxp3 expression early after activation, naïve CD4⁺ T cells were isolated via FACS and activated with antibodies in Th0 or TFH media overnight. Cells were then harvested and analyzed for RNA expression via microarray. In both media conditions, significant reductions in *foxp3* RNA transcript were found in fl/fl T cells (Figure 39 A). This was confirmed in an *in vivo* time course experiment. When mice were sacrificed one, three, and five days after immunization with SRBC and cells lysed for RNA directly *ex vivo*, *foxp3* was found to be significantly reduced both at the three and five day time points in fl/fl mice (Figure 39 B-left). *Ex vivo* stimulation with antibodies for 24 hours only exacerbated this difference (Figure 39-right). Therefore, unlike the inconsistencies seen with other master transcription factors after *in vitro* stimulation, Foxp3 appears to be down-regulated in the absence of BCL6, regardless of stimulation method.

Blimp-1 is not increased in the absence of BCL6

Many researchers have established a reciprocal expression model for Blimp-1 and BCL6 (62). However, this work has been primarily done with BCL6 GL KO mice and Blimp-1 cKO mice. Therefore, no one has examined the changes in Blimp-1 expression in the absence of BCL6 in a non-inflammatory prone model. Using our new conditional mouse model we were able address this issue, and found the repression of *prdm1*, the gene for Blimp-1, by BCL6 is not as clear as previously thought.

Total $CD4^+$ T cells from fl/fl mice showed no increase in *prdm1* expression either before (Figure 40 A) or nine days after immunization with SRBC (Figure 40 B). In a time course experiment, in which mice were sacrificed one, three, and five days after immunization, cells assessed directly *ex vivo* showed a significant decrease in *prdm1* expression in the absence of BCL6 early after immunization (Figure 40 C-top). This was also seen when cells were stimulated with antibodies for 24 hours (Figure 40 C-bottom). Interestingly, while cells analyzed *ex vivo* showed a decrease in *prdm1* expression over time in +/+ cells, the gene seemed to increase on day five when those cells were stimulated with antibody. However, that increase was never able to match the levels seen in *ex vivo* analyzed +/+ cells, even at their lowest levels (Figure 40 D).

When naïve Th cells were isolated and activated *in vitro* under different culture conditions, Th0 media resulted in no differences between +/+ and fl/fl cells, ThN conditions seemed to facilitate reduced *prdm1* transcript in fl/fl cells, while TFH-polarizing conditions were able to trigger a significant increase in *prdm1* in the absence of BCL6 (Figure 40 E). When cells were cultured for longer periods in ThN media, *prdm1* remained low in fl/fl cells until day five, at which point they seemed to equal that of the unchanged levels in +/+ cells (Figure 40 F). Together this data demonstrates while BCL6 may be up-regulated in the absence of Blimp-1, as has been reported, the opposite is not necessarily true. In fact, Blimp-1 appears to be somewhat reliant on BCL6 for its own transcription, and is only able to overcome the absence of BCL6 in the presence of TFH-polarizing cytokines.

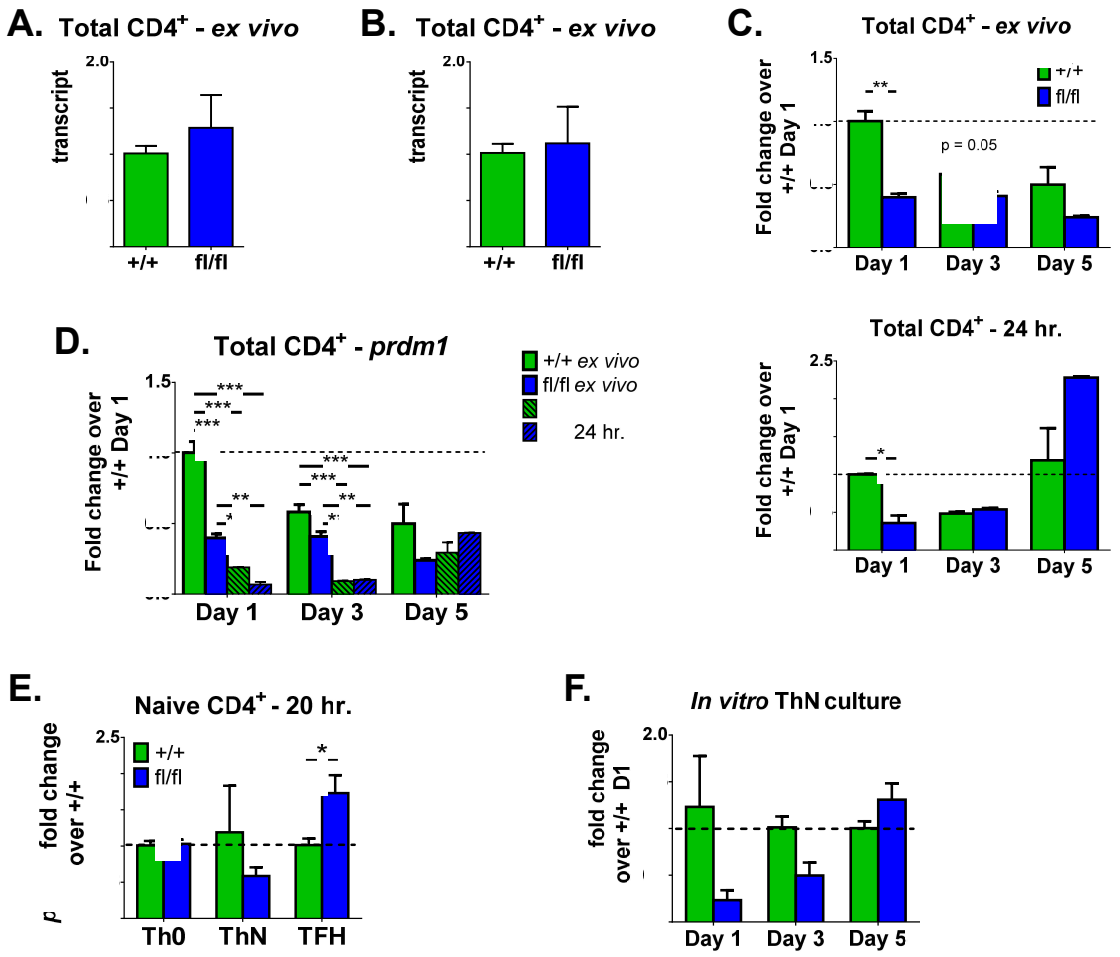

Figure 40. Blimp-1 is decreased in CD4⁺ T cells lacking BCL6. A. RNA expression of *prdm1* (Blimp-1) in total CD4⁺ T cells from unimmunized BCL6$^{+/+}$ Cre^{CD4} and BCL6$^{fl/fl}$ Cre^{CD4} mice. Total CD4⁺ T cells isolated via bead separation and lysed for RNA analysis directly *ex vivo* via qPCR. **B.** RNA expression of *prdm1* in mice immunized i.p. with SRBC and sacrificed on day 9. Total CD4⁺ T cells isolated via bead separation and lysed for RNA analysis directly *ex vivo* via qPCR. **C.** BCL6$^{+/+}$ Cre^{CD4} and BCL6$^{fl/fl}$ Cre^{CD4} mice were immunized i.p. with SRBC and sacrificed 1, 3, and 5 days after. Total CD4⁺ T cells were isolated via bead separation. RNA expression of *prdm1* in cells lysed directly *ex vivo* (top) or after 24 stimulation with anti-CD3 and anti-CD28 antibodies (bottom) in Th0 media. Samples normalized to Day 1 +/+ (dotted line at 1.0). Mean ± SE; *p < 0.05, **p < 0.01 by *t* test. **D.** Samples from (**C**) together normalized to levels in +/+ Day 1 *ex vivo* (dotted line at 1.0). Mean ± SE; *p < 0.05, **p < 0.01, ***p < 0.001 by ANOVA; Tukey post hoc. **E.** Naïve CD4⁺ T cells were isolated from BCL6$^{+/+}$ Cre^{CD4} or BCL6$^{fl/fl}$ Cre^{CD4} mice via FACS and stimulated with anti-CD3 and anti-CD28 antibodies in Th0, ThN, or TFH culture conditions for approximately 20 hours. RNA expression of *gata3* was assessed by microarray (Th0) or qPCR (ThN & TFH) analysis. Mean ± SE; *p < 0.05 by t test. **F.** Naïve CD4⁺ T cells were isolated via FACS and stimulated with anti-CD3 and anti-CD28 antibodies in ThN culture conditions. Cells were harvested and analyzed 1, 3, and 5 days after stimulation for *prdm1* RNA expression via qPCR. Mean ± SE

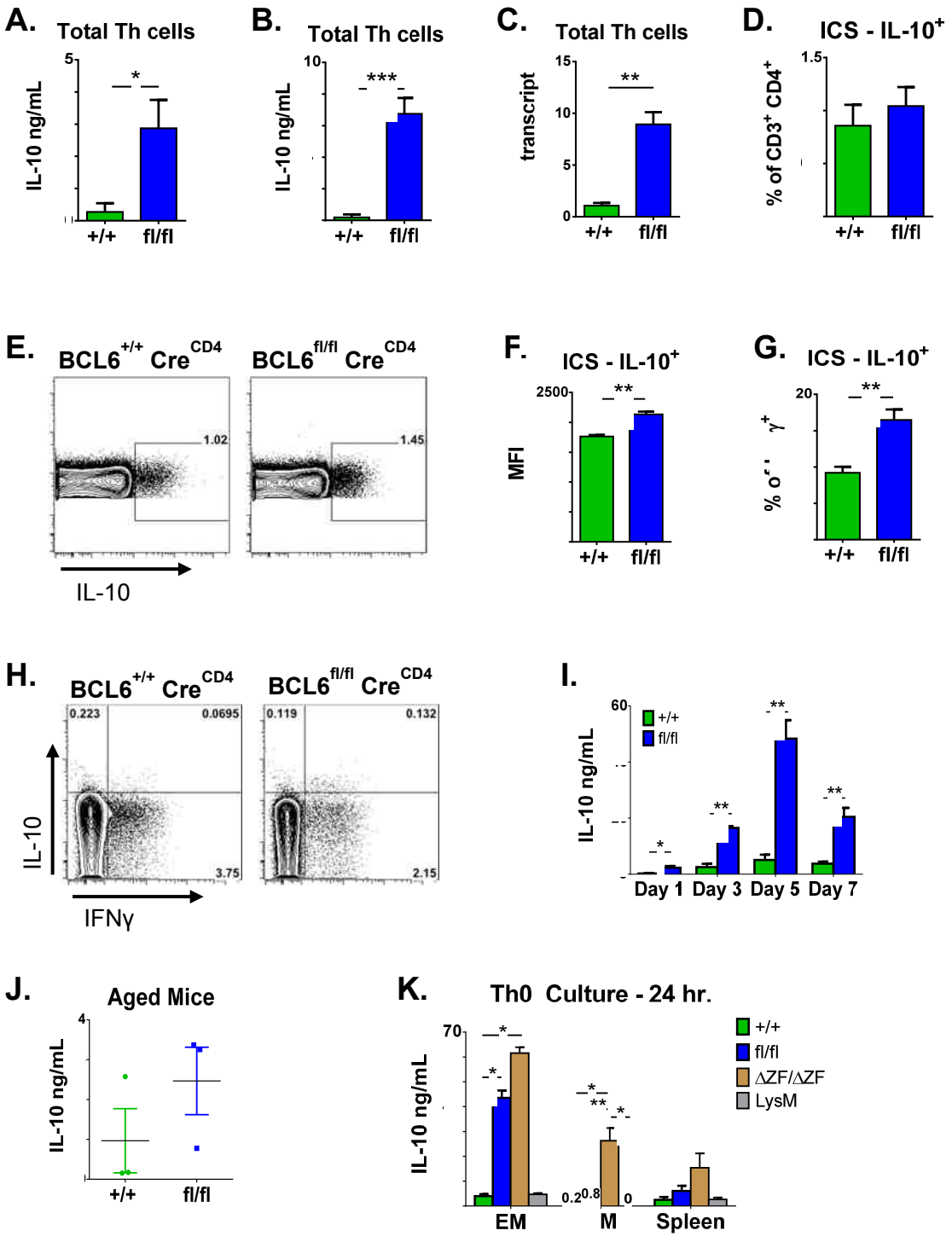

Figure 41. IL-10 is increased, in an intrinsic manner in BCL6$^{fl/fl}$ Cre^{CD4} CD4^{+} T cells. A. Unimmunized BCL6$^{+/+}$ Cre^{CD4} and BCL6$^{fl/fl}$ Cre^{CD4} mice were sacrificed and total CD4^{+} T cells isolated from spleen. Cells were activated with anti-CD3 and anti-CD28 antibodies in Th0 media for 24 hours. Supernatants were tested for IL-10 via ELISA. **B - F.** BCL6$^{+/+}$ Cre^{CD4} and BCL6$^{fl/fl}$ Cre^{CD4} mice were immunized with SRBC and sacrificed 9 days later. Total CD4^{+} T cells were isolated via bead separation. **B.** Cells

were stimulated with anti-CD3 and anti-CD28 antibodies in Th0 media for 24 hours and supernatants assessed for IL-10 via ELISA. **C.** Cells were stimulated as in (**B**) then lysed for RNA analysis. Transcript levels of *il10* were assessed via qPCR; levels normalized to +/+. **D.** Isolated T cells were stimulated with PMA and ionomycin in Th0 media for 5 hours then cytokines assessed via ICS. IL-10^{+} cells are shown as percent of CD3^{+} CD4^{+}. **E.** Representative flow plots of cells in (**B**). Gated on CD3^{+} CD4^{+}. **F.** MFI of IL-10^{+} cells in (**D**). **G.** Percent of IFNγ^{+} cells that are IL-10^{+} cells. Gated on CD3^{+} CD4^{+} IFNγ^{+}. **H.** Representative flow plots of cells in (**G**). Gated on CD3^{+} CD4^{+}. **I.** BCL6$^{+/+}$ Cre^{CD4} and BCL6$^{fl/fl}$ Cre^{CD4} mice were immunized with SRBC and sacrificed 1, 3, 5, and 7 days after. Total CD4^{+} T cells were isolated and stimulated as in (**A**). IL-10 levels in supernatant were measured via ELISA. Mean ± SE; *p < 0.05, **p < 0.01, ***p < 0.001 via *t* test. **J.** Mice were aged to 13 months and sacrificed without immunization. Total CD4^{+} T cells were isolated and stimulated as in (**A**). IL-10 levels in supernatants were measured via ELISA. Mean ± SE. **K.** Spleen cells were isolated from unimmunized BCL6$^{+/+}$ Cre^{CD4}, BCL6$^{fl/fl}$ Cre^{CD4}, BCL6$^{\Delta ZF/\,\Delta ZF}$, and BCL6$^{fl/fl}$ Cre^{LysM} mice. Effector memory (EM) and central memory (CM) cells were isolated via FACS and stimulated 24 hours with anti-CD3 and anti-CD28 antibodies in Th0 media. Total spleen cells were stimulated with LPS for 24 hours in Th0 media. Supernatants were assessed for IL-10 via ELISA. Mean ± SE; *p < 0.05, **p < 0.01 by ANOVA; Tukey post hoc.

IL-10 is suppressed by BCL6

During evaluation of our new mutant cKO mouse model, one cytokine, IL-10, which is not traditionally a signature cytokine of any of the Th subsets, was shown to be consistently increased in a variety of experimental conditions. When total CD4^{+} T cells from unimmunized mice were isolated and stimulated overnight with antibodies, BCL6$^{fl/fl}$ Cre^{CD4} cells showed a significant increase in IL-10 secretion (Figure 41 A). Nine days after immunization with SRBC, both protein and transcript levels of IL-10 were significantly increased in BCL6-deficient CD4^{+} T cells (Figure 41 B-C). When IL-10 production was assessed in immunized mice via ICS, no difference in the percentage of IL-10^{+} CD4^{+} T cells was found between the two mouse strains (Figure 41 D-E). However, the MFI of IL-10 in fl/fl T cells was significantly higher than +/+ cells (Figure 41 F). Therefore, although the same percentage of cells are making IL-10, those lacking BCL6 make more.

We next wished to determine if the cytokine secretion profile of the CD4 T cells in fl/fl mice was altered. Using ICS of CD4^{+} T cells from immunized mice, we saw no differences in IL-4/IL-10 dual positive cells, nor were there differences in IL-17A producing cells which also made IL-10 (data not shown). However, we did find an interesting result when analyzing IFNγ producing cells. As shown in Figure 30 C, no

differences in percent of IFNγ^{+} Th cells were found between BCL6$^{+/+}$ Cre^{CD4} and BCL6$^{fl/fl}$ Cre^{CD4} mice. However, the percent of IFNγ^{+} cells which also produce IL-10 was significantly higher in the fl/fl CD4^{+} T cells (Figure 41 G-H), suggesting in the absence of BCL6, more Th cells which make IFNγ are also producing IL-10.

Using a time course experiment, CD4^{+} T cells from fl/fl mice were shown to secrete more IL-10 at all time points checked after immunization, peaking on day five (Figure 41 I). Even the CD4^{+} T cells from mice aged to thirteen months trended toward secreting more IL-10 in the absence of BCL6 (Figure 41 J).

However, the IL-10 produced by fl/fl Th cells was not as high as the level seen in GL KO mice. Using FACS, we sorted effector memory (EM) and central memory (EM) cells from BCL6$^{+/+}$ Cre^{CD4}, BCL6$^{fl/fl}$ Cre^{CD4} and BCL6$^{\Delta ZF/\Delta ZF}$ mice and stimulated those cells, along with total spleen cells, overnight in Th0 media. While cells from +/+ mice produced very little IL-10, EM cells from fl/fl and ΔZF/ΔZF mice produced significantly more IL-10, although fl/fl cells did not produce as much IL-10 as ΔZF/ΔZF cells. When CM supernatants were evaluated, ΔZF/ΔZF cells were the only group to secrete measurable amounts of the cytokine. Finally, while total spleen cells from all three mice were able to produce IL-10 after stimulation with LPS, the levels appeared in a step-wise fashion, with +/+ making the least, fl/fl cells producing intermediate amounts, and ΔZF/ΔZF Th cells secreting the most.

To demonstrate that the propensity to secrete more IL-10 is due to Th cell intrinsic factors in BCL6$^{fl/fl}$ Cre^{CD4} mice, EM and CM cells were also sorted from BCL6$^{fl/fl}$ Cre^{LysM} mice. These LysM mice express the cre recombinase enzyme specifically in myeloid cells, thus inducing the inflammatory nature of myeloid cells seen in GL KO mice. T cells sorted from these mice, as well as total spleen cells, produced levels of IL-10 similar to that seen in BCL6$^{+/+}$ Cre^{CD4} mice. Therefore, increased IL-10 production of BCL6-deficient CD4^{+} T cells is due to loss of BCL6 specifically in CD4^{+} T cells and not to extrinsic stimulating factors.

Finally, we evaluated the expression and secretion of IL-10 in several *in vitro* culture conditions (Figure 42). Naïve CD4^{+} T cells were isolated from BCL6$^{+/+}$ Cre^{CD4} and BCL6$^{fl/fl}$ Cre^{CD4} mice and activated in different polarizing media conditions with

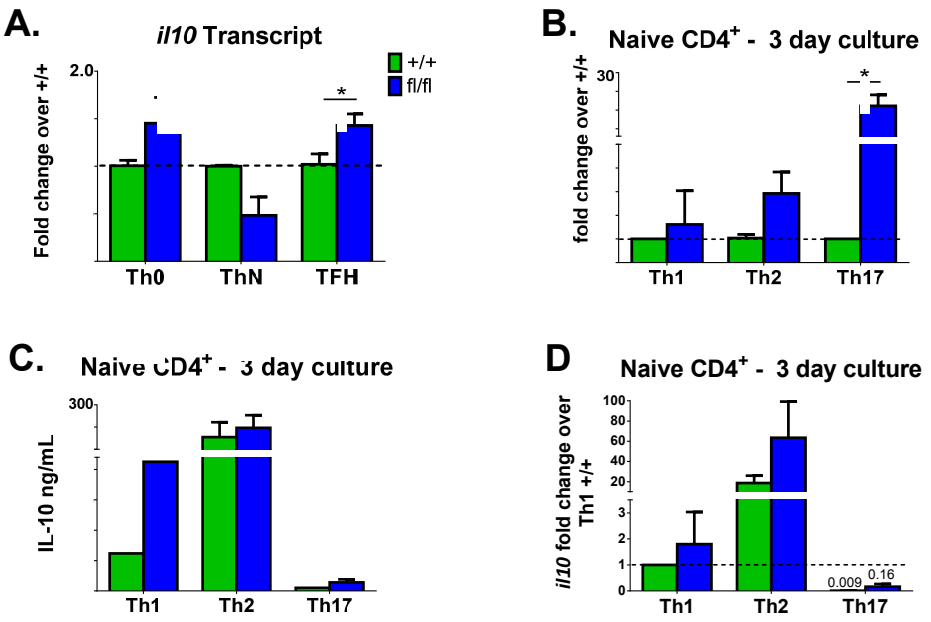

Figure 42 IL-10 is increased under different skewing culture conditions. A. Naïve CD4+ T cells were isolated from BCL6$^{+/+}$ Cre^{CD4} and BCL6$^{fl/fl}$ Cre^{CD4} mice via FACS and activated with anti-CD3 and anti-CD28 antibodies in Th0, ThN, or TFH media. After 24 hours, cells were lysed for RNA analysis. IL-10 transcript levels in Th0 and TFH cultures analyzed via microarray; ThN cultured cells analyzed via qPCR. **B.** Naïve CD4+ cells were isolated from spleen via FACS and activated with anti-CD3 and anti-CD28 antibodies in Th1, Th2, and Th17 polarizing media for 3 days. After a 6 hour restimulation with the same antibodies, cells were lysed for RNA analysis via qPCR. Samples normalized to +/+ for each culture condition (dotted line at 1). **C.** Cells in (**B**) were restimulated for 24 hours with antibodies and supernatants assessed for IL-10 via ELISA. **D.** Same samples as in (**B**) except all are normalized to Th1 +/+ cells (dotted line at 1). Mean ± SE; *p < 0.05 by *t* test.

antibodies. When naïve cells were activated overnight in Th0, ThN, and TFH culture conditions, *il10* transcript levels were increased in Th0 culture conditions and significantly increased in TFH conditions (Figure 42 A). Blocking IFNγ and IL-4 in ThN conditions led to a drop in *il10* RNA. When naïve cells were activated under Th1, Th2, and Th17 polarizing conditions for three days, *il10* transcript levels were elevated in fl/fl Th cells, and significantly so under Th17 conditions (Figure 42 B). This increase in RNA, however, did not necessarily translate to increases in cytokine secretion. Under Th1-polarizing culture conditions, fl/fl Th cells seemed to secrete more IL-10; however the sample size was too small to determine statistical significance (Figure 42 C). Th2-polarized cells showed no difference in IL-10 production between the two cell types. Finally, while Th17-polarizing conditions yielded the highest fold increase of *il10* transcript over +/+, these cells secreted the least IL-10 of all culture conditions. When

transcript levels were reanalyzed and all samples normalized to Th1 +/+ samples (Figure 42 D), the *il10* transcript profile seemed to match the IL-10 secretion by these cells. Therefore, while Th2 culture conditions facilitated the most IL-10 secretion of the three Th cell polarizing conditions, no difference in IL-10 was seen in BCL6-deficient cells. Therefore, the cytokine conditioning of the media must be abrogating any effects loss of BCL6 may have on the production of IL-10 by these cells.

BCL6 limits the proliferation of activated Th cells

As demonstrated in Chapter 3 of this thesis, $BCL6^{fl/fl}$ Cre^{CD4} mice appear to have a defect in Th cell activation. However there are effector Th cells in these mice. Therefore, we wished to analyze whether the proliferation of Th cells is affected by the absence of BCL6, once the cells are activated.

As was done previously, a time course experiment was performed, wherein mice were immunized i.p. with SRBC and sacrificed one, three, and five days after. Total spleen cells were assessed for Ki67, a proliferation marker, via flow cytometry. As shown in Figure 43 A, total $CD4^+$ T cells from $BCL6^{fl/fl}$ Cre^{CD4} mice had decreased Ki67 staining compared to $BCL6^{+/+}$ Cre^{CD4} mice. However, this could likely be due to fewer activated cells, as seen in Chapter 3. Therefore, cells were further gated on CXCR5, a surface marker which is up-regulated on many Th cells soon after activation. One day after immunization, $BCL6^{fl/fl}$ Cre^{CD4} mice showed a decrease in Ki67 in this population, however by days three and five, there were no differences between the two mouse strains (Figure 43 B). Th cells were also gated on an effector cell phenotype, which should include most activated cells. When this was done, no difference was seen between BCL6-deficient and WT Th cells one and three days after immunization. Furthermore, BCL6-deficient Th cells had significantly more Ki67 staining five days after immunization (Figure 43 C), suggesting BCL6 may actually be repressing proliferation starting at intermediate time points after immunization.

When mice were analyzed nine days after immunization, significantly more effector Th cells from fl/fl mice were expressing CD25, an activation marker, as compared to +/+ mice (Figure 43 D-left). Also, the amount of CD25 expressed on $CD25^+$ cells trended toward being higher in fl/fl cells, although the MFI levels were not statistically significant

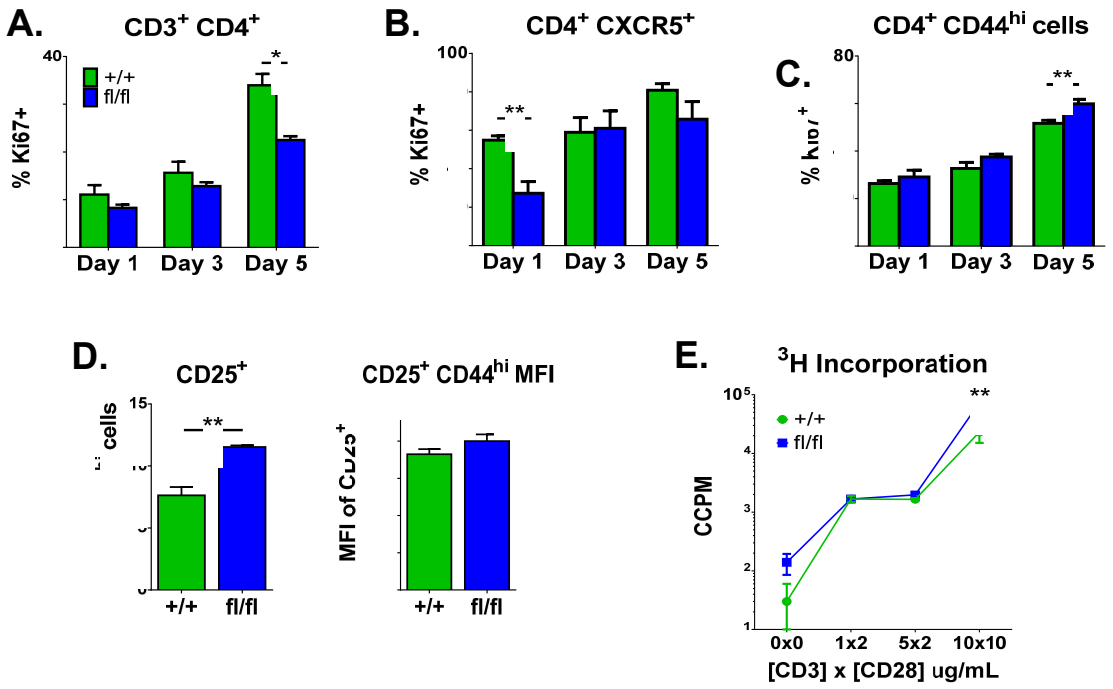

Figure 43. BCL6 limits proliferation of activated CD4⁺ T cells. A – C. BCL6$^{+/+}$ Cre^{CD4} and BCL6$^{fl/fl}$ Cre^{CD4} mice were immunized i.p. with SRBC and sacrificed 1, 3, and 5 days after. Total spleen cells were stained for CD3, CD4, and assessed for Ki67 expression via flow cytometry. **A.** Ki67⁺ cells in total Th cell population. **B.** Ki67⁺ cells that are CD3⁺ CD4⁺ CXCR5⁺. **C.** Ki67⁺ cells that are CD3⁺ CD4⁺ CD44^{hi}. **D.** Mice were immunized i.p. with SRBC and sacrificed on day 9. Total spleen cells stained for CD3⁺ CD4⁺ CD44^{hi} CD25⁺. Percent of CD25⁺ cells in CD44^{hi} Th cell population (left). MFI of CD25 in CD25⁺ population shown at left. **E.** Naïve CD4⁺ T cells were isolated via FACS and activated *in vitro* with different concentrations of anti-CD3 and anti-CD28 antibodies in Th0 media for 48 hours. Cells were then pulsed with tritiated thymidine for 18 hours. Incorporation shown as corrected counts per minute (CCPM). Mean ± SE; *p < 0.05, **p < 0.01 by *t* test.

(Figure 43 D-right). Therefore, it appears BCL6 limits the expression of activation markers on already activated Th cells.

To investigate the difference in cell activation markers *in vitro*, naïve Th cells were isolated via FACS and activated *in vitro* with different concentrations of anti-CD3 and anti-CD28 antibodies. After 48 hours in Th0 media, cells were pulsed with tritiated thymidine (^{3}H) for 18 hours. Scintillation counting of the incorporated thymidine revealed no differences in baseline proliferation (cultured without antibodies) (0x0) or at lower levels of activating antibodies (1 ug/mL anti-CD3 + 2 ug/mL anti-CD28 (1x2) and 5 ug/mL anti-CD3 + 2 ug/mL anti-CD28 (5x2)) (Figure 43 E). However, at the highest

concentrations of antibodies (10 ug/mL anti-CD3 and anti-CD28 (10x10)), which would activate the most Th cells and do so with strong stimulation, cells from fl/fl mice showed significantly more thymidine incorporation. This demonstrates a higher proliferative capability for Th cells lacking BCL6 in the presence of strong stimulation.

DISCUSSION

Overall, there appeared to be no overwhelming effects on Th subset cell differentiation in the absence of BCL6, contrary to what has been seen previously with GL KO mouse models. However, the mode of cellular activation (*in vitro* vs. *in vivo*) and the cell culture environment seemed to greatly affect the regulation of master transcription factors and cytokine secretion. In the case of Th1 cells, IFNγ production did not seem to be altered in the absence of BCL6 *in vivo*. However, when naïve fl/fl cells were activated *in vitro* for several days in Th0 media, which contains no skewing agents of any kind, the signature cytokine was reduced, as compared to +/+ cells. This would suggest that IFNγ production is at least somewhat facilitated by BCL6. These findings seem to contradict the findings of recent research in which BCL6 is necessary to limit excessive IFNγ production which is initiated by Tbet (39, 95). This finding is especially perplexing since Tbet protein levels were significantly elevated *in vivo* in the absence of BCL6. Our data demonstrates a role for BCL6 regulating Tbet at the post-transcriptional level in an *in vivo* immunization model. When fl/fl naïve cells were activated *in vitro*, we saw significant increases in *tbx21* transcript after 24 hours in Th0 media and after 3 days in ThN media. However, when cells were cultured in TFH-skewing conditions, *tbx21* mRNA was significantly reduced in the absence of BCL6. Therefore, it seems that BCL6 can limit *tbx21* transcription when no additional cytokines are present or when they are blocked, but in the presence of a cytokine rich environment, such as is found *in vivo* or in TFH *in vitro* conditions, *tbx21* transcription is abrogated. At the post-transcriptional level, though, it seems that BCL6 will limit Tbet production *in vivo*. However, most of these findings are quite nuanced and IFNγ production was not significantly altered in our cKO mice. Therefore, it appears that loss of BCL6 has very little effect on Th1 cell differentiation.

The one subset we expected to see overwhelming increases in in the $BCL6^{fl/fl}$ Cre^{CD4} mice was Th2 cells. This, however, did not prove to be true. In fact, we saw significant

reductions in IL-4 secretion and transcription, both *in vitro* and *in vivo*. Therefore, BCL6 clearly plays a role in the production of this cytokine. Overall, we saw few differences in *gata3* transcription in the absence of BCL6. Th cells activated *in vivo* had no difference in GATA3 mRNA without BCL6, while naïve cells activated *in vitro* showed increases in transcription in certain circumstances, particularly very early after activation (i.e. within 24 hours). Therefore, unlike the published findings using the BCL6 GL KO mouse model, we do not have evidence for increased Th2 differentiation in our cKO mice, and in fact, they appear to have a defect in IL-4 production.

Like Th1 and Th2 cell analysis, the differentiation of Th17 cells did not appear to be consistently affected by loss of BCL6. However, upon closer inspection, we detected a phenotype which adds further support for our model of graded expression, as set forth in Chapter 2. In that model, Th17 cells require low levels of BCL6 for differentiation. We can see evidence for this in the data presented in Figure 37. When +/+ cells were assessed *ex vivo* for *rorc* mRNA, levels did not change much over the first five days of the immune response (Figure 36 C-top). However, when WT total $CD4^+$ T cells were stimulated with antibodies overnight, the levels of *rorc* increased. Most interestingly, if you consider the transcript levels of BCL6 after *in vitro* stimulation (Figure 29 B), with day five having the lowest levels, we can see an inverse correlation between *rorc* transcripts and BCL6 RNA in WT mice. Furthermore, when WT naïve cells are activated *in vitro* for several days, we saw a time-dependent decrease in *rorc* transcript levels (Figure 38 D). However, that decrease was much slower than what was seen in fl/fl cells. BCL6 is up-regulated upon initial activation of naive Th cells (22, 23), thus, it appears that the low levels of BCL6 in recently activated cells reinforces the expression of RORγt for a few days, longer than when BCL6 is completely absent. Together, this analysis of BCL6 and RORγt in WT cells suggests that low levels of BCL6 are necessary for continued expression of RORγt.

Analysis of our fl/fl mice provides evidence that an enhanced cytokine environment can overcome any necessity for BCL6 in RORγt expression, and, in some cases, facilitate even higher expression. For example, cells assessed *ex vivo* show increases in *rorc* transcript levels one, three, and five days after immunization in the absence of BCL6. Therefore, when subjected to an *in vivo* environment, likely to be rich in cytokines, BCL6 appears to inhibit RORγt expression. *In vitro*, when naïve cells are activated in TFH

media, *rorc* mRNA is significantly increased in the absence of BCL6, while it is marginally increased in Th17-skewing media. When the contents of these two media types are compared, it appears that IL-6 may be facilitating the increase in RORγt expression.

To summarize our findings for Th17 cells, we propose that low levels of BCL6 are necessary to sustain RORγt expression, both *in vitro* and *in vivo*. However, BCL6 appears to limit RORγt expression, particularly in an environment that is rich in IL-6, such as the case *in vivo*, and in Th17 and TFH cultures *in vitro*. Without BCL6 or IL-6, *rorc* transcription is not sustained. Therefore, a careful balance between BCL6 expression levels and IL-6 stimulation from the surrounding environment is necessary to regulate Th17 differentiation (Figure 44).

While recent research has shown BCL6 and Foxp3 to be dually expressed in TFR cells, little work has been done to investigate the specific effect BCL6 may have on Foxp3 expression. Using our new cKO mouse model, we were able to establish that BCL6 contributes to *foxp3* expression, both *in vitro* and *in vivo*. While TFR cells do express both transcription factors, they are thought to be derived from Treg cells and not TFH cells (35, 36). Therefore these cells would express Foxp3 first, before up-regulating BCL6. However, it is possible that even low levels of BCL6 are necessary for Th cells to express Foxp3. What this means for nTreg cell development in the thymus cannot be determined here. However, our data does suggest that low levels of BCL6 would be necessary for iTreg development *in vivo*.

The balance between BCL6 expression and Blimp-1 is one which has been extensively studied, particularly in B cells and $CD8^+$ T cells. Current dogma states, in the absence of Blimp-1, BCL6 is up-regulated, and vice versa. However, work recently published by our lab shows *prdm1* transcript to only be significantly increased in the absence of BCL6 in TFH media conditions (110). Here, we present a more in-depth analysis of the expression of Blimp-1 in BCL6-deficient Th cells.

When mice are immunized with SRBC, a strong GC reaction is induced, and, thus, many Th cells will be expressing high levels of BCL6 in +/+ mice. It should follow then, that Blimp-1 levels would be particularly low in Th cells in this type of immune response.

Therefore, when transcript levels of *prdm1* are assessed in cKO mice and normalized to +/+ levels, any increases in the absence of BCL6 should be strongly evident, due to the assumed low levels in WT mice. However, when this was done, no differences in *prdm1* expression were found between the two types of cells. When WT cells were analyzed for *prdm1* transcript early after immunization, levels decreased over time, as expected. However, mRNA from fl/fl Th cells was low one day after immunization and remained low thereafter. This experiment showed that in WT Th cells, Blimp-1 levels increase just after immunization, but decrease over time, down to the levels seen in cKO Th cells by day nine. Interestingly, when those same Th cells are stimulated overnight with antibodies, the levels of *prdm1* transcript does increase, however, not to the levels seen in WT mice assessed *ex vivo*. Therefore, like BCL6, Blimp-1 transcription is severely abrogated with *in vitro* stimulation.

As we have previously published (110), when naïve cells are activated for 24 hours in different media conditions, Blimp-1 was increased only in the TFH culture. Furthermore, when naïve cells were cultured for several days in ThN media, Blimp-1 was severely decreased in the absence of BCL6 twenty four hours after activation. However over time, those cells were able to transcribe *prdm1* to the levels of +/+ cells. This would suggest BCL6 restricts Blimp-1 expression in TFH conditions, but facilitates its transcription in the limiting environment of ThN culture conditions.

Taken together, the data presented here demonstrate a much more complicated relationship between BCL6 and Blimp-1 than previously thought. While it seems clear that BCL6 is up-regulated in Blimp-1 KO cells, the converse is not necessarily true. Only in particular stimulatory and cytokine conditions is Blimp-1 increased in the absence of BCL6. In fact, it seems more probable from this data that BCL6 is necessary for Blimp-1 expression, particularly *in vivo*. Clearly more work needs to be done to fully analyze the effects of BCL6 loss on Blimp-1 expression, but the data presented here should at least trigger a reassessment of the current understanding of the relationship between these two transcriptional repressors.

The one cytokine in our extensive analysis of $BCL6^{fl/fl}$ Cre^{CD4} mice which was consistently increased in the absence of BCL6 was IL-10. We saw statistically significant increases in this cytokine at the transcriptional and protein levels in BCL6-

deficient $CD4^+$ cells from unimmunized mice, at various time points after immunization, and in aged mice. Because IL-10 is a suppressive cytokine, this would suggest that the immune response is trying to function in a limiting environment in cKO mice. It is possible that secretion of IL-10 by activated Th cells in $BCL6^{fl/fl}$ Cre^{CD4} mice is contributing to the decreased activation seen in these mice, as discussed in Chapter 3. However, BCL6 GL KO mice are known to have large proportions of activated Th cells that secrete IL-10 (61), yet there appears to be no activation defect in these mice. In fact, GL KO mice typically have increases in activated Th cells and decreases in naive Th cells. The role IL-10 is playing in $BCL6^{fl/fl}$ Cre^{CD4} mice cannot be determined from the data presented. However, it is clear that BCL6 works to repress IL-10 in WT Th cells.

We can also deduce from our data that IFNγ may be playing a role in the increased secretion of IL-10 by BCL6-deficient cells. Firstly, using ICS, we determined that only $IFN\gamma^+$ cells from immunized mice, and not $IL\text{-}4^+$ or $IL\text{-}17A^+$ cells, had a larger percentage of cells also producing IL-10. Secondly, analyses using *in vitro* assays showed a reduction in IL-10 secretion in a ThN environment, which blocks IFNγ and IL-4. This suggests that IFNγ or IL-4 may be facilitating IL-10 secretion. When cells were cultured in Th1- and Th2-skewing environments, IL-10 production was only increased in the presence of IFNγ, and not IL-4. This would suggest that IFNγ facilitates increased IL-10 production by Th cells in the absence of BCL6.

Finally, we utilized our new cKO mouse model to determine if BCL6 has any role in the proliferation of already activated cells. Analysis using Ki67 staining and tritiated thymidine incorporation provided data which suggests BCL6 limits the proliferation of activated cells. Therefore, while BCL6 is necessary for proper Th cell activation, as was presented in Chapter 3, here we show that once activated, the transcriptional repressor will actually limit cellular proliferative capabilities.

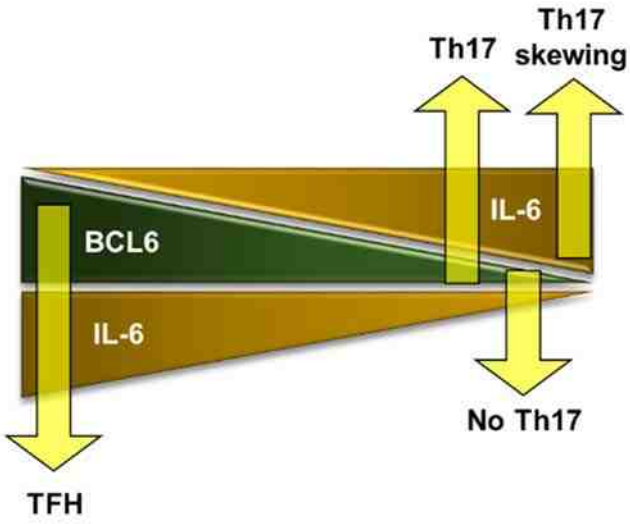

Figure 44. Th17 differentiation and BCL6. In the presence of high BCL6 and high IL-6 expression, TFH cells will differentiate. Proper differentiation of Th17 cells is dependent on moderate levels of IL-6 and low levels of BCL6. When BCL6 is absent and IL-6 is present at high levels, excessive Th17 skewing occurs. In the absence of both BCL6 and IL-6 no Th17 differentiation will occur.

CHAPTER 5 – ROLE OF BCL6 IN TFH CELL SURFACE MARKER EXPRESSION

INTRODUCTION

Follicular T helper (TFH) cells are an important $CD4^+$ T cell subset responsible for facilitating the production of high affinity antibodies from B cells (24). Historically, this task was associated with Th2 cells, and only recently have TFH cells emerged as the primary T cell responsible for assisting B cells (26). While TFH cells have been shown to migrate into the B cell follicle for some time, only in the last five years has their master transcription factor, BCL6, been identified (37-39, 62). Under the control of this transcriptional repressor, TFH cells up-regulate CXCR5, ICOS, PD-1, and several other surface markers. However, the majority of studies focus on CXCR5, ICOS, and PD-1 when identifying these cells (24). While expression of these markers is not exclusive to TFH cells, their combination and high level expression is.

Upon activation of naïve $CD4^+$ T cells, BCL6 becomes up-regulated at low levels (22, 23). During this time, the chemokine receptor CXCR5 also becomes up-regulated, although this increase in surface expression has been shown to be independent of BCL6 (81). Expression of CXCR5 enables $CD4^+$ T cells to follow a CXCL13 chemokine gradient toward the B cell follicle. Once these cells reach the T/B cell border region, interactions with B cells will determine whether they will become TFH cells or not (24, 26). During the peak of the immune response, the vast majority of $CXCR5^+$ Th cells are TFH cells (26). Furthermore, prolonged expression of this surface marker has been shown to be dependent on BCL6 expression (81). CXCR5 is widely used to identify TFH cells, however, how BCL6 controls its expression has yet to be fully understood.

ICOS is a CD28-like costimulatory molecule which is expressed on several Th subsets, but is particularly highly expressed on TFH cells (111, 112). Its up-regulation occurs early after cell activation and is crucial for sustaining cell-cell contact with B cells (26). Furthermore, it has been shown that ICOS signaling can program Th cells to become TFH very early in the immune response (113). Continued ICOS-ICOSL interactions between TFH and APCs, has been shown to be vital for continued TFH differentiation (113).

Programmed death-1, or PD-1, is encoded by the gene *pdcd1* and plays a crucial role in controlling T cell proliferation (114, 115). While expressed on many different T cell subsets, including $CD8^+$ T cells, this inhibitory marker is highly expressed on TFH cells (116). PD-1 has been shown to block TCR activation signals through the recruitment of two phosphatases: Src homology region 2 domain-containing phosphatase-1 (SHP-1) and SHP-2 (114, 117-119). These phosphatases can then, in turn, abrogate downstream activity of PI3K, which is necessary for Th cell activation and cytokine secretion (117, 120). Furthermore, PD-1 signaling can inhibit TCR signals facilitating ongoing interactions with APCs (121). An additional study demonstrated a role for PD-1 signaling in blocking $CD4^+$ T cell entry into S phase of the cell cycle (122). It is believed that high expression of PD-1 on TFH cells limits the proliferation of these cells (24, 114), and blockade of PD-1 signaling leads to increased TFH populations (123).

Like the above mentioned TFH markers, PD-1 has been shown to be up-regulated soon after cell activation (114, 117). Recent publications have demonstrated a role for epigenetics in the regulation of PD-1 expression in $CD8^+$ T cells. One study in particular demonstrated a loss of methylation at the PD-1 promoter upon T cell activation, while remethylation of the region allowed cells to become long-lived memory cells (124). Additionally, exhausted $CD8^+$ T cells had complete demethylation of the PD-1 promoter. While epigenetic modifications to the PD-1 promoter have been well studied, what controls those epigenetic changes has not been identified. Furthermore, although it has been suggested that PD-1 signaling controls TFH cell proliferation, by what means this is done has not yet been discussed. Here, we present data which attempts to elucidate these issues.

The fact that PD-1 expression has been shown to be controlled, to some extent, by methylation is important, as DNA methylation is one of the only epigenetic modifications which can be passed on to daughter cells efficiently (125). Methylating DNA, typically cytosines at CpG dinucleotides, is one way of remodeling chromatin into a less accessible state, leading to silencing of genes (125, 126). This activity is carried out by DNA-methyltransferases (Dnmt). Initial methylation patterns, or *de novo* methylation, in unactivated cells, is thought to be carried out by Dnmt3a and Dnmt3b, while maintaining the established methylation pattern of DNA during cell division is the job of Dnmt1 (126-128). When a cell divides, the daughter DNA is hemi-methylated, and Dnmt1 recognizes

and targets this pattern for full methylation to maintain the epigenetic modifications (127). Conversely, the Ten-Eleven-Translocation, or TET, proteins can also recognize these hemi-methylated regions and further reduce the methyl groups at those sites (127, 129). This makes it less likely Dnmt1 will recognize the region and target it for templated methylation. Therefore, TET proteins play a critical role in the demethylation of gene promoters over successive cell differentiations (127, 129).

How *de novo* methylation patterns are established has not been well studied *in vivo*, however, cell line experiments have provided several hypothesizes. Two potential ways in which Dnmt3a and Dnmt3b are targeted to genes for silencing are 1) by recognition of specific domains directly by the Dnmts, or 2) via recruitment to gene regions by transcriptional repressors (128). Once localized to a promoter region, Dnmts can block transcription either by physically interfering with the binding of transcriptional machinery or through methylation modifications to the chromatin structure. Furthermore, Dnmts can also associate with histone deacetylases (HDACs), and this association, combined with targeting to a specific gene, will lead to remodeling of the chromatin and silencing of gene transcription (128).

At this time, no data has shown that BCL6 can activate genes directly. Therefore, in order to activate genes that define the TFH phenotype, BCL6 must activate transcription indirectly, such as by repressing other transcriptional repressors or by binding these suppressors and sequestering them away from their targets (46, 50). The exact mechanisms by which this is accomplished are not known at this time. Multiple models for how TFH cells differentiate have been proposed (17, 24, 99). One model postulates that activated Th cells differentiate into another subset first, before up-regulating BCL6 and becoming a TFH cell (94, 130). The thought behind this model is that by down-regulating the master transcription factors of other Th subsets, any repression these factors held over TFH genes will be consequently lifted, thus allowing activation of TFH-related genes. Research using GL KO mice has shown that BCL6 can directly repress GATA3 and RORγt, the master transcription factors for Th2 and Th17 cells respectively (61, 97).

A second theory for how TFH cells develop is by directly differentiating from activated naïve Th cells (131). Multiple studies have shown this, using both *in vivo* and *in vitro*

methods (24). The interplay between BCL6 and other Th subsets proved even more complex when several groups published data showing a subset of Treg cells which were able to acquire TFH-like characteristics, such as up-regulated BCL6 and CXCR5 expression, and traffic into the GC, where they helped to regulate the GC reaction (35, 36). Therefore, the role BCL6 plays in Th cells is complicated and not well understood. However, here we provide evidence for how BCL6 may be regulating the expression of some TFH cell markers and what role this master transcription factor plays in TFH cell survival.

METHODS AND MATERIALS

Mice and immunizations

$Bcl6^{fl/fl}$ mice were mated to CD4-cre mice (82) to generate $Bcl6^{fl/fl}$ Cre^{CD4} mice. Mice with the wild type BCL6 allele were bred to CD4-Cre mice for use as controls ($BCL6^{+/+}$ Cre^{CD4}). C57BL/6 mice were obtained from Jackson Laboratories.
The floxed allele was genotyped by PCR using the following primers:

5' loxP forward (5' – TGAAGACGTGAAATCTAGATAGGC – 3')
5' loxP reverse (5' – ACCCATAGAAACACACTATACATC – 3')
3' loxP forward (5' –TCACCA ATCCCAGGTCTCAGTGTG–3')
3' loxP reverse (5' – CTTTGTCATATTTCTCTGGTTGCT–3')

Cre-CD4 transgene was genotyped using the following primers:

Forward (5' –ATCGCCATCTTCCAGCAGGCGCACT– 3')
Reverse (5' –ATTTCCGTCTCTGGTGTAGCTGAT– 3')

Mice were immunized i.p. with 1 x 10^9 sheep red blood cells (SRBC; Rockland Immunochemicals Inc., Gilbertsville, PA) in PBS.

Serum antibody analysis

Blood was collected from sacrificed mice. After clotting, blood was centrifuged for 10 minutes at 10,000 RPM and serum collected. For total IgG, capture antibody was anti-

mouse kappa chain antibody (Sigma Cat. # SAB3701212) and an anti-mouse IgG-Peroxidase detection antibody used was used (Sigma Cat. # A9044). SRBC-specific Ig was measured as previously described (132). Briefly, wells were coated with SRBC membrane extract (prepared as described (132)) overnight at 4˚C. Wells were blocked with 10% FCS and diluted serum was incubated in wells for 2 hours at RT. A peroxidase labeled Fc-specific anti-mouse Ig detection antibody was used for each isotype (Sigma). Titration method was used to determine concentration. For total IgM, IgG1, IgG2b, IgG3, and IgA, capture antibodies were isotype-specific (Sigma Cat. # ISO2) and an anti-mouse Ig-Peroxidase detection antibody was used. Concentrations determined according to a standard curve. Standards were purchased from Southern Biotech (IgM Cat. # 0101-01; IgG1 Cat. # 0102-01; IgG2b Cat. # 0104-01; IgG3 Cat. # 0105-01; IgA Cat. # 0106-01).

Flow cytometry

Total spleen or thymus cells were incubated with anti-mouse CD16/CD32 (Fcγ receptor) for 20 minutes, followed by surface staining for the indicated markers. A fixable viability dye (eFluor 780, eBioscience) was used for all samples. The following antibodies were used for staining GC B cells: α-mCD19 Alexa Fluor 700, clone eBio1D3 (eBioscience); α-mB220 PE, clone RA3-682 (BD Bioscience); α-mFas Biotin, cat. # 554256 (BD Bioscience); Streptavidin-PECy7 (Biolegend); α-mGL7 APC, clone GL7 (BD Bioscience); PNA FITC (Vector Laboratories Inc.). The following antibodies were used to stain TFH cells: α-mCD3 Alexa Fluor 700, clone 500A2 (BD Bioscience); α-mCD4 PECy7, clone RM4-5 (BD Bioscience); α-mCXCR5 PerCP-efluor 710, clone SPRCL5 (eBioscience); α-mPD-1 APC, clone 29F.1A12 (Biolegend); α-mICOS FITC, clone C398.4A (eBioscience). Samples were run on a BD LSR II flow cytometer using FACSDiva software. Data was analyzed using FlowJo software.

Cell isolation

Total $CD4^+$ T cells were isolated via magnetic bead separation (Miltenyi Biotec); naïve $CD4^+$ T cells were isolated via FACS and gated on $CD3^+$ $CD4^+$ $CD44^-$ $CD62L^+$. Propidium iodide was used as a viability gate.

Gene expression analysis

Total RNA was prepared using a kit (Qiagen) after lysis of the cells via Trizol (Life Technologies); cDNA was prepared with the Transcriptor First Strand cDNA synthesis kit (Roche). Quantitative PCR (qPCR) reactions were run by assaying each sample in triplicates using the Fast Start Universal SYBR Green Mix (Roche Applied Science) with custom primers or specific Taqman assays (ABI). Assays were run with a Stratagene Mx3000P Real-Time QPCR machine. Levels of mRNA expression were normalized to beta-tubulin mRNA levels, and differences between samples analyzed using the ΔΔCT method. Primers for SYBR Green assays were previously described (14, 19).

Microarrays

Naïve $CD4^+$ T cells were isolated via FACS using the following surface markers: $CD3^+$ $CD4^+$ $CD62L^+$ $CD44^-$. A cell viability gate was also used. Cells were activated *in vitro* with anti-CD3 and anti-CD28 antibodies, as described above, in Th0 or TFH media conditions. TFH conditions contain IL-6 and IL-21 [10 ng/ml each (R&D Systems)], plus anti-IFNγ (10 μg/mL), anti-IL-4 (10 μg/mL), and anti–TGF-β (20 μg/mL) antibodies. Cells were cultured for 20 hours. Cells were lysed, RNA prepared using an RNeasy kit (Qiagen), and cDNA prepared with the Transcriptor First Strand cDNA synthesis kit (Roche). Affymetrix gene expression microarrays were carried out by Center for Medical Genomics at the Indiana University School of Medicine.

Chromatin immunoprecipitation assay

$BCL6^{+/+}$ Cre^{CD4} and $BCL6^{fl/fl}$ Cre^{CD4} mice were sacrificed either unimmunized or five days after immunization with SRBC. Total $CD4^+$ T cells were isolated from spleen via bead separation (Miltenyi Biotech). ChIP assay was performed as previously described (133). Briefly, cells were cross-linked for 10 min with 1% formaldehyde and lysed by sonication. After pre-clearing with salmon sperm DNA, bovine serum albumin, and protein agarose bead slurry (50%), cell extracts were incubated with either Dnmt3a antibody (IMG-268A; IMGENEX), Dnmt3b antibody (804-233-c100; Alexis), H3ac antibody (Millipore), H4ac antibody (06-866; Millipore), or normal rabbit IgG (Millipore) overnight at 4 °C. The immunocomplexes were precipitated with protein agarose beads at 4 °C for 2 h, washed,

eluted, and cross-links were reversed at 65 °C overnight. DNA was purified, resuspended in H2O, and analyzed by quantitative PCR with SYBR primers as described previously (134). Additional primers were as follows:

PD-1 CRB forward (5' –CTCTGACTAGCTGTCCTTGCCTC– 3')
PD-1 CRB reverse (5' –CTCGACACCCACCCTCCAAAG– 3')
PD-1 CRC forward (5' –CCTCACCTCCTGCTTGTCTCTC– 3')
PD-1 CRC reverse (5' –GTGAGACCCACACATCTCATTGC– 3')
CXCR5 forward (5' –CAGTGCTTCGTCAGCTCCAGAC– 3')
CXCR5 reverse (5' –CTCAGGTAGTCATGTTTGATGGC– 3')

Statistical analysis

Statistical analysis was done using IBM SPSS Statistics 21 software. Statistics for microarray data was done using GraphPad Prism software. In all figures, *$p < 0.05$, **$p < 0.01$, ***$p < 0.001$.

RESULTS

Germinal center cells fail to develop at any time after immunization in $BCL6^{fl/fl}$ Cre^{CD4} mice

Using our new cKO mice, we wanted to verify that GCs fail to develop in the absence of BCL6 in Th cells. Nine days after immunization with SRBC, $BCL6^{fl/fl}$ Cre^{CD4} mice failed to generate GC B cells or TFH cells, while $BCL6^{+/+}$ Cre^{CD4} mice had robust populations of these cells (Figure 45 A-B). Next, we wondered whether these cell populations are able to differentiate early in the immune response, but are not sustained when Th cells are BCL6-deficient. When mice were sacrificed one, three, and five days after immunization and analyzed for GC cell populations, we found no evidence of TFH cell development in fl/fl mice (Figure 45 C-D). This experiment also demonstrated the exponential expansion of GC B cells and TFH cells in +/+ mice between days three and five.

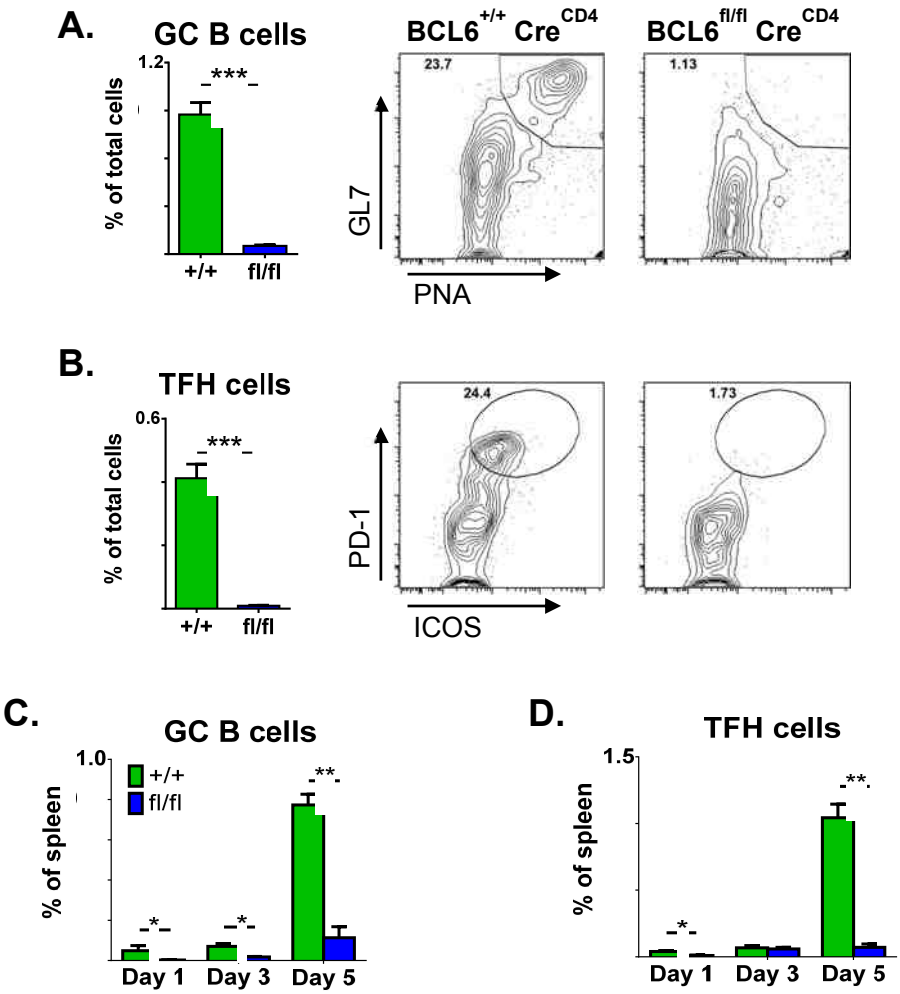

Figure 45. BCL6$^{fl/fl}$ Cre^{CD4} mice fail to generate germinal centers. A – B. Mice were immunized i.p. with SRBC and sacrificed on day 9. Spleen cells were analyzed via flow cytometry. **A.** GC B cells, shown as percent of total spleen, with representative flow plots. Cells gated on B220$^+$ CD19$^+$ Fas$^+$ PNA$^+$ GL7$^+$. **B.** TFH cells, shown as percent of total spleen, with representative flow plots. Cells gated on CD3$^+$ CD4$^+$ CXCR5$^+$ ICOS$^+$ PD-1^{hi}. **C – D.** Mice were immunized i.p. with SRBC and sacrificed 1, 3, and 5 days after. Spleen cells were analyzed via flow cytometry. **C.** GC B cells, gated as in (**A**). **D.** TFH cells, gated as in (**B**). Mean ± SE; *p < 0.05, **p < 0.01, ***p < 0.001 by *t* test.

To determine the functional effects of loss of GCs in fl/fl mice, serum from unimmunized mice and mice sacrificed nine days after immunizing with SRBC was analyzed for antibody concentrations. When total IgG was assessed, we found the titer in both +/+ and fl/fl to increase with immunization and no significant difference in titer levels were found between the two mouse strains either before or after immunization (Figure 46 A).

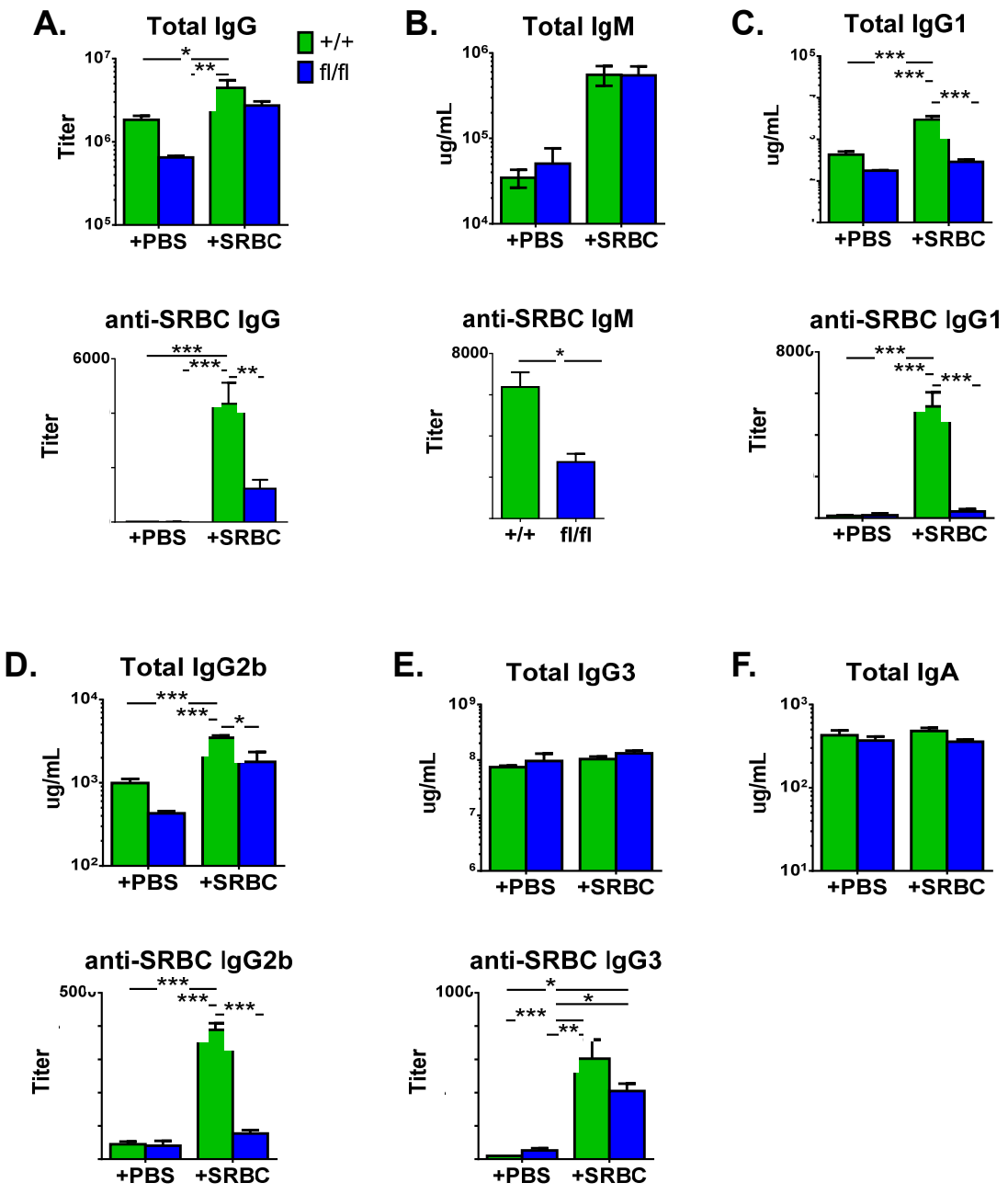

Figure 46. Antibody titers in BCL6$^{+/+}$ Cre^{CD4} and BCL6$^{fl/fl}$ Cre^{CD4} mice. Mice were immunized with either SRBC or PBS (control) and sacrificed on day 9, when serum was harvested. Antibody titers assessed via ELISA. **A.** Total IgG (top) and SRBC-specific IgG (bottom) determined using titration method. **B.** Total IgM (top) determined using standard curve and SRBC-specific IgM (bottom) determined via titration method. *$p < 0.05$ via *t* test. **C.** Total IgG1 (top) and SRBC-specific IgG1 (bottom) determined as in (**B**). **D.** Total IgG2b (top) and SRBC-specific IgG2b (bottom) determined as in (**B**). **E.** Total IgG3 (top) and SRBC-specific IgG3 (bottom) determined as in (**B**). **F.** Total IgA determined as in (**B**). Mean ± SE. For all analysis except (**B**): *$p < 0.05$, **$p < 0.01$, ***$p < 0.01$ by two-way ANOVA; Tukey post hoc analysis.

However, when antigen-specific IgG was measured, fl/fl mice were found to have a significant reduction in these antibodies, compared to serum from +/+ mice. Total IgM, while increasing with immunization, was not found to be different between the two types of mice, but again, SRBC-specific IgM was reduced, approximately three-fold, in fl/fl mice (Figure 46 B). When total IgG1 and IgG2b were analyzed, +/+ mice were found to have significantly higher levels after immunization (Figure 46 C-D). Also, fl/fl mice were shown to have almost no production of antigen-specific antibodies of these isotypes (Figure 46 C-D). Finally, while no differences in total IgG3 and IgA were found, after immunization, +/+ mice had a slightly higher SRBC-specific IgG3 titer compared to fl/fl mice, although it was not significant (Figure 46 E-F).

TFH surface marker expression in BCL6-deficient Th cells

Because TFH cells are so often identified by their surface marker expression via flow cytometry, we did further analysis on the expression of frequently used TFH markers to determine what effects loss of BCL6 has on their expression. First, the canonical marker for TFH, CXCR5, was found to be expressed at fairly similar levels between +/+ and fl/fl mice before immunization, however, nine days after immunization, the percentage of $CD4^+$ T cells expressing CXCR5 significantly increased in +/+ mice, but remained fairly stagnant in fl/fl mice (Figure 47 A). While significantly more Th cells in +/+ mice were expressing the surface marker after immunization, the relative surface expression per $CXCR5^+$ cell remained unchanged between WT and BCL6-deficient Th cells (Figure 47 A). To assess how early the difference in $CXCR5^+$ cell percentages takes place, mice were immunized with SRBC and sacrificed one, three, and five days later. When total spleen cells were analyzed for $CXCR5^+$ Th cells, no significant differences in percentages were seen until day five, when the +/+ cells had more (Figure 47 B). This increase also correlated with mRNA analysis of *cxcr5* transcript in *ex vivo* Th cells (Figure 47 C). But again, while the percentage of $CXCR5^+$ cells significantly increased in +/+ mice, compared to fl/fl mice, no differences in the relative expression of CXCR5 per cell were found (Figure 47 B). Therefore, while $BCL6^{fl/fl}$ Cre^{CD4} mice appear to have significantly fewer Th cells expressing CXCR5 by day five, the amount of CXCR5 on each cell is not changed compared to $BCL6^{+/+}$ Cre^{CD4} mice.

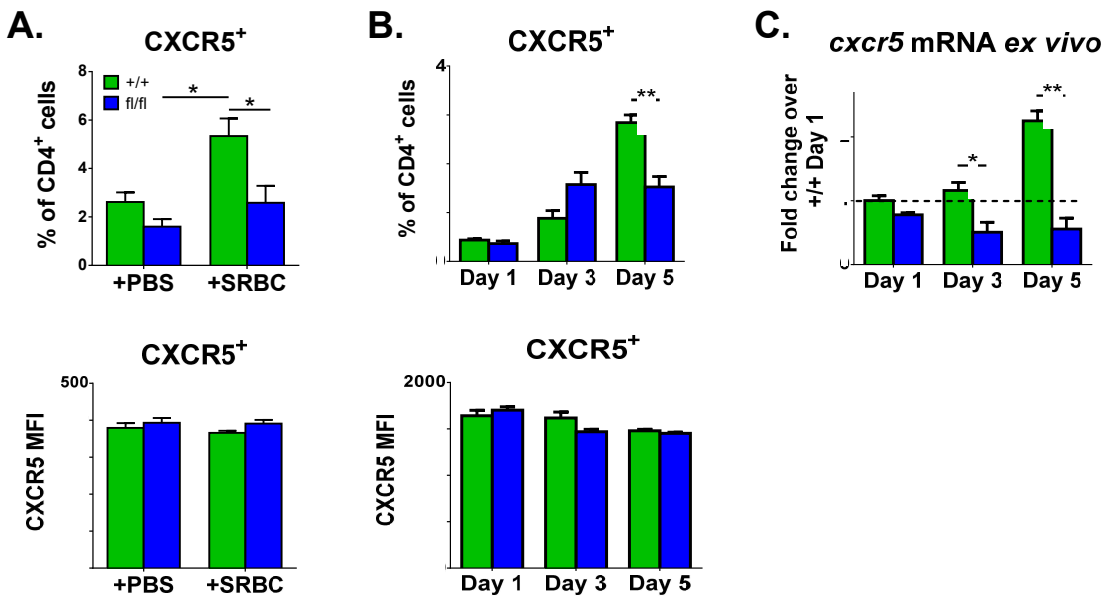

Figure 47. CXCR5 expression in BCL6-deficient CD4⁺ T cells. A. CXCR5 surface expression on Th cells from spleen was evaluated in unimmunized (+PBS) mice and mice immunized with SRBC and sacrificed on day 9 via flow cytometry. The percent of CXCR5⁺ cells is shown as a percentage of CD4⁺ cells (top) and the MFI of CXCR5 in the CXCR5⁺ population is shown (bottom). Cells gated on CD3⁺ CD4⁺ CXCR5⁺. Mean ± SE. *p < 0.05 by two-way ANOVA; Tukey post hoc. **B.** Mice were immunized with SRBC and sacrificed 1, 3, and 5 days after. Spleen cells were assessed for CXCR5 expression as in (**A**). Mean ± SE. **p < 0.01 by *t* test. **C.** Total CD4⁺ T cells were isolated via bead separation from spleen of mice immunized in (**B**) and lysed for RNA analysis. Transcript levels of *cxcr5* were assessed and normalized to Day 1 +/+ samples (dotted line at 1). Mean ± SE. *p < 0.05, **p < 0.01 by *t* test.

The next marker we analyzed was ICOS. By first gating cells on CXCR5 expression, we were able to evaluate the potential for ICOS expression on TFH and non-TFH cells in +/+ mice. Because fl/fl mice are unable to produce TFH cells, in this way we can equalize any bias in ICOS expression on TFH cells in +/+ mice. First, when ICOS⁺ cells were evaluated in CXCR5⁺ cells, those which are poised to become TFH cells, we saw a significant increase in ICOS⁺ cells after immunization in +/+ mice, which was expected as these mice have TFH cells (Figure 48 A). Like CXCR5, we saw no significant difference in ICOS MFI on ICOS⁺ cells within this CXCR5⁺ gate (Figure 48 A). Next, we evaluated ICOS expression on CXCR5⁻ Th cells. While the percentage of ICOS⁺ cells significantly increased in both BCL6$^{+/+}$ Cre^{CD4} and BCL6$^{fl/fl}$ Cre^{CD4} mice after immunization, +/+ Th cells still had a significantly larger proportion expressing the surface marker (Figure 48 B). However, once again, there was no difference in the

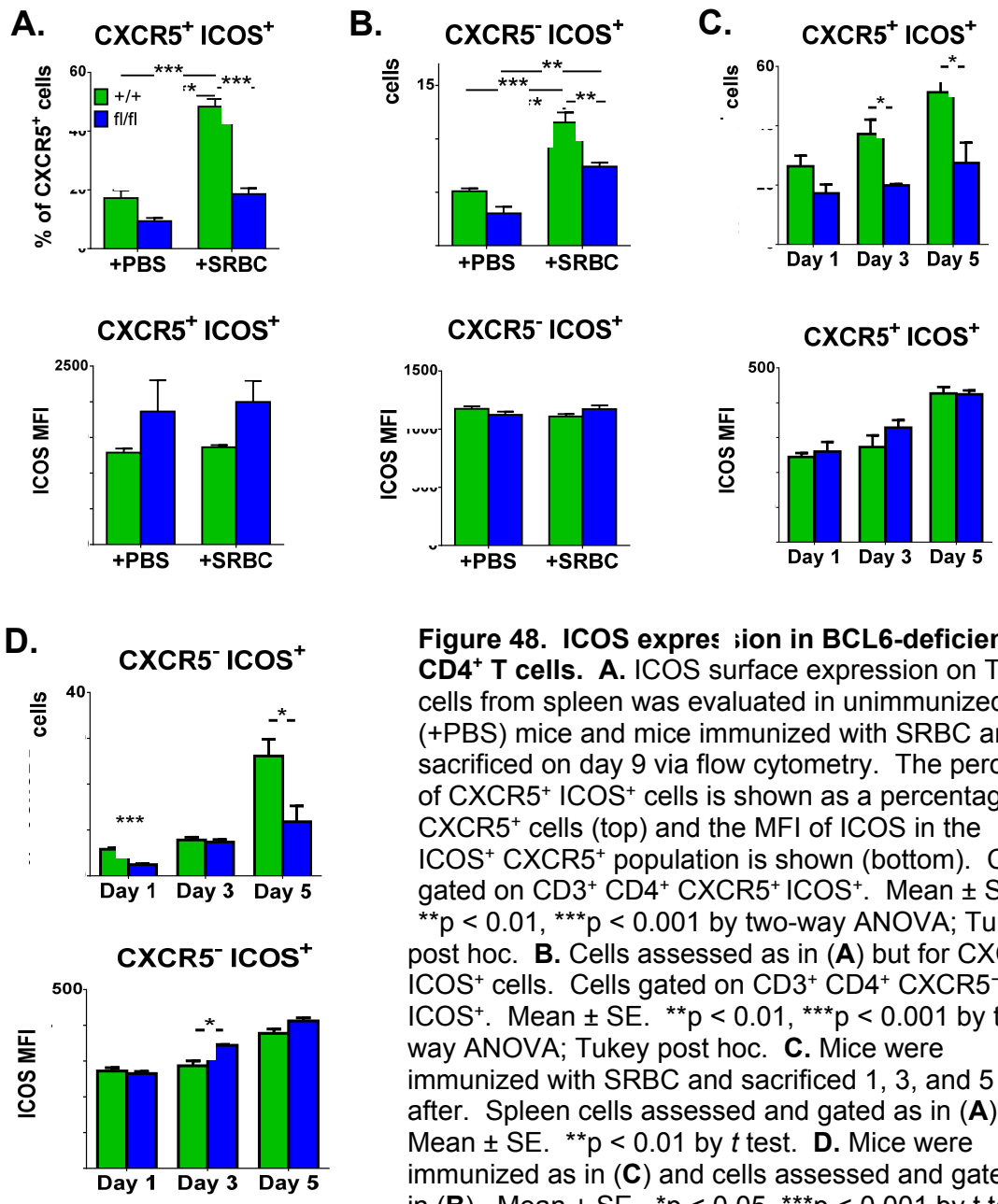

Figure 48. ICOS expres ion in BCL6-deficient CD4⁺ T cells. A. ICOS surface expression on Th cells from spleen was evaluated in unimmunized (+PBS) mice and mice immunized with SRBC and sacrificed on day 9 via flow cytometry. The percent of CXCR5⁺ ICOS⁺ cells is shown as a percentage of CXCR5⁺ cells (top) and the MFI of ICOS in the ICOS⁺ CXCR5⁺ population is shown (bottom). Cells gated on CD3⁺ CD4⁺ CXCR5⁺ ICOS⁺. Mean ± SE. **p < 0.01, ***p < 0.001 by two-way ANOVA; Tukey post hoc. **B.** Cells assessed as in (**A**) but for CXCR5⁻ ICOS⁺ cells. Cells gated on CD3⁺ CD4⁺ CXCR5⁻ ICOS⁺. Mean ± SE. **p < 0.01, ***p < 0.001 by two-way ANOVA; Tukey post hoc. **C.** Mice were immunized with SRBC and sacrificed 1, 3, and 5 days after. Spleen cells assessed and gated as in (**A**). Mean ± SE. **p < 0.01 by *t* test. **D.** Mice were immunized as in (**C**) and cells assessed and gated as in (**B**). Mean ± SE. *p < 0.05, ***p < 0.001 by t test.

amount of ICOS expressed per cell when comparing +/+ and fl/fl Th cells (Figure 48 B).

To evaluate any differences early in the immune response, the same time course experiment was done and ICOS was evaluated on CXCR5⁺ and CXCR5⁻ cells one, three, and five days after immunization. Th cells from fl/fl mice had significantly fewer CXCR5⁺ cells expressing ICOS five days after immunization (Figure 48 C). Like CXCR5 expression, this was expected, as +/+ mice have TFH cells which significantly increased

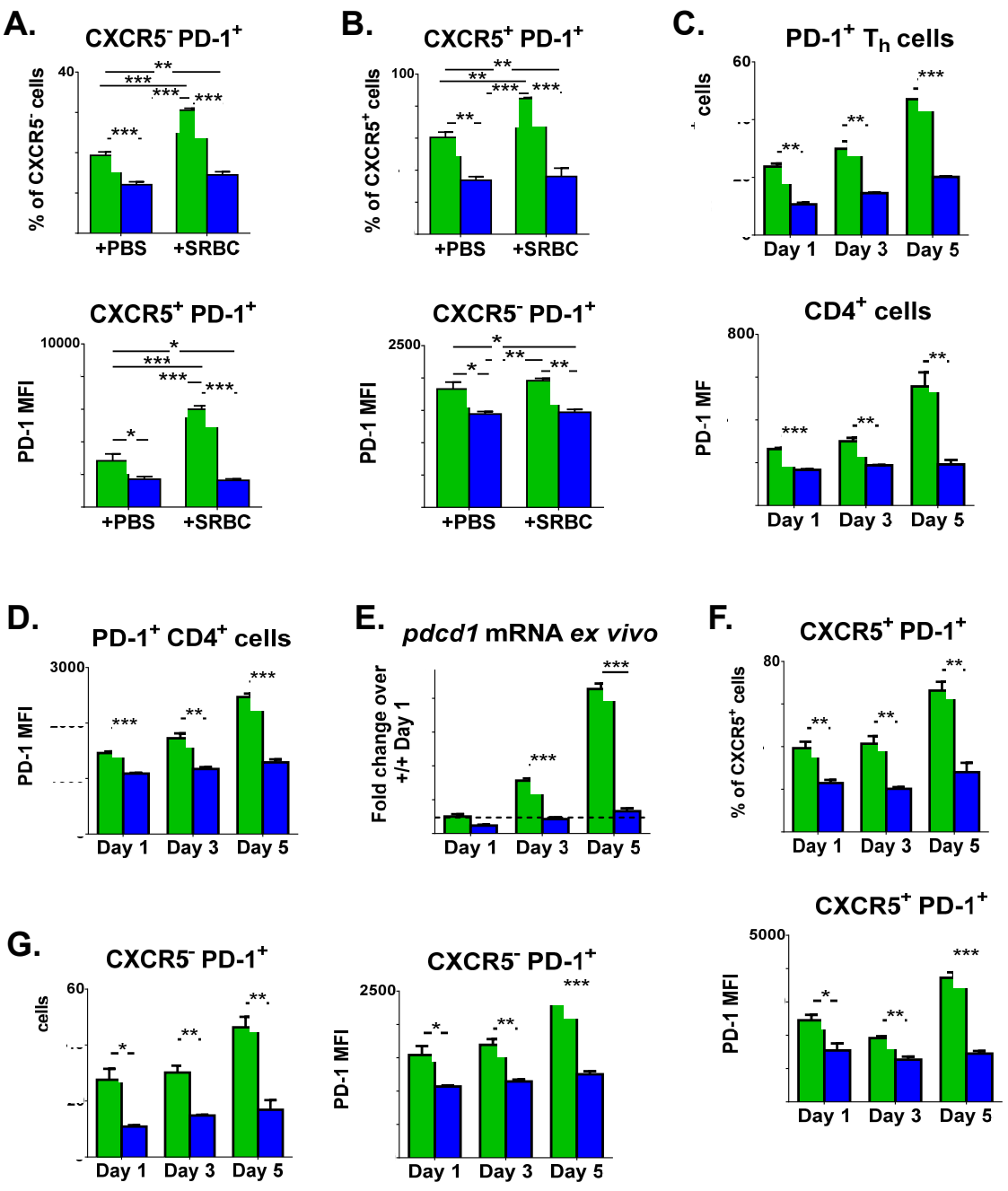

Figure 49. PD-1 expression s altered in the absence of BCL6. A. PD-1 surface expression on Th cells from spleen was evaluated in unimmunized (+PBS) mice and mice immunized with SRBC and sacrificed on day 9 via flow cytometry. The percent of CXCR5$^+$ PD-1$^+$ cells is shown as a percentage of CXCR5$^+$ cells (top) and the MFI of PD-1 in the PD-1$^+$ CXCR5$^+$ population is shown (bottom). Cells gated on CD3$^+$ CD4$^+$ CXCR5$^+$ PD-1$^+$. Mean ± SE. *p < 0.05, **p < 0.01, ***p < 0.001 by two-way ANOVA; Tukey post hoc. **B.** Cells assessed as in (**A**) but for CXCR5$^-$ PD-1$^+$ cells. Cells gated on CD3$^+$ CD4$^+$ CXCR5$^-$ PD-1$^+$. Mean ± SE. *p < 0.05, **p < 0.01, ***p < 0.001 by two-way ANOVA; Tukey post hoc. **C.** Mice were immunized with SRBC and sacrificed 1, 3, and 5 days after. Total CD4$^+$ T cells were assessed for PD-1 expression. Cells gated on CD3$^+$

$CD4^+$ $PD\text{-}1^+$; shown as percent of $CD4^+$ (top) and MFI of PD-1 in total $CD4^+$ T cells shown (bottom). Mean ± SE. **p < 0.01, ***p < 0.001 by *t* test. **D.** PD-1 MFI of $PD\text{-}1^+$ cells in (**C**). Mean ± SE. **p < 0.01, ***p < 0.001 by *t* test. **E.** Total $CD4^+$ T cells were isolated from mice in (**B**) and lysed for RNA analysis. Transcript levels of *pdcd1* (PD-1) were normalized to Day 1 +/+ samples. Mean ± SE. ***p < 0.001 by *t* test. **F.** Cells from (**C**) were further gated on $CXCR5^+$ cells, then assessed for PD-1 expression. Cells gated on $CD3^+$ $CD4^+$ $CXCR5^+$ $PD\text{-}1^+$; shown as percent of $CXCR5^+$ (top) and MFI of PD-1 in $CXCR5^+$ $PD\text{-}1^+$ population (bottom). Mean ± SE. *p < 0.05, **p < 0.01, ***p < 0.001 by *t* test. **G.** Cells assessed the same as in (**F**) except in the $CXCR5^-$ population. Mean ± SE. *p < 0.05, **p < 0.01, ***p < 0.001 by *t* test.

on day five (Figure 45 D). However, ICOS MFI was not changed between +/+ and fl/fl mice in this $CXCR5^+$ gate (Figure 48 C). When ICOS expression was evaluated on non-TFH, or $CXCR5^-$ cells, fl/fl mice had significantly fewer Th cells expressing the marker one and five days after immunization (Figure 48 D). Interestingly, while the MFI of ICOS on those days was unchanged between the two types on mice, on day three, when the percentages of $ICOS^+$ cells were equivalent, fl/fl $ICOS^+$ cells had a higher MFI (Figure 48 D). These data demonstrate that while fewer Th cells in $BCL6^{fl/fl}$ Cre^{CD4} mice are expressing ICOS on their surface, their potential to do so is not changed, as is indicated by ICOS MFI levels.

PD-1 expression is altered in BCL6-deficient Th cells

When PD-1, another key marker for TFH cells, was assessed in unimmunized mice, irrespective of CXCR5 expression, the percentage of PD-1-expressing Th cells was reduced, significantly so in $CXCR5^-$ cells (Figure 49 A-B). Nine days after immunization, the difference in $PD\text{-}1^+$ cells between +/+ and fl/fl mice was even more significant, regardless of the CXCR5 expression status of the cells (Figure 49 A-B). What was most interesting, though, was, unlike CXCR5 and ICOS expression, the MFI of PD-1 was significantly reduced, both before and after immunization, and on both $CXCR5^+$ and $CXCR5^-$ cell subsets (Figure 49 A-B). In fact, the amount of PD-1 expressed on fl/fl $PD\text{-}1^+$ cells after immunization was still significantly less than the amount of PD-1 seen on +/+ cells from unimmunized mice.

Using our time course experiment, we saw that the percent of $PD\text{-}1^+$ cells in total $CD4^+$ T cells was significantly reduced on day one after immunization and the difference is only exacerbated over time (Figure 49 C). This is not surprising, as +/+ mice are generating

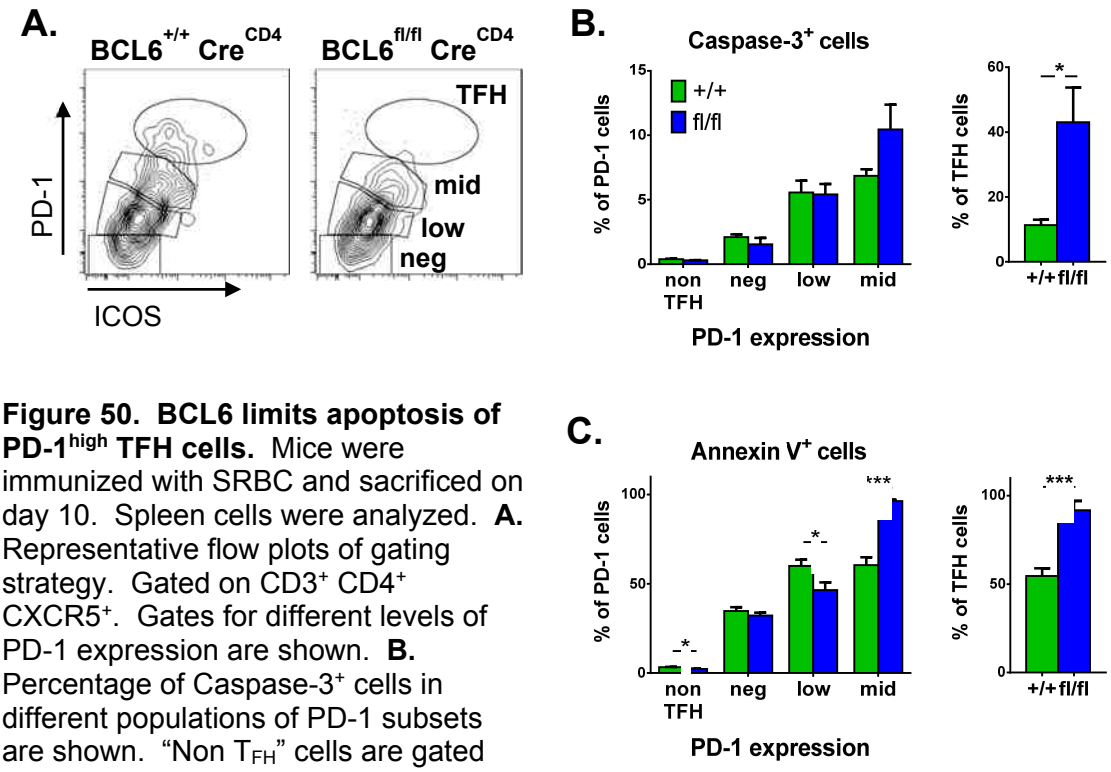

Figure 50. BCL6 limits apoptosis of PD-1^{high} TFH cells. Mice were immunized with SRBC and sacrificed on day 10. Spleen cells were analyzed. **A.** Representative flow plots of gating strategy. Gated on CD3$^+$ CD4$^+$ CXCR5$^+$. Gates for different levels of PD-1 expression are shown. **B.** Percentage of Caspase-3$^+$ cells in different populations of PD-1 subsets are shown. "Non T_{FH}" cells are gated on CD3$^+$ CD4$^+$ CXCR5$^-$ ICOS$^-$ PD-1$^-$. **C.** Percentage of Annexin V$^+$ cells in different populations of PD-1 subsets. Same gating as in (**B**). Mean ± SE. * $p < 0.05$, *** $p < 0.001$ by *t* test.

TFH cells, and they are likely contributing to the overall increase in PD-1$^+$ cells in +/+ mice. The MFI of PD-1 in total Th cells also mirrored these differences (Figure 49 C), as did the mRNA levels of PD-1 (as expressed by the gene *pdcd1*) in total Th cells (Figure 49 E). When PD-1 expression in PD-1$^+$ cells was assessed over time, saw see significantly lower levels of PD-1 surface expression in fl/fl mice (Figure 49 D). Since these assessments are likely skewed by the development of TFH cells in +/+ mice, we further gated Th cells on CXCR5$^+$ (TFH) and CXCR5$^-$ (non-TFH) cells. In the TFH gate, +/+ mice had significantly more cells expressing PD-1 one and five days after immunization (Figure 49 F). However, the amount of PD-1 on the surface of these PD-1$^+$ cells was significantly reduced in fl/fl cells at all time points (Figure 49 F). When non-TFH cells were assessed, significantly fewer fl/fl Th cells were expressing PD-1 at all time points, and the MFI of PD-1 on PD-1$^+$ cells was also significantly reduced (Figure 49 G). Therefore, taken together, this data demonstrates not only a lowered potential for Th cells from fl/fl mice to express PD-1, but those cells expressing this marker, unlike CXCR5 and ICOS, do so at significantly lower levels than +/+ Th cells. This would

suggest a role for BCL6 in promoting the elevated expression of PD-1 in $CD4^+$ T cells.

BCL6 limits apoptosis in PD-1^{high} Th cells

Because PD-1 has been shown to limit T cell proliferation, and, in some cases, facilitate apoptosis, we wanted to evaluate the fate of Th cells expressing high levels of PD-1 in the absence of BCL6. To do this, we immunized mice and sacrificed them ten days later. Spleen cells were assessed for PD-1 expression on Th cells via flow cytometry. $CD4^+$ T cells were subdivided into "non TFH" cells ($CD4^+$ $CXCR5^-$ $ICOS^-$ $PD\text{-}1^-$), PD-1 negative ("neg": $CD4^+$ $CXCR5^+$ $ICOS^-$ $PD\text{-}1^-$), PD-1 low-expressing ("low": $CD4^+$ $CXCR5^+$ $ICOS^{+/-}$ $PD\text{-}1^{low}$), PD-1 mid-level-expressing ("mid": $CD4^+$ $CXCR5^+$ $ICOS^{+/-}$ $PD\text{-}1^{mid}$), and TFH, or PD-1 high-expressing ("TFH": $CD4^+$ $CXCR5^+$ $ICOS^+$ $PD\text{-}1^{hi}$) cells. An example of these gates for both +/+ and fl/fl mice is shown in Figure 50 A. Cells within each gate were then assessed for active Caspase-3 staining (Figure 50 B) or Annexin V staining (Figure 50 C). Our results show a striking correlation between PD-1 expression and positive staining for apoptosis markers. In both +/+ and fl/l mice, as PD-1 MFI increased, so did the percentage of cells which were Caspase-3^+ or Annexin V^+. Interestingly, at lower levels of PD-1 expression, BCL6-deficient cells had less Annexin V staining than +/+ cells (Figure 50 C). At higher levels of PD-1 though (PD-1 mid and TFH), +/+ cells seemed to be protected from apoptosis, while almost 100 percent of the few BCL6-deficient cells to be included in the TFH gate were Annexin V^+, and, to a lesser extent, Caspase-3^+. This data suggests that at low levels of PD-1 surface expression, BCL6 seems to facilitate apoptosis, while at the highest levels of PD-1, BCL6 limits apoptosis of TFH cells.

Methylation and deacetylation machinery is increased in the absence of BCL6

To investigate what may be restricting the expression of PD-1 in our BCL6-deficient Th cells, we revisited the data produced from our microarray experiment (See Table 1 in Chapter 3). Upon closer inspection, we observed significant increases in the chromatin remodeling enzymes responsible for adopting a more closed conformation. In the case of our results, Dnmt1, which is responsible for maintaining the methylation profile of replicated DNA, was not changed in fl/fl mice (Figure 51 A). However, one Dnmt which is responsible for *de novo* methylation of DNA, Dnmt3b, was significantly increased in

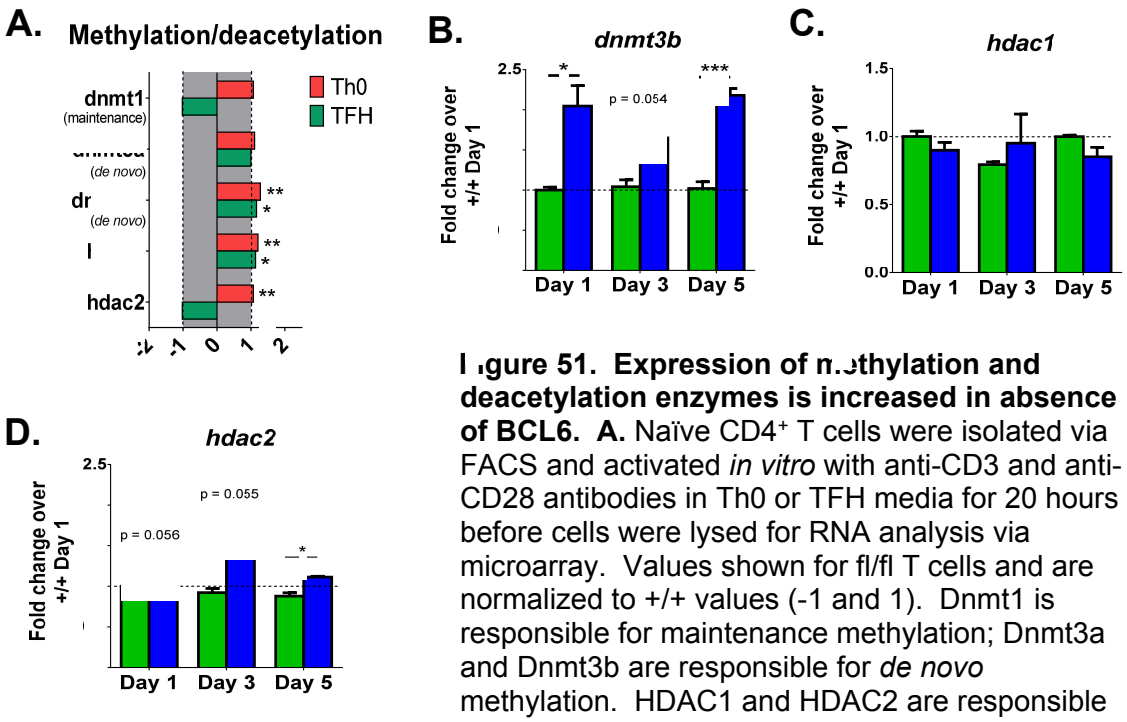

I gure 51. Expression of n.thylation and deacetylation enzymes is increased in absence of BCL6. A. Naïve CD4⁺ T cells were isolated via FACS and activated *in vitro* with anti-CD3 and anti-CD28 antibodies in Th0 or TFH media for 20 hours before cells were lysed for RNA analysis via microarray. Values shown for fl/fl T cells and are normalized to +/+ values (-1 and 1). Dnmt1 is responsible for maintenance methylation; Dnmt3a and Dnmt3b are responsible for *de novo* methylation. HDAC1 and HDAC2 are responsible for deacetylation of histones. Naïve cells gated on CD3⁺ CD4⁺ CD44⁻ CD62L⁺. **B-D.** Mice were immunized with SRBC and sacrificed 1, 3, and 5 days after. Total CD4⁺ T cells were isolated from spleen via bead separation and lysed *ex vivo* for RNA analysis via qPCR. Transcript levels for **B.** *dnmt3b*, **C.** *hdac1*, and **D.** *hdac2* are normalized to Day 1 +/+ (dotted line at 1.0). Mean ± SE. *p < 0.05, **p < 0.01, ***p < 0.001 by *t* test.

both culture conditions. Furthermore, the HDAC which Dnmt3b has been shown to associate with, HDAC1, was significantly increased in a similar fashion (Figure 51 A).

To verify these changes, we tested the RNA from our time course experiment (Figure 45 C) for expression of these enzymes. Transcript levels of *dnmt3b* were increased in the Th cells from fl/fl mice at all time points after immunization (Figure 51 B). Unlike the microarray data, *hdac1* expression was not increased in an *in vivo* model (Figure 51 C), however *hdac2* was (Figure 51 D). It is important to note, though, that this RNA analysis was done on Th cells with mixed statuses of activation, while the microarray was used to analyze naïve Th cells which were all, presumably, activated in the *in vitro* culture. Therefore, taken together, these data show that Dnmt3b is significantly increased in all Th cells, regardless of activation status, while expression of HDAC enzymes may be affected more by the *in vitro* culture conditions and level of cellular activation. But overall, these data provide evidence that epigenetically, the DNA structure of Th cells in

fl/fl mice may be altered and in a more closed confirmation, thus blocking access to transcriptional machinery.

The promoter region of PD-1 has increased binding of DNA-methyltransferases

To test if PD-1 is being repressed by epigenetic modifications to the gene *in vivo*, we performed a chromatin immunoprecipitation (ChIP) assay. First, total $CD4^+$ T cells were isolated from unimmunized $BCL6^{+/+}$ Cre^{CD4} and $BCL6^{fl/fl}$ Cre^{CD4} mice, or from mice immunized with SRBC and sacrificed on day five. We chose to evaluate T cells from five day immunized mice because this is the time point at which we saw the most significant differences in PD-1 and Dnmt3b expression. For ChIP analysis, isolated chromatin was immunoprecipitated (IP) for Dnmt3a (as a control) or Dnmt3b. The DNA pulled down with these proteins was then assessed for the presence of the PD-1 (*pdcd1*) promoter region. Before immunization (Day 0), no differences in Dnmt3a binding to either of the two PD-1 promoter sites checked were found between +/+ and fl/fl cells (Figure 52 A-B). Five days after immunization, fl/fl samples were shown to have significantly more Dnmt3a present at one region of the PD-1 promoter (Figure 52 A). When cells were IP for Dnmt3b, fl/fl samples had more of the methyltransferase present at the PD-1 promoter, both before and after immunization (Figure 52 C-D). Interestingly, +/+ cells had no detectable presence of Dnmt3b at the PD-1 promoter before immunization (Figure 52 C-D).

Next, using a ChIP assay, we investigated the acetylation status of the PD-1 promoter. When samples were IP for acetylated histone 3 (H3AC), then assessed for the presence of the PD-1 promoter, +/+ cells were found to have more acetylated histone at both regions of the PD-1 promoter checked (Figure 53 A-B). The same was found when samples were IP for H4AC (Figure 53 C-D). These data show fl/fl Th cells have less acetylation of their H3 and H4 histones at the PD-1 promoter. Therefore, it is likely the PD-1 promoter in fl/fl Th cells has a less open conformation than the PD-1 promoter region in +/+ Th cells.

Another crucial TFH marker, CXCR5, has been shown to be dependent on BCL6 expression later in the immune response. As shown in Figure 47, expression of CXCR5

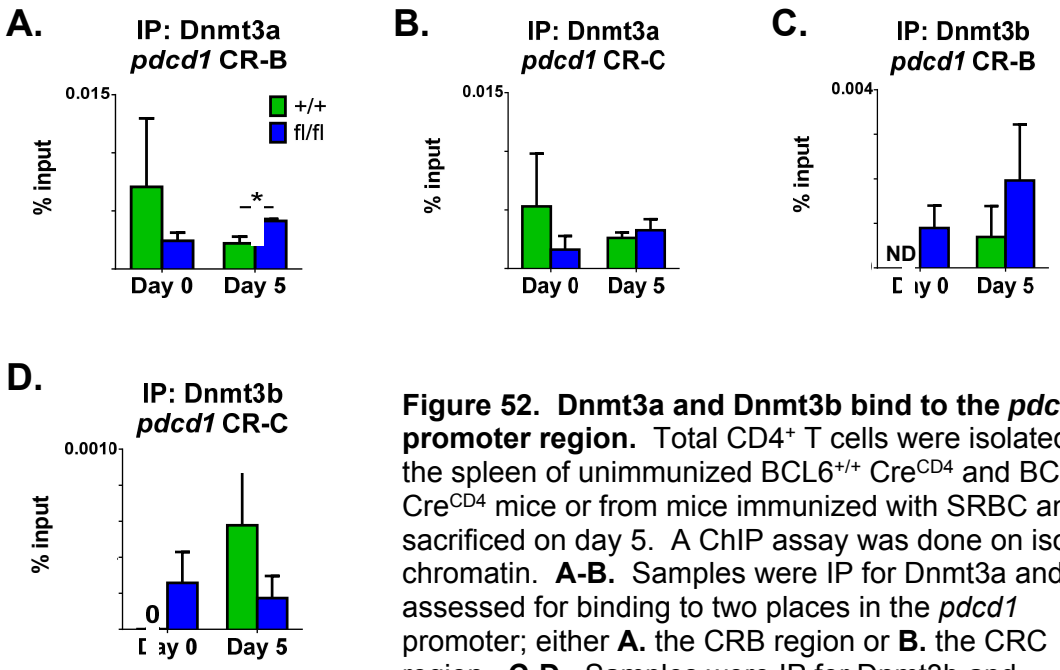

ND

Figure 52. Dnmt3a and Dnmt3b bind to the *pdcd1* promoter region. Total CD4^{+} T cells were isolated from the spleen of unimmunized BCL6$^{+/+}$ Cre^{CD4} and BCL6$^{fl/fl}$ Cre^{CD4} mice or from mice immunized with SRBC and sacrificed on day 5. A ChIP assay was done on isolated chromatin. **A-B.** Samples were IP for Dnmt3a and assessed for binding to two places in the *pdcd1* promoter; either **A.** the CRB region or **B.** the CRC region. **C-D.** Samples were IP for Dnmt3b and assessed for binding to two places in the *pdcd1* promoter; either **C.** the CRB region or **D.** the CRC region. Shown as percent of input. ND = none detected. Mean ± SE. *p < 0.05 by *t* test. Done in collaboration with Dr. Duy Pham.

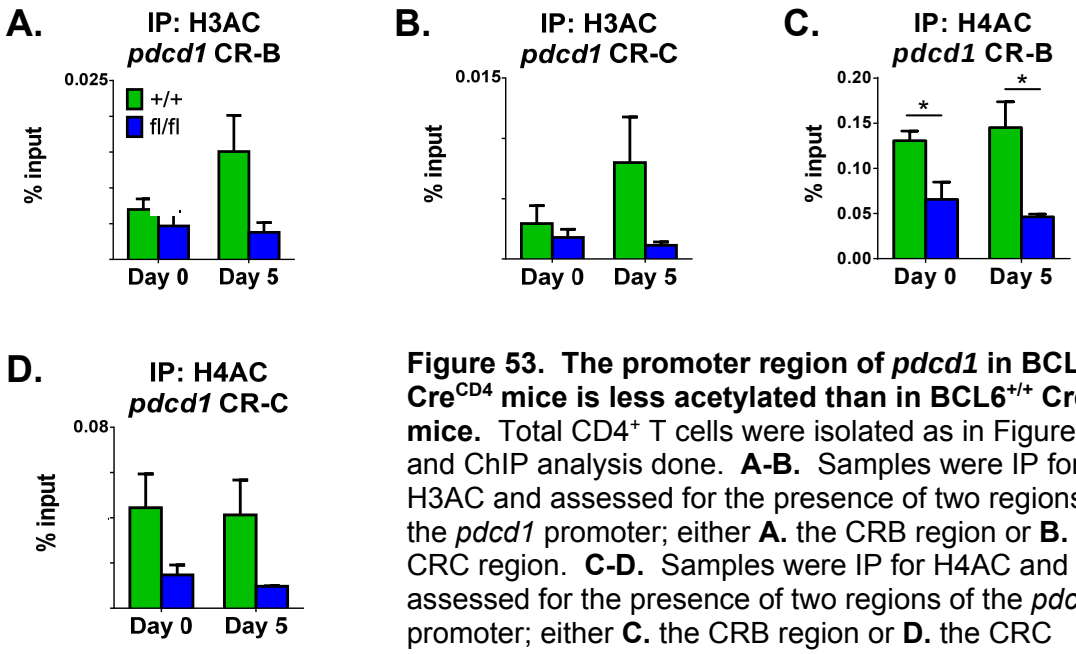

Figure 53. The promoter region of *pdcd1* in BCL6$^{fl/fl}$ Cre^{CD4} mice is less acetylated than in BCL6$^{+/+}$ Cre^{CD4} mice. Total CD4^{+} T cells were isolated as in Figure G and ChIP analysis done. **A-B.** Samples were IP for H3AC and assessed for the presence of two regions of the *pdcd1* promoter; either **A.** the CRB region or **B.** the CRC region. **C-D.** Samples were IP for H4AC and assessed for the presence of two regions of the *pdcd1* promoter; either **C.** the CRB region or **D.** the CRC region. Shown as percent of input. Mean ± SE. *p < 0.05 by *t* test. Done in collaboration with Dr. Duy Pham.

was significantly decreased on fl/fl cells beginning five days after immunization. When the promoter region of CXCR5 was assessed for the presence of Dnmt3a and Dnm3b binding via ChIP analysis, we saw no differences between +/+ and fl/fl samples either before or five days after immunization (Figure 54 A-B). However, the acetylation status of the H3 and H4 histones was significantly altered. While there was significantly less acetylated H3 histone at the *cxcr5* promoter of fl/fl cells after immunization (Figure 54 C), H4 was significantly less acetylated both before and after immunization (Figure 54 D). Because the CXCR5 promoter in fl/fl mice did not have altered Dnmt binding, but did have decreased acetylation, it would appear that increased methylation via Dnmt3b is a mechanism for repression of PD-1 in fl/fl Th cells, while this method does not repress CXCR5.

Blocking methylation increases PD-1 expression, but not CXCR5 expression

To test the hypothesis that PD-1 expression is controlled by the methylation status of its promoter, we carried out *in vitro* experiments in which we block methylation. Total $CD4^+$ T cells were isolated from C57BL/6 mice and activated *in vitro* with anti-CD3 and anti-

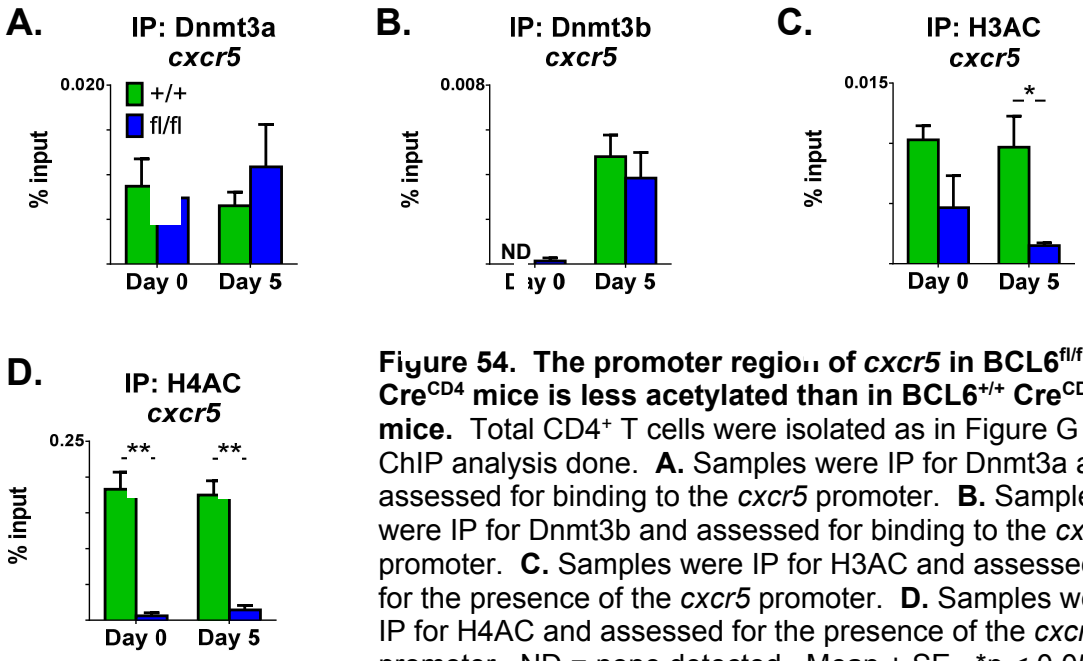

Figure 54. The promoter region of *cxcr5* in $BCL6^{fl/fl}$ Cre^{CD4} mice is less acetylated than in $BCL6^{+/+}$ Cre^{CD4} mice. Total $CD4^+$ T cells were isolated as in Figure G and ChIP analysis done. **A.** Samples were IP for Dnmt3a and assessed for binding to the *cxcr5* promoter. **B.** Samples were IP for Dnmt3b and assessed for binding to the *cxcr5* promoter. **C.** Samples were IP for H3AC and assessed for the presence of the *cxcr5* promoter. **D.** Samples were IP for H4AC and assessed for the presence of the *cxcr5* promoter. ND = none detected. Mean ± SE. *$p < 0.05$, **$p < 0.01$ by *t* test. Done in collaboration with Dr. Duy Pham.

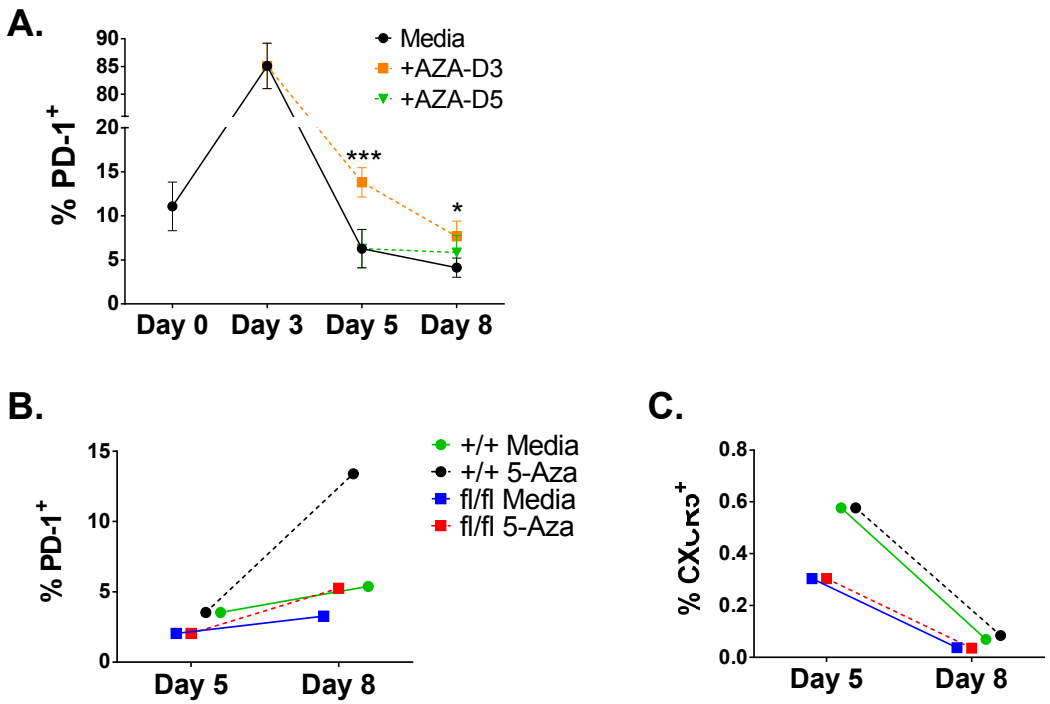

Figure 55. Blocking methylation increases PD-1 expression, but not CXCR5 expression. A. Total CD4$^+$ T cells were isolated from C57BL/6 mice via bead separation. Cells were activated *in vitro* with anti-CD3 and anti-CD28 antibodies in Th0 media. On day 0, cells were checked for surface expression of PD-1 via flow cytometry. On day 3, cells were again assessed for PD-1 expression, and half of the remaining cells were treated with 5-Aza-2′-deoxycytidine (+AZA-D3). On day 5, all cells were assessed for PD-1 expression. Half of the remaining untreated cells (media only) then had 5-Aza-2′-deoxycytidine added to their media (+AZA-D5). On day 8, all cells were harvested and assessed for PD-1 expression. Shown as percent of total cells. Gated on CD4$^+$. Mean ± SE; n = 4. *p < 0.05, ***p < 0.001 by ANOVA, Tukey post hoc. **B-C.** Total CD4$^+$ T cells were isolated from unimmunized BCL6$^{+/+}$ Cre^{CD4} and BCL6$^{fl/fl}$ Cre^{CD4} mice via bead separation and activated *in vitro* with anit-CD3 and anti-CD28 antibodies in Th0 media. On day 5 of the culture, cells were checked for surface marker expression via flow cytometry. Also, half of the cells were treated with 5-Aza-2′-deoxycytidine. On day 8, all cells were harvested and checked for surface marker expression via flow cytometry. **B.** Surface expression of PD-1. **C.** Surface expression of CXCR5.

CD28 antibodies in Th0 media. Three days later, samples were assessed for PD-1 expression. At this time, approximately 85% of cells were PD-1$^+$ (Figure 55 A). The remaining cells were then split; half continued to be culture in media and half were treated with 5-Aza-2′-deoxycytidine (Azacytidine), a methylation inhibitor. On day five, all cells were assessed for PD-1 expression. Cells which received Azacytidine on day three (+Aza–D3) had significantly more cells expressing PD-1 on the surface compared to untreated cells (Figure 55 A). The remaining untreated cells were again split in half,

leaving one group in media only and the other group treated with Azacytidine (+Aza–D5). Eight days after the initial activation, all cells were harvested and assessed for PD-1 expression via flow cytometry. As shown in Figure 55 A, cells treated with Azacytidine on day three (+Aza–D3) were significantly increased in the percentage of cells expressing PD-1 on the surface compared to untreated cells. While treatment with Azacytidine on day 5 did increase the percent of cells expressing PD-1, it was not significantly more than what untreated cells expressed (Figure 55 A).

Using this approach, we next wanted to test if treatment with Azacytidine could restore PD-1 surface expression levels on fl/fl cells to those seen on +/+ cells. As before, total $CD4^+$ T cells from mice were isolated and activated *in vitro*. Five days later, cells were treated with Azacytidine. At this time point, untreated cells from +/+ and fl/fl mice had fairly low percentages of PD-1^+ cells, although +/+ mice had more (Figure 55 B). On day eight, when all samples were checked, treatment of +/+ Th cells with Azacytidine increased the percent of PD-1^+ cells above what was seen on day five (Figure 55 B). While treatment of fl/fl Th cells was able to increase the percent of cells expressing PD-1, it was only able to raise the level to that of untreated +/+ cells (Figure 55 B). To verify that the increases seen with Azacytidine treatment were specific to PD-1 and not a genome-wide increase in expression, cells were also assessed for CXCR5 surface expression. As shown in Figure 55, Azacytidine treatment did not increase the percent of $CXCR5^+$ cells for either mouse group (Figure 55 C). Therefore, it appears that PD-1, to some extent, is controlled by methylation of its promoter.

DISCUSSION

Using our new mouse model, we were able to verify the necessity of BCL6 in Th cells for the development of TFH cells and GCs. Without this transcription factor, mice were unable to establish GCs at any time after immunization. The functional effects of GC loss were observed by sharp reductions in antigen-specific antibody production, and, in some cases, decreases in total isotype production. Therefore, these results demonstrate an inherent necessity for BCL6 expression in Th cells for not only the development of GCs, but also for high titers of antigen-specific antibodies.

These findings can be applied to human therapeutics in two distinct ways. First, patients suffering from autoimmune disorders associated with increased TFH differentiation could benefit from protein inhibitors which target BCL6 in T cells. As demonstrated in Chapter 4, deletion of BCL6 in $CD4^+$ T cells has little effect on the differentiation of other Th cell subsets. Additionally, the antibody data presented here suggests that by inhibiting the development of TFH cells, antigen-specific antibody titers can be drastically reduced as well. Therefore, a BCL6 protein inhibitor could provide a therapeutic alternative to those immune modulating drugs already on the market for autoimmune disease patients.

Secondly, because the ultimate goal of vaccines is to trigger the development of B cells which secrete high affinity, antigen-specific antibodies, and survive long term, if said vaccines could be programmed to facilitate increased TFH differentiation upon immunization, more robust GCs could develop, and, theoretically, higher affinity antibodies would result. Data presented in Chapter 6 concerning a prime/boost vaccine scheme would suggest that increased GCs may actually limit antibody quality in that type of approach. However, whether increased GC development is beneficial when only one immunization is necessary has yet to be investigated.

When evaluating TFH surface marker expression, we found evidence that CXCR5 can, in fact, be expressed in a BCL6-independent fashion, up to five days post-immunization. After that time point, it appears the BCL6-deficient Th cells cannot sustain surface expression and decrease the amount of CXCR5 expressed, as demonstrated by qPCR and flow cytometry analysis. Furthermore, by day five, while $BCL6^{fl/fl}$ Cre^{CD4} Th cells are still expressing CXCR5 above background levels, they cannot up-regulate the chemokine receptor to the levels seen in +/+ mice. Evaluation of ICOS showed a similar trend, wherein Th cells from fl/fl mice can in fact up-regulate the marker in both TFH-like and non-TFH cells ($CXCR5^+$ and $CXCR5^-$ subsets, respectively), but not as many cells are able to do so by day five. However, in the case of both CXCR5 and ICOS, those cells which do express the markers in fl/fl mice are able to do so with the same potential as +/+ mice, as evidenced by similar MFI levels of $CXCR5^+$ and $ICOS^+$ cells.

When PD-1 was assessed for surface expression, we found that while the percentage of $PD\text{-}1^+$ cells was significantly reduced in fl/fl mice, unlike ICOS and CXCR5, the MFI of this TFH marker was also significantly reduced in BCL6-deficient Th cells. This

difference was seen irrespective of whether a Th cell was $CXCR5^+$ (TFH-like) or $CXCR5^-$ (non-TFH). Therefore, the expression of PD-1 on Th cells is affected by loss of BCL6 even in non-TFH cells. Also of interest was the observation that CXCR5 and ICOS deficiencies in fl/fl mice were only really seen as of day five after immunization. However, with PD-1 expression, a truly significant loss of positive cells and the amount of PD-1 expressed by those cells was seen in unimmunized mice. After immunization, the difference in PD-1 expression was significantly lower in fl/fl mice and this difference only exacerbated over time. It appears, though, that these differences are mainly due to the increased expression by +/+ Th cells, while $CD4^+$ T cells in fl/fl mice fail to increase the percentage of $PD\text{-}1^+$ cells and the existing $PD\text{-}1^+$ cells are unable to increase their surface expression, as shown by decreases in MFI. Therefore, the mechanism controlling PD-1 expression in TFH and non-TFH cells is affected even before immunization in BCL6-deficient Th cells and cannot be overcome with immunization.

Data provided by our microarray analysis demonstrate a potential role for chromatin remodeling enzymes in the repression of PD-1 in the Th cells of $BCL6^{fl/fl}$ Cre^{CD4} mice. After identifying Dnmt3b as a potential inhibitor of PD-1 expression, ChIP analysis confirmed that this DNA-methyltransferase does in fact bind to the promoter region of PD-1 in fl/fl Th cells before immunization, while it is not present in +/+ cells. Because Dnmt3b is responsible for *de novo* methylation of DNA, this data would suggest that Dnmt3b is actively methylating the PD-1 promoter of unactivated Th cells in the absence of BCL6. After immunization, significantly more Dnmt3a was found at one PD-1 promoter site in fl/fl cells. Because both Dnmt3a and 3b can silence genes by physically binding to the promoter and blocking the transcriptional machinery, this may be an additional way in which Dnmt activity is limiting PD-1 expression in fl/fl Th cells. Therefore, not only is it probable that the promoter region of PD-1 is hyper-methylated before cell activation, after immunization, binding of Dnmt3a to the promoter is likely inhibiting access of RNA polymerase to the region. Furthermore, the consistent and significant decrease in acetylation of the H3 and H4 histones at the PD-1 promoter regions suggests an even more closed conformation of this gene.

To verify that this activity is unique to PD-1, we assessed the presence of these enzymes at a promoter site of CXCR5. We found no evidence of differential Dnmt3a or Dnmt3b binding at the CXCR5 promoter in +/+ and fl/fl mice. However, when the

acetylation levels of H3 and H4 were examined, it was found that the CXCR5 promoter in fl/fl Th cells has significantly less acetylation, both before and after immunization. Therefore, expression of CXCR5 may be somewhat controlled by acetylation of its promoter, but Dnmts do not appear to be affecting its expression exclusively in BCL6-deficient mice.

Finally, to further investigate a potential role for methylation in PD-1 repression, activated $CD4^+$ T cells were treated with 5-Aza-2′-deoxycytidine (Azacytidine). This methylation inhibitor was able to increase PD-1 levels in C57BL/6 and $BCL6^{+/+}$ Cre^{CD4} cells. However, while the percent of $PD\text{-}1^+$ cells did increase when $BCL6^{fl/fl}$ Cre^{CD4} cells were treated, the levels were only increased to that of untreated +/+ cells. Therefore, blocking methylation is able to partially overcome the decrease in PD-1 expression in the absence of BCL6. Whether prolonged exposure to Azacytidine can further increase the levels seen in fl/fl Th cells needs to be investigated.

In addition to describing how BCL6 may control PD-1 expression, we also found that BCL6 may be limiting the intracellular signals of PD-1 in TFH cells. When $CD4^+$ T cells were subdivided by PD-1 expression levels, we found that in the absence of BCL6, more PD-1-high Th cells were marked for apoptosis than their WT counterparts. Because high levels of PD-1 are typically associated with exhausted T cells, researchers have wondered how TFH cells are able to remain functionally active while expressing this marker. Here we demonstrate that the high expression levels of BCL6 found in TFH cells may be somehow limiting the quiescence or death signals coming from PD-1 engagement, thus allowing for continued activity by these cells.

Data presented in this chapter has established a new method for how BCL6 can activate gene expression: by repressing methylation. Previous data (Chapter 2, Figure 9 A) has demonstrated a correlation between BCL6 and PD-1 expression. Therefore, when we observed not only a reduction in the percent of Th cells expressing PD-1 in fl/fl mice, but a drop in the MFI of $PD\text{-}1^+$ cells as well, we hypothesized that BCL6 controls PD-1 expression through an as-yet identified mechanism. Microarray and ChIP analysis enabled us to identify epigenetic modifiers which were increased in the absence of BCL6, and they were found to bind specifically to the PD-1 promoter, and not to other TFH markers, like CXCR5. Identification of Dnmt3b as a BCL6 target is a unique finding

and the first of its kind as a way to describe how BCL6 controls TFH gene expression. Further work needs to be done to verify the specific nature of the relationship between BCL6 and Dnmt3b, but we are confident that we have, for the first time, described a method for BCL6-mediated gene activation.

CHAPTER 6 – GERMINAL CENTER DYNAMICS IN AN HIV-1-gp120 DNA PRIME/PROTEIN BOOST VACCINE SCHEME

INTRODUCTION

The Human Immunodeficiency Virus-1 (HIV-1) has affected hundreds of millions of people worldwide since its discovery in the early 1980s (135). In 1996, hope was given to millions of infected patients with the release of the Highly Active Anti-Retroviral Therapy, or HAART (136). This combination drug therapy meant people with HIV were no longer sentenced to die, but instead could manage their infection and extend their life. The quality of that life, however, was not as high as their pre-infection standards. Side effects, including, but not limited to, nausea, vomiting, mental health issues, renal and liver failure, and heart attacks were common (136, 137). Furthermore, the cost of these treatments meant life-extension remained out of reach for the vast majority of HIV^+ patients (138). While drug development over the last two decades has decreased the number and severity of these side effects, as well as substantially lowered the cost of anti-retroviral drugs, millions of people are still infected each year. To date, six different human vaccine trials have taken place (139-142), with one ending early due to unexplained increases in HIV-1 susceptibility (143), and one showing modest protection of approximately thirty percent (144). Therefore, the challenge remains to create an effective HIV-1 vaccine which prevents the transmission of all clades and, ultimately, eradicates this virus from the human population.

HIV is a lentivirus which packages two identical single strand RNA transcripts into its capsid, along with several viral enzymes (Figure 56) (138, 145). The surface glycoprotein (gp) 160 is composed of a transmembrane section, termed gp41, and a surface section, called gp120 (Figure 56) (138, 145, 146). After gp120 attaches to its main receptor, CD4, on a host cell, a conformational change in the structure of the surface glycoprotein facilitates binding to a coreceptor, either CCR5 or CXCR4 (Figure 57 A-B) (146). Coreceptor binding then triggers an additional conformational change, allowing a section of gp41, called HR1, which is typically covered to become exposed and bind to the host cell surface (Figure 57 C) (146). Once two gp160 glycoproteins have bound to the host cell surface, the viral capsid can then be deposited into the host cell (Figure 57 D) (145, 146). Release of the capsid contents into the cytoplasm of the

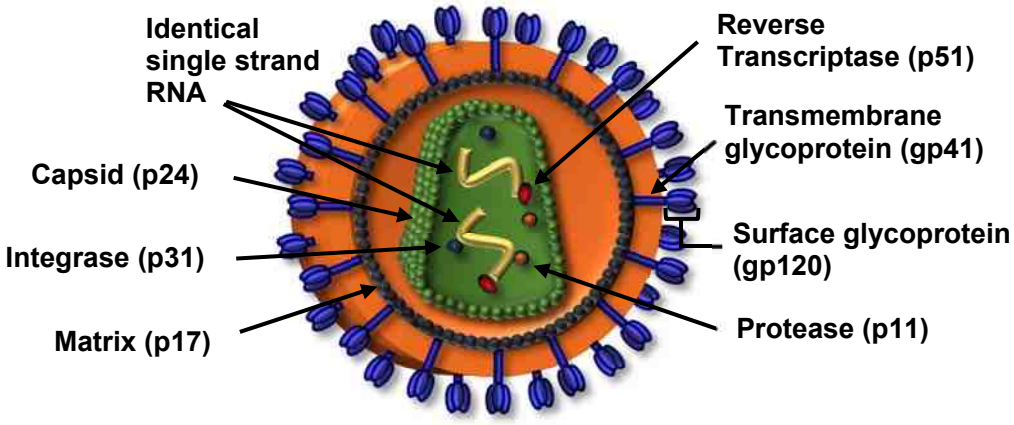

Figure 56. Structure of HIV virion. HIV is a single strand RNA virus which carries two identical copies of its genome. The RNA is surrounded by a capsid made from protein 24 (p24). Accessory proteins and enzymes are also packaged within the capsid with the RNA, including integrase (p31), reverse transcriptase (p51), and protease (p11). The nuclear capsid is surrounded by a matrix made from p17. The surface of the virus is covered in glycoproteins. The surface portion is termed gp120, while the transmembrane section is gp41. Together, these glycoproteins make gp160.

host cell allows the viral reverse transcriptase enzymes to transcribe DNA from the viral RNA genome (Figure 57 E) (145, 147). That DNA can then be transported into the host nucleus and integrated into the host genome via the viral integrase enzyme (Figure 57 F) (147, 148). Once integrated, the virus is now referred to as a provirus and can lay dormant for years, even decades, before beginning to replicate uncontrollably, leading to the decimation of the helper T cell response, and the patient to develop AIDS-related diseases (135, 147, 148). Because genomic integration cannot be undone, an effective vaccine must produce antibodies which block viral entry into its host cell.

The challenge for the immune system to produce such antibodies during an active infection is two-fold. First, the virus infects and kills the cells (Th cells) which are responsible for helping B cells mutate and produce high affinity antibody. Furthermore, the Th cells which are responsible for triggering the highest affinity antibodies, TFH cells, have recently been shown to contain the highest reservoir of virus of all the Th cell subsets. Therefore, HIV-1 targets and removes the cells which could most effectively contribute to eliminating the virus. Secondly, HIV-1 mutates at such a high rate the regions of gp120 and gp41 targeted by antibodies change just enough to facilitate viral escape from existing antibodies. However, there are a few select regions on these

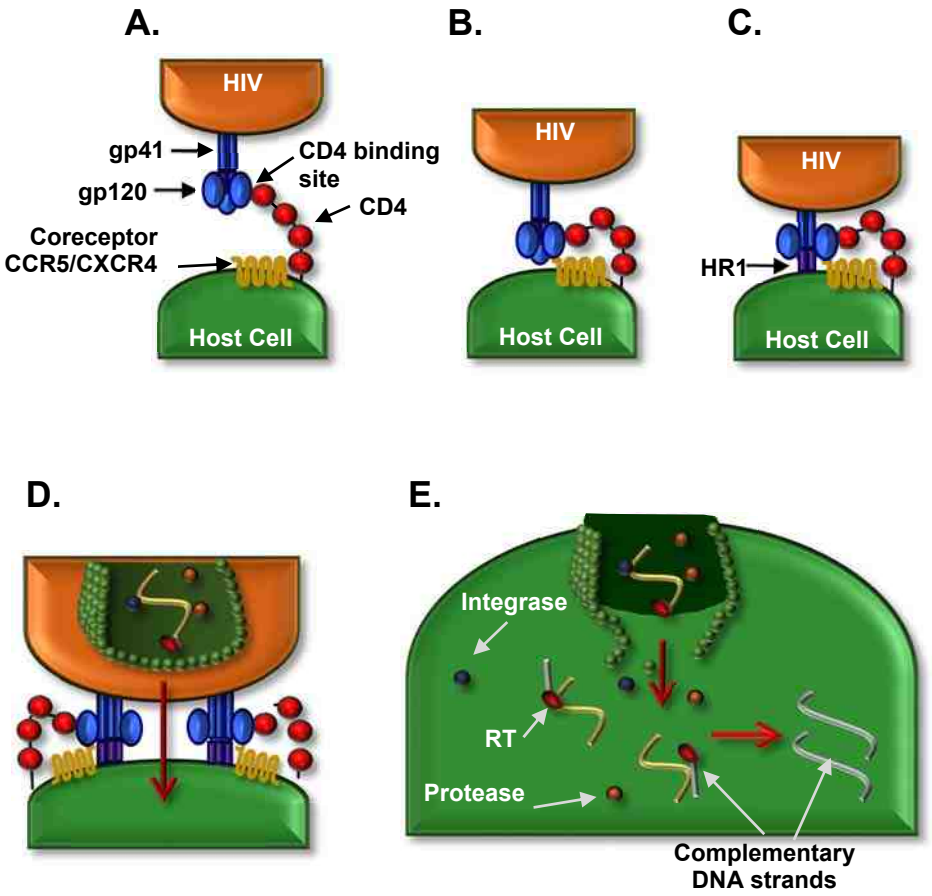

Figure 57. Attachment and fusion of HIV to host cell. A. HIV will first bind to a host cell via its main receptor, CD4, at a conserved binding site on gp120. **B.** Binding of CD4 to its site on the surface glycoprotein causes a conformational change in gp120 that exposes the binding site for the coreceptor. The coreceptor, either CCR5 or CXCR4, then binds its conserved site on gp120, called the V3 loop. **C.** Binding of the coreceptor triggers a conformational change in the surface glycoproteins, revealing a portion of gp41 normally not exposed. This domain of gp41 is called HR1. **D.** When two gp160 proteins have bound a host cell, fusion of gp41 to the cell surface allows transport of the viral capsid from the virion into the host cell. **E.** Once the capsid enters the host cell, it releases its RNA and enzymes into the host cytoplasm. Next, the reverse transcriptase (RT) will synthesize complementary DNA strands of the viral RNA using host cell nucleotides. **F.** Finally, the viral DNA will traffic into the host cell nucleus along with the viral integrase enzymes. Integrase will selectively splice viral DNA into the host genome. Once this occurs, the virus is referred to as a provirus.

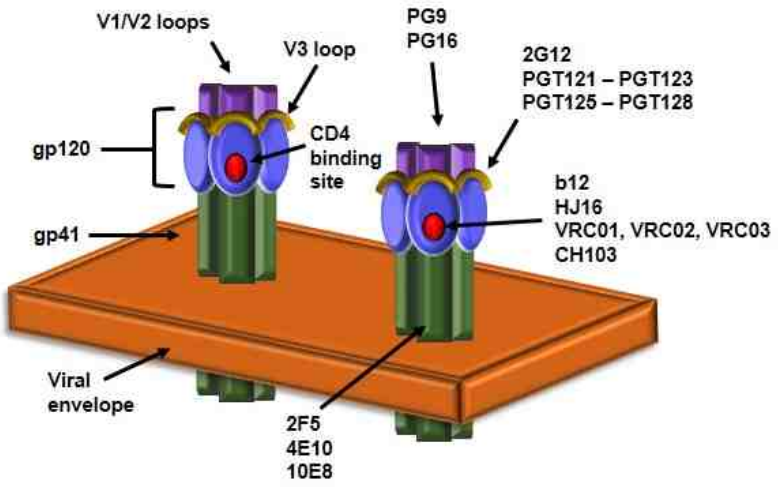

Figure 58. Binding sites of broadly neutralizing antibodies to HIV. Many anti-HIV antibodies have been isolated from the serum of infected patients which possess neutralizing capabilities. The breadth of these antibodies is quite variable, but most can neutralize at least 30% of viruses. The binding sites which these antibodies are directed to are not only crucial for virus attachment and fusion with host cells, but they are highly conserved among viruses as well, allowing these viruses to efficiently neutralize most virus they bind to. Unfortunately, many of these binding sites are hidden and are not revealed until the virus begins to bind a host cell and the surface glycoproteins undergo conformational changes. The antibodies b12, HJ16, VRC01, VRC02, VRC03, and CH103 have been shown to bind the CD4 binding site on gp120. The V1 and V2 loops have been shown to be targeted by the PG9 and PG16 antibodies. The V3 loop, which binds the viral coreceptor, has several characterized antibodies targeting it, including 2G12, PGT121 – PGT123, and PGT125 – PGT128. Finally, a conserved region on gp41 near the viral envelope has also been shown to be targeted by neutralizing antibodies. The three with the highest affinity are 2F5, 4E10, and 10E8. Figure adapted from Clapham PR and Lu S, *Nature medicine*, 2012.

surface glycoproteins which are conserved. These regions include the binding sites for CD4 and the coreceptors (Figure 58). The difficulty with targeting these regions is due to their physical inaccessibility. These areas are mainly shielded until the virus begins binding to a target cell, at which time the surface glycoproteins undergo conformational changes to facilitate infection (Figure 57). It is then when the conserved regions are exposed and vulnerable to antibody binding.

While the majority of HIV-1-infected individuals lack the ability to target these areas, a number of antibodies with known neutralizing capabilities have been characterized in a subset of infected patients (149-153). These individuals' immune systems have developed antibodies which target the CD4 binding site, the V3 loop (which binds

coreceptors), as well as a few conserved regions on gp41 (Figure 58) (149-153). Unfortunately, these antibodies usually take years to develop, and, by that point, an infected individual likely has millions of established proviruses. Furthermore, the B cells from these patients have typically undergone five- to tenfold higher affinity maturation rates than cells from patients lacking these neutralizing antibodies (154). This level of mutation is rarely seen in non-HIV$^+$ people, and thus difficult to characterize (154). However, it seems indisputable that the GC must be involved in this affinity maturation, and, consequently, TFH cells likely play a pivotal role in aiding the development of neutralizing antibodies. Therefore, any effective vaccine which is to elicit broadly neutralizing antibodies must not only target and stimulate B cell activity, but activate highly specific TFH cells as well.

Because CD4$^+$ T cells are the primary target for the virus, these cells have been largely ignored in the search for an effective vaccine. While the importance of TFH cells in the humoral immune response has become clear in recent years, the role of TFH cells in an HIV vaccine strategy remains uncertain. Furthermore, while much focus has been placed on serum antibody analysis in the development of HIV vaccines, little research has been done on evaluating the robustness of GC development with different vaccination approaches. The GC has been shown to peak earlier in a secondary response than after a primary immunization (155), but nothing is known about the kinetics of the TFH response and the GC reaction with vaccines that require repeated immunizations. Therefore, it is critical to study the development of TFH cells and GCs to gain insights into effective HIV vaccine strategies.

Currently, heterologous prime-boost vaccination strategies employing a DNA priming component are making headways in different disease fields, such as HIV, influenza, malaria and tuberculosis (156-159). Previously, our collaborators have shown mice immunized with a DNA vector encoding gp120, followed by injection of recombinant gp120 protein, yield antibodies with higher specificity and avidity than either vaccine alone, and, more importantly, develop improved neutralizing antibodies against primary viral isolates (160-162). Because TFH cells are crucial for the development of plasma cells secreting mutated high affinity antibodies from the GC, we hypothesized DNA priming causes more TFH cell differentiation, thereby triggering a more robust GC response.

MATERIALS AND METHODS

Mice and immunizations

Eight to ten week old C57BL/6 mice were obtained commercially from The Jackson Laboratory. $BCL6^{fl/fl}$ mice were generated as described in Chapter 2 and mated to Cre-ERT2 mice, which were also acquired from The Jackson Laboratory (stock # 007001). Mice were bred under specific pathogen-free conditions at the laboratory animal facility at the Indiana University School of Medicine (IUSM) and were handled according to protocols approved by the IUSM Animal Use and Care Committee.

Pilot study mice were immunized i.m. with 1 x 10^9 sheep red blood cells (SRBC; Rockland Immunochemicals Inc., Gilbertsville, PA) in 100 uL of PBS. A codon optimized JR-FL gp120 DNA vaccine construct in the pJW4303 vector was used for all DNA-based immunizations, as previously reported (161). DNA vaccine plasmid was produced in HB101 bacterial cells then isolated and purified using the Qiagen Plasmid Mega Kit.

Recombinant HIV-1 gp120 proteins were produced from Chinese Hamster Ovary (CHO) cells, as previously reported (161). Mice were immunized i.m. with either 100 ug of DNA or 10 ug gp120 protein in ALUM (Sigma-Aldrich Corp., St. Louis, MO, USA). A total of 100 uL was injected, 50 uL per hind leg.

Tamoxifen

Mice were given i.p. injections of 4 mg Tamoxifen (Sigma-Aldrich Corp., cat. # T5648) in sunflower seed oil.

Flow cytometry

Total spleen or thymus cells were incubated with anti-mouse CD16/CD32 (Fcγ receptor) for 20 minutes, followed by surface staining for the indicated markers. A fixable viability dye (eFluor 780, eBioscience) was used for all samples. The following antibodies were used for staining GC B cells: α-mCD19 Alexa Fluor 700, clone eBio1D3 (eBioscience); α-mB220 PE, clone RA3-682 (BD Bioscience); α-mFas Biotin, cat. # 554256 (BD

Bioscience); Streptavidin-PECy7 (Biolegned); α-mGL7 APC, clone GL7 (BD Bioscience); PNA FITC (Vector Laboratories Inc.). The following antibodies were used to stain memory B cells: α-mCD19 Alexa Fluor 700, clone eBio1D3 (eBioscience); α-mB220 PerCP, clone RA3-6B2 (Biolegend); α-mIgD FITC, clone 11-26C (eBioscience); α-mGL7 APC, clone GL7 (BD Bioscience); α-mCD38 PE, clone 90 (eBioscience); α-mCD73 PECy7, clone TY/11.8 (eBioscience). The following antibodies were used to stain naïve and memory T cells: α-mCD3 Alexa Fluor 700, clone 500A2 (BD Bioscience); α-mCD4 PECy7, clone RM4-5 (BD Bioscience); α-mCD8a APC, clone 53-6.7 (BD Bioscience), α-mCD44 PE, clone IM7 (eBioscience); α-mCD62L FITC, clone MEL-14 (BD Bioscience). The following antibodies were used to stain TFH cells: α-mCD3 Alexa Fluor 700, clone 500A2 (BD Bioscience); α-mCD4 PECy7, clone RM4-5 (BD Bioscience); α-mCXCR5 PerCP-efluor 710, clone SPRCL5 (eBioscience); α-mPD-1 APC, clone 29F.1A12 (Biolegend); α-mICOS FITC, clone C398.4A (eBioscience).

Antibody analysis

Antibody titers of gp120-specific IgG were measured by ELISA as previously reported (160). Antibody avidity was measured via the NaSCN displacement method, as previously described (160). This work was done by Dr. Shan Lu's laboratory at the University of Massachusetts Medical School.

RNA analysis

Total spleen cells from Cre-ERT2 mice were lysed using Trizol three days after final immunizations. Total RNA was isolated using an RNeasy mini kit (Qiagen). cDNA was constructed using a Transcriptor First Strand cDNA synthesis kit (Roche). Expression of BCL6 mRNA was quantified using SYBR Green analysis (Roche) with the following primers:

BCL6 exon 2/3 forward (5' – GCACTGGGCAAACACAACAT – 3')
BCL6 exon 2/3 reverse (5' – AGCGTGCCGGGTAAACTG – 3')
BCL6 exon 8 forward (5' – GAAGACCCACACTCGAATTCACT – 3')
BCL6 exon 8 reverse (5' – CCCCACAGGTTTCACATTTGT – 3')

Statistical Analysis

All data analysis was done using SPSS Statistics 20 software. Unless otherwise stated, ANOVA with Tukey post hoc analysis was used.

RESULTS

Immunization with gp120-encoding DNA yields a stronger GC response than gp120 protein

To test the hypothesis that gp120-encoding DNA triggers stronger GC responses than gp120 protein alone, C57BL/6 mice were injected i.m. with either gp120-encoding DNA, gp120 protein, or empty vector DNA, three times, two weeks apart (Figure 59). In our collaborators' previous HIV-1 gp120 immunogenicity studies, the priming phase included three immunizations. Traditionally, GC responses tend to peak between days seven and ten of the immune response. In our initial experiments with this gp120 immunization scheme, we looked at these time points, only to find little evidence of an active GC (data not shown). Also, to our knowledge, no data has been published demonstrating the

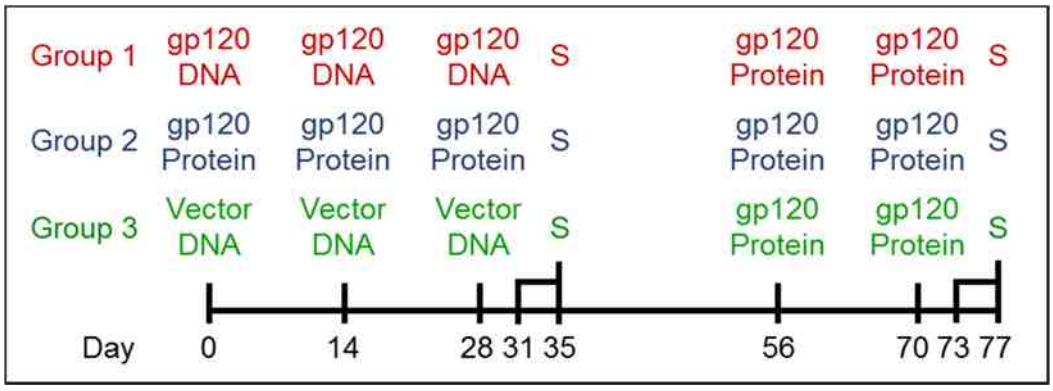

Figure 59. Experimental design for testing DNA vs. protein priming. C57BL/6 mice were primed i.m. with either gp120-encoding DNA, gp120 protein, or empty vector, 3 times, 2 weeks apart. Some mice were sacrificed 3 and 7 days after final priming injections. The remaining mice were rested for 4 weeks, then all groups were given 2 booster shots of gp120 protein, 2 weeks apart. Mice were then sacrificed 3 and 7 days after the final boosters.

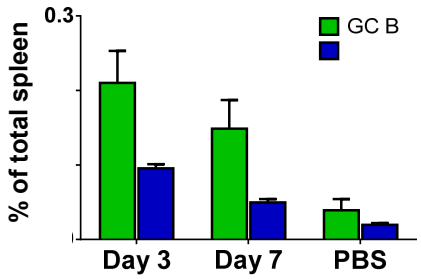

Figure 60. Germinal centers appear earlier with repeated immunizations. C57BL/6 mice were immunized 3 times, 2 weeks apart, i.m. with SRBC or control mice were given PBS. Mice were sacrificed 3 and 7 days after final injections and analyzed for TFH and GC B populations. PBS mice were sacrificed with day 3 mice. TFH cells gated on $CD3^+$ $CD4^+$ $CXCR5^+$ $ICOS^+$ $PD\text{-}1^{hi}$. GC B cells gated on $B220^+$ $CD19^+$ Fas^+ PNA^+ $GL7^+$. Percent of total spleen; mean ± SE.

kinetics of TFH cell differentiation with repeated immunizations. Therefore, to determine the optimal time to analyze mice given multiple injections, we immunized C57BL/6 mice i.m. with SRBC three times, two weeks apart and sacrificed them at different times afterward. Our data showed GC B cells and TFH cells peaking earlier, on day three, after final injections (Figure 60). Therefore, we chose to analyze mice for the following experiments on days three and seven after final injections.

With this information in mind, we then examined TFH cells and GC B cells after just the priming phase of the immunization scheme (Figure 61). Mice which received gp120-encoding DNA had increased TFH cells and significantly more GC B cells in the spleen three days after the last priming injections (Figure 61 A-B). However, by day seven after the last priming injections, these amounts equaled that of mice primed with gp120 protein. Antibody analysis revealed priming with gp120 DNA induced significantly higher antigen-specific IgG titers, both three and seven days after final injections (day 28; Figure 61 C). The avidity of these antibodies was somewhat higher on day three with gp120 DNA priming (Figure 61 D). This data demonstrates priming with gp120 DNA alone, without booster injections, already triggered more robust GC responses and antigen-specific IgG production than does gp120 protein.

Priming with gp120-encoding DNA enhances GCs and the proportion of TFH cells in spleen

After initially priming with gp120-encoding DNA, gp120 protein, or empty vector DNA, all groups were rested for four weeks, then received two gp120 protein booster immunizations, two weeks apart (Figure 59). TFH cells from spleen were elevated in

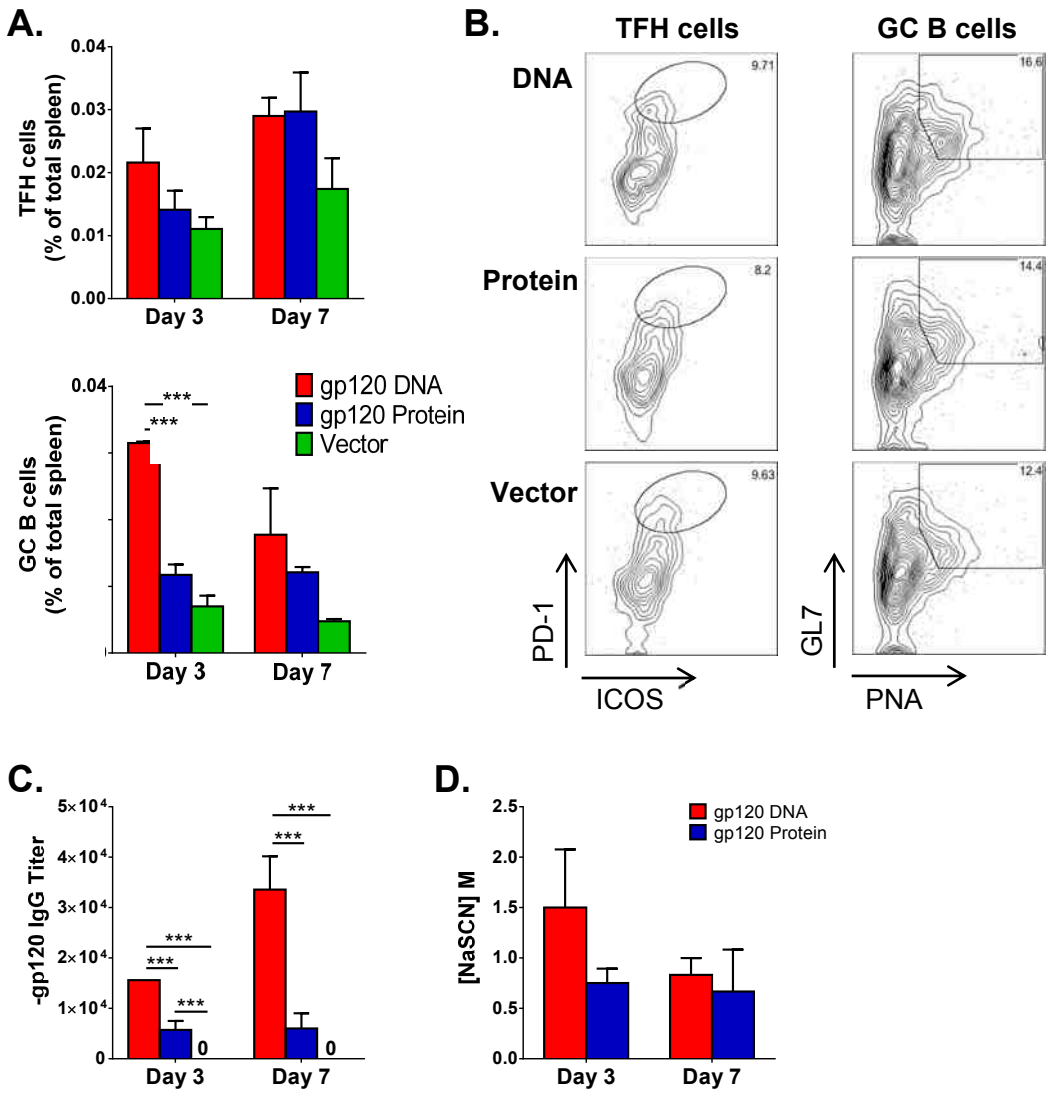

Figure 61. Increased GC activity after gp120 DNA priming. Mice were immunized according to Figure 59 and sacrificed 3 and 7 days after final priming injections immunizations. **A.** TFH and GC B cell populations after priming only. TFH cells gated on $CD4^+$ $CXCR5^+$ $ICOS^+$ $PD\text{-}1^{hi}$. GC B cells gated on $B220^+$ Fas^+ PNA^+ $GL7^+$. Percent of total spleen; mean ± SE. **B.** Representative flow plots of TFH cells and GC B cells in (**A**) from day 3 after final immunization. **C.** Serum anti-gp120-specific IgG titers after prime only; mean ± SE. **D.** Anti-gp120-specific IgG affinity after prime only; mean ± SE. n = 3; *p < 0.05, **p < 0.01, ***p < 0.001. **C** & **D** done in collaboration with Dr. Shan Lu.

mice receiving gp120 DNA three days after the final injections, but tapered off by day seven (Figure 62 A-B). GC B cell populations, however, remained significantly higher in mice primed with gp120 DNA on both day three and seven after final immunizations (Figure 62 A-B). This data demonstrated the advantage of priming with gp120 DNA

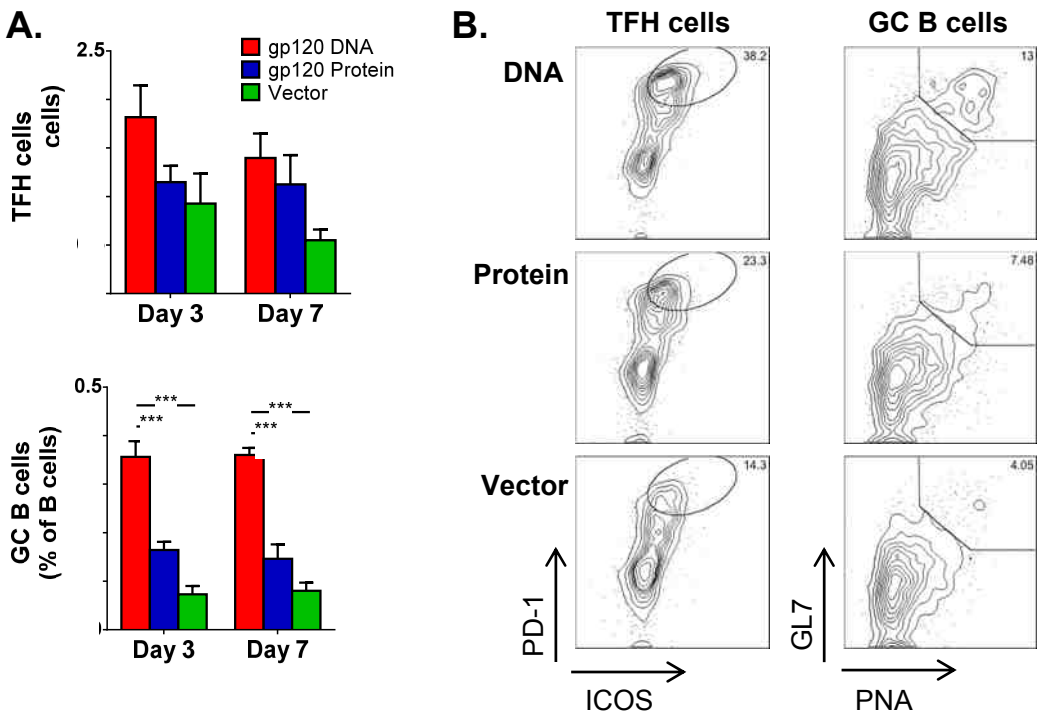

Figure 62. Enhanced GC B cells and TFH cell populations with gp120 DNA priming. Mice were immunized as in Figure 59 and sacrificed 3 and 7 days after final gp120 protein booster injections. **A.** TFH and GC B cell populations after prime-boost regimen. Cells gated as in Figure 61. Percent of total spleen; n = 3-5; mean ± SE. **p < 0.01, ***p < 0.001 **B.** Representative flow plots of TFH cells and GC B cells in (**A**) from day 3 after final protein booster.

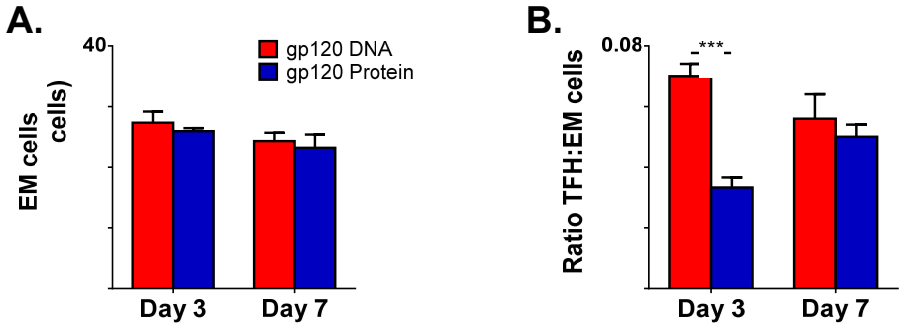

Figure 63. Proportion of TFH cells increased with gp120 DNA priming. Mice were immunized as in Figure 59 and sacrificed 3 and 7 days after final gp120 protein booster injections. **A.** Percent EM T cells ($CD3^+$ $CD4^+$ $CD44^{hi}$ $CD62L^-$) in gp120 DNA and protein primed mice after protein boosters. Percent of total spleen; n = 5-6; mean ± SE. **B.** Ratio of TFH to EM cells. n = 5-6; mean ± SE. **p < 0.01 by *t* test.

rather than protein, as GC cell populations were increased and arose earlier in the immune response.

When EM $CD4^+$ T cells were analyzed in the spleen of these mice, no significant differences were seen on either day three or seven after final immunization (Figure 63 A). Because TFH cells are activated Th cells, phenotypically they are included in the EM population of $CD44^+$ $CD62L^-$ cells. Therefore, we analyzed the proportion of TFH cells within this EM population. On day three, the proportion of TFH cells within the EM population was significantly higher with gp120 DNA priming than with protein alone (Figure 63 B). By day seven, however, the proportion of TFH cells from gp120 protein priming caught up to the levels from gp120 DNA priming. Therefore, after boosting with gp120 protein, mice primed with DNA showed a clear advantage in TFH and GC B cell development.

Priming with gp120 DNA improves GC activity

Like EM T cells, neither priming method yielded significantly higher percentages of splenic memory B cells (Figure 64 A). Therefore, we were interested in what percentage of these memory cells were of GC origin. Recent literature has shown CD73 to be an accurate marker for defining former GC B cells (163). When the fraction of memory B cells of GC origin was examined, we saw significantly higher percentages with gp120 DNA priming both three and seven days after final immunization (Figure 64 B). Titers of anti-gp120 IgG with DNA priming were significantly higher three days after final immunizations, as was the avidity (Figure 64 C-D). It was not until day seven that the antibodies of mice primed with gp120 protein equaled the levels seen in gp120 DNA mice. Not only was the functionality of these B cells increased with gp120 DNA priming, but, again, the increase in antibody secretion occurred earlier.

While analyzing memory B cell populations, we observed a decrease in this cell population from day three to day seven, even though the memory cells of GC origin expanded during the same period with both immunization methods. Therefore, we utilized the surface markers CD38 and GL7 to differentiate memory B cells (MB: $CD38^+$ $GL7^-$) from transitional B cells (TB: $CD38^+$ $GL7^+$) (Figure 65 A-B). In terms of B cell kinetics, it was interesting to observe that regardless of which priming method was used,

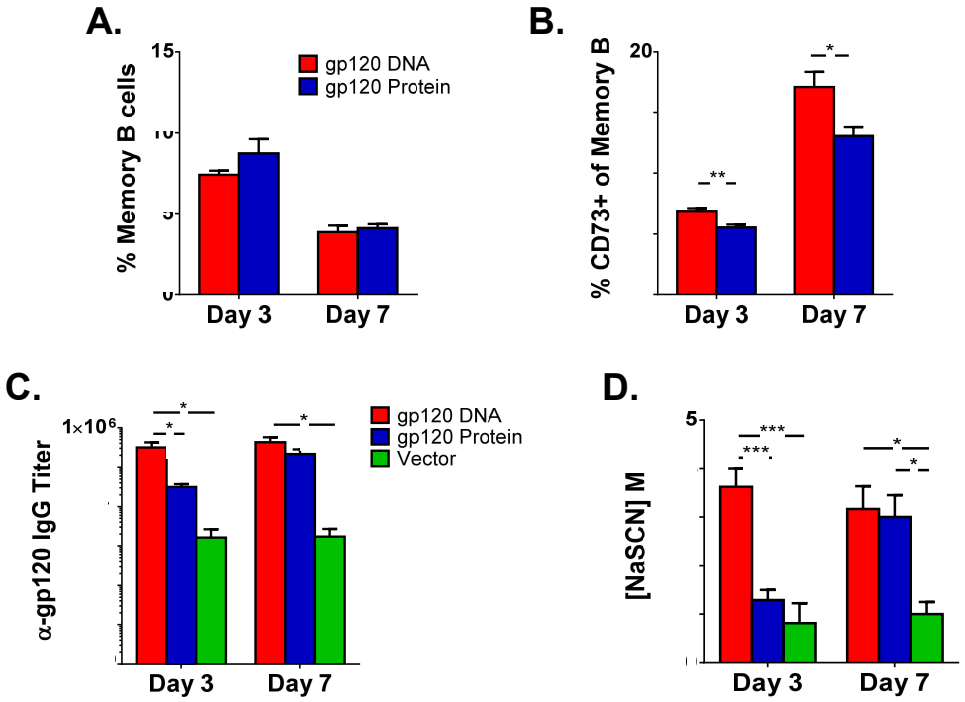

Figure 64. Priming with gp120-encoding DNA improves GC activity. Mice were immunized and sacrificed as in Figure 59. **A.** Memory B cells (gated as CD19$^+$ IgD$^-$ GL7$^-$ CD38$^+$) in mice primed with gp120-encoding DNA or gp120 protein. Percent of total spleen; mean ± SE. **B.** Memory B cells originating from the GC. Gated as CD19$^+$ IgD$^-$ GL7$^-$ CD38$^+$ CD73$^+$. Percent of memory B cells; n = 4-6; mean ± SE. *p < 0.05, **p < 0.01 by *t* test. **C.** Serum anti-gp120-specific IgG titers after boosting. Mean ± SE. **D.** Avidity of serum anti-gp120-specific antibodies after boosting. Mean ± SE. n = 4-6; *p < 0.05, ***p < 0.001

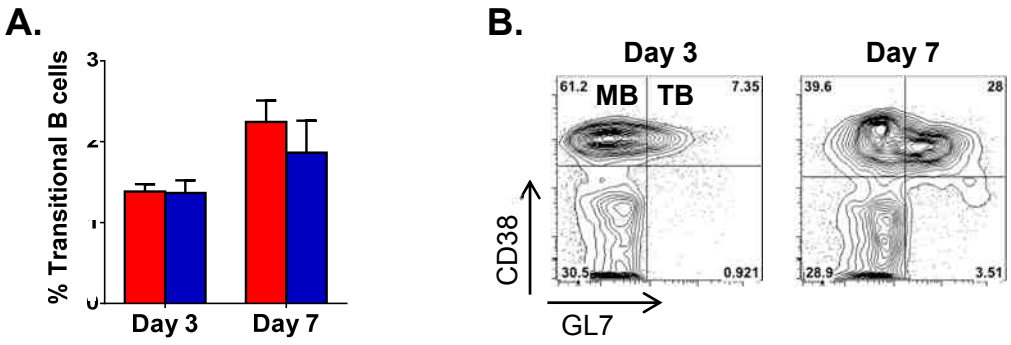

Figure 65. Dynamics of transitional B cells during repeated immunizations. Mice were immunized and sacrificed as in Figure 59. **A.** Transitional B cells (gated on CD19$^+$ IgD$^-$ GL7$^+$ CD38$^+$); percent of total spleen; mean ± SE. **B.** Representative flow plots of day 3 and day 7 from mice primed with gp120 DNA. Quadrants show memory B cells (MB) (top left) and transitional B cells (TB) (top right).

B cells seem to be differentiating out of a memory B cell phenotype into a transitional cell state between days three and seven, while memory cells of GC origin retain their phenotype and proliferate. Thus, while not increasing overall memory B cell numbers, priming with gp120 DNA significantly increased the percentage of memory cells of GC origin. Furthermore, in the context of repeated immunizations, between days three and seven, memory B cells in all mice decreased, while those with a transitional cell phenotype increased, demonstrating a transition from a memory to a more active cell state.

Deletion of BCL6 results in a significant increase of gp120-specific IgG

Previously, we have generated a mouse wherein exons 7 – 9 of the BCL6 gene are flanked with loxP recombination sites ($BCL6^{fl/fl}$) (See Chapter 2). In this study we created a new cKO mouse model in which $BCL6^{fl/fl}$ mice were mated to mice expressing a Cre recombinase fused to a human estrogen receptor (Cre-ERT2). Under control of the estrogen receptor, we can functionally delete BCL6 by administering tamoxifen to these mice. Unlike our earlier cKO mouse, in which Cre was under the control of the CD4 promoter, $BCL6^{fl/fl}$ Cre^{ERT2} mice will have BCL6 functionally deleted in all cells once

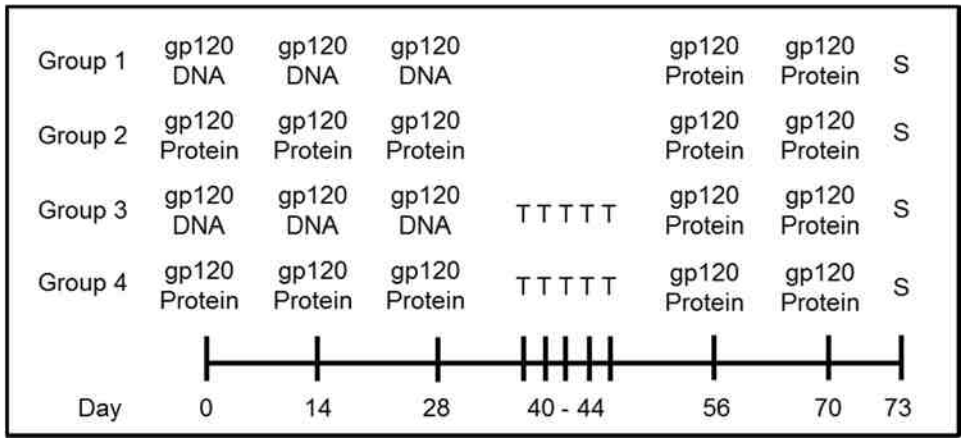

Figure 66. Experimental design for deletion of BCL6. ERT2-Cre $BCL6^{fl/fl}$ mice were primed with either gp120-encoding DNA or gp120 protein, followed by 2 booster shots of gp120 protein. Some ERT2-Cre $BCL6^{fl/fl}$ mice also received 5 i.p. injections of tamoxifen (T) (4 mg in sunflower seed oil) between the prime and boost injections to delete BCL6. Mice were sacrificed 3 days after final injections.

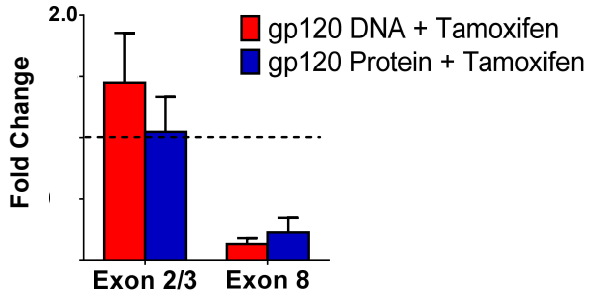

Figure 67. Deletion of BCL6 in tamoxifen treated mice. Total spleen cells from ERT2-Cre BCL6$^{fl/fl}$ mice were analyzed for deletion of BCL6. RNA from total spleen was analyzed via qPCR for BCL6 transcripts. Transcript levels were normalized to mice not given tamoxifen (dotted line at 1.0). Exons 2-3 and Exon 8 are shown.

tamoxifen is administered. As in the initial experiments, mice were primed with either gp120-encoding DNA or gp120 protein, three times, two weeks apart (Figure 66).

During the four week rest period, half of the mice received i.p. injections of tamoxifen every day, for five days. Twelve days after the final tamoxifen injection, mice were given the first of two gp120 protein booster injections. Administration of tamoxifen effectively and functionally deleted BCL6 from mice (Figure 67). Since the most drastic changes in GC dynamics were seen three days after final immunizations in our earlier studies, we chose this time point to analyze these mice. Once again, gp120 DNA triggered significantly higher TFH and GC B cell populations in the spleen of mice not treated with tamoxifen (Figure 68 A-B). As expected, deletion of BCL6 severely and significantly reduced the TFH and GC B cell populations (Figure 68 A-B). Surprisingly, deletion of GCs led to an increase in gp120-specific IgG, (Figure 68 C). Priming with gp120 DNA, followed by functional deletion of BCL6 significantly enhanced antigen-specific IgG titers compared to all other groups. Furthermore, the avidity of these antibodies was increased as well (Figure 68 D). This data verifies the necessity of BCL6 for GC development, while demonstrating the dispensability of these structures for antibody secretion and affinity maturation in the context of repeated immunizations.

DISCUSSION

While a number of research publications have shown the protective advantage of incorporating a DNA priming step into heterologous prime-boost vaccination strategies, few studies have looked into the mechanism by which DNA priming affords this advantage. Furthermore, almost nothing is known about the role of the TFH cell and the

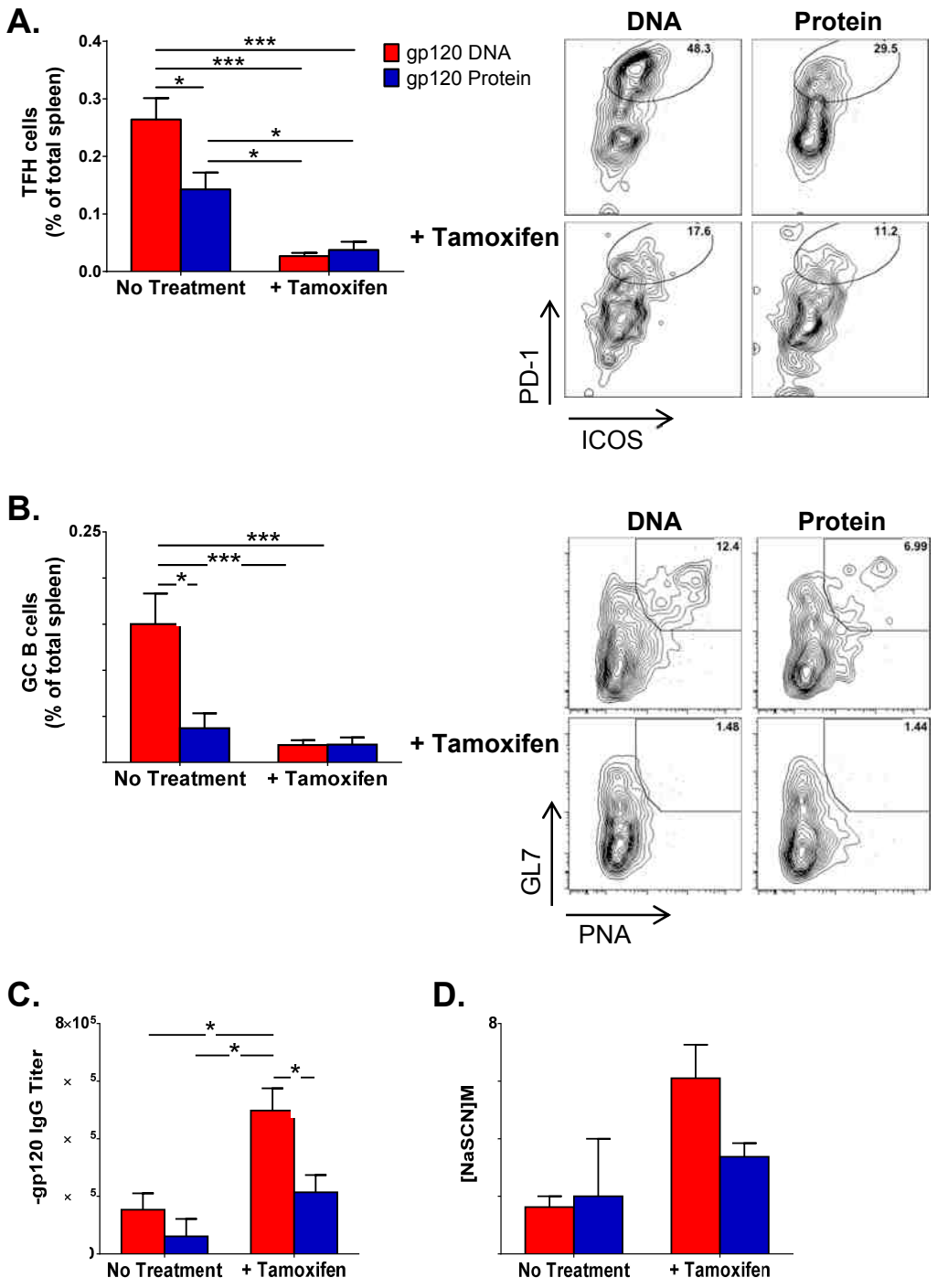

Figure 68. GCs are lost with deletion of BCL6. Cre-ER BCL6$^{fl/fl}$ mice were immunized as in Figure 66 and sacrificed 3 days after final protein booster injections. Some mice were given tamoxifen injections between prime and boost injections to delete BCL6. **A.** TFH cells (gated as in Figure 61) in spleen of mice either untreated or given i.p. tamoxifen injections before boosting. Representative flow plots of each treatment condition. **B.** GC B cells (gated as in Figure 61) in spleen after prime-boost regimen with representative flow plots of each treatment condition. Percent of total spleen; n = 3-4; mean ± SE. **C.** Serum anti-gp120-specific IgG titers after boosting. **D.** Avidity of anti-

gp120-specific antibodies after boosting. Mean ± SE. n = 3-4; *p < 0.05, **p < 0.01, ***p < 0.001

GC response in prime-boost vaccinations. Here, we demonstrate, using an HIV gp120 vaccine scheme, priming with gp120-encoding DNA yields increased TFH and GC B cell populations compared to priming with gp120 protein. Furthermore, this increase occurs at an earlier time-point after immunization. The early antibody response induced by DNA priming was seen after the priming phase, as well as following the boost injections. While literature exists explaining the possible different mechanisms of antigen processing and presentation with plasmid vector vaccines (159, 164), it is not yet clear how the protein from these plasmids affords an advantage.

Human trials of HIV-1 DNA vaccines consisting only of injections of HIV-1-encoding DNA (i.e. not prime-boost approaches) have been disappointing for eliciting the production of antibodies (165, 166). More recently, several prime-boost HIV-1 vaccines have been tested in humans that use a pure DNA component, as well as protein, and these systems have succeeded in provoking a significant antibody response (167-169). Studies with cancer vaccines in humans have also supported the utility of DNA priming in a prime-boost system (170). Thus, understanding how DNA priming can augment immunity in a prime-boost vaccination system is warranted.

Memory cell development is considered critical for an effective vaccine. We found no apparent increase in memory T cell populations after DNA priming. However, when looking at the proportion of effector Th cells which are TFH cells, we saw that gp120 DNA priming lead to more activated $CD4^+$ T cells becoming TFH cells, rather than other Th cell subsets. For B cells, priming with DNA effectively enhanced GC memory B cell outcomes, in this case by triggering the development of more $CD73^+$ memory B cells, which are derived from the GC. This data, combined with the earlier peak in antigen-specific IgG, would suggest that priming with gp120 DNA not only triggers more memory B cell development from GCs, but that those memory cells underwent affinity maturation and differentiated into plasma cells more quickly than with protein priming. The decrease in memory B cell populations between days three and seven, and the concurrent increase in transitional cells (Figure 65), shows an interesting trend in terms of B cell kinetics. It would be worthwhile to investigate how repeated immunizations

affect the timing of this cell transition; perhaps the increased number of immunizations is decreasing the time necessary to make this transition.

To investigate the necessity of GCs in the context of repeated immunizations, our inducible Cre mouse model allowed us to delete BCL6, the master transcription factor for GCs, after priming the mice. Our data suggests that once memory B cells are formed in the priming stage, further formation of GCs actually limits the antibody production of antigen-specific IgG-secreting B cells. Since we observed more memory B cells of GC origin developing with gp120 DNA priming (Figure 64 B), we reasoned that during protein booster injections, forming GCs limits the antibody-secreting potential of these memory cells, as they appear to be better able to differentiate into antibody-secreting plasma cells independent of the constrains of the GC. How these memory cells underwent additional affinity maturation, as evident by their increased avidity, outside the GC is not understood at this time. It is possible these B cells are interacting with Th cells outside the B cell follicle.

These results have highly significant implications for the field of B cell immunology, HIV-1 vaccine development, and AIDS therapy. When and where B cells can undergo affinity maturation needs to be fully understood to design an optimal immunization schedule that elicits high-affinity, broadly neutralizing antibodies by a prophylactic HIV-1 vaccine. Further studies are warranted to determine how much of a role repeated immunizations play in extra-follicular antibody development. At what point GCs are no longer needed to develop antigen-specific antibodies with high avidity is of great importance to the vaccine field. Our findings also have potential impact for the design of immune therapy strategies for HIV-1 infected people. Published works have demonstrated TFH cells as being a major target and reservoir for HIV-1 (171-173). Therefore, it is undesirable to stimulate these cells when treating infected patients. However, if there is a way to trigger high-affinity antibody production without involving TFH cells, patients could increase their antibody-mediated protection without activating the production of new virus from TFH cells.

In conclusion, the key goal of this study was to provide insight into how DNA priming provides an advantage in the antibody response, and here we have pinpointed, for the first time, the ability of DNA priming to augment the GC reaction, as well as to transiently

increase TFH cells. Thus, the improved antibody response in a heterologous prime-boost vaccination system with DNA priming can be explained by increased TFH and GC function. At the same time, we have found that the GC reaction appears to limit antibody production in the boost phase. These results should prompt a reevaluation of HIV vaccine design.

FUTURE DIRECTIONS

Part I – Elucidating the role of BCL6 in repressing DNA methylation

Determining the methylation status of BCL6-deficient naive CD4$^+$ T cells

Using our new cKO mouse model, we were able to determine a relationship between BCL6 and Dnmt3b, which is responsible for *de novo* methylation of DNA. While we were able to establish the presence of Dnmt3b at the PD-1 promoter before immunization, it remains undetermined what the genome-wide methylation status is of naïve Th cells in BCL6$^{fl/fl}$ Cre^{CD4} mice is.

To investigate this aim, naïve CD4$^+$ T cells should be isolated from naïve BCL6$^{+/+}$ Cre^{CD4} and BCL6$^{fl/fl}$ Cre^{CD4} mice via FACS. Unstimulated naïve cells can then be lysed and assessed for DNA methylation via MeDIP analysis. Briefly, methylated DNA immunoprecipitation works by targeting methylated DNA with a methyl cytosine (5-mC)–specific antibody. Following this immunoprecipitation, captured DNA can be assessed for total quantity, via Nanodrop technology, or sequenced to identify specific genes being modified, also known as MeDIP-seq.

In addition to naïve unactivated cells being analyzed, sorted naïve Th cells can also be activated *in vitro* with anti-CD3 and anti-CD28 antibody stimulation. These cells can be harvested over time, such as days three and seven, to track changes in methylation overtime using the same analysis tools stated above. In this way, we can analyze the role BCL6 has in suppressing methylation machinery in the cell at different points after activation.

To model this experiment *in vivo*, our cKO mice should first be bred onto an OT-II background. This will cause all the TCRs of CD4$^+$ cells in the mouse to be specific for OVA, and, thus, after immunization, have equal opportunities to become activated. After sorting naïve CD4$^+$ T cells from mice to use as a baseline for methylation status, an additional set of mice should be immunized and sacrificed at various time points after. Naïve (CD44$^-$ CD62L$^+$) and effector (CD44$^+$ CD62L$^-$) cells should be isolated from these mice. Analysis of effector cells can shed light on the changing methylation status of cells

over time, while analyzing naïve Th cells may provide interesting insights into changes in DNA methylation due to environmental cues without cellular activation.

Determine the types of methylation modifications in BCL6-deficient Th cells

While several types of methylation modifications exist, one of the most frequent is 5-methylcytosine (5mC) (129). This modification is associated with closed chromatin, and, thus, gene repression. After DNA has been methylated *de novo*, how it becomes demethylated is currently a controversial topic in the field of epigenetics. The first way in which this occurs, which is not contested, is via passive demethylation. When a cell divides and the DNA replicates, the 5mC areas become hemimethylated because the new complementary DNA strand is without modifications. Dnmt1 identifies these areas and methylates the new DNA strand in daughter strands, thus returning it to a fully methylated state. If Dnmt1 fails to recognize a hemimethylated area of DNA, that segment will become passively demethylated with subsequent cell divisions.

What is controversial is the current proposal that certain enzymes can actively target and demethylate 5mC (129). In this model, TET enzymes can oxidize 5-methylcytosine (5mC) to 5-hydroxymethylcytosine (5hmC). This modified cytosine has been shown to be a crucial intermediate in demethylation activity. Additionally, TET can further oxidize 5hmC into 5-formylcytosine (5fC) and 5-carboxylcytosine (5caC). These modified bases are then targeted for removal by thymine DNA glycosylase (TDG). TDG, which plays a critical role in base excision repair, will remove the methylated cytosine, generating an abasic site. This is followed by replacement with an unmethylated cytosine by DNA polymerase.

One reason the type of methylation present in cKO Th cells should be assessed is because TET1 and TDG are significantly up-regulated in microarray analysis (Figure 69 A). Therefore, not only is DNMT3b increased in the absence of BCL6, but the machinery which modifies those methylation modifications put in place by Dnmt3b are increased also. Furthermore, TET1 transcript levels were also found to be increased in total Th cells in our time course experiment (Figure 69 B). For these reasons, not only should the total methylation status of DNA in cKO Th cells be assessed, but the type of methylation should be addressed as well.

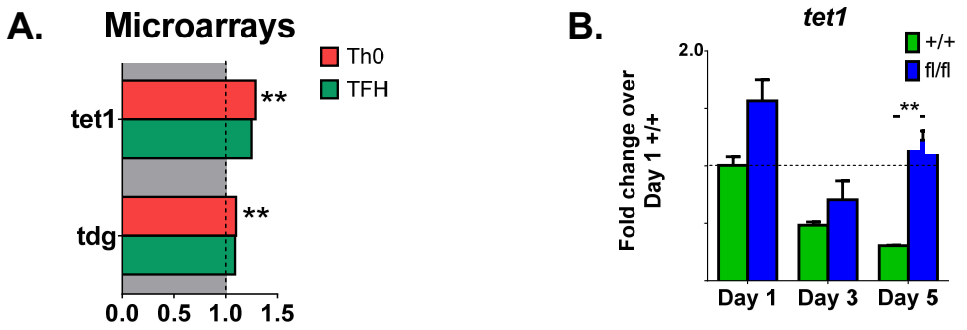

Figure 69. Tet1 and Tdg are up-regulated in the absence of BCL6. A. Naïve Th cells from BCL6$^{+/+}$ Cre^{CD4} and BCL6$^{fl/fl}$ Cre^{CD4} mice, cultured, and assessed via microarray as described in Chapter 3. **B.** BCL6$^{+/+}$ Cre^{CD4} and BCL6$^{fl/fl}$ Cre^{CD4} mice were immunized with SRBC and sacrificed 1, 3, and 5 days after. Total Th cells were lysed ex vivo and analyzed for tet1 transcript. Levels normalized to Day 1 +/+ (dotted line at 1.0). **p < 0.01 by *t* test.

To determine whether the methylation modifications are 5mC, 5hmC, 5fC, or 5caC, a ChIP analysis can be performed, as antibodies against these methylation forms are available for commercial purchase. After IP, the captured DNA can be quantified for total concentration (Nanodrop) or analyzed for the presence of gene promoters, via qPCR or genome wide sequencing (ChIP-seq). This data can help shed light on the current controversy surrounding active DNA demethylation.

An additional reason why the increased expression of TET1 and TDG is interesting is the finding that once activated, BCL6-deficient Th cells proved to be more proliferative than their WT counterparts. Perhaps the increased activity of TET1 and TDG in these cells is leading to more gene activity via demethylation once the cells are activated.

Determine the physical relationship between BCL6 and Dnmt3b

At this point, we know that Dnmt3b is up-regulated in the absence of BCL6, but how BCL6 represses the methyltransferase has not been determined. Therefore, using several different analyses, we can determine at what level BCL6 is repressing Dnmt3b. First, by immunoprecipitating for BCL6, using ChIP analysis, we can determine whether BCL6 directly binds the Dnmt3b promoter. To do this, mice should be immunized with SRBC and TFH cells sorted to ensure the highest expression of BCL6. Also, qPCR promoters will need to be designed to span the entire Dnmt3b promoter.

Through its zinc fingers, BCL6 also has the capability to bind RNA. Therefore, BCL6 may be repressing translation of Dnmt3b by bindings its transcripts. To test this, RNA immunoprecipitation (RIP) can be employed (174). Like ChIP analysis, samples are IP for a protein of interest and the RNA it associates with is isolated and analyzed. In this way, we can test if BCL6 binds to Dnmt3b mRNA.

Finally, to determine if BCL6 is repressing Dnmt3b by direct protein-protein interactions, TFH cells can also be co-IP for BCL6, followed by Dnmt3b. This standard procedure will reveal if these repressors interact on the protein level.

While data using mouse Th cells is crucial for establishing targets of interest, it is also important to test these theories in human models. Using human tonsil samples, we can sort TFH cells and test BCL6-Dnmt3b interactions in these cells using the above techniques. If we can identify this association in human T cells, our data could have great contributions for the study of human T cell activation.

Effects of BCL6 on the cell cycle

When a naïve Th cell is activated, in addition to up-regulating surface markers and secreting cytokines, it will enter the G1 phase of the cell cycle and, ultimately, divide. Because we saw decreased activation of naïve Th cells and increased proliferation of already activated cells in fl/fl mice, it remains to be investigated what affects BCL6 has on the cell cycle. As discussed in Chapter 5 of this thesis, the chromatin in BCL6-deficient Th cells appears to be more methylated than its WT counterpart. Therefore, this increased epigenetic modification may be affecting a cell's ability to enter the cell cycle and replicate.

In addition to our methylation findings, further analysis of our microarray data revealed significant increases in the expression of genes which play a role in cell cycle progression (Figure 70 A). Nek6 becomes activated during M phase and its inhibition will trigger apoptosis. It associates with Kif11, which plays a role in organizing spindles prior to cell division. Jub was also significantly increased and, in addition to playing roles in cell activation and proliferation, it activates Aurora A (*aurka*) which facilitates mitosis.

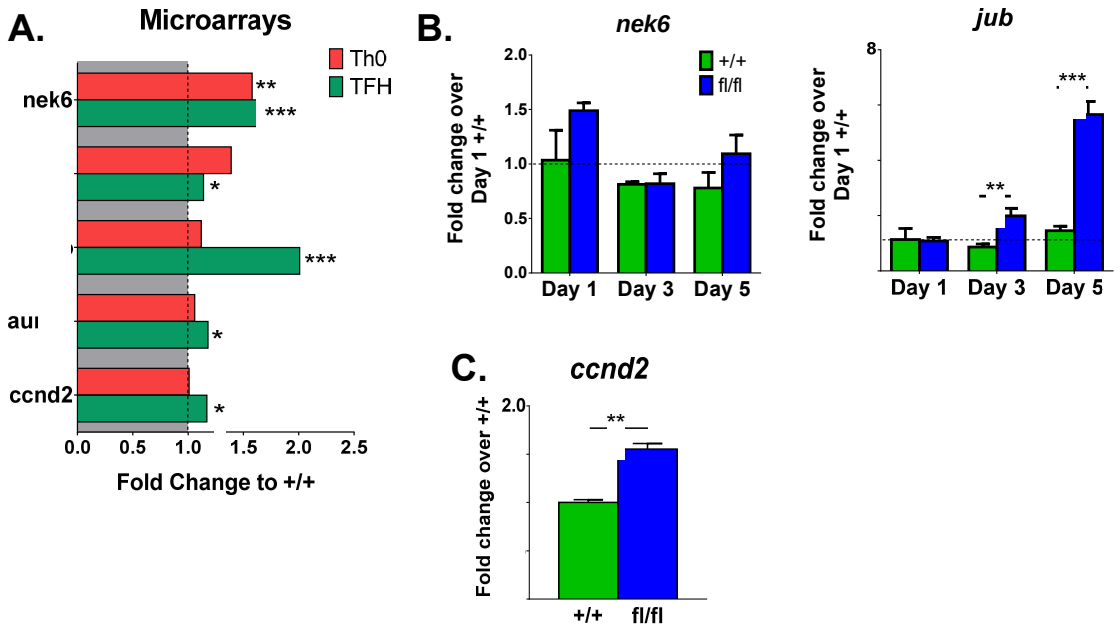

Figure 70. Cell cycle genes are up regulated in the absence of BCL6. A. Microarray analysis was done as in Chapter 3. **B.** Time course experiment as described in Figure 69 B. **C.** Naïve CD4$^+$ T cells were isolated via bead separation and activated in vitro with anti-CD3 and anti-CD28 antibodies in Th0 media for 24 hours. Cells were then lysed for RNA analysis. Mean ± SE. *p < 0.05, **p < 0.01, ***p < 0.001 by *t* test.

Finally, cyclin D2 (*ccnd2*) plays a role in the transition from G1 to S phase. When Th cells from our time course experiment were analyzed for *jub* and *nek6* transcription, increased levels were found in the absence of BCL6 as well (Figure 70 B). Also, when naïve Th cells were activated *in vitro* with antibodies for 24 hours, transcript levels of cyclin D2 were significantly decreased in the absence of BCL6 (Figure 70 C). Therefore, it seems apparent that BCL6 is in some way, repressing cell cycle genes.

This idea seems reasonable when you consider the role of BCL6 in B cells. BCL6 is most highly expressed in the B cells of the GC. Once there, it is beneficial to control the differentiation of these cells and limit it to those with the highest affinity. Therefore, while cell machinery responsible for isotype class switching and somatic hypermutation is highly active in these cells, rampant cell differentiation would not be beneficial. Only once these cells have been selected to become plasma cells, secreting the developed and mutated antibodies, is BCL6 down-regulated. The same idea can be applied to TFH cells. Patients with certain autoimmune diseases have been shown to have significantly more TFH cells in circulation than healthy controls. Therefore, massive cell division of

TFH cells would be detrimental for human health and makes it possible that BCL6 works to limit the cell cycle in TFH cells.

To test the ability for a cell to enter and complete cell cycling, a propidium iodide (PI) analysis can be done. Once naïve Th cells from +/+ and fl/fl mice are activated in vitro with antibodies for twenty four hours, they can be fixed and stained with PI to check what part of the cell cycle they are currently in. Using flow cytometry, this assay can differentiate cells which are in G0/G1 phase, S phase, and G2/metaphase. Based on the genes which are up-regulated in the microarray, it is possible that BCL6-deficient cells are more likely to be going through mitosis than WT cells.

Another way to test a cell's ability to divide is via BrdU incorporation *in vivo*. By injecting mice with BrdU before immunizing, we can assess a Th cell's ability to divide with and without BCL6 using our cKO mouse model.

Part II – Further investigate the limiting nature of GCs in a prime/boost vaccine scheme

Reevaluate our vaccine strategy in a BCL6$^{fl/fl}$ Cre$^{CD4\text{-}ER}$ model

A noticeable caveat to our gp120 DNA-prime/protein boost vaccine scheme (Chapter 6) is that we deleted BCL6 in all cells in our animals, not just in T and B cells which make up GCs. Therefore, deletion in other cells could be affecting antibody development via extrinsic factors. Considering the extrinsic factors at play in BCL6 GL KO mice, which I have revealed in this thesis, this is a realistic concern. Therefore, this vaccine experiment should be repeated with BCL6$^{fl/fl}$ Cre$^{CD4\text{-}ER}$ mice (B6(129X1)-Tg(Cd4-cre/ERT2)11 Gnri/J) (JAX cat. 022356). Using this inducible cre model, we can restrict BCL6 deletion to T cells. This will enable us to determine whether the altered antibody secretion we observed is due to the lack of GCs, deletion of BCL6 in B cells, or some other unidentified extrinsic factor.

Evaluate somatic hypermutation rates in gp120 DNA-prime versus protein-prime B cells

While our analysis of antibodies using an HIV gp120 DNA prime versus gp120 protein prime demonstrated an advantage when the former was used, we did not test the mutation rate of immunoglobulin (Ig) genes in B cells. Therefore, I propose isolating GC B cells and non-GC B cells from mice receiving either DNA or protein priming, and after they all receive protein boosts. These cells can be lysed and their Ig genes cloned and sequenced.

The complementary determining region of the Ig gene is the site most targeted for somatic hypermutation (175). It undergoes mutation at the approximate rate of 0.05 – 1 x 10^{-3} changes per base pair per cell division (175). Using a database for germline sequences in mice (www.vbase2.org) we can determine the rate at which somatic hypermutation is taking place in B cells primed with gp120 DNA versus B cells primed with gp120 protein.

Determine why GCs are limiting for antibodies resulting from a prime/boost vaccine scheme.

As demonstrated in Chapter 6, once GCs were inhibited by injecting mice with tamoxifen (and thus deleting BCL6), antibody titers and affinity actually increased without the reassembly of these structures. One way to determine the reason for this is to evaluate the somatic hypermutation rates with and without deletion of BCL6. This can be done utilizing methods stated above. Identifying whether B cells outside the GC undergo additional somatic hypermutation can shed light on why these cells seem to secrete higher quality antibodies. If they cannot undergo additional mutations, then it is possible that additional booster shots may only be impeding the antibody response.

Table 2. Summary of mutant mice presented in this thesis

MOUSE	$BCL6^{-/-}$	$BCL6^{\Delta ZF/\Delta ZF}$	$BCL6^{Neofl/Neofl}$	$BCL6^{fl/fl}$	$BCL6^{fl/fl}$ Cre^{CD4}	$BCL6^{+/+}$ Cre^{CD4}
ALIAS (in thesis)	Original GL KO	New GL KO	Neo-floxed	Floxed	Conditional knockout (cKO)	Wild type (WT)
STRAIN BACKGROUND	Mixed C57BL/6-129Sv	Mixed C57BL/6-129Sv	Mixed C57BL/6-129Sv	Mixed C57BL/6-129Sv	Mixed C57BL/6-129Sv	Mixed C57BL/6-129Sv
BIRTH RATE	Significantly reduced	Significantly reduced	Moderately reduced	Normal	Normal	Normal
PHENOTYPE	Severely runted; early death	Severely runted; early death	Moderately runted; early death	Normal	Normal	Normal
HISTOLOGY	Severe inflammation of heart and lung; myocarditis	Slight inflammation of heart and lung	Slight inflammation of heart and lung	Normal	Normal	Normal
BCL6 ZF REGION TRANSCRIPT ($CD4^+$ CELLS)	Deficient	Deficient	Severely reduced	Normal	Deficient	Normal
TH CELL SKEWING	Severe Th2	Slight Th17	Slight Th17	None	None	None

Table 2 (continued). Summary of mutant mice presented in this thesis

MOUSE	$BCL6^{-/-}$	$BCL6^{\Delta ZF/\Delta ZF}$	$BCL6^{Neofl/Neofl}$	$BCL6^{fl/fl}$	$BCL6^{fl/fl}$ Cre^{CD4}	$BCL6^{+/+}$ Cre^{CD4}
GC DEVELOPMENT	None	None	None	Normal	None	Normal
NAÏVE/ EFFECTOR $CD4^{+}$ T CELLS	Increased effector population	N/A	N/A	N/A	Increased naïve and reduced effector populations	Normal
OTHER NOTES		Appears to have less inflammation and little-to-no Th2 skewing (as assessed by cytokine secretion) compared to $BCL6^{-/-}$			Th cells have significant decrease in IL-4 secretion and significant increase in IL-10 secretion	

REFERENCES

1. Litman GW, Cannon JP, & Dishaw LJ (2005) Reconstructing immune phylogeny: new perspectives. *Nat Rev Immunol* 5(11):866-879.
2. Beck G & Habicht GS (1996) Immunity and the invertebrates. *Sci Am* 275(5):60-63, 66.
3. Stirewalt DL & Radich JP (2003) The role of FLT3 in haematopoietic malignancies. *Nature reviews. Cancer* 3(9):650-665.
4. Ceredig R, Rolink AG, & Brown G (2009) Models of haematopoiesis: seeing the wood for the trees. *Nat Rev Immunol* 9(4):293-300.
5. Corey SJ*, et al.* (2007) Myelodysplastic syndromes: the complexity of stem-cell diseases. *Nature reviews. Cancer* 7(2):118-129.
6. Rosenberg HF, Dyer KD, & Foster PS (2013) Eosinophils: changing perspectives in health and disease. *Nat Rev Immunol* 13(1):9-22.
7. Weber C & Noels H (2011) Atherosclerosis: current pathogenesis and therapeutic options. *Nat Med* 17(11):1410-1422.
8. Siracusa MC, Perrigoue JG, Comeau MR, & Artis D (2010) New paradigms in basophil development, regulation and function. *Immunol Cell Biol* 88(3):275-284.
9. Voehringer D (2013) Protective and pathological roles of mast cells and basophils. *Nat Rev Immunol* 13(5):362-375.
10. Murray PJ & Wynn TA (2011) Protective and pathogenic functions of macrophage subsets. *Nat Rev Immunol* 11(11):723-737.
11. Ziegler-Heitbrock L*, et al.* (2010) Nomenclature of monocytes and dendritic cells in blood. *Blood* 116(16):e74-e80.
12. Banchereau J & Steinman RM (1998) Dendritic cells and the control of immunity. *Nature* 392(6673):245-252.
13. Sargeant D*, et al.* (2011) HIVToolbox, an Integrated Web Application for Investigating HIV. *PLoS ONE* 6(5):e20122.
14. Purcell AW, McCluskey J, & Rossjohn J (2007) More than one reason to rethink the use of peptides in vaccine design. *Nature Reviews Drug Discovery* 6(5):404-414.
15. Vyas JM, Van der Veen AG, & Ploegh HL (2008) The known unknowns of antigen processing and presentation. *Nat Rev Immunol* 8(8):607-618.

16. Vivier E, Ugolini S, Blaise D, Chabannon C, & Brossay L (2012) Targeting natural killer cells and natural killer T cells in cancer. *Nat Rev Immunol* 12(4):239-252.
17. O'Shea JJ & Paul WE (2010) Mechanisms Underlying Lineage Commitment and Plasticity of Helper CD4+ T Cells. *Science* 327 (5969):1098-1102
18. Zhu J, Yamane H, & Paul WE (2010) Differentiation of Effector CD4 T Cell Populations. *Annual Review of Immunology* 28:445-489.
19. Zhou L, Chong MMW, & Littman DR (2009) Plasticity of CD4+ T Cell Lineage Differentiation. *Immunity* 30(5):646-655.
20. Zhu J & Paul WE (2010) Heterogeneity and plasticity of T helper cells. *Cell research* 20(1):4-12.
21. Gray D (2002) A role for antigen in the maintenance of immunological memory. *Nat Rev Immunol* 2(1):60-65.
22. Kerfoot Steven M*, et al.* (2011) Germinal Center B Cell and T Follicular Helper Cell Development Initiates in the Interfollicular Zone. *Immunity* 34(6):947-960.
23. Baumjohann D, Okada T, & Ansel KM (2011) Cutting Edge: Distinct Waves of BCL6 Expression during T Follicular Helper Cell Development. *The Journal of Immunology* 187(5):2089-2092.
24. Crotty S (2011) Follicular Helper CD4 T Cells (TFH). *Annual Review of Immunology* 29(1):621-663.
25. King C (2009) New insights into the differentiation and function of T follicular helper cells. *Nature Reviews Immunology* 9(11):757-766.
26. King C, Tangye SG, & Mackay CR (2008) T Follicular Helper (TFH) Cells in Normal and Dysregulated Immune Responses. *Annual Review of Immunology* 26(1146):741-766.
27. Fazilleau N, McHeyzer-Williams LJ, Rosen H, & McHeyzer-Williams MG (2009) The function of follicular helper T cells is regulated by the strength of T cell antigen receptor binding. *Nature Immunology* 10(4):375 - 384.
28. Victora GD & Nussenzweig MC (2012) Germinal Centers. *Annual Review of Immunology* 30(1):429-457.
29. Dent AL, Shaffer AL, Xin Yu DA, & Staudt LM (1997) Control of Inflammation, Cytokine Expression, and Germinal Center Formation by BCL-6. *Science* 276(5312):589-592.
30. Stavnezer J, Guikema JEJ, & Schrader CE (2008) Mechanism and Regulation of Class Switch Recombination. *Annual Review of Immunology* 26(1):261-292.

31. Stavnezer J (1996) Antibody Class Switching. *Advances in Immunology*, ed Frank JD (Academic Press), Vol Volume 61, pp 79-146.
32. Vinuesa CG, Sanz I, & Cook MC (2009) Dysregulation of germinal centres in autoimmune disease. *Nat Rev Immunol* 9(12):845-857.
33. Chang P-P*, et al.* (2012) Identification of Bcl-6-dependent follicular helper NKT cells that provide cognate help for B cell responses. *Nat Immunol* 13(1):35-43.
34. Tsai LM & Yu D (2014) Follicular helper T-cell memory: establishing new frontiers during antibody response. *Immunol Cell Biol* 92(1):57-63.
35. Chung Y*, et al.* (2011) Follicular regulatory T cells expressing Foxp3 and Bcl-6 suppress germinal center reactions. *Nat Med* 17(8):983-988.
36. Linterman MA*, et al.* (2011) Foxp3+ follicular regulatory T cells control the germinal center response. *Nat Med* 17(8):975-982.
37. Schaerlia P*, et al.* (2009) Cxc Chemokine Receptor 5 Expression Defines Follicular Homing T Cells with B Cell Helper Function. *JEM* 192(11):1553-1562.
38. Kim CH*, et al.* (2001) Subspecialization of Cxcr5+ T Cells: B Helper Activity Is Focused in a Germinal Center–Localized Subset of Cxcr5+ T Cells. *The Journal of Experimental Medicine* 193(12):1373-1382.
39. Yu D*, et al.* (2009) The Transcriptional Repressor Bcl-6 Directs T Follicular Helper Cell Lineage Commitment. *Immunity* 31(3):457-468.
40. Ansel KM, McHeyzer-Williams LJ, Ngo VN, McHeyzer-Williams MG, & Cyster JG (1999) In Vivo–Activated Cd4 T Cells Upregulate Cxc Chemokine Receptor 5 and Reprogram Their Response to Lymphoid Chemokines. *The Journal of Experimental Medicine* 190(8):1123-1134.
41. Huynh KD & Bardwell VJ (1998) The BCL-6 POZ domain and other POZ domains interact with the co-repressors N-CoR and SMRT. *Oncogene* 17(19):2473-2484.
42. Dhordain P*, et al.* (1997) Corepressor SMRT binds the BTB/POZ repressing domain of the LAZ3/BCL6 oncoprotein. *Proceedings of the National Academy of Sciences* 94(20):10762-10767.
43. Huynh KD, Fischle W, Verdin E, & Bardwell VJ (2000) BCoR, a novel corepressor involved in BCL-6 repression. *Genes & Development* 14(14):1810-1823.
44. Olivier A-C (2003) Ambivalent role of BCL6 in cell survival and transformation. *Oncogene* 22(4):507-516.

45. Polo JM*, et al.* (2004) Specific peptide interference reveals BCL6 transcriptional and oncogenic mechanisms in B-cell lymphoma cells. *Nat Med* 10(12):1329-1335.
46. Dent AL, Vasanwala FH, & Toney LM (2002) Regulation of gene expression by the proto-oncogene BCL-6. *Crit Rev Oncol Hematol* 41(1):1-9.
47. Dhordain P*, et al.* (1998) The LAZ3(BCL-6) oncoprotein recruits a SMRT/mSIN3A/histone deacetylase containing complex to mediate transcriptional repression. *Nucleic Acids Research* 26(20):4645-4651.
48. Parekh S*, et al.* (2007) BCL6 programs lymphoma cells for survival and differentiation through distinct biochemical mechanisms. *Blood* 110(6):2067-2074.
49. Fujita N*, et al.* (2004) MTA3 and the Mi-2/NuRD Complex Regulate Cell Fate during B Lymphocyte Differentiation. *Cell* 119(1):75-86.
50. Basso K & Dalla-Favera R (2010) Chapter 7 - BCL6: Master Regulator of the Germinal Center Reaction and Key Oncogene in B Cell Lymphomagenesis. *Advances in Immunology*, ed Frederick WA (Academic Press), Vol Volume 105, pp 193-210.
51. Miki T, Kawamata N, Hirosawa S, & Aoki N (1994) Gene involved in the 3q27 translocation associated with B-cell lymphoma, BCL5, encodes a Kruppel-like zinc-finger protein. *Blood* 83(1):26-32.
52. Kerckaert J-P*, et al.* (1993) LAZ3, a novel zinc−finger encoding gene, is disrupted by recurring chromosome 3q27 translocations in human lymphomas. *Nature Genetics* 5:66-70.
53. Ye B*, et al.* (1993) Alterations of a zinc finger-encoding gene, BCL-6, in diffuse large-cell lymphoma. *Science* 262(5134):747-750.
54. Baron BW*, et al.* (1995) BCL6 encodes a sequence-specific DNA-binding Protein. *Genes, Chromosomes and Cancer* 13(3):221-224.
55. Kawamata N*, et al.* (1994) Recognition DNA Sequence of a Novel Putative Transcription Factor, BCL6. *Biochemical and Biophysical Research Communications* 204(1):366-374.
56. Chang CC, Ye BH, Chaganti RS, & Dalla-Favera R (1996) BCL-6, a POZ/zinc-finger protein, is a sequence-specific transcriptional repressor. *Proceedings of the National Academy of Sciences* 93(14):6947-6952.

57. Basso K*, et al.* (2010) Integrated biochemical and computational approach identifies BCL6 direct target genes controlling multiple pathways in normal germinal center B cells. *Blood* 115(5):975-984.
58. Ci W*, et al.* (2009) The BCL6 transcriptional program features repression of multiple oncogenes in primary B cells and is deregulated in DLBCL. *Blood* 113(22):5536-5548.
59. Ye BH*, et al.* (1997) The BCL-6 proto-oncogene controls germinal-centre formation and Th2-type inflammation. *Nat Genet* 16(2):161-170.
60. Dent AL, Hu-Li J, Paul WE, & Staudt LM (1998) T helper type 2 inflammatory disease in the absence of interleukin 4 and transcription factor STAT6. *Proceedings of the National Academy of Sciences* 95(23):13823-13828.
61. Kusam S, Toney LM, Sato H, & Dent AL (2003) Inhibition of Th2 Differentiation and GATA-3 Expression by BCL-6 *The Journal of Immunology* 170(5):2435-2441.
62. Johnston RJ*, et al.* (2009) Bcl6 and Blimp-1 Are Reciprocal and Antagonistic Regulators of T Follicular Helper Cell Differentiation. *Science* 325(5943):1006-1010.
63. Fazilleau N, Mark L, McHeyzer-Williams LJ, & McHeyzer-Williams MG (2009) Follicular Helper T Cells: Lineage and Location. *Immunity* 30(3):324-335.
64. Bhandoola A & Sambandam A (2006) From stem cell to T cell: one route or many? *Nat Rev Immunol* 6(2):117-126.
65. Kiel MJ*, et al.* (2005) SLAM Family Receptors Distinguish Hematopoietic Stem and Progenitor Cells and Reveal Endothelial Niches for Stem Cells. *Cell* 121(7):1109-1121.
66. Weissman IL & Shizuru JA (2008) The origins of the identification and isolation of hematopoietic stem cells, and their capability to induce donor-specific transplantation tolerance and treat autoimmune diseases. *Blood* 112(9):3543-3553.
67. Kondo M, Weissman IL, & Akashi K (1997) Identification of Clonogenic Common Lymphoid Progenitors in Mouse Bone Marrow. *Cell* 91(5):661-672.
68. Koichi A, David T, Toshihiro M, & Irving LW (2000) A clonogenic common myeloid progenitor that gives rise to all myeloid lineages. *Nature* 404(6774):193-197.

69. Spits H (2002) Development of alpha beta T cells in the human thymus. *Nature Reviews Immunology* 2(10):760-772.
70. Goldrath AW & Bevan MJ (1999) Selecting and maintaining a diverse T-cell repertoire. *Nature* 402(6759):255-262.
71. Morris GP & Allen PM (2012) How the TCR balances sensitivity and specificity for the recognition of self and pathogens. *Nature Immunology* 13(2):121-128.
72. Takahama Y (2006) Journey through the thymus: stromal guides for T-cell development and selection. *Nature Reviews Immunology* 6(2):127-135.
73. Ciofani M & Zúñiga-Pflücker JC (2010) Determining γδ versus αβ T cell development. *Nat Rev Immunol* 10(9):657-663.
74. Jenkins MK*, et al.* (2001) IN VIVO ACTIVATION OF ANTIGEN-SPECIFIC CD4 T CELLS. *Annual Review of Immunology* 19(1):23-45.
75. Zikherman J & Weiss A (2009) Antigen receptor signaling in the rheumatic diseases. *Arthritis research & therapy* 11(1):202.
76. Smith-Garvin JE, Koretzky GA, & Jordan MS (2009) T cell activation. *Annu Rev Immunol* 27:591-619.
77. Vang T*, et al.* (2012) LYP inhibits T-cell activation when dissociated from CSK. *Nature Chemical Biology* 8(5):437-446.
78. Béné MC (2006) What is ZAP-70? *Cytometry Part B: Clinical Cytometry* 70B(4):204-208.
79. Acuto O & Michel F (2003) CD28-mediated co-stimulation: a quantitative support for TCR signalling. *Nat Rev Immunol* 3(12):939-951.
80. Sieber M & Baumgrass R (2009) Novel inhibitors of the calcineurin/NFATc hub - alternatives to CsA and FK506? *Cell Communication and Signaling* 7(1):25.
81. Liu X*, et al.* (2012) Bcl6 expression specifies the T follicular helper cell program in vivo. *The Journal of Experimental Medicine* 209(10):1841-1852.
82. Lee PP*, et al.* (2001) A Critical Role for Dnmt1 and DNA Methylation in T Cell Development, Function, and Survival. *Immunity* 15(5):763-774.
83. Mombaerts P*, et al.* (1992) RAG-1-deficient mice have no mature B and T lymphocytes. *Cell* 68(5):869-877.
84. Mosmann TR, Cherwinski H, Bond MW, Giedlin MA, & Coffman RL (1986) Two types of murine helper T cell clone. I. Definition according to profiles of lymphokine activities and secreted proteins. *The Journal of Immunology* 136(7):2348-2357.

85. Mosmann TR & Coffman RL (1989) TH1 and TH2 Cells: Different Patterns of Lymphokine Secretion Lead to Different Functional Properties. *Annual Review of Immunology* 7:145-173.
86. Harrington LE*, et al.* (2005) Interleukin 17-producing CD4+ effector T cells develop via a lineage distinct from the T helper type 1 and 2 lineages. *Nat Immunol* 6(11):1123-1132.
87. Park H*, et al.* (2005) A distinct lineage of CD4 T cells regulates tissue inflammation by producing interleukin 17. *Nat Immunol* 6(11):1133-1141.
88. Chen W*, et al.* (2003) Conversion of Peripheral CD4+CD25− Naive T Cells to CD4+CD25+ Regulatory T Cells by TGF-β Induction of Transcription Factor Foxp3. *The Journal of Experimental Medicine* 198(12):1875-1886.
89. Itoh M*, et al.* (1999) Thymus and Autoimmunity: Production of CD25+CD4+ Naturally Anergic and Suppressive T Cells as a Key Function of the Thymus in Maintaining Immunologic Self-Tolerance. *The Journal of Immunology* 162(9):5317-5326.
90. Veldhoen M*, et al.* (2008) Transforming growth factor-beta 'reprograms' the differentiation of T helper 2 cells and promotes an interleukin 9-producing subset. *Nature Immunology* 9(12):1341-1346.
91. Dardalhon V*, et al.* (2008) IL-4 inhibits TGF-beta-induced Foxp3+ T cells and, together with TGF-beta, generates IL-9+ IL-10+ Foxp3(-) effector T cells. *Nat Immunol* 9(12):1347-1355.
92. Duhen T, Geiger R, Jarrossay D, Lanzavecchia A, & Sallusto F (2009) Production of interleukin 22 but not interleukin 17 by a subset of human skin-homing memory T cells. *Nature Immunology* 10(8):857-863.
93. Trifari S, Kaplan CD, Tran EH, Crellin NK, & Spits H (2009) Identification of a human helper T cell population that has abundant production of interleukin 22 and is distinct from TH-17, TH1 and TH2 cells. *Nature Immunology* 10(8):864-871.
94. Nakayamada S*, et al.* (2011) Early Th1 Cell Differentiation Is Marked by a Tfh Cell-like Transition. *Immunity* 35(6):919-931.
95. Oestreich KJ, Huang AC, & Weinmann AS (2011) The lineage-defining factors T-bet and Bcl-6 collaborate to regulate Th1 gene expression patterns. *The Journal of Experimental Medicine* 208(5):1001-1013.

96. Korn T, Bettelli E, Oukka M, & Kuchroo VK (2009) IL-17 and Th17 Cells. *Annual Review of Immunology* 27(1):485-517.
97. Mondal A, Sawant D, & Dent AL (2010) Transcriptional Repressor BCL6 Controls Th17 Responses by Controlling Gene Expression in Both T Cells and Macrophages. *The Journal of Immunology* 184(8):4123-4132
98. Nurieva RI*, et al.* (2009) Bcl6 Mediates the Development of T Follicular Helper Cells. *Science* 325(5943):1001-1005.
99. Crotty S, Johnston RJ, & Schoenberger SP (2010) Effectors and memories: Bcl-6 and Blimp-1 in T and B lymphocyte differentiation. *Nat Immunol* 11(2):114-120.
100. Bauquet AT*, et al.* (2008) The costimulatory molecule ICOS regulates the expression of c-Maf and IL-21 in the development of follicular T helper cells and TH-17 cells. *Nature Immunology* 10(2):167 - 175.
101. Cimmino L*, et al.* (2008) Blimp-1 Attenuates Th1 Differentiation by Repression of ifng, tbx21, and bcl6 Gene Expression. *The Journal of Immunology* 181(4):2338-2347.
102. Martins GA*, et al.* (2006) Transcriptional repressor Blimp-1 regulates T cell homeostasis and function. *Nature Immunology* 7(5):457-765.
103. Shaffer AL*, et al.* (2000) BCL-6 Represses Genes that Function in Lymphocyte Differentiation, Inflammation, and Cell Cycle Control. *Immunity* 13(2):199-212.
104. Ziegler SF (2006) FOXP3: Of Mice and Men. *Annual Review of Immunology* 24(1):209-226.
105. Hawrylowicz CM & O'Garra A (2005) Potential role of interleukin-10-secreting regulatory T cells in allergy and asthma. *Nat Rev Immunol* 5(4):271-283.
106. Maloy KJ & Powrie F (2001) Regulatory T cells in the control of immune pathology. *Nat Immunol* 2(9):816-822.
107. Saraiva M & O'Garra A (2010) The regulation of IL-10 production by immune cells. *Nat Rev Immunol* 10(3):170-181.
108. Sawant DV*, et al.* (2012) Bcl6 Controls the Th2 Inflammatory Activity of Regulatory T Cells by Repressing Gata3 Function. *The Journal of Immunology* 189(10):4759-4769.
109. Breitfeld D*, et al.* (2000) Follicular B Helper T Cells Express Cxc Chemokine Receptor 5, Localize to B Cell Follicles, and Support Immunoglobulin Production. *The Journal of Experimental Medicine* 192(11):1545-1552.

110. Hollister K*, et al.* (2013) Insights into the Role of Bcl6 in Follicular Th Cells Using a New Conditional Mutant Mouse Model. *The Journal of Immunology*.
111. Rasheed A-U, Rahn H-P, Sallusto F, Lipp M, & Müller G (2006) Follicular B helper T cell activity is confined to CXCR5hiICOShi CD4 T cells and is independent of CD57 expression. *European Journal of Immunology* 36(7):1892-1903.
112. Linterman MA*, et al.* (2009) Roquin Differentiates the Specialized Functions of Duplicated T Cell Costimulatory Receptor Genes Cd28 and Icos. *Immunity* 30(2):228-241.
113. Choi Youn S*, et al.* (2011) ICOS Receptor Instructs T Follicular Helper Cell versus Effector Cell Differentiation via Induction of the Transcriptional Repressor Bcl6. *Immunity* 34(6):932-946.
114. Chemnitz JM, Parry RV, Nichols KE, June CH, & Riley JL (2004) SHP-1 and SHP-2 Associate with Immunoreceptor Tyrosine-Based Switch Motif of Programmed Death 1 upon Primary Human T Cell Stimulation, but Only Receptor Ligation Prevents T Cell Activation. *The Journal of Immunology* 173(2):945-954.
115. Carter LL*, et al.* (2002) PD-1:PD-L inhibitory pathway affects both CD4+ and CD8+ T cells and is overcome by IL-2. *European Journal of Immunology* 32(3):634-643.
116. Haynes NM*, et al.* (2007) Role of CXCR5 and CCR7 in Follicular Th Cell Positioning and Appearance of a Programmed Cell Death Gene-1High Germinal Center-Associated Subpopulation. *The Journal of Immunology* 179(8):5099-5108.
117. Keir ME, Butte MJ, Freeman GJ, & Sharpe AH (2008) PD-1 and Its Ligands in Tolerance and Immunity. *Annual Review of Immunology* 26(1):677-704.
118. Sheppard K-A*, et al.* (2004) PD-1 inhibits T-cell receptor induced phosphorylation of the ZAP70/CD3ζ signalosome and downstream signaling to PKCθ. *FEBS Letters* 574(1–3):37-41.
119. Okazaki T, Maeda A, Nishimura H, Kurosaki T, & Honjo T (2001) PD-1 immunoreceptor inhibits B cell receptor-mediated signaling by recruiting src homology 2-domain-containing tyrosine phosphatase 2 to phosphotyrosine. *Proceedings of the National Academy of Sciences* 98(24):13866-13871.

120. Parry RV*, et al.* (2005) CTLA-4 and PD-1 Receptors Inhibit T-Cell Activation by Distinct Mechanisms. *Molecular and Cellular Biology* 25(21):9543-9553.
121. Zinselmeyer BH*, et al.* (2013) PD-1 promotes immune exhaustion by inducing antiviral T cell motility paralysis. *The Journal of Experimental Medicine* 210(4):757-774.
122. Patsoukis N*, et al.* (2012) Selective Effects of PD-1 on Akt and Ras Pathways Regulate Molecular Components of the Cell Cycle and Inhibit T Cell Proliferation. *Sci. Signal.* 5(230):ra46-.
123. Good-Jacobson KL*, et al.* (2010) PD-1 regulates germinal center B cell survival and the formation and affinity of long-lived plasma cells. *Nat Immunol* 11(6):535-542.
124. Youngblood B*, et al.* (2011) Chronic Virus Infection Enforces Demethylation of the Locus that Encodes PD-1 in Antigen-Specific CD8+ T Cells. *Immunity* 35(3):400-412.
125. Wilson CB, Rowell E, & Sekimata M (2009) Epigenetic control of T-helper-cell differentiation. *Nature Reviews Immunology* 9(2):91-105.
126. Bestor TH (2000) The DNA methyltransferases of mammals. *Human Molecular Genetics* 9(16):2395-2402.
127. Kriukienė E, Liutkevičiūtė Z, & Klimašauskas S (2012) 5-Hydroxymethylcytosine – the elusive epigenetic mark in mammalian DNA. *Chemical Socitey Reviews* 41(21):6916-6930.
128. Klose RJ & Bird AP (2006) Genomic DNA methylation: the mark and its mediators. *Trends in Biochemical Sciences* 31(2):89-97.
129. Kohli RM & Zhang Y (2013) TET enzymes, TDG and the dynamics of DNA demethylation. *Nature* 502(7472):472-479.
130. Zaretsky AG*, et al.* (2009) T follicular helper cells differentiate from Th2 cells in response to helminth antigens. *The Journal of Experimental Medicine* 206(5):991-999.
131. Nurieva RI*, et al.* (2008) Generation of T Follicular Helper Cells Is Mediated by Interleukin-21 but Independent of T Helper 1, 2, or 17 Cell Lineages. *Immunity* 29(1):138-149.
132. Temple L, Kawabata TT, Munson AE, & White Jr KL (1993) Comparison of ELISA and Plaque-Forming Cell Assays for Measuring the Humoral Immune

Response to SRBC in Rats and Mice Treated with Benzo[a]pyrene or Cyclophosphamide. *Fundamental and Applied Toxicology* 21(4):412-419.

133. Thieu VT*, et al.* (2008) Signal Transducer and Activator of Transcription 4 Is Required for the Transcription Factor T-bet to Promote T Helper 1 Cell-Fate Determination. *Immunity* 29(5):679-690.
134. Stritesky GL*, et al.* (2011) The Transcription Factor STAT3 Is Required for T Helper 2 Cell Development. *Immunity* 34(1):39-49.
135. Moss AR & Bacchetti P (1989) Editorial review: Natural history of HIV infection. *AIDS* 3(2):55-61.
136. Bartlett JG (2006) Ten Years of HAART: Foundation for the Future. (Medscape, LLC).
137. McNicholl I (2012) Adverse Effects of Antiretroviral Drugs. (UCSF Center for HIV Information).
138. Moore JP & Stevenson M (2000) New targets for inhibitors of HIV-1 replication. *Nat Rev Mol Cell Biol* 1(1):40-49.
139. McElrath MJ*, et al.* (HIV-1 vaccine-induced immunity in the test-of-concept Step Study: a case–cohort analysis. *The Lancet* 372(9653):1894-1905.
140. Group TrHVS (2005) Placebo-Controlled Phase 3 Trial of a Recombinant Glycoprotein 120 Vaccine to Prevent HIV-1 Infection. *Journal of Infectious Diseases* 191(5):654-665.
141. Pitisuttithum P*, et al.* (2006) Randomized, Double-Blind, Placebo-Controlled Efficacy Trial of a Bivalent Recombinant Glycoprotein 120 HIV-1 Vaccine among Injection Drug Users in Bangkok, Thailand. *Journal of Infectious Diseases* 194(12):1661-1671.
142. Hammer SM*, et al.* (2013) Efficacy Trial of a DNA/rAd5 HIV-1 Preventive Vaccine. *New England Journal of Medicine* 369(22):2083-2092.
143. Gray GE*, et al.* (2011) Safety and efficacy of the HVTN 503/Phambili Study of a clade-B-based HIV-1 vaccine in South Africa: a double-blind, randomised, placebo-controlled test-of-concept phase 2b study. *The Lancet Infectious Diseases* 11(7):507-515.
144. Rerks-Ngarm S*, et al.* (2009) Vaccination with ALVAC and AIDSVAX to Prevent HIV-1 Infection in Thailand. *New England Journal of Medicine* 361(23):2209-2220.

145. Karlsson Hedestam GB*, et al.* (2008) The challenges of eliciting neutralizing antibodies to HIV-1 and to influenza virus. *Nature reviews. Microbiology* 6(2):143-155.
146. Melikyan GB (2008) Common principles and intermediates of viral protein-mediated fusion: the HIV-1 paradigm. *Retrovirology* 5:111.
147. Li M & Craigie R (2006) Virology: HIV goes nuclear. *Nature* 441(7093):581-582.
148. Savarino A (2007) In-Silico docking of HIV-1 integrase inhibitors reveals a novel drug type acting on an enzyme/DNA reaction intermediate. *Retrovirology* 4:21.
149. Clapham PR & Lu S (2011) Vaccinology: precisely tuned antibodies nab HIV. *Nature* 477(7365):416-417.
150. Langedijk JP & Schuitemaker H (2012) A sweet surprise for HIV broadly neutralizing antibodies. *Nature medicine* 18(11):1616-1617.
151. Haynes BF, Kelsoe G, Harrison SC, & Kepler TB (2012) B-cell-lineage immunogen design in vaccine development with HIV-1 as a case study. *Nat Biotechnol* 30(5):423-433.
152. Kwong PD, Mascola JR, & Nabel GJ (2013) Broadly neutralizing antibodies and the search for an HIV-1 vaccine: the end of the beginning. *Nat Rev Immunol* 13(9):693-701.
153. Burton DR*, et al.* (2004) HIV vaccine design and the neutralizing antibody problem. *Nat Immunol* 5(3):233 - 236.
154. Streeck H, D'Souza MP, Littman DR, & Crotty S (2012) Harnessing CD4+ T cell responses in HIV vaccine development. *Nature Medicine* 19(2):143-149.
155. Hollowood K & Macartney J (1992) Cell kinetics of the germinal center reaction - a stathmokinetic study. *European Journal of Immunology* 22(1):261-266.
156. Wei C-J*, et al.* (2010) Induction of Broadly Neutralizing H1N1 Influenza Antibodies by Vaccination. *Science* 329(5995):1060-1064.
157. Dou J*, et al.* (2012) Protection against Mycobacterium tuberculosis challenge in mice by DNA vaccine Ag85A-ESAT-6-IL-21 priming and BCG boosting. *International Journal of Immunogenetics* 39(2):183-190.
158. Chuang I*, et al.* (2013) DNA Prime/Adenovirus Boost Malaria Vaccine Encoding *P. falciparum* CSP and AMA1 Induces Sterile Protection Associated with Cell-Mediated Immunity. *PLoS ONE* 8(2):e55571.
159. Lu S (2009) Heterologous prime–boost vaccination. *Current Opinion in Immunology* 21(3):346-351.

160. Vaine M, Wang S, Hackett A, Arthos J, & Lu S (2010) Antibody responses elicited through homologous or heterologous prime-boost DNA and protein vaccinations differ in functional activity and avidity. *Vaccine* 28(17):2999-3007.
161. Wang S*, et al.* (2005) Enhanced Immunogenicity of gp120 Protein When Combined with Recombinant DNA Priming To Generate Antibodies That Neutralize the JR-FL Primary Isolate of Human Immunodeficiency Virus Type 1. *Journal of Virology* 79(12):7933-7937.
162. Wang S*, et al.* (2006) Polyvalent HIV-1 Env vaccine formulations delivered by the DNA priming plus protein boosting approach are effective in generating neutralizing antibodies against primary human immunodeficiency virus type 1 isolates from subtypes A, B, C, D and E. *Virology* 350(1):34-47.
163. Taylor JJ, Pape KA, & Jenkins MK (2012) A germinal center–independent pathway generates unswitched memory B cells early in the primary response. *The Journal of Experimental Medicine* 209(3):597-606.
164. Coban C, Koyama S, Takeshita F, Akira S, & Ishii KJ (2008) Molecular and cellular mechanisms of DNA vaccines. *Human Vaccines* 4(6):453-457.
165. Vasan S*, et al.* (2010) Phase 1 Safety and Immunogenicity Evaluation of ADVAX, a Multigenic, DNA-Based Clade C/B' HIV-1 Candidate Vaccine. *PLoS ONE* 5(1):e8617.
166. Catanzaro AT*, et al.* (2007) Phase I clinical evaluation of a six-plasmid multiclade HIV-1 DNA candidate vaccine. *Vaccine* 25(20):4085-4092.
167. Koblin BA*, et al.* (2011) Safety and Immunogenicity of an HIV Adenoviral Vector Boost after DNA Plasmid Vaccine Prime by Route of Administration: A Randomized Clinical Trial. *PLoS ONE* 6(9):e24517.
168. Bakari M*, et al.* (2011) Broad and potent immune responses to a low dose intradermal HIV-1 DNA boosted with HIV-1 recombinant MVA among healthy adults in Tanzania. *Vaccine* 29(46):8417-8428.
169. Koup RA*, et al.* (2010) Priming Immunization with DNA Augments Immunogenicity of Recombinant Adenoviral Vectors for Both HIV-1 Specific Antibody and T-Cell Responses. *PLoS ONE* 5(2):e9015.
170. Lu S, Wang S, & Grimes-Serrano JM (2008) Current progress of DNA vaccine studies in humans. *Expert Review of Vaccines* 7(2):175-191.
171. Lindqvist M*, et al.* (2012) Expansion of HIV-specific T follicular helper cells in chronic HIV infection. *The Journal of Clinical Investigation* 122(9):3271-3280.

172. Perreau M*, et al.* (2013) Follicular helper T cells serve as the major CD4 T cell compartment for HIV-1 infection, replication, and production. *The Journal of Experimental Medicine* 210(1):143-156.
173. Xu Y*, et al.* (2013) Simian Immunodeficiency Virus Infects Follicular Helper CD4 T Cells in Lymphoid Tissues during Pathogenic Infection of Pigtail Macaques. *Journal of Virology* 87(7):3760-3773.
174. Keene JD, Komisarow JM, & Friedersdorf MB (2006) RIP-Chip: the isolation and identification of mRNAs, microRNAs and protein components of ribonucleoprotein complexes from cell extracts. *Nat Protoc* 1(1):302-307.
175. Bowers E*, et al.* (2014) Decreased Mutation Frequencies among Immunoglobulin G Variable Region Genes during Viremic HIV-1 Infection. *PLoS ONE* 9(1):e81913.

CURRICULUM VITAE

KRISTIN N. HOLLISTER

EDUCATION

Indiana University — Indianapolis, IN
Ph.D., Microbiology and Immunology — 2008 – 2014

Kelley School of Business — Indianapolis, IN
Indiana University — 2012 – 2013
Certificate in Business of Life Sciences program

Hanover College — Hanover, IN
B.A., Biology and Mathematics — 2003 – 2007

Denmark International Study Program, 2006 — Copenhagen, DK
Course work: HIV/AIDS in Western Europe — London, UK
Paris, FR
Amsterdam, NL

RESEARCH/WORK EXPERIENCE

Indiana University School of Medicine — 2008 – 2014
Ph.D. Student; Advisor: Dr. Alexander L. Dent, Ph.D. — Indianapolis, IN
Thesis: Elucidating the role of BCL6 in T helper cell activation, proliferation, and differentiation

Dow AgroSciences (Kelly Scientific) — 2008
Research scientist and laboratory technician — Indianapolis, IN

Alpharma – Animal Health Division (KForce Scientific) — 2007
Chemist laboratory technician — Chicago Heights, IL

TEACHING EXPERIENCE

Indiana University-Purdue University Indianapolis — 2012
Teaching Assistant, Microbiology and Immunology — Indianapolis, IN

Indiana University School of Medicine — 2013 – 2014
Teaching Assistant, Immunology I – Introduction to the Immune System — Indianapolis, IN

GRANTS AND AWARDS

Immunology and Infectious Disease Training Grant — 2009 – 2010
NIH/NIAID: T32 AI060519-06

Basic Science Studies on Gene Therapy of Blood Disease Training Grant 2011 – 2013
NIH/NIAID: T32 HL007910-14

Keystone Symposia Travel Award, HIV Vaccines 2013
NIAID: 1R13AI104364-01

AAI Laboratory Travel Grant 2013
AAI Annual Meeting

Educational Enhancement Grant 2012
IUPUI Graduate Student Professional Government

Co-chair of Fong-Clontech Award Committee 2012 – 2013

Employee of the Month 2008
Kelly Scientific (Dow AgroSciences)

CONFERENCE PRESENTATIONS

Hollister, K., Dent, A. (2011). Accidents Happen: Discovery of a new BCL6 knockout model. Poster and oral presentation delivered at the Autumn Immunology Conference, Chicago, IL.

Hollister, K., Chen, Y., Wu, H., Lu, S., Dent. A. (2013). Enhanced expansion of follicular T helper cells following vaccination with gp120-encoding DNA. Poster and oral presentation delivered at the Keystone Symposia – HIV Vaccines, Keystone, CO.

Hollister, K., Wu, H., Dent, A. (2013). Role of BCL6 and PD-1 in CD4 memory T cell development. Poster presentation at the American Association of Immunologists Annual Meeting, Honolulu, HI.

PEER-REVIEWED PUBLICATIONS

Hollister, K., Kusam, S., Wu, H., Clegg, N., Mondal, A., Sawant, D.V., Dent, A.L. (2013). Insights into the role of BCL6 in follicular Th cells using a new conditional mutant mouse model. *Journal of Immunology*, 191(7):3705-11.

Hollister, K., Yuxin, C., Wang, S., Wu, H., Mondal, A., Clegg, N., Dent, A.L., Lu, S. (2014). The role of follicular helper T cells and the germinal center in HIV-1 gp120 DNA prime and gp120 protein boost vaccination. Accepted for publication. *Human Vaccines and Immunotherapeutics*.

Pham, D., Walline, C.C., **Hollister, K.**, Dent, A.L., Blum, J.S., Firulli, A.B., Kaplan, M.H. (2013). The Transcription Factor Twist1 Limits T Helper 17 and T Follicular Helper Cell Development by Repressing the Gene Encoding the Interleukin-6 Receptor α Chain. *The Journal of Biological Chemistry*, 288(38):27423-33.

Walline, C.C., Deffit, S.N., Wang, N., Guindon, L.M., Crotzera, V.L., Liu, J., **Hollister, K.**, Eisenlohr, L.C., Brutkiewicz, R.R., Kaplan, M.H., Blum J.S. (2014). Virus Encoded CD74 Enhances Poxvirus Vaccine Efficacy. *Immunology*, 141(4):531-539.

Mathew, R., Mao, A., Chiang, A., Bertozzi-Villa, C., Bunker, J., Scanlon, S., McDonald, B., Constantinides, M., **Hollister, K.**, Singer, J., Dent, A., Dinner, A., Bendelac, A. (2014). A negative feedback loop mediated by the Bcl6-cullin3 complex limits Tfh differentiation. Accepted for publication. *The Journal of Experimental Medicine*.